Waste-to-Energy: Solar pyrolysis of sludge, as a part of global solid waste issue, to produce oil.

Initial Trial to Design a Household Solar Pyrolysis Device

SEPTEMBER 8, 2020

UNIVERSITY OF WAIKATO
Faculty of Engineering

Acknowledgements

Greeting to those great people standing in my back.

This work has done with much support given by my lovely supervisor, Dr. Mark Lay. He did all his best to make this project alive. I can not also forget my wife, Noor Amerah and my family who have dedicated themselves and sacrified their time to support me during difficult sitiuations. My idol who has not stopped inducing and encouraging me, my elder brothe, Dr. Meqdad Hasan. I would like to thank them all, my supervisor, my wife, my brother and my family for their help and support during this research.

Waste-to-Energy

Solar pyrolysis of sludge, as a part of global solid waste issue, to produce oil

Initial Trial to Design a Household Solar Pyrolysis Device

Abstract

Daily, huge amounts of solid waste are produced around the world with 70% increase rate. Municipal solid waste (MSW) including sewage sludge is the main waste generated in cities and towns. Proper waste management approaches are urgently needed. Despite numerous social and technical approaches were presented, this paper aims to employ plenty of solar energy specifically in the Middle East into a waste-to-energy solution. By using solar pyrolysis technology, this study aims to present a solar-powered design to convert sludge into oil. This design can be easily upgraded to a household device as a household waste management approach. Like other thermochemical reactions, solar pyrolysis of sludge produces bio-oil which has a reasonable calorific value making this technology is useful as a fuel source. However, unlike others, solar pyrolysis has low operation cost and not dependent on fossil fuel. Although this device is designed only for sludge, it can be used also to convert all kinds of domestic wastes including waste oils, plastics, rubbers, and municipality solid waste (MSW) into energy and oil. This research illustrates a novel design for a dryer that produce “a slude flacks” by using solar energy. Factors such as feasibility, continuity, productivity, drying time, and quality of the yield were considered in this design. A rotational dryer with ϕ 1m and 1m length was modelled by Solidwork software application to dry wet sludge of 75% water content. Different types of solar concentrators were employed to maximize productivity and minimize cost and area. However, the average daily production of this dryer per 8 sunny working hours was around 51.87 litters of bio-oil, 31.78 Kg bio-char, and 58.785 Kg syngas. The best results were measured when the average mass flow into the reactor is 21 kg/hr.

This study highlights solar pyrolysis efficiency in waste management. This research aims to develop a solar-powered system, using the sludge as fuel to generate energy. The experiments were done at Waikato University, NZ. As known, Waikato district is wet and cloudy most days in comparison to those countries on the Sunbelt such as Jordan. Interestingly, figures show that solar pyrolysis of sludge has high potential in Jordan and Middle East countries in term of plenty of solar energy and sunny days. However, although solar pyrolysis can be described as an affordable eco-friendly technology that can be used directly by householders as a source of energy, its viability and feasibility in Middle East still need further study.

Table of Contents

TABLE OF FIGURES

TABLE OF TABLES

Waste-to-Energy

Solar pyrolysis of sludge, as a part of global solid waste issue, to produce oil

Initial Trial to Design a Household Solar Pyrolysis Device

1. Introduction

1.1 Overview

This thesis aims to bring together three fields; a reasonable solution for solid waste management, invest the solar energy as a sustainable energy, and to produce bio-oil, bio-char, and syngas as renewable sources of energy by designing a solar unit (receiver-reactor) suitable for this purpose, from sewage sludge.

Therefore, this thesis has included seven subjects; 1) the issue of solid waste including its volume and causes, 2) the sludge as a part of solid waste issue and the potential energy recovery processes from sludge, 3) Pyrolysis technique which is a preferable thermochemical treatment method of sludge because of its high potential of bio-oil yield, 4) solar pyrolysis as a sustainable and eco-friendly technique to reduce fossil fuel using and operational cost. This subject discusses the feasibility of solar pyrolysis of sludge in Sunbelt countries such as Middle East and Jordan specifically as well as present technologies of harvesting solar energy and enhancing the productivity. 5) Drying process as an initial step in solar pyrolysis of sludge including present thermal techniques and challenges. 6) Finally, a novel design for a solar pyrolysis unit, mainly the solar dryer to produce “Sludge Flacks”. Schemes, calculation, and results are included to present the potential economic value of using this design for solar pyrolysis.

This design is presented as first step in the final goal which is Household Solar Pyrolysis Unit (HSPU). HSPU can be a potential disposal option in waste management.

However, although this design has limited scope at the moment, it can be easily upgraded to include very wide range of waste. Waste combustibility as an end-life process is the criteria

for useful waste for solar pyrolysis unit regardless to its biodegradability, properties, sources, materials, or its usage. Solid waste from municipalities, factories, forests and farms, meat processing companies and wastewater treatment facilities can be used as a feedstock for this unit. In addition, all types of plastic, tires, rubbers and waste oils are considered ideal feedstock for this unit due to its zero water content. Gaseous wastes and water-based liquid wastes are excluded. However, this study is to complete the great efforts are done globally to recover energy from solid waste specifically sewage sludge.

2. Solid Waste

2.1 Background

Waste issue is a major source of global concern. Despite waste is companied with human being (Chandler et al, 1997) because most his activities generate waste (Brunner and Rechberger, 2014) and he is only who decides what waste is (Amasuomo & Baird, 2016), industrial revolution in the sixteenth century can be blamed as a main cause of the beginning of substantial increase in wastes generation. This comes as a result of hundreds of new and innovative materials and products (Tchobanoglous et al, 1993), population growth and economic development (Hoornweg & Bhada-Tata, 2012) as well as urban spread and population explosion in cities (Wilson, 2007). It has led to change in human behaviours, activities and consumption and then a surge in the quantity and variety of wastes generated (Williams, 2005). Recognizing the waste issue requires determining the waste volume and this in turn needs an adequate understanding for the meaning of term of waste (Amasuomo & Baird, 2016). Natural waste is produced as returned substances to the environment by organisms or living things. These wastes are recycled by other organisms as a part of the life cycle (EPA, 2006). However, human overloads the capacity of environmental recycling processes by generating continuous stream of material residues that are non-biodegradable or need long time to be degraded naturally (The Environmental Literacy Council, 2015) and thus need to be managed to reduce their effects. Therefore, waste can be defined concisely as any useful or useless matter that is unwanted, rejected, abandoned leftover and/or surplus which is then discharged or disposed into the environment (Lamb, Pogson & Schliebs, 2012) while The Australian/New Zealand Standard, AS/NZS 3831:1998, sees that waste can be

“materials and energy which have no further use and are released to the environment as a means of disposal”. The U.S. Environmental Protection Agency (EPA) is more specified in its definition to solid waste as

> *"any garbage or refuse, sludge from a wastewater treatment plant, water supply treatment plant, or air pollution control facility and other discarded material, including solid, liquid, semi-solid, or contained gaseous material resulting from industrial, commercial, mining, and agricultural operations, and from community activities."*

While Jordan Green Building Council (2016) defines Municipal Solid Waste (MSW) as

> *“solid and semi-solid materials produced by households, as well as other waste similar in nature and composition resulting from any activity (commerce, offices, public institutions, etc.) and not included in the definition of harmful and hazardous waste, that are collected by or on behalf of municipal authorities or by the private sector (business or private non-profit institutions) and disposed of through the waste management system”.*

This includes broad range of compositions that are categorised into several groups based on different characteristics. Some of these common criteria include waste biodegradability: organic waste and inorganic waste, its direct impact on health and environment: hazardous and non-hazardous waste, its physical form: Solid, liquid and gaseous waste, its source of production: household or domestic waste, industrial waste, commercial waste, institutional waste, agricultural waste, construction and demolition waste, and mining waste, its reusable potentials: by-products waste, e-waste and recyclable waste, and its physical properties: compostable, combustible, and recyclable as well as its material: plastic, paper, glass, cardboard, etc., and its original use: food waste, packaging waste, etc. (American Veterinary Medical Association AVMA, 2019; The U.S Environmental Literacy Council, 2015; Hoornweg & Bhada-Tata,2012; Demirbas,2011; Dixon & Jones, 2005; White et al., 1995).

Interestingly, Dijkema et al. (2000) defined the waste as anything labelled by the owner as such even if it is not. Meaning that what is waste for one individual can be a resource to another. This definition forms the concept of Waste-to-Energy.

The majority of Municipal Solid Waste (MSW) is produced by household and commercial practice. Household waste is treated as solid waste regardless of whether it is physically "solid" in actual (American Veterinary Medical Association, 2019). This waste is known as one of the hardest wastes in term of management due to its nature that consists of various range of materials. These materials are found totally mixed together (Fullerton & Raub, 2004).The Organisation for Economic Co-operation and Development, 2010). MSW includes household waste and commercial waste. MSW, including sewage sludge, is also variable in term of composition; geographically and seasonally.

Economically, solid waste management is very expensive in term of the issue itself and in term of its consequences. Often, the cost of addressing solid waste impacts is many times higher than the cost of operating and developing simple and adequate waste management systems. Investing in sustainable waste management was suggested by The World Bank and the United Nation because it does make economic sense. According to the World Bank report: What a Waste 2.0 (2016), the current techniques of waste management and disposal are comprising 20%–50% of municipal budgets. For example, on average, every single ton of solid waste costs 30 $US for recycling, 50 $US for dumping, and 75 $US for incineration (University of Southern Indiana). Since 2000, the World Bank alone has committed over $4.7 billion to more than 340 solid waste management programs around the globe. However, all of these programs are focusing on operating the essential municipal services which requires integrated systems that are efficient, sustainable, and socially supported but don’t involve deeply in technologies of energy recovery and potential renewable energy sources from solid waste.

2.2 Solid Waste volume

The solid waste issue began in the 16th century as a result of industrial revolution. This in turn resulted in waves of migrants to cities. This huge increase in cities population caused a substantial increase in wastes generation (Wilson, 2007). In these days, the world produces more than five billion tonnes per year of solid waste (Fullerton & Raub, 2004). As the waste volume increases, the diversity of the waste increases with various new types of wastes that are hardly degraded (Vergara and Tchobanoglous, 2012). Currently, Waste is one of the main environmental issues globally especially with current huge volumes. According to World Bank

Report WBR (2018), the world cities generated 2.01 billion tonnes of solid waste. This amount increases with increasing of the world population. With urbanization and rapid population growth, annual waste generation is expected to jump up to 70% increasing from 2016 levels. The waste production will likely increase to 2.2 billion tonnes per year by 2025 (about 1.42 kg/capita/day) (Hoornweg & Bhada-Tata, 2012) and to 3.40 billion tonnes in 2050 (WBR, 2018).

According to WBR, the average production of person in 2016 was 0.74 kilograms per day. This rate varies around the world. High-income and developed countries only account for 16% of the world's population but they generate over 34% of the world's waste. For example, the United States and Canada come in the top of the world countries as the highest generators of solid waste by producing about 2.58 kg and 2.33 kg per capita, per day, respectively (Wang, 2019). This means that Americans who form 5% of the world population generate 40% of the global waste as the highest solid waste producers in the world (University of Southern Indiana). However, the waste issue may be worse with huge unaccounted amount of waste that can be seen clearly in streets and cities of poor and developing countries (Walsh, 2017).

Consequently, more attention have been given to the environmental development when public officials began in the 19th century to use a safe controlled manner for waste disposal (Tchobanoglous et al, 1993). In addition to the remarkable reduction in side effects of solid waste disposal, due to the new regulation, this also resulted in increasing the benefits of waste itself. For instance, the trash production of the US alone in 2006 was 250 million ton. Nearly 33 percent of this volume had been recycled. This process had saved energy equivalent of about 38 billion litter of gasoline (The Environmental Literacy Council, 2015).

Components percentage of MSW varies from city to another. However, the global urban solid waste production contains more than 46% organic materials (Hoornweg and Bhada-Tata, 2012). According to statics of Food and Agriculture Organization of the United Nations FAO in 2011, the MSW generated worldwide contains 1.3 billion tons of the edible food (Grilli, Bildstein & Lambertucci, 2019). Packaging materials which are mainly plastic have formed about one-third of global waste production (University of Southern Indiana). In term of plastic, there is estimation that 8.3 billion tons of plastic were produced in the period from 1950 to 2015 (Geyer et al. 2017). More than 5.7 billion tons of this production had discharged as waste

and about 4.9 billion tons of this waste had found their way to landfills and the natural environment (Barnes, 2019).

In Jordan, Jordanians generate daily about 3800 tons of MSW; 2620 tons in the middle region, 780 tons in the northern region, and about 400 tons in the southern region (Daradki, 2008; Aljaradin, 2014). The total annual generation of MSW in Jordan according to a recent governmental estimation is 2.7 million tons which is estimated to increase by 2034 to 5.2 million tons. Organic or bio-waste forms 60% of total generated MSW (European Commission, 2018). However, the current policies in Jordan (Three R's approach; Reduce, Reuse, Recycle) have aimed to reduce the bio-waste landfilled by 75% in 2024 (European Commission, 2018).

Dry sludge is considered as a part of municipal solid waste. In addition to other factors, the volume of sludge production depends significantly on dietary habits (Niwagaba, Mbéguéré & Strande, 2014). Communities with a diet consisting of a high fibre content produce a higher mass and volume of solid sludge compared to communities who have a higher meat based or highly processed food diet. However, wastewater treatment, in total, produces about 0.94 kg of dry solids per 3.78 m3 of wastewater treated (National Research Council, 1996). Means that every person, in average, deposits about 70 g of solids into wastewater per day. Counting 'garbage grinders' that find their way to wastewater will raise this production to 100g per day (Boucher & Van Eeden, 1994). However, knowing that the activated sludge often has solids content of about three percent by weight, the following equation can be used to calculate the daily production of sludge (Lenntech BV):

$$P_{X,TSS} = \frac{QY(S_0 - S)}{1 + k_d(\mathrm{SRT})} \cdot \frac{1}{0.85} + \frac{f_d k_d Y Q(S_0 - S)(\mathrm{SRT})}{1 + k_d(\mathrm{SRT})} \cdot \frac{1}{0.85} + QX_{0,i} + Q(\mathrm{TSS}_0 - \mathrm{VSS}_0)$$

Where

Q = wastewater flowrate (m^3/d)

S_0 = influent soluble substrate concentration (bsCOD) (BOD or bsCOD g/m^3)

S = effluent soluble substrate concentration (bsCOD)

$X_{0,i}$ = nbVSS concentration in influent (g/m^3 or mg/l)

iTSS = inert inorganics Total Suspended Solids (iTSS) (g/m^3)

X_T = total MLVSS concentration (g/m^3 or mg/l)

SRT = Sedimentation Retention Time (SRT) (day)

VSS_0 = influent Volatile Suspended Solids [g VSS/m^3] or [mg/l]

TSS_0 = influent Total Suspended Solids [g TSS/m^3] or [mg/l]

Kinetic Coefficients

k = maximum rate of soluble substrate utilization (g COD/g·d)

Y = biomass yield (g VSS/g COD used)

k_d = endogenous decay coefficient (g VSS/g VSS·d)

K_s = half-velocity constant (g COD/m^3)

f_d = fraction of biomass that remains as cell debris (g VSS/g VSS)

The daily sludge production is:

$P_{X,T,VSS}$ (kg VSS/d)

$P_{X,T,TSS}$ (kg TSS/d)

In term of using thermochemical treatment methods for solid waste management, this equation can provide the designer with the approximate volume of required treatment plant.

2.3 Why solid waste is an issue?

Unprocessed MSW including sludge has many negative impacts on the environment and human health. Its environmental impacts includes global warming due to harmful gases emissions (such as methane, Dioxins, sulphur, and PAN), health issues and diseases (such as different types of cancer), air pollution and groundwater contamination (El-Naqa, 2005), vegetation and cattle issue as a result of plastic bags, heat exchange which results mainly from direct burning of rubbish, and the financial cost of recovery (Amasuomo & Baird, 2016). Open dumps that are world widely used specifically in developing countries are breeding grounds for vermin and rats. This likely to result in outbreak of epidemics and then high death tolls (Amasuomo & Baird, 2016).

Non-biodegradable waste such as plastic is also another tragedy issue (Barnes, 2019). Plastic alone forms 12% of the total annual generation of waste. With only 5.5% of global waste is composted and 13.5% is recycled, high percentage of this plastic chokes oceans, ecosystems,

and waterways and then the food chain (Auta, Emenike & Fauziah, 2017). According to Islam & Tanaka (2004), plastic makes up 90% of marine debris which threatens curtails biodiversity and potentially everyone on the planet (Barnes, 2019). Although physical blockages from plastic debris as well as ingestion stress problems are direct harms to aquatic organisms, leakage of plasticizers, exposure to persistent organic pollutants (POPs) are other harms (Barnes, 2019). These contaminants are able to cause changes in endocrine disruption and metabolic processes and hence changes in behaviour (Oliveira et al., 2013; Rochman et al., 2014). Moreover, plastic debris in aquatics reduces photosynthesis and growth of primary food producers such as algae, causes entanglement of aquatic organisms, and affects the reproductive ability of crustaceans (Barnes, 2019). However, although plastic waste affects the land-based ecosystems, its impacts still not well understood (Horton et al., 2017).

2.4 The causes behind waste issue

Up-normal change in human life style can be generalized as the main reason behind waste issue. Industrial revolution, migration, wellbeing, and forced migration due to wars (refugee) are some examples for this change. However, causes of waste issue can be classified into two main groups; Social reasons, and high production of non-degradable products such as plastic, tires, and waste oil.

2.4.1 High production of non-degradable products

The industrial revolution was the milestone in the history of waste generation (Wilson, 2007). This revolution has resulted in producing heaps of non-degradable products such as different types of plastic, tires, rubber, and waste oil. A single use products such as packaging and catering plastic has maximized the issue. This led to increase in waste flux and then the total volume of wastes generated. The wide variety in waste composition has deepened the waste issue significantly (Amasuomo & Baird, 2016).

2.4.2 Social issues (population density, demographic, convenience and motivation)

Industrial revolution and wars led to a significant demographic changes. Migration from rural areas to towns and cities to seek wellbeing as well as huge migration from country to another to seek asylum from wars has led to more urban spread. Sudden urbanization changes the population density and lead to population explosion in hosting cities or countries and then a surge in waste volume generated (Amasuomo & Baird, 2016). For instance, 20% of total solid waste volume in Jordan being generated by Syrian refugees (European Commission Annex, 2018).

The poor education system results in poor behaviour in regard of waste management. The large population in cities with high level of non-educated people give rise to indiscriminate littering as well as open dumps. According to Walsh (2017), "One of the surest signs that you're in a developing country is the trash beneath your feet". Developing countries suffers from poor education system and low levels of wellbeing.

Economic development also leads to more wellbeing and high rates of income. This results in more waste production. Developed and high-income countries combined are generating over one-third (34%) of the world's waste although they only account for 16% of the world's population (The World Bank Report, 2018).

2.5 Current solutions

2.5.1 Social and political options

Current waste management development stands on three main balanced pillars; environmental, economic, and social (McDougall et al., 2008). These pillars rely on society awareness and governmental legislations; both strategic and end-of- pipe (White, Franke & Hindle, 2012). However, to achieve the best waste management, great efforts are done nationally and globally to recover solid waste. United Nation has a special department that concern about waste issues. This department has launched The United Nation Environmental Programme (UNEP) to support the implementation of integrated solid waste management

systems in several countries. Its work also focuses on the proper treatment of special wastes (electronics, agricultural biomass, plastics) in developing countries. Since 2000, the World Bank has committed over $4.7 billion to more than 340 solid waste management programs around the globe (The World Bank Report, 2018).

In Jordan, several national projects have been launched in the last two decades to raise up the social awareness about solid waste issue. Many national organisations such as Environmental society of Jordan, Green Generation Environmental Association, Jordanian Society for the Environment, and Association of Treated Water Users and Environmental Protection are working in Jordan to achieve the three Rs approach (Reduce, Reuse & Recycle). In addition to their regular public meetings with locals in urban suburbs and rural areas, they have launched regular campaigns to clean up Jordan. Their actual projects target paper, glass, plastic, metal cans, bags and different types of solid wastes.

However, all of these programs are focusing on operating the essential municipal services which requires integrated systems that are efficient, sustainable, and socially supported but don't involve deeply the technology and renewable energy sources in solid waste recovery. Implementing technology can be introduced as the fourth pillar of waste management development.

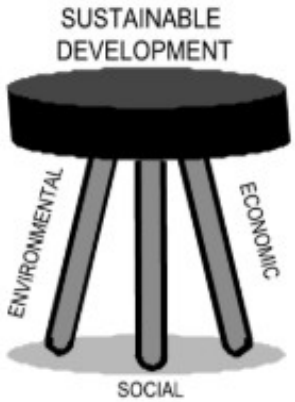

Figure 1: Pillars of balanced sustainable development. (McDougall et al., 2008)

2.5.2 Current waste disposal options

Governmental legislations and local laws are strictly control any project to dispose waste. The Reduce, Reuse, and Recycle approach is the step before waste disposal. The most commonly

applied technical processes to dispose urban waste are anaerobic digestion AD and composting (for bio-waste or biodegradable waste), landfills (due to its relatively low cost), and incineration (Morero et al., 2020). Without using high detecting levels, composting can produce some pathogens that find their way to the environment as fertilizers (EPA). Potential pollution, local laws, high investment cost and the need to huge volumes of waste supply continuously are limiting incineration implement at a large scale especially in low populated areas (Fernández-Gonzalez et al., 2017; Morero et al., 2020).

Thermochemical processes such as carbonization, pyrolysis, and gasification are also introduced as the end-life waste treatment methods or energy recovery methods from waste. These methods rely mainly on fusel fuel and electricity to produce high temperature to start up the process which minimizes their sustainability as well as reduces their economic benefit. Some projects at a labritory scale have been developed to heat up the pyrolysis feedstock by solar energy (Zadik & Israel, 2011, Rahman & Aziz, 2018; Zeaiter et al., 2018). Developing a sustainable and fundable pyrolysis unit is required.

3. Sludge

3.1 Overview

Globally, finite resources such as food, water, land space and energy are facing high demands due to the rapidly urbanization growth and increasing population. Escalating volume of sewage sludge gives clear and direct indication about the increasing waste globally and its overlooked consequence. On other hand, environmental challenges such as pollution, global warming, and waste management issues have been also intensified as a result of that. In the last two decades, the global trend has been toward sustainable strategies and policies. Sludge processing technologies for energy production and waste management such as anaerobic digestion (AD), and composting, or final disposal treatment such as incineration and landfills have been popular currently due to their relatively low investment cost (Hoornweg & Bhada-Tata, 2012). However, they have high potential risk on the environment and human health. Sustainable waste-to-energy techniques such as solar pyrolysis and gasification can be introduced as a reasonable and valuable solution.

3.1.1 Overview of the global volume of sludge production

Sludge production increases continuously due to the rapid increasing in population. Urbanization, economic and population growth have led to deepens sludge issue. Huge volume of sludge that produced daily is a prominent global concern. Sewage sludge production is estimated at the rate of 0.1 to 30.8 (kg/p.e/year) (Peccia & Westerhoff, 2015; Yang, Zhang & Wang, 2015; Kelessidis & Stasinakis, 2012). According to Spinosa (2007), global generates annually more than twenty million tonnes of dry matter. This volume increases rapidly due to continue growing in population, urbanisation, and industrialisation. For instance, Europe alone produced approximately 8.2 million tons of dry solids (DS) in 2003 (Sanin et al. 2011). Later in 2010, European Commission estimated in its report that the annual production of sludge has increased to be 11.5 to 12 million tons of DS (Peeters, Dewil & Smets, 2014), whereas this number is estimated to jump up to 13.0 million tons of DS in 2020 (Milieu

Ltd., 2008). In the same vein, the United States produced 8 million tons of DS in 2010 (Peeters, Dewil & Smets, 2014) and about 49 trillion litres of sludge in 2017 (Seiple, Coleman & Skaggs, 2017) while the annual production of sludge has been estimated at 20 million tons of DS in China for the same year 2017 (Syed-Hassan et al., 2017; Hu et al., 2016; Han et al., 2015; Li et al., 2015) and more increase has been projected in the future (Seiple, Coleman & Skaggs, 2017). Sludge production and treatment in turn is one of main global sources of methane emissions which plays a key role in global warming as green gas (Meegoda et al., 2018). For instance, wastewater treatment in the U.S. in 2015 had constituted the seventh largest sources of this gas (Figure 2) and collectively, wastewater treatment, animal waste treatment, and landfills had produced almost 45% of methane gas as a CO2 equivalent (EPA, 2018).

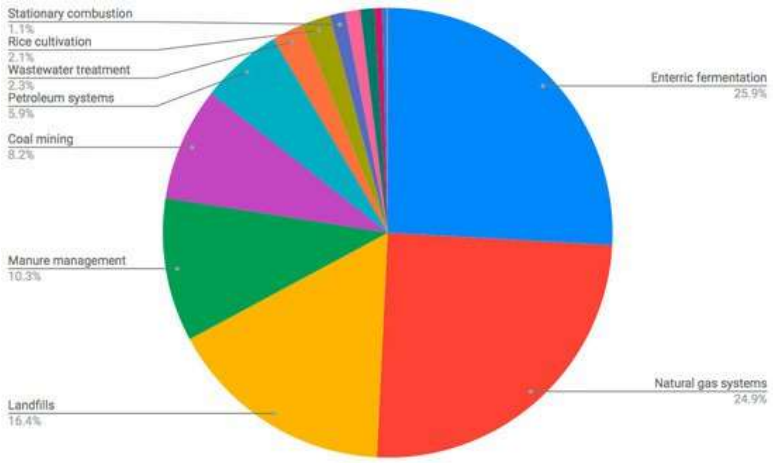

Figure 2: The sources of methane emissions in US in 2015 by percentage (EPA, 2018).

Jordan, in turn, despite approximately 85% of Jordanians are now served by wastewater pipe network, there are 18 wastewater treatment plants. The annual production of these facilities is about 300000 m^3 of liquid sludge and 15,000 m^3 of dewatered sludge (Suleiman et al., 2010). Solar drying beds are the common used method in these plants for thickening of sludge or to produce dry sludge (bio-solids). Most of this dry sludge in turn is either hauled off at nearby landfills or stored on-site. The annual cost of hauling dry sludge in Jordan (transportation cost) is more than one million US dollars.

The regulations of sludge disposal in Jordan have been changed. The current regulations aim to invest any potential opportunity to create beneficial use of the sludge (Suleiman et al., 2010). Thus, the As-Samra plant has established in 2003 as the largest plant in Jordan to serve

more than 3 million people. The hydraulic influent flow rate of As-Samra plant is 364,000 m^3 per day (SUEZ - As Samra, 2014). Mesophilic anaerobic digestion is used to treat the sludge. Sludge is treated to about 20 days to generate biogas which is used for energy production (electricity) as well as to produce Class B liquid bio-solids (USEPA Rule 503 requirements, 1993). The total solid content of liquid bio-solid is about 3% which is dried into solar beds up to 90% solid content before landfill disposal (Suleiman et al., 2010).

As-Samra plant is the first wastewater treatment plant in the world in term of energy efficiency. It is almost fully energy sufficient. It generates 230,000 kWh of green energy per day and save 300,000 tons of CO_2 emissions per year (SUEZ - As Samra, 2014). However, currently, there is no plan in Jordan to reuse or to get more benefit from dry sludge. In As-Samra plant and all the other plants, most volume of generated dry sludge is sent to landfills (Suleiman et al., 2010).

3.1.2 Treatment process and components of sludge

Sludge is a part of municipal solid waste that is produced as a result of human nature. Sewage sludge is generated from wastewater treatment plants or facilities as liquid, semi-solid or solid waste. The water content of sludge can reach 98% when it arrive treatment plants which requires further chemical, mechanical and thermal treatment to get it in dried solid phase with moister content less than 10 wt%. Briefly, sludge is produced through many stages. The preliminary treatment process starts when wastewater arrives to wastewater treatment facilities by screening. This followed by using initial straining to remove large particles such as stones, grits, sand, etc. Wastewater is moved then to sedimentation tanks. In these tanks sludge settles down due to gravitational force. Gravity takes a place to form slurry sludge which becomes easy to be removed from the bottom of sedimentation tanks (Syed-Hassan et al., 2017; Harrison et al., 2006). Sedimentation marks the point of elementary sludge generation which is followed by coagulation and flocculation for more settlement or flotation and then filtration (Daud et al., 2015). In most waste water plants, sludge goes after that through aerobic and anaerobic digestion processes for more treatment (Liu & Wang, 2017; Lofrano & Brown, 2010). Produced sludge is known by its physical properties as high ratio of liquid to solid matter. Concentration of solid particles in treated sludge ranges from

10 to 25 wt% from <3 wt% in the original wastewater (Syed-Hassan et al., 2017; Seiple, Coleman & Skaggs, 2017; Magdziarz, Dalai, & Koziński, 2016; Cieślik, Namieśnik & Konieczka, 2015). Components of sludge and its solid-liquid ratio is affected also by the source of wastewater itself such as domestic, industrial or commercial processes (Oladejo et al., 2019). Sludge as a solid phase is an in-homogenous mix of carbohydrates, proteins, oils, fats, range of living and dead micro-organisms and inorganic matters. This mixture results in a putrid matter which is volatile, unstable, and consists of many toxic elements (Cieślik, Namieśnik & Konieczka, 2015).

Calorific value of sludge depends on its organic contents. They, in turn, depend significantly on sludge's properties. Properties of sludge are highly variable and influenced by its origin (domestic, industrial, medicine, cosmetics and textile materials, etc.), seasonal variations, environmental requirements, treatment system of wastewater, and its production process such as drying method (Magdziarz, Dalai, & Koziński, 2016; Mulchandani & Westerhoff, 2016). However, in addition to water content, constituents of sludge can be categorized as following (Meegoda et al., 2018; Roubík et al., 2018; Syed-Hassan et al., 2017; Tsai, 2012):

1. Toxic inorganic compounds which are highly concentrated in sludge more than other solid fuels. These compounds mostly come from biological, physiochemical processes and corrosion in pipelines. For instance, heavy metals which are mostly pollutants such as arsenic, lead, mercury, cadmium, silver, copper, nickel, cobalt, zinc, and chromium.

2. Toxic organic compounds like Polycyclic Aromatic Hydrocarbons, and dioxins which are also pollutants.

3. Non-toxic inorganic compounds such as compounds that contain silicon, calcium, iron, and aluminium.

4. Non-toxic organic compounds which descend mostly from plant origin. They have highly volatile content and form about 48% of the dry solid. Their heating value ranges from 11.10 MJ/Kg to 22.10 MJ/Kg which forms about 60% of the total energy content in wastewater.

5. Nitrogen and phosphorus compounds which come from sugars, proteins, peptides, and fatty acids.

6. Living and dead micro-organisms which are biological pollutants and pathogens.

3.1.3 Present methods of sludge disposal

From a long time, sea dumping has been the preferable choice for sludge disposal particularly in developing countries or may be continents like Asia and Africa due to the high cost of appropriate disposal and treatment (Syed-Hassan et al., 2017; Mills et al., 2014). In China for example, water bodies currently improperly receive approximately 85% of its produced sludge as a last station in sludge' lifecycle (Syed-Hassan et al., 2017). In developed countries which in turn have been stricter and have banned sea dumping to offer other disposal alternatives such as landfilling, incineration, composting, and reclamation of land. Sludge constituents such as heavy metals, phosphate, pathogens, and organic pollutants rise high concerns from health and environmental perspective especially due to its predominant utilization as a fertilizer in agricultural applications as a recovery method (Ding, Chang, & Liu, 2017; Włodarczyk-Makuła, 2016; Chan & Wang, 2016; Xu, Chen & Hong, 2014; Lee, Parameswaran & Rittmann, 2011). However, restrictive environmental standards are increasingly enforced (Fonts et al., 2012), therefore, these methods are also subjected to strict laws to avoid improper dumping. Due to the increase of global demand on sustainability, the requirements to process sludge in energy recovery applications such as thermal reactors including incineration (Niessen, 2010), thermochemical reactors including pyrolysis, gasification (Basu, 2018), hydrothermal liquefaction (Gollakota, Kishore & Gu, 2018), torrefaction, hydrogenation and esterification (Strezov & Evans, 2015; Elliott et al., 1991) have increased (Seiple, Coleman & Skaggs, 2017) because of their positive impact in term of reducing environmental footprint, landfill requirements as well as minimizing sludge' impact on the food supply, land, and groundwater (Cieślik, Namieśnik & Konieczka, 2015). In addition, these processes offer verity of sludge derived products such as phosphorus, raw rare metals, ash, syngas, chemicals and biofuel or organic fuels (Oladejo, et al., 2019).

Treatment and disposal methods of sludge are highly challenging because of its high content of heavy metals, toxics, and activated organics which are recognized as environmental hazards affect living being, soil and water sources (Cieślik, Namieśnik & Konieczka, 2015). Different methods can be apply for consequent treatment. Most them can be classified into three categories: physical such as heat, pressure, vibration, or microwaves; biological such as digestion or composting; and chemical such as alkalinity adjustments or oxidations. Stability

of the organic matters in the primary sludge such as odour elimination, pathogens destruction, and decrease of volatile contents is the main goal of these methods which in turn maximizes nutrient recovery, improves effluent's quality, and/or facilitates disposal process by making it safer. Product of stabilisation process may undergo further biological treatment to produce secondary sludge (Syed-Hassan et al., 2017; Mulchandani & Westerhoff, 2016; Chan & Wang, 2016; Vaxelaire & Cézac, 2004). For example, anaerobic digestion is used as a technique for energy recovery due to its capability to produce biogas from the anaerobic digester and to produce secondary sludge that can be used as a fertilizer (Winkler et al., 2013). Thermal treatment techniques are other example for stabilisation methods. Utilizing these techniques requires drying as one of initial pre-treatments (Chen, Lock Yue, & Mujumdar, 2002; Vaxelaire, et al., 2000; Grüter, et al., 1990) and produces normally char and ash as solid output rather than secondary sludge (Oladejo, et al., 2019).

3.2 Potential energy recovery from sludge

Despite properties of the sludge are variable physically and chemically as a result of the variety of sewage types (Spinosa, 2011; Fytili & Zabaniotou, 2008), energy content of dried sludge varies between 11.10 to 22.10 MJ/Kg due to its high volatile organic content that ranges from 21% to 48%. However, stabilization or biological digestion (aerobic and anaerobic) also affects the sludge calorific value and organic content of sludge. Raw sludge consists of 70-85% organics of DS which decreases after digestion to become 45-60% of DS. Organic content represents the combustible fraction of sludge, therefore, the high calorific value of activated sludge ranges approximately between 15-22 MJ/kg of DS due to the mineral content of sludge that does not degrade by thermal processes. The mineral content of sludge ranges between 33.3%-55% of sludge dry mass. In opposite, the high calorific value of dried digested sludge is lower than activated or raw sludge. It usually ranges between 11-16 MJ/kg of DS (Flaga, 2007).

This energy content indicates that dried sludge may be the best biomass for thermochemical treatment because of its high calorific values (Syed-Hassan et al., 2017; Tsai, 2012). Heating value of sludge and the necessity to efficiently eliminate its organic content before disposal

are the core of its suitability as a solid fuel. Consequently, using dried sludge for energy recovery may be the most attractive techniques to reduce waste volume as well as recover heavy metals and/or nutrients (Oladejo, et al., 2019).

Each sludge has two different values Low calorific value LCV and high calorific value HCV. These two values of the same sludge are used as energy parameters of sludge that used as a fuel, therefore, combustible fraction or the moisture content should be defined in sludge dry solids. HCV which is the most reliable and precise parameter of energy content of sludge indicates to the energy from water-free sludge or completely dry solids (DS) whilst LCV indicates to the energy from wet sludge solid and its real value can be calculated by the following equations (Flaga, 2007):

$$W_d = W_g \times (1 - w) - r \times (w + 9H)$$

[MJ/kg of wet sludge]

$$\boldsymbol{W_d = W_{g,s.m.bp} \times (1 - w - p) - r \times (w + 9H)}$$

[MJ/kg of wet sludge]

Where

$\boldsymbol{W_d}$ = *low calorific value from wet sludge.*

$\boldsymbol{W_g}$ = *high calorific value of sludge [MJ/kg of water-free sludge]*

$\boldsymbol{W_{g,s.m.bp}}$ = *high calorific value of ash- and water-free sludge*

$\boldsymbol{r}$ = enthalpy of water evaporation at the ambient temperature.

$\boldsymbol{H}$ = weight of fraction of combustible hydrogen in combustible mass of wet sludge.

If weight of combustible hydrogen is not specified, then empirical formulas for different types of sludge that assume typical values of H can be used (Flaga, 2007):

For raw sludge:

$$\boldsymbol{W_d = 14,235 - 1,683 \times w}$$

[MJ/kg of wet sludge]

For digested sludge:

$$W_d = 10,467 - 1,306 \times w$$

[MJ/kg of wet sludge]

It is important to notice that high calorific value of sludge is not equivalent to the quantity of practically heat used. Although Tanner's triangle has been designed for communal or municipal solid waste combustion (Figure 3), it can be used to estimate the possibility of autothermic combustion of sludge without supplementary fuel (Flaga, 2007). The triangle demonstrates mass shares of ash or mineral content, water or moisture content, and combustible or volatiles content corresponding with coordinates. The total summation of mass shares must count 100% of primary sludge mass. The limits of autothermic combustion of sludge are presented in the darkened area.

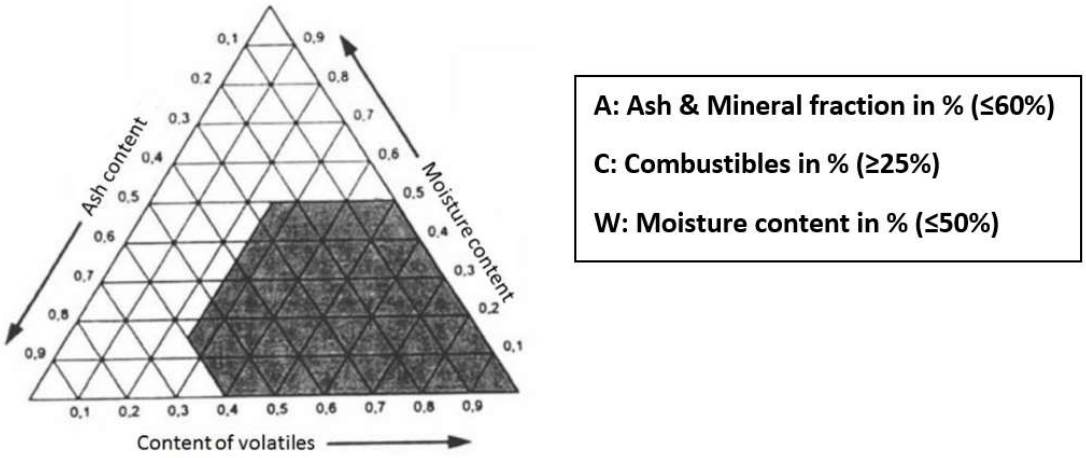

Figure 3: Tanner's triangle for possibility of autothermic combustion of sludge without supplementary fuel. (Flaga, 2007 as cited in Hoffman & Marmsjö, 2014)

3.3 Properties of sludge: Challenges and benefits

Differences in the properties of sludge present many technical challenges such as reducing the moisture content, nitrogen and heavy metal content which influence the energy recovery reactions and process. These factors namely moisture content is a prominent challenge particularly for thermochemical processes and must to be considered for any successful

deployment of sewage sludge to energy recovery (Oladejo, et al., 2019). Drying sludge has been addressed by several research and studies to offer practical and sustainable solutions (Vaxelaire & Cézac, 2004). However, highly distinctive and complex compositions of sludge (Chan & Wang, 2016) as well as its behaviour during drying process such as sticky phase (Tunçal & Uslu, 2014; Peeters, Dewil & Smets, 2014, Bennamoun, Arlabosse & Léonard, 2013) and its degradation behaviour during thermal processing (Lu et al., 2012; Inguanzo et al., 2002) have led to examine the effectiveness of mixing sludge with other solid fuels such as biomass like rice husk or sawdust (Ding & Jiang, 2013), biomass ash, pyrolysis ash, and polyelectrolyte (Wójcik & Stachowicz, 2019) dried sludge (Peeters, Dewil & Smets, 2014; Flaga, 2005) and polyaluminiumchloride (PACl) (Peeters et al., 2013) to improve its properties, performance during processing and hence pyrolysis yield distribution and properties.

Previous proximate and ultimate analyses of sludge indicate that sludge, in compression to other biomass, has higher volatile content, lower fixed carbon (Syed-Hassan et al., 2017; Mulchandani & Westerhoff, 2016), higher mass content which is mostly calcium, sodium, magnesium, aluminium, titanium, iron, silicon, and phosphorus (Chan & Wang, 2016), higher hydrogen, higher nitrogen because of its peptides and protein content, higher oxygen and sulphur content, while its carbon contents are still comparable to lignite and biomass (Chan & Wang, 2016; Vaxelaire & Cézac, 2004). Therefore, sludge can be one of most valuable renewable feedstock for thermochemical processes such as pyrolysis.

4. Pyrolysis

Pyrolysis has been given high attention as a process that has zero-waste energy recovery and its emissions namely gas require limited clean-up facilities (Oladejo, et al., 2019). Pyrolysis can be considered as a sequence of development in waste and sludge management technologies because of the restrictions on sea dumping, land disposal, agricultural reuse (Fonts et al., 2012). Furthermore, microorganism activities in anaerobic treatment of sludge cause potential emissions of greenhouse gases (Wang et al., 2013) and incineration generate huge amount flue gas which needs to be treated with extra cost (Gradus et al., 2017; Kishimoto et al., 2001). Therefore, thermochemical treatment technologies might be a current suitable alternative economically and environmentally (Chan & Wang, 2016).

Pyrolysis is one of thermochemical energy recovery methods in addition to others such as combustion or incineration, gasification, and hydrothermal liquefaction which are characterised by their short reaction time (Oladejo, et al., 2019). They are also characterized by their high energy consumption (Jin et al., 2004) which results from the necessity to reduce the moisture content of sludge by drying or dewatering sludge as an important pre-processing requirement (Grüter et al., 1990) and for reactors. Despite incineration has been the predominant energy recovery method (Oladejo, et al., 2019) right now, pyrolysis conversion process has the capability to convert sludge into valuable product (Czernik & Bridgwater, 2004) instead of only heat. Moreover, pyrolysis could recover the resources of hydrogen and carbon from the residues, reduce the waste' volume, degrade the toxic organic compounds, fix or minimise present of heavy metals in residues (Nordin, 2015; Nzihou & Stanmore, 2013) and hence reducing landfilling and sludge disposal cost (Marrero et al., 2004). From environmental perspective, pyrolysis also could reduce the furans formation as well as the formation of dioxins, NOx, SOx, and greenhouse gas emissions (Yi, Jang & An, 2018; Arena, 2012).

Pyrolysis of sludge can be defined as a controlled rapid thermal degradation or decomposition of 80% or more of sludge organic matter or feedstock at moderate reacting temperatures (range from 350◦C to 600 ◦C) (Basu, 2018) to high reacting temperatures (up to 900 ◦C) (Ruiz et al., 2013; Zhang, Xu & Champagne, 2010) in inert (non-reactive) atmospheres with completely absence of oxygen which is considered as one of the main benefits of

pyrolysis process in comparison to others such as anaerobic (Ruffino et al., 2016). The complete absence of oxidation agent can be the main difference between gasification and pyrolysis which is referred to sometimes as incomplete gasification (Kirubakaran et al., 2009). Depends on sludge properties and the nature of wanted yield (oil, gas, char), reaction time ranges from seconds to a min. In addition to reaction time which is defined as residence time of sludge in the reactor, the product distribution and hence energy content of products are also affected by heating rate and operating temperature (Basu, 2018). Depending on these variables, pyrolysis produces biochar, bio-oil, and two types of gases; primary and secondary gases. Other aqueous products of sludge pyrolysis might appear such as tar, acetic acid, water, acetone and methanol (Basu, 2013).

Primary gaseous products of pyrolysis are two types: non-condensable such as light hydrocarbons, CO, CO_2, H_2, CH_4, C_2H_4 and C_2H_6 (Chan & Wang, 2016; Valo, Carrere & Delgenes, 2004) which are used predominantly for heat and electricity generation via combustion (Bianchini et al., 2015). Second type is heavy molecules gases which are condensed by cooling and added to liquid yield. Furthermore, condensable gases can be cracked to produce additional non-condensable gases known as secondary gases. Primary gas has LHV 11 MJ/Nm3 while LHV of secondary gas is 20 MJ/Nm3 (Basu, 2013).

Biochar forms about 10-20 wt% of biomass. It is a mixture of ash (from minerals) and carbonaceous residue. Biochar contains oxygen, hydrogen and about 85% of its components is carbon. Its LHV is 32 MJ/Kg which is higher than LHV of biomass (Basu, 2013). Biochar can be used as a catalyst, in adsorption application, and as a solid fuel to generate heat and then electricity via combustion.

Bio-oil in turn has a colour differs between black to dark brown. Bio-oil is a tarry liquid consists of organic compounds and water. Water forms around 20-30 wt% of its total components (Lehto et al. 2014). Organic compounds consist of alcohols, acids, aldehydes, alkene, aromatics, esters, furans, guaiacols, ketones, phenols, syringols, sugars, and miscellaneous oxygenates and nitrogen compounds (Ringer, Putsche & Scahill 2006). In other words, bio-oil is a complex mixture of homologous phenolic compounds namely water, complex hydrocarbons and huge amount of oxygen. However, the lower heating value (LHV) of bio-oil ranges between 13 to 18 MJ/Kg and its molecular weight exceeds 500 Daltons (Basu,

2013). Bio-oil is highly polar and non-immiscible with petroleum-based hydrocarbons (Campuzano, Brown & Martínez, 2019).

Bio-oil can be subjected for further treatment to produce H_2 and CO which called syngas or synthesis gas for chemical production or can be upgraded to be used as a liquid fuel for diesel engines or for combustion. Upgrading process works to improve the physical-chemical properties of bio-oil such as its acidity, viscosity, and heating value as well as to decrease its high oxygen content to be used as liquid fuel. Current bio-oil upgrading techniques are catalytic cracking, hydroprocessing, and distillation (fractional and reactive) (Kabir & Hameed, 2017; Gollakota et al. 2016; Martínez et al. 2014).

However, due to its reasonable caloric value and high storage availability, liquid yield is highly preferable (Basu, 2018) and pyrolysis is mostly applied to maximize this yield (Oladejo, et al., 2019). According to Fonts et al., (2012), pyrolysis can produce around 50 wt% dry and ash free (daf) liquid yield. Therefore, low residence time of feedstock in the reactor at high temperature promotes liquid production while high residence time of feedstock at the same temperature promotes gas production (Campuzano, Brown & Martínez, 2019). On the other hand, the yield of char decreases with increase in temperature (Balat et al., 2009). The energy density of the liquid produced can be 5 times higher than the original feedstock. Therefore, fast pyrolysis is more attractive than other pyrolysis types as well as other treatment methods such as combustion and gasification (Williams, 2013).

Figure (4) demonstrates the main stages of the sludge pyrolysis process and main parts of sludge pyrolysis unit. Pyrolysis unit mainly consists of three subunits: preparing or pre-processing unit, reactor, and condenser. Pyrolysis process starts from drying process to reduce the moisture content. The moisture content of input sludge fed into pyrolysis reactor plays important role in pyrolysis success, cost and quality of output yield (Xiong et al., 2013). For efficient pyrolysis, moisture tolerance of pyrolysis feedstock should be <10% wt, therefore, drying process is highly required as a pre-process of pyrolysis which raise up pyrolysis energy consumption and hence pyrolysis total cost (Oladejo et al., 2019). Three sources are mainly used in present pyrolysis units to provide heat energy to initiate the reaction: electricity, thermal sources such as gas and fossil fuel, and solar energy via solar concentrators or harvesters (Joardder et al., 2017; Sharuddin et al., 2016). Despite its low efficiency to provide a self-sustainability pyrolysis, the partial combustion of bio-oil or biogas which are the

pyrolysis outputs can be utilize also as a source or assisted source of heat energy in pyrolysis units (Rollinson & Oladejo, 2019).

Heat energy is applied on pyrolysis reactor to heat it to pyrolysis temperature and hence initiate the reaction. Reaction or thermal decomposition of sludge is complex and occurs in the reactor in various stages due to the sludge heterogeneous nature. First stage is decomposition of decomposable organic matters which occurs at ⩽200 ◦C. Second stage is decomposition of lipids and dead organisms when temperature increased to (200◦C –300◦C). At temperatures ≥300◦C and ⩽700 ◦C, decomposition of cellulosic constituents, organic polymers, and proteins takes place as third stage (Alvarez et al., 2015; Font et al., 2001). Typically, because of high heating rates in reactors, these three stages run simultaneously at temperatures <600 ◦C as a primary reaction. This reaction produces light gases, heavy tars, and chars. At temperatures almost 600 ◦C, secondary reactions are motivated to maximize the liquid product. Secondary reactions produce secondary gases and tar via further pyrolysis of unstable primary products. Further progress in pyrolysis reaction may polymerize some tar to give coke (Oladejo et al., 2019).

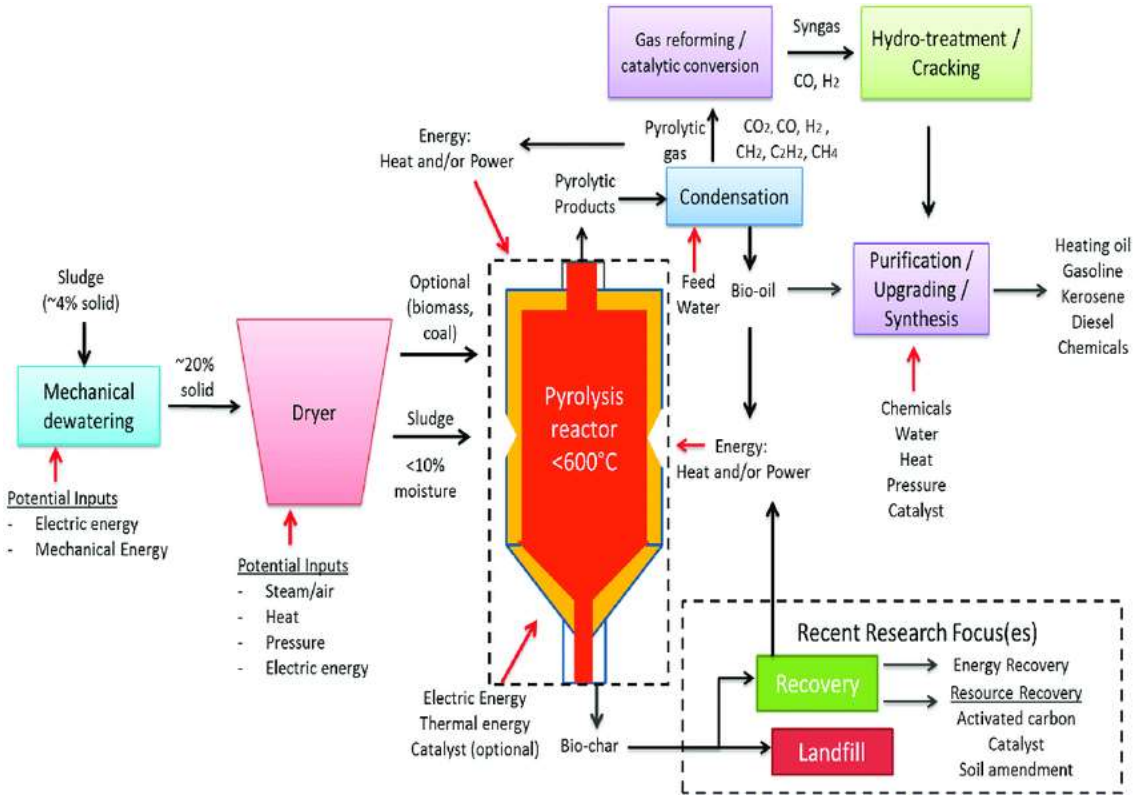

Figure 4: Schematic Diagram of the Pyrolysis of Sludge. (Oladejo, et al., 2019)

Different factors affect the yield quality and distribution (solid, liquid, and gas) which also complicate pyrolysis as energy recovery method. These factors have been addressed by numerous studies to improve bio-oil production which is the main goal of pyrolysis process. They depend mainly on characteristics of feedstock of pyrolysis unit, operating conditions and reactor type. Feedstock characteristics such as particle size and its physical nature such as digested, primary, wet sludge, dried, and blends as well as its chemical compositions. While operating conditions such as pyrolysis reaction temperature, residence time in the reactor, turbulence, pressure, catalyst, feed rate, power, and type and rate of fluidizing gas (Basu, 2018; Syed-Hassan et al., 2017). Although fluidised bed reactor is mostly predominant in present pyrolysis units (Oladejo et al., 2019; Park, Kang & Kim, 2008), other types are also used such as batch and semi-batch reactors (Kim & Parker, 2008), fixed bed reactors (Chen et al., 2018), conical spouted bed reactor (CSBR) (Alvarez et al., 2016), microwave and microwave-assisted technology (Zhou et al., 2018; Ma et al., 2018; Lin et al., 2017; Huang et al., 2015; Xie et al., 2014), screw reactors (Morgano, et al., 2018; Gao et al., 2017) and continuous and semi-continuous (Pedroza et al., 2014; Pokorna et al., 2009; Fonts et al., 2008), horizontal furnace (Gao et al., 2014). In addition, transport phenomena, phase transitions, and intricate reaction chemistry are considered further complications for this technology (Oladejo et al., 2019).

Biochar has a wide range of applications depending on its energy content, nutrients content, and heavy metals contents such as solid fuel for direct combustion applications, agricultural applications, and catalyst applications due to its high adsorptive capability, respectively or as a value-added resource (Oladejo et al., 2019). Moreover, ash produced after direct combustion of biochar can be used for the construction and building applications as well as road surfacing products (Chen, Lock Yue, & Mujumdar, 2002). Gaseous yield of pyrolysis or biogas is condensed to produce bio-oil. It also can be subjected to further treatment to upgrade it to synthesis gas or can be burnt directly as fuel. Synthesis gas can be either processed for chemical synthesis or liquid fuel.

Liquid fuel or bio-oil is heterogeneous liquid and typically separates into up to three phases such as organic phases. Organic phases have a reasonable gross heating values as high as those of petroleum-based fuels. The heating value of bio-oil reaches to ~33 MJ/kg (Xu & Wu, 2015; Fonts et al., 2012). In addition to the flexibility of storage and transportation, bio-oil is

flexible in utilization as well. It can be either refined to be used similarly as petroleum liquid fuels, used for electricity generation or heat as combustion fuel, or reformed by further reactions to produce syngas for chemicals production (Zafar, 2018). However, the moisture content of sludge' bio-oil is mostly over 23% wt. This percentage is high relatively and reduces flame temperature and energy density and hence the fuel quality. Moreover, when sludge' bio-oil used in engines, the high moisture content causes deterrent combustion properties (Alvarez et al., 2016; Lehto et al., 2014). Commercially, bio-oil that is generated from sludge is used widely for chemical production rather than fuel oil due to its high O-containing compounds which form around 33%. These compounds significantly limit the thermal output of sludge' bio-oil and cause its intrinsic instability (Alvarez et al., 2016). Pedroza et al., (2014) and others found that the optimal pyrolysis temperature to maximize the liquid yield ranges between 450 ◦C to 550 ◦C such that higher temperatures cause thermal cracking for tar and hence increase the gas yield while lower temperatures wouldn't be adequate for optimum breakdown of char (Shen & Zhang, 2003; Alvarez et al., 2002). Therefore, reducing the residence time can be adopted to prevent further reaction (Park et al., 2010; Shen & Zhang, 2003). On the other hand, impact of moisture in wet sludge feedstock on output oil quality, increasing of non-condensable gases, and operating conditions of the reactor due to vapour-rich atmosphere challenges conventional pyrolysis technologies (Dominguez, Menéndez & Pis, 2006). On the way to find suitable technology to overcome that, Xie et al. (2014) and others investigated the efficiency of using microwaves technology as a pyrolysis reactor which interestingly resulted in limited influence on oil production and quality regardless of catalysts presence (Lin et al., 2017; Jin et al., 2016; Gao et al., 2014).

Different factors had been examined to optimize bio-oil production such as reactor types, operating conditions, and sludge nature as fuel. The maximum production of bio-oil from sludge was 57.5 wt% as reported by Pokorna et al. (2009). He achieved that in laboratory by using semi-continuous reactor and conducting flash pyrolysis (very fast or very low residence time) at 500 ◦C. He used samples of dried activated and digested sludge with moisture content less than 10 wt%. This resulted in quality of output bio-oil including low water content (10.3% to 17%) and moderate heating value (23.9 MJ/kg to 29.0 MJ/kg) while the output char has (5.2 to 10.6 MJ/kg) heating value. Alvarez et al. (2016) conducted flash pyrolysis (<100 ms residence time) in a conical spouted bed reactor at temperatures from 450 ◦C to 600 ◦C. He

achieved up to 48.5 wt% liquid product at 500◦C with quality more suitable for chemicals. In term of catalysts, Zhou et al. (2018) and others reported that catalysts and acid pre-treatment improve the quality of bio-oil and other pyrolytic products but they also have negative to negligible influence on the liquid yield (Xie et al., 2014; Ischia et al., 2011; Kim & Parker, 2008). Quantity of liquid yield is also influenced by sludge inorganic content. High inorganic compounds in sludge reduce bio-oil production due to presence of some metal oxides such as ZnO and CaO which impede decomposition of organic matters and promote secondary reactions (Longo et al., 2015).

Similarly, although low temperature pyrolysis minimize the oil production, it can be used to retain heavy metals in biochar which means eliminating transfer heavy metals to bio-oil and biogas and hence minimizing risk of potential toxic emissions. Meanwhile, decrease of bioavailable heavy metals results in increase of residual and oxidative fractions which lessen of ecological risks of biochar usage or disposal (Lee, Kim & Yoo, 2018; Jin et al., 2016).

To mitigate the impact of input wet sludge on pyrolysis process and output oil quality, microwave technology has been examined as a technology capable to cope with high moisture content of input wet sludge (Jin et al., 2016; Gao et al., 2014; Xie et al., 2014). Studies indicate that maximum heating value of bio-oil can be obtained at temperatures range from 550◦C to 600◦C. Lin et al., 2017 used wet sludge with >84 wt% water content to feed a 900 W microwave reactor at 600 ◦C. After 30 min of residence time, he obtained 20% bio-oil yield to be the maximum liquid yield has been reported by microwave right now (Oladejo et al., 2019). However, it can be observed that sewage sludge pyrolysis production of bio-oil ranges from 14 wt% to 57.5 wt% and optimal production of bio-oil can be achieved at temperature between 500◦C to 600 ◦C (Oladejo et al., 2019). Operating temperature influences quality of output bio-oil due to its influence on the bio-oil moisture content, aliphatic and aromatic compounds (Zhou et al., 2018; Gao et al., 2017; Xie et al., 2014). In the same concept, Zhuang et al. (2011) reported that operating temperature at <700 ◦C may result in minimal amounts of some kinds of metal such as mercury and cadmium in pyrolytic oil because of their low boiling points.

Solid yield of char and ash remains the highest among other pyrolysis products with about 50 wt% (Gao et al., 2017). Although it is not preferable yield, pyrolysis char reduces pollutant emissions to atmosphere and heavy metal emissions to landfill as well as offers wide range of

utilization methods. However, bio-char needs to further treatment before usage regardless of its usage method (Chen, Chen & Hong, 2015).

In term of energy source for heating, solar pyrolysis is a promising candidate where using solar concentrator was approved to be capable to raise pyrolysis reactor temperature to 500-600◦C which is the optimum to obtain the maximum liquid yield (Weldekidan, Strezov & Town, 2018; Joardder et al., 2017).

4.1 Pyrolysis Types

Pyrolysis can be classified based on many factors. Heating rate is widely used to describe the process as slow, fast or flash pyrolysis. This in turn indicates clearly to residence time and distribution of pyrolysis products. According to Basu (2013), pyrolysis is classified mainly based on heating rate, presence of pyrolysis medium and pressure, and the lodging time of gases in the reaction zone (vapour residence time).

4.1.1 Heating rate

This factor is calculated mathematically based on two times: required time to heat feedstock ($t_{heating}$), and required time for characteristic pyrolysis reaction (t_r). By using these two features, pyrolysis classified into two types slow and fast. Slow pyrolysis if $t_{heating} > t_r$ and fast pyrolysis if $t_{heating} < t_r$. In fast pyrolysis, the heating rate ranges from 1000 to 10000 ^{o}C/second with taking in account that peak temperature should not exceed 650 ^{o}C. Temperature higher than 650 ^{o}C up to 1000 ^{o}C produces mainly gas especially non-condensable gas such as CO, CO_2, H_2 and CH_4.

4.1.2 Presence of pyrolysis medium and pressure

Environment of reaction affects pyrolysis process. Pyrolysis is carried out typically in absence of medium and pressure. However, sometimes to produce specific products such as

chemicals, H_2 and H_2O are involved as non-oxidizing mediums in pyrolysis process. Using these mediums conducts two types of pyrolysis: hydrous pyrolysis in presence of water (H_2O) and hydro-pyrolysis in presence of hydrogen (H_2). Hydro-pyrolysis occurs in ambience of high pressure hydrogen to increase the gaseous yield and hydrocarbons with low molecule mass. Although the main product of hydro-pyrolysis is gas, bio-oil can be produced by reducing oxygen in reaction atmosphere. On the other hand, hydrous pyrolysis occurs in ambience of high temperature and pressured water.

4.1.3 The lodging time of gases in the reaction zone (vapour residence time)

Traditional pyrolysis is used to produce liquid as a main goal. In this process pyrolysis vapour stays in the reaction zone for seconds or milliseconds. In case the main target is char, then slow pyrolysis more likely to be used. In this case, pyrolysis vapour stays in the reaction zone minutes or more to conduct two types: torrefaction and carbonization. Although these two types require very slow heating rate, the residence time of torrefaction ranges from 10 to 60 minutes while for carbonization the residence time may extend for days.

In contrast, fast pyrolysis is divided mainly to flash and ultra-rapid based on the residence time which ranges from milliseconds up to 2 seconds. For example, the vapour in flash pyrolysis leaves the reactor within 30 to 1500 ms to produce bio-oil reaches to 70-75% of total flash pyrolysis products. Ultra-rapid pyrolysis in turn needs shorter residence time in reactor than flash pyrolysis to produce mainly gases. The peak temperature for ultra-rapid pyrolysis is 1000 ^{0}C while it is 650 ^{0}C for flash pyrolysis.

The following table shows the characteristics of pyrolysis types (Basu, 2013).

Pyrolysis Process	Residence Time	Heating Rate	Final Temperature (°C)	Products
Torrefaction	10–60 min	Very small	280	Torrefied biomass
Carbonization	Days	Very low	>400	Charcoal
Fast	<2 s	Very high	~500	Bio-oil
Flash	<1 s	High	<650	Bio-oil, chemicals, gas
Ultrarapid	<0.5 s	Very high	~1000	Chemicals, gas
Vacuum	2–30 s	Medium	400	Bio-oil
Hydropyrolysis	<10 s	High	<500	Bio-oil
Methanopyrolysis	<10 s	High	>700	Chemicals

Table 1: pyrolysis types: process conditions & major products. (Basu, 2013)

Finally, various types of reactors were experimented in sludge pyrolysis. In addition to other parameters, recent studies utilised batch reactors (e.g., cylindrical batch reactor), fluidized bed reactors (e.g., conical spouted bed reactor, fixed bed tubular furnace), continuous and semi-continuous reactors (e.g., continuous feed rotating cylinder reactor, continuous feed screw reactor), horizontal furnace reactors, horizontal tubular furnace reactor, and microwave reactors (Park, Kang & Kim, 2008, Pokorna et al., 2009, Zhuang et al., 2011, Gao et al., 2014, Chen et al., 2014, Longo et al., 2015, Chen, Chen, & Hong, 2015, Jin et al., 2016, Lin et al., 2017, Gao et al., 2017). More details about reactors of sludge pyrolysis are discussed in chapter 7.3 of this study. However, there is no literature available right now about the best type of reactors for sludge pyrolysis.

4.2 Pyrolysis reactor types

Different types of reactors are commonly used for fast pyrolysis of biomass to produce bio-oil. Every reactor is used for specific type of pyrolysis (fast, intermediate, or slow) to generate specific kind of energy (electricity, heat, carbonaceous materials, liquid yield or gaseous products) based on the feedstock characteristics. Every reactor also has its own technical and economic advantages and disadvantages. Some of pyrolysis reactors include high mass and high heat transfer rates such as fluidized bed reactors, spouted reactors, and both circulating bed (CFB) and bubbling bed (BFB) reactors. Other reactors have been used also rotating cone reactors, rotary kiln reactors, cyclonic reactors as well as the ablative process reactors. Other reactors involve melting vessels, autoclaves, plasma reactors. For vacuum pyrolysis, particular arrangements are required (Meier et al. 2013). However, following is explanation for several types of the more commonly employed reactors for pyrolysis of biomass cited from (Malkow, 2004; Mohan, Pittman & Steele, 2006; Elordi et al., 2007; Olazar et al., 2009; Fogler, 2010; Venderbosch & Prins, 2010; Bridgwater, 2012; Jahirul, et al. 2012; Abbas-Abadi, Haghighi & Yeganeh, 2013; Basu, 2013; Chen et al. 2014; Sharuddin, et al., 2016; Czajczynska, et al. 2017).

4.2.1 Batch and semi-batch reactor

This type of reactors gives high conversion by giving the reaction extended time into the reactor. Batch reactor is a closed system (Figure, 5) which means that while the reaction is being carried out, no inflow or outflow of both reactants and products. This is considered as one of its advantages. However, batch reactor requires high labour cost and its product is variable from one batch to another one. In addition, batch reactor is difficult to be used for large scale production (Fogler, 2010). In contrast, addition of reactants and removal of products during the reaction is allowed in semi-batch reactors (Sakata, Uddin & Muto, 1999). This flexibility in feeding over time gives continuous reaction and reaction selectivity. However, semi-batch is more suitable for small scale production because it has the same disadvantages of batch reactors. Despite these reactors are recommended because of their high liquid yield, they are not suitable from industrial perspective because of their low scale production (Abbas-Abadi, Haghighi & Yeganeh, 2013).

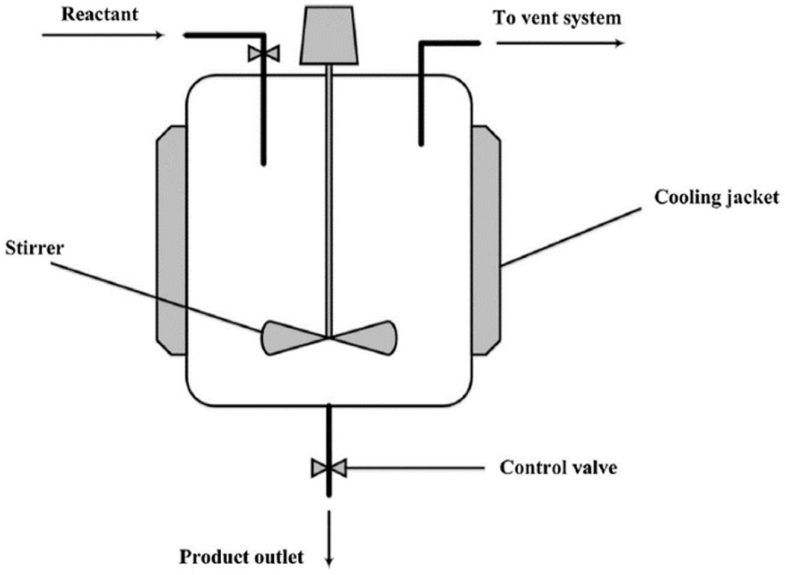

Figure 5: Batch reactor with stirrer equipment. (Sharuddin, et al., 2016)

4.2.2 Fixed and fluidized bed reactor

In this type of reactors, the catalyst is used in palletized form and packed in static bed (Figure, 6). Irregular size and shape of feeding particles are constraints of this reactor design. Besides,

catalyst' area that available for the reaction is limited, thus, it is preferable to be used as a secondary reactor (Fogler, 2010).

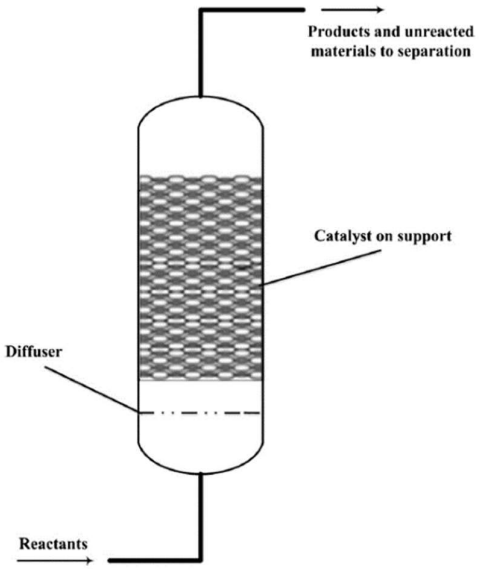

Figure 6: Fixed-bed reactor. (Sharuddin, et al., 2016)

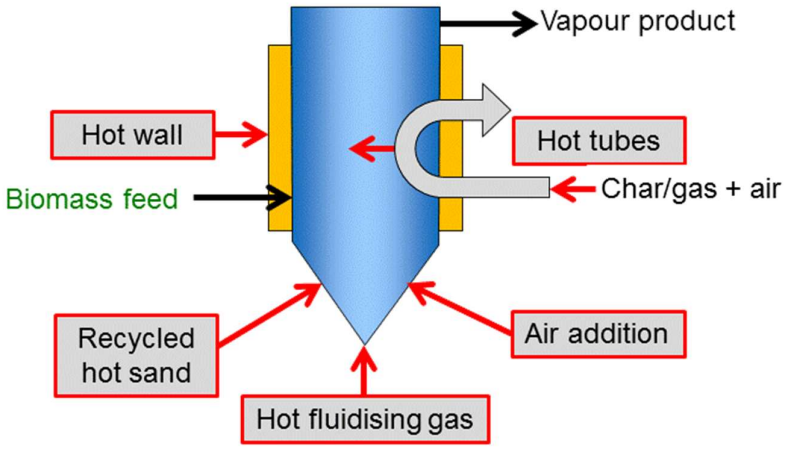

Figure 7: schematic diagram of fluidized bed reactor. (IEA bioenergy)

Fluidized bed reactor comes as a normal development for fixed bed reactor to solve some of its problems. Fluidized bed reactor has been developed where the catalyst sits over a distributer plate (Figure, 8). The primary products are divided to gas and particles which are carried in a liquid state to give best mix with catalyst and hence best use of catalyst surface area. This type is more flexible than batch reactor because there is no need for frequent charging or resuming process as well (Kaminsky & Kim, 1999). Garfoth et al. (1998) asserted

that this reactor is preferred to be used in catalytic pyrolysis rather than fixed bed reactor because the catalyst is able to be reused several times without need for discharging. In comparison to batch reactor, fluidized bed reactor is more flexible because the frequent feeing and resuming process can be avoided. However, from economic perspective, fluidized bed reactor is considered as the most suitable reactor for pyrolysis plants and large scale operations (Sharuddin, et al., 2016). In addition to its good and constant performance, its liquid yield is typically 70-75%wt.

The heating rate of fluid bed reactor is usually the rate limiting step. Therefore, it requires small size particles of biomass less than 3mm to achieve high biomass heating rates (International Energy Agency (IEA) Bioenergy, 2017).

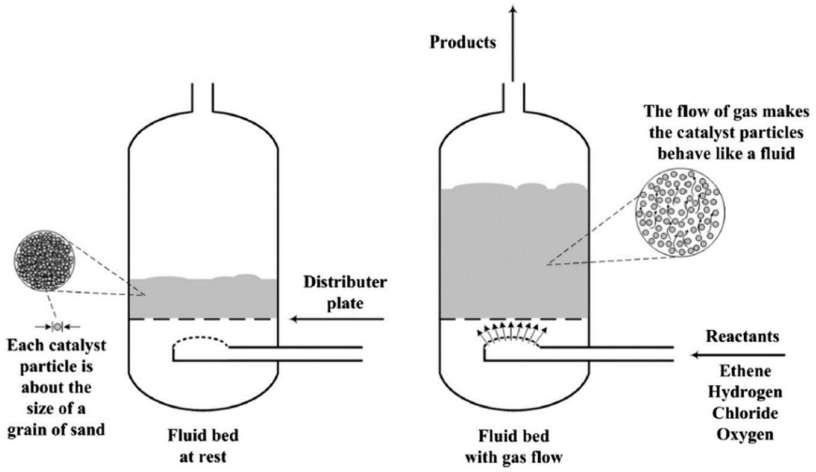

Figure 8: working process of fluidized bed reactor. (Sharuddin, et al., 2016)

4.2.3 Conical spouted bed reactor (CSBR)

This reactor is known by its ability to handle different particle sizes and densities. It is also able to provide good mixing process (Fogler, 2010). In opposite, CSBR relatively has low bed segregation and lower attrition than bubbling fluidized bed (Olazar et al., 2009). Moreover, it has high rate of heat transfer between phases and it has also minor defluidization during sticky solids handling. All of these disadvantages besides its complicated design make it unfavourable reactor because it requires several pumps in the system and hence high capital and operational cost (Figure, 9) (Elordi et al., 2007).

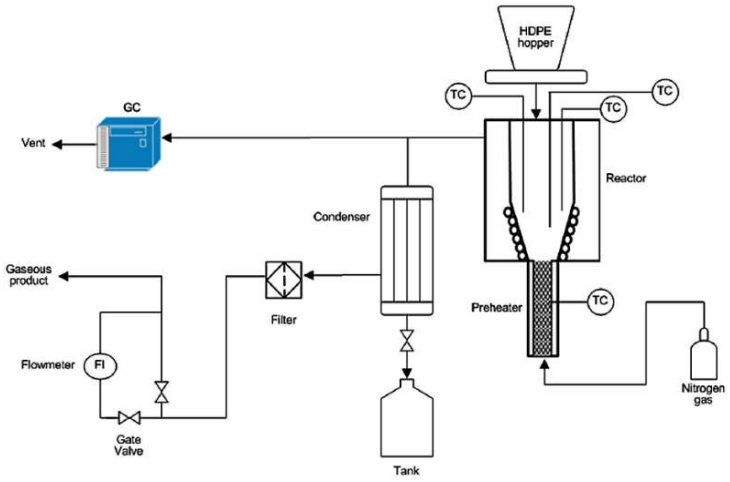

Figure 9: Conical Spouted Bed Reactor (CSBR). (Sharuddin, et al., 2016)

4.2.4 Auger reactor (screw reactor)

Auger reactor is versatile and can be used to transform a wide range of feedstock. It is attractive technologies because of its relatively simple design (a screw into a tube to convey feedstock with/out solid heat carriers down along of a tube (Figure 10) with better strengths for all types of pyrolysis specifically fast pyrolysis. It is able to overcome some of conveying heat problems for pyrolyzing biomass and solid wastes. Its design enhances heat transfer and particle mixing which are key factors to achieve successful pyrolysis with high liquid yield. Therefore, it is used at industrial scale in several plants able to process up to 700 kg/h (Campuzano, Brown & Martínez, 2019). However, although ablative and rotating cone reactors are more compact and relatively consume small amounts of inert gases, commercially, auger reactor has more market attractiveness in comparison to other reactors according to The Biomass Pyrolysis Network (PyNe) (Figure 11).

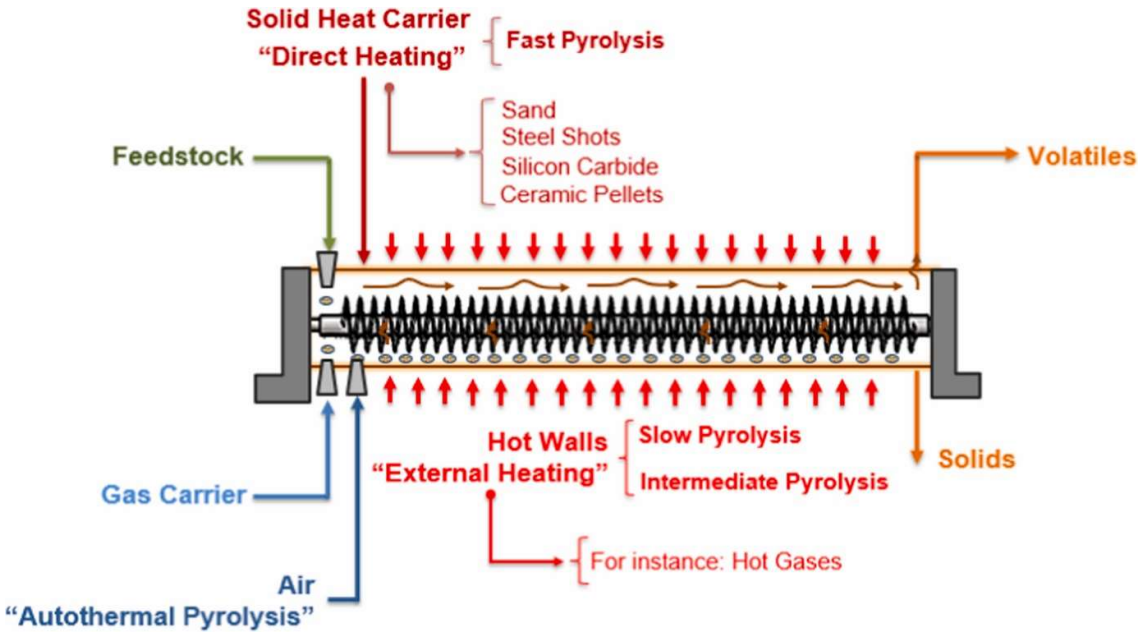

Figure 10: schematic diagram of auger pyrolyzer. (Campuzano, Brown & Martínez, 2019)

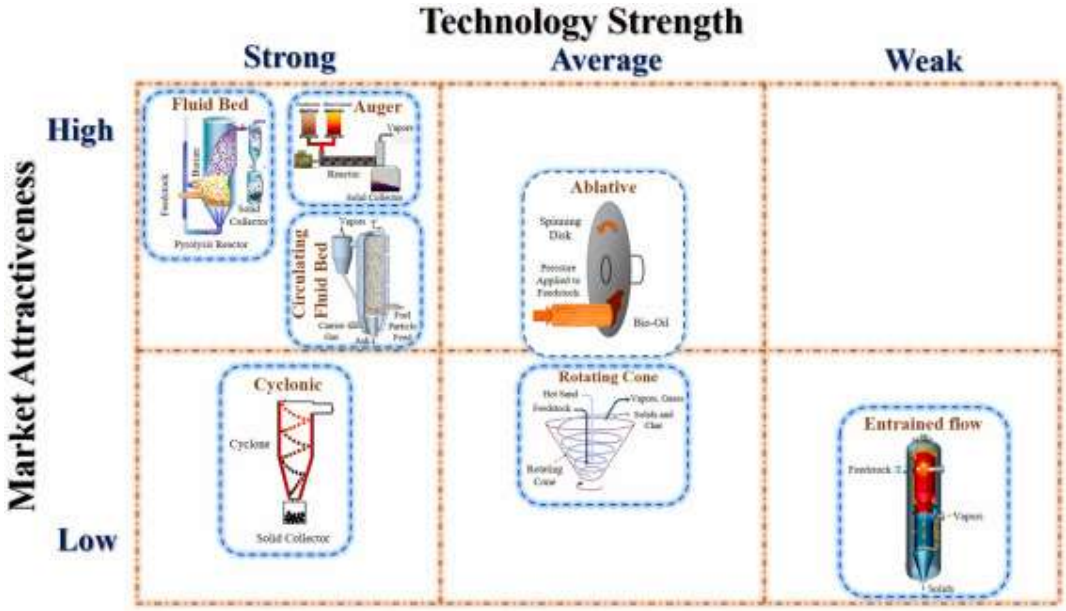

Figure 11: attractiveness & strength of auger reactor in comparison to some other pyrolysis technologies. (Van de Velden et al. 2010)

As observed in figure (10), the typical auger reactor consists of an enclosed shell with a helical screw rotating inside it (Rackl & Günthner, 2016). The screw rotates to convey the feed materials into the shell (reaction vessel) and to evacuate the biochar (residual solid fraction). The rotating movement of screw exposes the feedstock particles to a higher uniformity of

heating in the length of time and hence, enhances particle mixing as well as the heat transfer among the reactants (Nachenius et al. 2015). Despite a single-screw auger reactor is commonly used, auger reactor may have twin screws to enhance its overall performance (mixing, heat transfer, lower blogging, faster reaction, and higher liquid yield) (Brown, 2009; Brown & Brown, 2012; Sirijanusorn, Sriprateep & Pattiya, 2013; Brassard, Godbout & Raghavan, 2017; Garcia-Nunez et al. 2017).

When wall of the shell is subjected to heat, the shell of auger pyrolyzer works itself as a reactor and the screw as conveyer. The heat energy provided to the wall in a reactor of single-auger should be sufficient to raise up its wall temperature above the desired temperature of pyrolysis. When feed materials fed into the shell, the endless screw convoys it to another side by rotation providing good mixing and good contact between feedstock particles and the heated wall. The residence time is controlled by means of screw speed and the inert gas flowrate respectively. However, feed materials are totally volatilized at the end of the reactor (Aramideh et al. 2015).

Auger reactor are favourable because of many advantages. These advantages include its ability to use different kinds of heat carriers and catalysts, its excellent ability to control catalyst-feedstock ratio, mass flow rate and residence time, its low solid yield with simple separation process of solid fraction (falling down by gravity), and its gaseous yield is less diluted (good for further utilization). It is also versatile and fixable to be installed horizontally or vertically. Some arrangements, employ inclined installation which offers a steadier and smoother flow (Campuzano, Brown & Martínez, 2019). Auger reactor requires also limited infrastructure which make it suitable for different mobile applications and locations. It can be transported to the waste generation place to reduce the operation costs. In addition to the simplicity in term of its design, operation, and maintenance, it has low energy demand because of its low specific size. The screw conveyer makes it suitable as pyrolysis reactor for feed materials of different typology or particle sizes with no sensitivity to hydrodynamic bed conditions. Auger reactor is more favourable in term of reducing pollution because it prevents low density particles from leaving it before the complete conversion and consume low amount of inert gas. Finally, its capital and operational cost is relatively low (Brassard, Godbout & Raghavan, 2017).

In opposite, auger reactor may cause secondary reactions due to long residence time of vapours. Using such kind of reactors (that have parts moving at high temperatures) may result in risk of plugging and mechanical tears and wear. Despite its high mixing performance, the mixing effectiveness might be reduced due to flow-induced segregation phenomena under specific operating conditions (Brassard, Godbout & Raghavan, 2017).

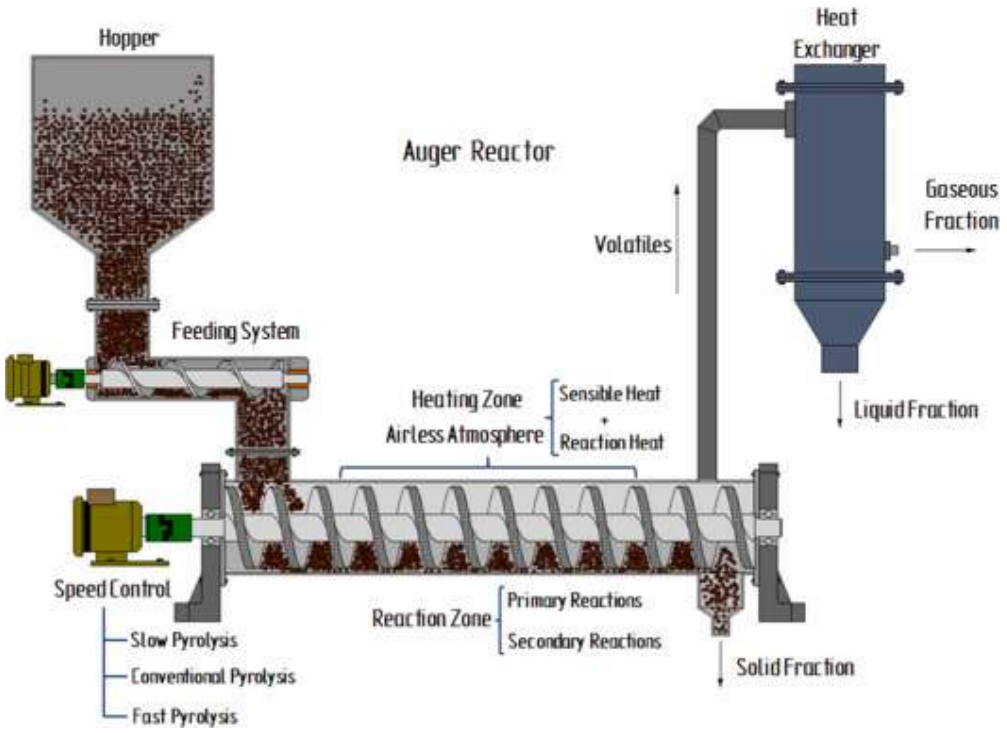

Figure 12: schematic diagram of a single-auger reactor. (Campuzano, Brown & Martínez, 2019)

Although auger is designed as a conveyer not a mixer, there are some practices should be taken in consideration in auger reactor design such as the inside and outside diameter of the shaft (screw), the length of screw, the pitch size which is the distance between nigh or adjacent flights, and the clearance (Figure 13).

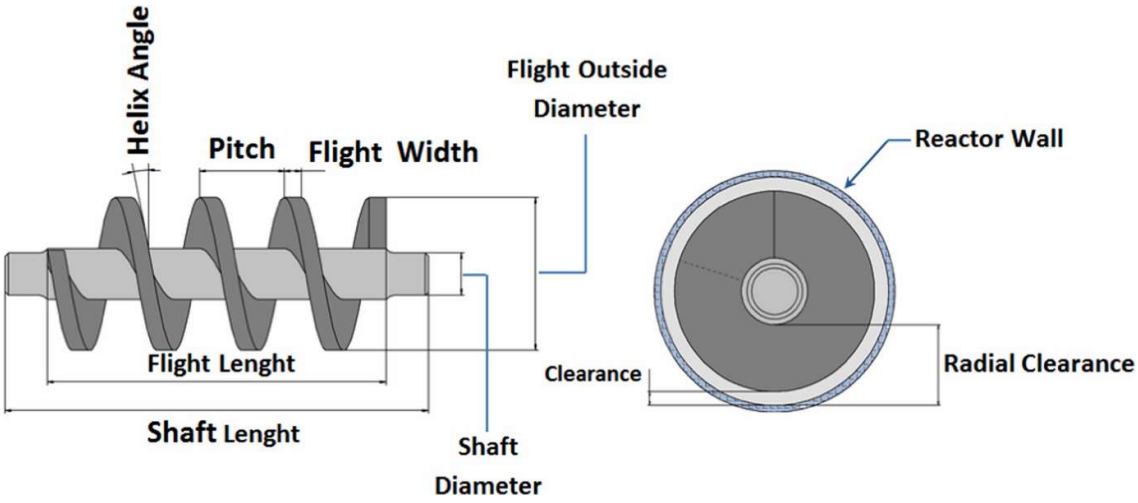

Figure 13: dimensional characteristics of auger. (Campuzano, Brown & Martínez, 2019)

Auger reactor design rely on empirical correlated obtained data (Owen & Cleary, 2010). Therefore, designer of auger reactor should consider many operating parameters such as the feedstock flow rate which in turn depends on the load factor, the rotational speed, the geometry of the screw, geometry of the tube and the feed hopper, inclination, and feedstock flow ability (Bortolamasi & Fottner, 2001). However, the most important factors in auger reactor design are the pitch-diameter ratio, the load factor, the characteristics of auger flighting, the mixing process, modelling the granular flow to visualize their movement in auger reactors, and scaling up the design considerations to understand the various phases of the process which probably change at different scales (laboratory, mathematical modelling, and actual design at pilot scale and industrial plant (Funke et al. 2017; Marmur & Heindel, 2016; Bridgwater, 2012; Kingston, 2013; Marmur, 2015; Morgano et al. 2015; Bortolamasi & Fottner, 2001; Kapoor, Mekala & Bose, 2016).

4.3 Pyrolysis process conditions

4.3.1 Catalysts

Catalytic degradation is involved to obtain great commercial products such as diesel, gasoline and C2–C4 olefins which are highly demanded in automotive and petrochemical

industry (Elordi et al., 2009). However, Catalysts are used in pyrolysis to lower down the activation energy of the reaction and then optimum temperature required and hence speed up the chemical reaction, besides, optimizing the product distribution and increasing the product selectivity. Interestingly, catalysts are used also to obtain liquid with similar properties to gasoline and diesel via pyrolysis process (Basu, 2013).

However, there are many types of catalysts which are classified mainly into two groups: heterogeneous which involves more than one phase, and homogeneous which involves only one phase. Homogeneous catalyst such as $AlCl_3$ (Stelmachowski, 2010). Due to the easy separation process of the mixture (fluid product from the solid catalyst), the heterogeneous is the most common catalyst type and most preferable catalyst economically. However, heterogeneous catalyst can be classified as nano-crystalline zeolites (such as HZSM-5, Hb, HMOR and HUSY), mesostructured catalyst, conventional acid solid, basic oxides and metal supported on carbon (Aguado, Serrano & Escola, 2008). Besides, there is non-zeolites catalysts which includes many types such as silica–alumina, silicalite, and MCM-41 (Aguado, Serrano & Escola, 2008).

As conclusions, formulating optimal catalysts for pyrolysis system is important. For example, the impact of metal oxide catalysts on pyrolysis varies based on the type of catalyst. CaO, TiO_2, and Al_2O_3 help to reduce the production of solid residues by promoting the degradation of organic matters in the sludge. On the other hand, Fe_2O_3 and ZnO help to produce more solid residues because they likely prevent the decomposition of organic matters in demineralized sludge (Chen et al. 2012). In term of their impact on pyrolysis time, Fe_2O_3, CaO and ZnO probably prolong it, while TiO_2 and Al_2O_3 may decrease it (Shao et al. 2010).

4.3.2 Type and rate of fluidizing gas

Fluidizing gas or carrier gas is an inert gas engages only in transportation of vaporized products but does not take part in the pyrolysis reaction itself. Despite the commonly used fluidizing gas for pyrolysis is N2 (specifically for auger reactors) (Campuzano, Brown & Martínez, 2019), it can be any inert gas such as hydrogen, argon, helium, ethylene and propylene which have different reactivity features depending on its molecular weight. The

lighter gas produces high amount of liquid oil (Abbas-Abadi, Haghighi & Yeganeh, 2013). Carrier gas plays an important role in enhancing the desired product yield in pyrolysis. Moreover, it influences the coke formation. For example, ethylene produces liquid yield more than nitrogen and lower coke formation because of its reactivity. Nevertheless, although helium is the second high liquid yield fluidizing gas after hydrogen, using nitrogen is easier, cheaper and safer (Basu, 2013).

Furthermore, fluidizing gas flow rate may affect the distribution of final product as well. Lowest fluidizing gas flow rate leads to drop the rate of degradation and high residue yield. Whilst, the large volume of inert carrier gases (highest fluidizing flow rate) maximizes the pyrolysis yield of diluted pyrolytic gases, namely gasoline and hydrocarbon (Abbas-Abadi, Haghighi & Yeganeh, 2013). These diluted pyrolytic gases makes bio-oil recovery very difficult (Garcia-Nunez et al. 2017).

5. Solar pyrolysis

Using fossil fuels excessively for energy production and managing its gas emissions especially greenhouse gases may be the most complicated challenges of today. Although fossil fuels are dominant energy source, there is prediction of vanishing fossil fuels in coming decades due to excessive usage and its non-renewable resources which raise high concerns about the environmental and sustainable problems. Unless other renewable and eco-friendly energy sources are put in place as alternatives for fossil fuel, these problems will continue. Sludge is considered a sustainable energy source. Thermochemical conversion technologies such as pyrolysis and gasification are introduced as processes of converting sludge to higher value oil. Fossil fuel either directly or via electricity generation, still a predominant source in heat energy production which is required in these processes to treat sludge. Such kinds of non-renewable energy sources greatly reduce the process efficiency economically and environmentally. Combustion of fossil fuels decreases the economic benefit of the pyrolysis process by about 35% (Weldekidan, Strezov & Town, 2018) which threatens the sustainability of biofuel production. Solar energy is nominated as a promising alternative to generate heat in thermochemical processes. This will significantly improve the process performance and overall sustainability.

High living standards with rapid growth of global population have resulted in a significant increase in energy consumption over the last century (Chen, Peng & Bi, 2015). Total energy consumption by 2040 is predicted to increase by about half of current use (Cronshaw, 2015) due to the increase in the world population which is estimated to reach 9.3 billion by 2050 (Morales et al., 2014). Although expectations say that fossil fuel will still remain the main source of energy by over quarter of the global energy demands (Cronshaw, 2015), its usage will decrease sharply due to its significant depletion after 70 years (Metzger & Hüttermann, 2009). Thus, the existing energy supply may not be sustained for coming few decades (Rahman et al., 2014). In addition, environmental impacts of fossil fuels and the over-exploitation of forests and natural resources are considered one of main reasons behind climate changes (Morales et al., 2014).

The percentage of main component and typical combustible elements of sludge such as hydrogen, carbon, and sulphur and their thermochemical degradation as well as their

thermochemical products show comparable characteristics up to closely analogy to those of lignite (Flaga, 2007) and biomass species (Barneto et al., 2009; Thipkhunthod et al., 2007). According to Hertwich & Zhang (2009), solar pyrolysis of biomass can produce over 60 wt% liquid bio-oil. Therefore, sludge can be introduced as an alternative source of energy. Utilization of sludge is seen as one of the most beneficial as well as promising ubiquitous energy sources due to its valuable products and its impacts to reduce greenhouse gas emissions. Adoption of such kind of sustainable energy sources might mitigate economic, social and environmental problems faced by urban life (Khan et al., 2009).

Despite existing processes offer economic benefits through their high value products, they are highly endothermic and require large heat input which is mostly provided from non-renewable sources of energy (Morales et al., 2014). Numerous studies asserted that solar energy can be utilized as a sustainable source of energy. Solar energy can be converted directly to heat energy or can be stored in fuels or chemicals (solar fuel) to ease transportation and storage (Weldekidan, Strezov & Town, 2018). Utilization of solar energy to convert sludge through thermochemical processes such as solar pyrolysis may significantly improve the performance of biofuel life cycle. These days, pyrolysis process are run using solar energy as a source of required heat energy which is known as solar pyrolysis. In solar pyrolysis, solar energy have been concentrated to extract biofuel via solar reactors from different types of feedstock such as biomass (Zeng et al., 2017), plastic (Caballero et al., 2016; Shakya, 2007), and scraped tires (Rahman & Aziz, 2018; Zeaiter et al., 2018; Zeaiter et al., 2015), and sewage sludge (Zadik & Israel, 2011). It is important to mention that solar pyrolysis of sewage sludge has investigated only in a very few number of literatures that can be counted on one hand. Thus, more studies need to be done to examine its feasibility and sustainability as well as its efficiency from commercial perspective.

This research will study solar pyrolysis with more focus on solar dewatering of both raw and digested sludge as preparing process for pyrolysis via solar dryer. Novel design has been employed to produce sludge flux. This design can dry sludge quickly and easily.

5.1 Energy supply from the sun

Sun is a massive source of energy. Annually, earth's surface receives more than 885 million terawatt hours of solar energy which is according to the International Energy Agency (IEA) Current Policies Scenario 4200 times of mankind need in 2035. According to Smil (2006), the earth – includes land masses, oceans, and atmosphere- absorbs approximately 1070.3 million TWh which means that the earth receives in one hour more energy than the total world use of the whole year of 2002 (Lewis & Nocera, 2006; Morton, 2006). Interestingly, the problem of energy supply will totally disappear if one-tenth of 0.01 of solar energy has been collected because three hours are enough for the earth to collect energy from the sun more than total world demand for one year (Philibert, 2011). Comparing to the energy that can be obtained from all available non-renewable resources of energy on the earth, the solar energy reaching the earth surface in one year is about the double (Global Climate and Energy Project (GCEP), 2018). Generally, the average insolation of the earth is about 7.0 kWh/m² or 300 watts/m² per day.

However, employment of solar energy as a source of heat energy in pyrolysis is promising. The liquid yield of fast solar pyrolysis of biomass is able to recovery about 65–77% of solar energy which can be enhanced by increasing the liquid yield by 1.5–3 if supplementary energy that is recovered from solar radiation is put in place (Agrawal & Singh, 2010). In this regard, solar concentrators are also used to harvest sunrays and hence considerably improve these numbers.

Using solar energy is might be challenging. The potential usable solar energy that can be acquire by humans depends on the density of solar flux reach the earth surface. This differs based on many factors such as time variation, seasonal variation or cloud cover, and geography. One of main challenges is unavailability of sunrays at night. Variation of sunrays intensity during daytime and seasons as well as the cost of solar systems affect negatively using solar technology widely. Using solar energy storage system might be important in solar pyrolysis units for continuous availability of energy. This will increase the productivity and hence the efficiency of the unit. Although there is a current trend to invest the sun as a sustainable source of energy in Sun Belt countries, the high cost of solar systems reduces spreading this technology in these countries which are generally developing countries (Figure

14). Targeting these countries, specifically Middle East countries will be promising. Solar pyrolysis can be described as a project harnesses the plenty of solar energy in Middle East countries such as Jordan to dispose solid wastes. Sludge as a part of solid waste issue in Jordan is the scope of this paper.

Figure 14: global prevalence of harnessing the solar energy. (Bielinskas, 2012)

Solar pyrolysis unit of sludge consists of three main parts: solar dryer, solar concentrator and solar reactor. Solar energy concentrating part in present technologies consists of glass mirror or polished aluminium as a reflecting surface whereas borosilicate glasses or quartz and metals are used to make solar pyrolysis reactors. Other parts such as sensors, controllers, tracking units, and condenser are almost similar to those of conventional pyrolysis (Weldekidan, Strezov & Town, 2017). However, pyrolysis unit of sewage sludge that is entirely run by solar energy will need a drying unit as a pre-processing unit of sludge. Although

5.1.1 Targeted countries by solar pyrolysis

The geometry of the earth and the sun affects the amount of solar radiation received at the earth surface. The elliptical orbit that the earth follows during its revolution around the sun and the inclined axis of rotation cause variations in the amount of daily insolation at latitudes of the earth as well as large seasonal variations (Bhatia, 2014), (Figure 15). Therefore, solar

energy is affected by geography. The countries that are closer to the equator receives higher amount of solar radiation and known by Sunbelt countries (Figure 16). Despite photovoltaics are used effectively to track the sun position in countries that are farther from the equator (Goldemberg, 2000), targeting those countries that receive high solar radiation seems more efficient. Sunbelt countries are located where sunlight is shining on a perfect receiving angle for long term per year. Sunbelt countries include Middle East countries particularly Jordan. This paper will focus on the feasibility of employing solar energy in sludge pyrolysis in Jordan and Middle East countries surrounding Jordan.

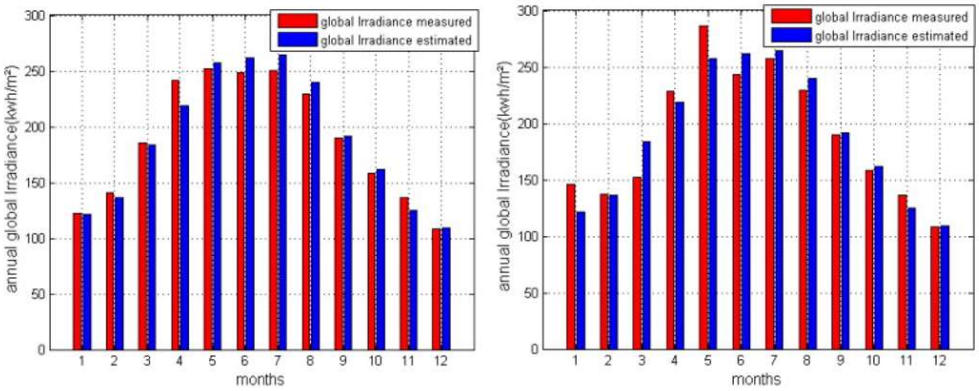

Figure 15: annual global irradiation for 2012 & 2013 respectively. (El Mghouchi et al., 2014)

Figure 16: Sunbelt countries. (Sănduleac, 2019)

5.1.2 Solar Intensity in Jordan and Middle East (Gulf countries, Iraq, Syria and Egypt)

Middle East countries and North Africa are located in what so called “the Sun Belt”; the fact that makes them one of the highest countries of receiving solar radiation (Jaffer, 2011),

(Figure 17). Jordan is located in the middle of Middle East countries surrounded by Saudi Arabia, Syria, Iraq and Palestine. Lebanon and Egypt do not have shared border with Jordan but they are very close to it. Jordan, specifically the southern region, is located in the middle of the highest annual average irradiation intensity of this area (Figure 18). Following is illustration of the amount of solar irradiation for the countries around Jordan and the current situation of insolation energy in those countries.

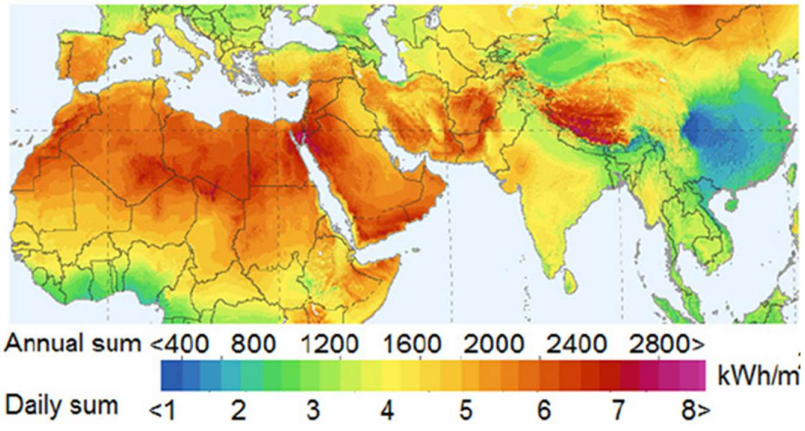

Figure 17: Annual summation of Horizontal Solar Irradiation for Sunbelt countries in Middle East and North-Africa. (Global Solar Atlas)

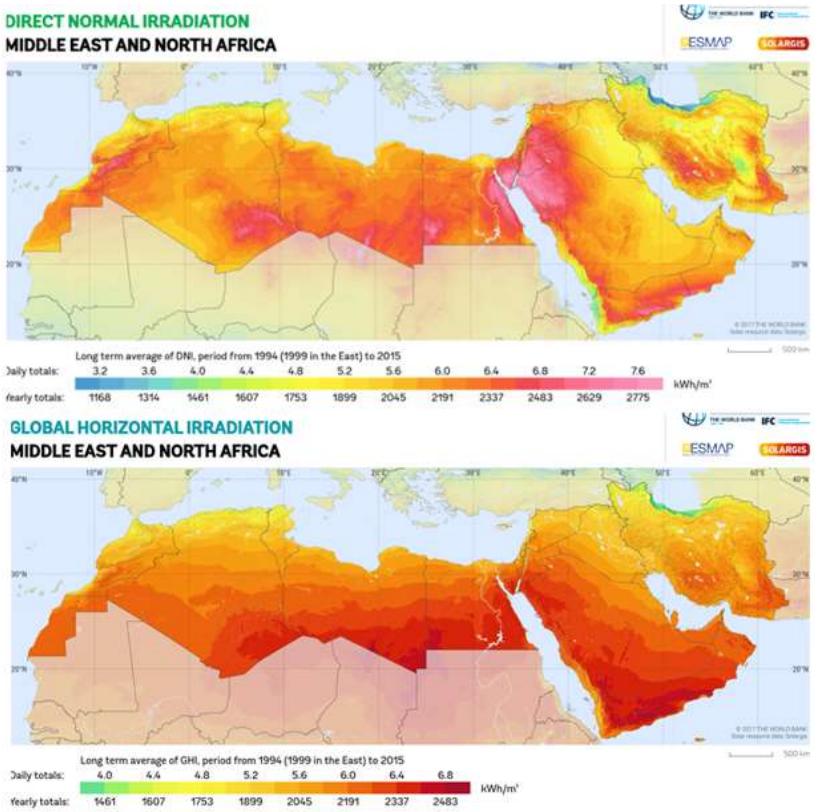

Figure 18: Jordan as one of highest receiving areas for solar irradiation in Middle East. (Global Solar Atlas)

Insolation power of Middle-East

The global solar map shows that the maximum value of normal irradiation in Middle East is around 3200kwh/m2/annum. This value can be obtained in the northern region of Saudi Arabia and the southern region of Jordan, Palestine, and Siena-Egypt. Whilst east of Iraq and south of Egypt receive the minimum solar irradiation in the area with average of 1500kWH/m2/ annum. The maximum global horizontal irradiation is received in west of Egypt, south of Saudi Arabia and in Yemen with average value over than 2400 kwh/m2/annum. The area of north of Iraq and Syria receives the lowest global horizontal irradiation in the region with average value between 1900 and 1800 kwh/m2/annum. Remarkably, Jordan receives almost the highest amount of direct and horizontal irradiation (Figure 19).

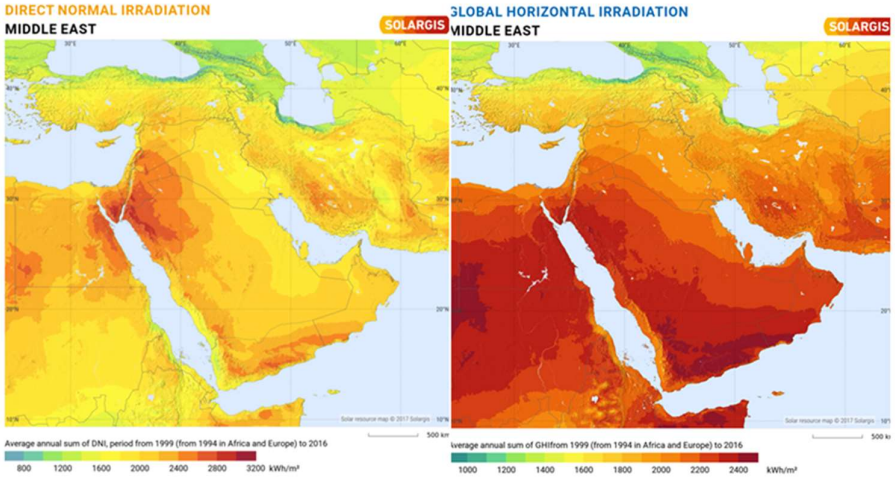

Figure 19: Middle-East insolation map, the direct normal radiation & the global horizontal irradiation respectively. (Global Solar Atlas)

Despite the shortage in studies that represent the total sunny days in this wide area as one region, the individual reports for every country separately demonstrate that the total sunny days in this area is often more than 280 days a year. Some regions such as Ma'an in south of Jordan has more than 326 sunny days a year (Alrwashdeh, 2018). The temperature of Middle East divers based on the location and its altitude above the sea level. Due to the location of ME in the north of equator, the temperature in some regions such as east of Saudi Arabia, south east of Jordan, mid and south of Iraq, west of Egypt and in Sudan touches 50 oC in June and July. However, the average temperature over the year is 35oC which makes this area very suitable for all solar applications (Jaffer, 2011). Currently, solar applications in Middle East include solar thermal systems that are widely used to heat water in commercial and

residential properties as well as industry. There are also huge projects in the area that apply solar energy for Water Desalination such as those in Bahrain (Abdelrassoul, 1998). Photovoltaic systems are widely used in some none-petroleum countries such as Jordan that relies on the solar plants to reduce the total demand on the grid. However, photovoltaic systems are promising in the region and have a great potential (Jaffer, 2011).

Insolation power in Syria

Studies show that Syria has a great potential with solar applications specifically the southern region. As shown in (Figure, 1117), Syria has in average 1800 kWH/m2/annum (5kWh/m2/day) of horizontal solar irradiation. The total sunny days in Syria varies from 282 to 326 days (2820 to 3270 sunny hours) (Ramadan and Elistratov, 2019). Figure (20) below illustrates the annual GHI and annual NDI for Syria.

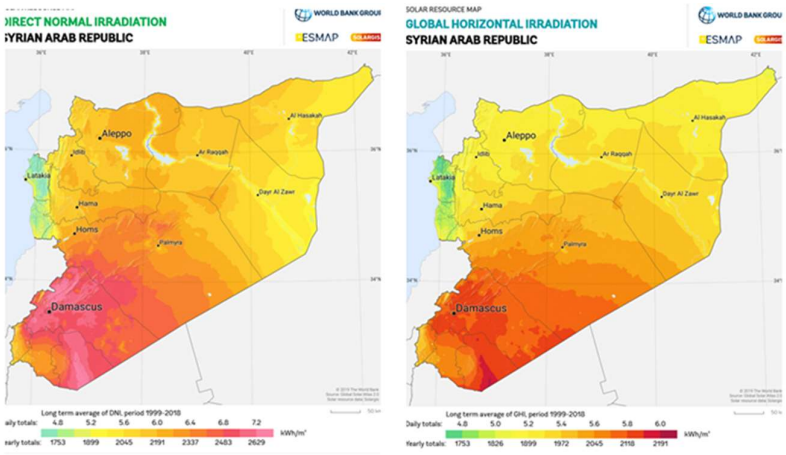

Figure 20: Insolation Power map of Syria governorate. (Global Solar Atlas, no date)

However, Syria investments in solar energy is still very low comparing with others countries in the ME. Most utilization of solar energy are private and made by locals. They generally use solar energy for water heating purposes by using the top roof solar water heating systems. Flat cells are the common solar collector in Syria. A current study shows that over than 300k dwelling have such systems that produce about 15.9MW annually. The same systems are also used commercially and in industry in many locations. The Solar photovoltaic systems (PV) are also used at a limited level. The major three PV projects in Syria have 5kW, 10kW, and 150

kW power generation capacity and they are located in the eastern desert specifically. There is also a limited utilisation for PV by locals in the rural areas (Ramadan and Elistratov, 2019).

Insolation power in Saudi Arabia (KSA)

The available data about the solar intensity in KSA shows that DNI of Saudi Arabia ranges between 1626 kWH/m2/annum and 2922 kWH/m2/annum. The lowest DNI is recorded in the eastern province of the country whilst the highest DNI is recorded in Tabok province in the northern region of Saudi Arabia. The lowest GHI average is 2118 kWH/m2/annum while the highest GHI annual average is (>= 2410 kWH/m2) in the southern provinces of Saudi Arabia (Nejran, Bishah and Khamis Moshaite) (Almasoud and Gandayh, 2015), (Zell et al., 2015) and (Mas'ud et al., 2018).

Saudi is blessed with plenty of solar energy. Most of areas of Saudi Arabia have 365 sunny days annually. However, feasibility of solar applications in KSA is challenged by two main issues; the high temperature (the average between 35oC-40oC) (Zell et al., 2015) and the moving sand and dust (Almasoud and Gandayh, 2015). The high temperature decreases the output efficiency of solar systems such as PV for less than the half of the original efficiency and the moving sand makes planting solar arrays almost impossible in more than third of Saudi Arabia area. The best 10 cities in KSA for PV power plants as a solar energy investment have been determined by (Rehman, 1998). According to him, these cities are Nejran, Sulayyll, Alnumas, Helfa, Bishah, Derab, Shaqra, Madina Monawarah, Hanakiya and Uqlat Al-soqur. Figure (21) below illustrates the annual average of the both DNI and GHI of Saudi Arabia.

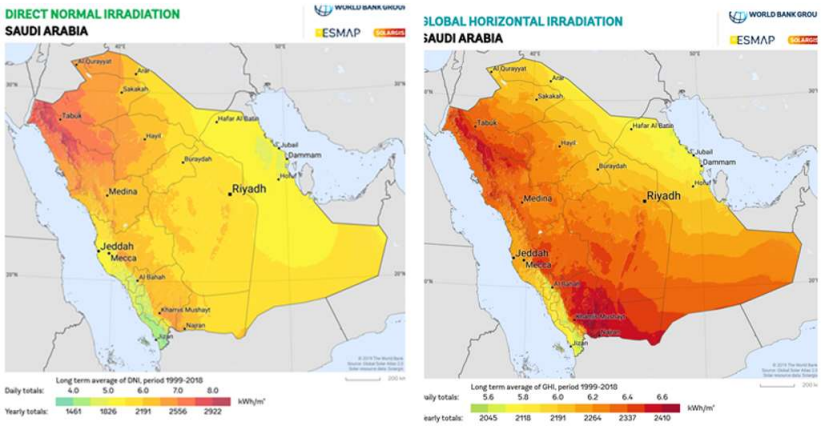

Figure 21: map of insolation power distribution (DNI & GHI, resp.) in KSA. (Global Solar Atlas)

Although Saudi Arabia is the first country in ME invested in Solar Energy research by creating a research solar village in Madina Monauarah in the mid of 80's of the past century, the actual commercial investment started in the beginning of the current century. Among other countries in Arab Gulf Cooperation Council (GCC), Saudi was leading the investment in PV until the late of 2011. Currently, KSA has retreated to the 3rd place after UAE and Kuwait. However, many transformation PV projects are lunched with starting of 2030 vision to decrease the dependency on the fossil fuel in KSA. Present projects produce together about 50MW. The 2030 vision aims to generate 41GW of electrical power by 2032 AD (Mas'ud et al., 2018). Following are some solar projects in KSA and their production capacity (Figure, 22 & table 2).

Figure 22: Solar PV projects in KSA: (a) King Abdullah Petroleum Studies and Research Center Solar Park; (b) Saudi Aramco solar car park, and (c) King Abdullah University of Science and Technology Solar Park. (Mas'ud et al., 2018)

Solar Project	Location	Generating Capacity (MW)	Purpose	Type of Equipment
King Abdullah Petroleum Studies and Research Center Solar Park	Riyadh	3.5	To feed up to 2900 MWh yearly into KAPSARC's medium voltage grid.	Polycrystalline silicon substrate (Suntech STP 280-24Vd)
Saudi Aramco Solar Car Park	Dhahran	10.5	To supply solar power to 4500 MW car park spaces.	Thin film solar cells (CIS type modules)
King Abdullah University of Science and Technology Solar Park	Thuwal	2	To supply solar power to certain university buildings.	Thin film solar cells(SPR 215 W Solar Panels)
King Abdulaziz International Airport Development Project	Jeddah	5.4	To supply remote car parking canopies.	Thin film technology (ARCO solar cells)

Table 2: location, generating capacity, and type of used equipment for selected solar projects in KSA. (Mas'ud et al., 2018)

Generally, all presented projects are standalone projects and they are not connected to the national grid. At the individual level, the usage of solar energy applications still in its beginning though the awareness of importance of solar energy among locals has increased dramatically since 2015 (Mas'ud et al., 2018).

Insolation power in Palestine (Israel)

Similar to other neighbours country located in the Sunbelt, Palestine (Israel) has GHI varies between 2400 kwh/m2/annum in the southern region (Naqab) and 1750 kwh/m2/annum in the northern region (Jaliel), (Figure, 23). The daily average in Red Sea area is 6.18kwh/m2. The number of sunny days in the southern region is more than 300 days/year.

Israel government is the biggest investor in solar energy in the ME with several mega projects. Ketura Sun (4.95MW generation Capacity) is the first mega project for PV systems.

Solar heaters of water provide almost 77% of dwelling with hot water in Israel regions. Hot water from solar systems are widely used in industry, agriculture as well as households there.

Solar thermal energy has a huge investment. “Ashalim power station in Naqab has the tallest solar tower; 250m. This project is expected to generate 310 MW of power” (Abu Hamed and Bressler, 2019).

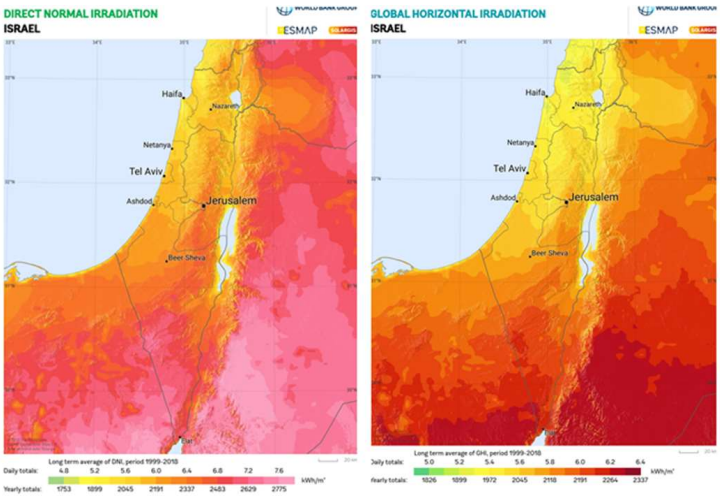

Figure 23: GHI and NDI distribution in Palestine (Israel). (Global Solar Atlas)

Insolation power in Egypt

Egypt also located in the Sunbelt. Its average GHI varies between 2000kWH/m2/annum in the northern regions; Delta and Meditation Sea coast and 2400 kWH/m2/annum in the south-western desert (Hemeda, Aboukarima and El-Bakhshawan, 2015), (Figure, 24). As all other

ME countries, Egypt is blessed with more than 320 sunny days annually in average. This fact, in addition, the geographical nature of Egypt and the high energy bill encourage Egypt to invest in solar energy. The current vision in Egypt which has been lunched two years ago is to create the world largest PV power plant. This solar plant is expected to generate (1.6 to 2) GW of electricity (20% of the total required energy in Egypt). The power plant is set into construction in the early 2018 and it was expected to start working in the mid of 2019 (Tawfeek, 2018). However, no updated information is available.

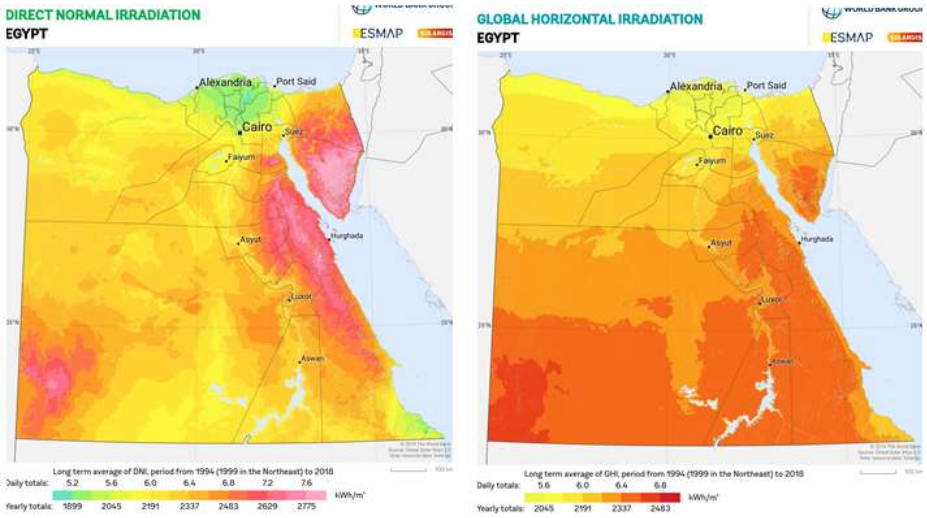

Figure 24: GHI and NDI distribution over Egypt. (Global Solar Atlas)

Insolation power in Lebanon

GHI in Lebanon is less than other neighbour's country although it has in average over than 300 sunny days (Moore and Collins, 2020) annually. GHI varies between 1600 kwh/m2 annually in the western cost to 2100 kwh/m2 annually in the eastern border region between Lebanon Mountains and Syria (Figure, 25). Similar to other ME countries, Lebanon utilizes solar energy in two main ways; solar water heater, and solar PV systems. Lebanon aims to reach a solar water heater on each roof top of its building by the end of 2020. Lebanon also generates 26% of its total power demand by using PV systems. However, many projects have been lunched in 2018 to increase the production capacity up to 450MW (Ayoub et al., 2013; Lebanon Ministry of Energy and Water report, 2018).

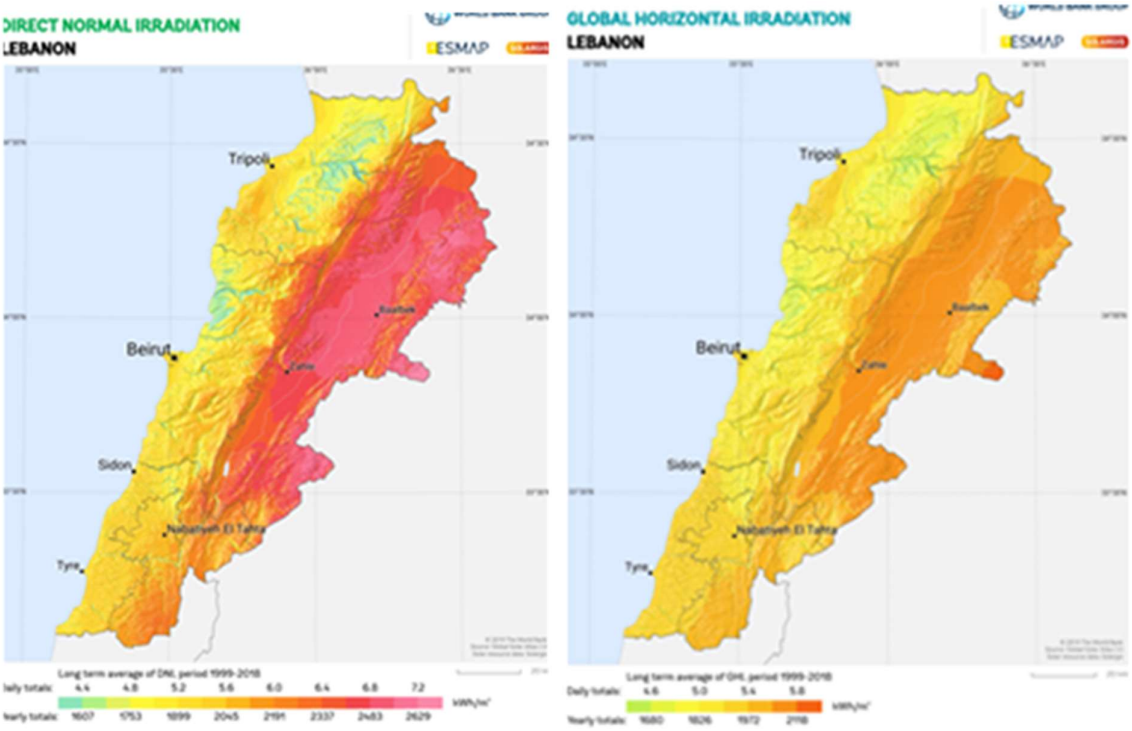

Figure 25: GHI and NDI distribution over Lebanon. (Global Solar Atlas)

Insolation power in Iraq

Iraq has a wide area extended over different climate regions. However, it is one of the Sunbelt countries like other ME countries. It has annually average solar irradiation GHI of 2000kWH/m2 (Abed, Al-douri and Al-shahery, 2014). However, the lowest GHI is in the northern mountain near the Turkish boarders (1600kWH/m2) and the highest irradiation is located near the Jordanian boarders (2200kWH/m2) in the western desert of the country (Ahmad, Al-Hamadani and Ibrahim, 1983), (Figure, 26). Moreover, the southern, middle, western and eastern regions of Iraq have over than 300 sunny days annually (Ahmad, Al-Hamadani and Ibrahim, 1983). However, the best location to be used for PV investment and solar power plants is considered to be “the western boarded quadrangle as from Sinjar, Sur, Wadi Al-Myah, Rutba, Wadi Horan, Wadi Tibil, Al-Thurthar, Al-Breet, Al-Ma’aniya, Al-Salman, Ansab and Al-Rukhaimiya” (Abed, Al-douri and Al-shahery, 2014). These locations are considered to be the best location after long analysis of hazardous criteria and other factors such as dust, rain and water floods.

Unfortunately, there is no available information about the current situation of investment in solar energy in Iraq.

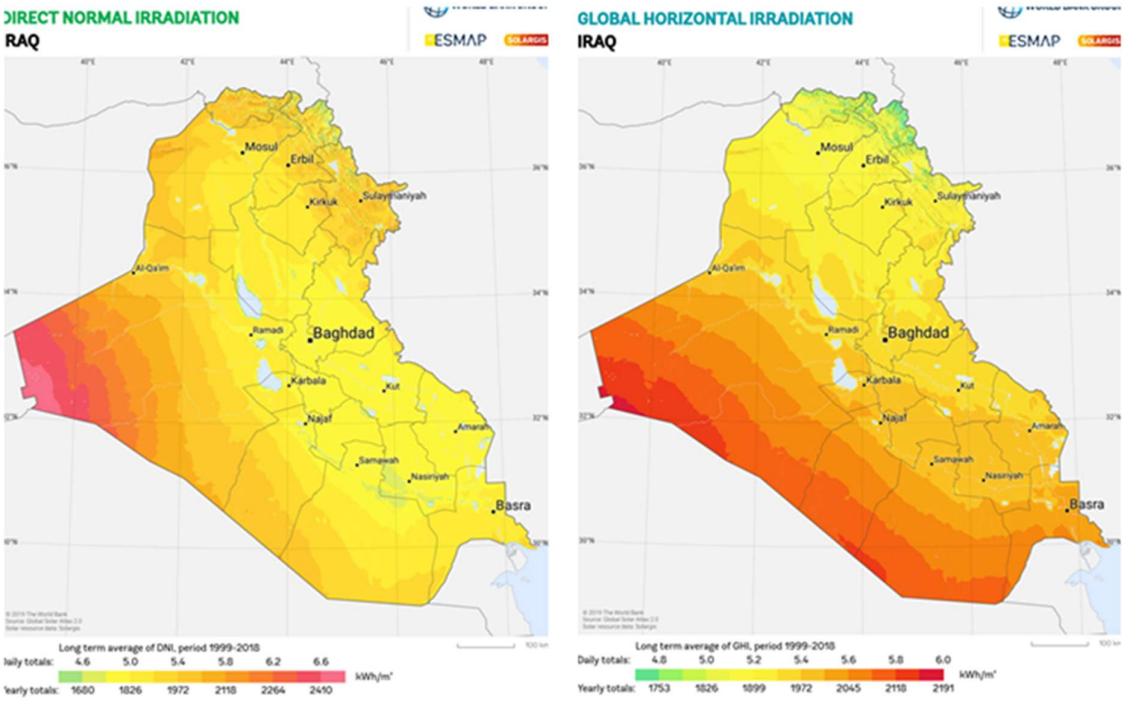

Figure 26: GHI and NDI distribution over Iraq. (Global Solar Atlas)

Solar Intensity in Jordan

Jordan, similar to most Middle East countries, has a high level of solar irradiation; DNI and GHI. Jordan is located at (32.05_N and 36.06_E). It has more than 300 sunny days in average (Alrwashdeh, 2018) and moderate temperature. Temperature average in Jordan varies between 20 oC and 30 oC (Etier, Al and Ababne, 2010) which makes it one of the best places to invest in solar energy applications such as solar pyrolysis. Furthermore, the efficiency of solar projects in Jordan is expected to be one of the best Middle East due to the clarity and good receiving angle. Jordan annually GHI varies between 1900 to 2300 kwh/m2 and the GHI average in Jordan is 2150 kwh/m2. Whilst, NDI of Jordan varies between 2045 to 2922 kwH/m2 with average of 2600 kwh/m2, (Figure, 27).

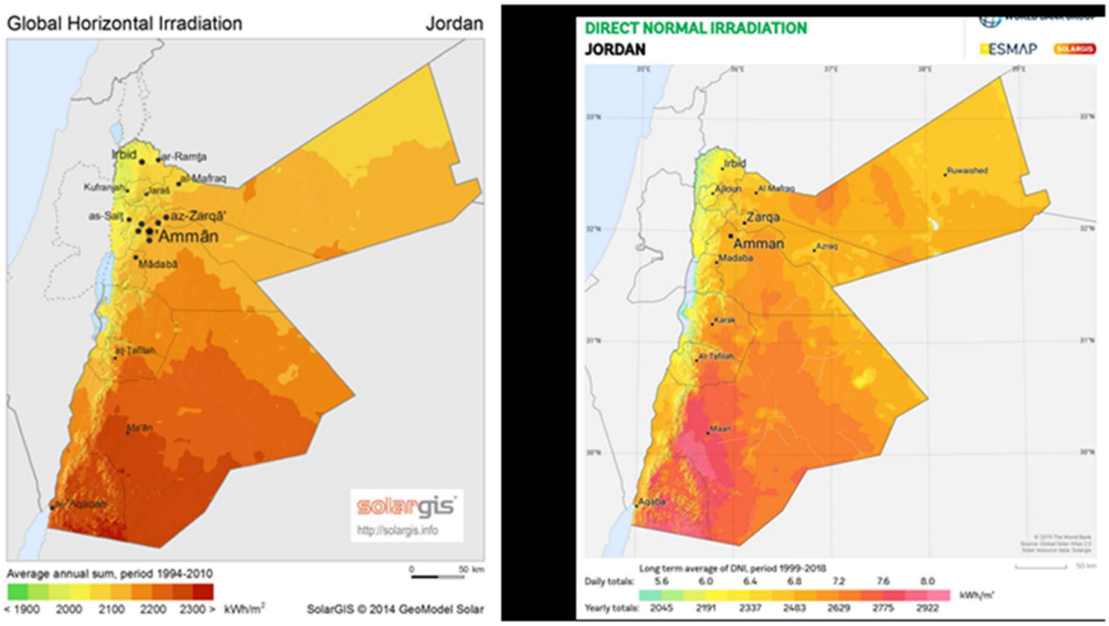

Figure 27: Jordan insolation map, lift is the direct normal radiation, right is the global horizantal irradiation. (Global Solar Atlas)

According to Global Solar Atlas, Jordan is divided into 5 different regions based on the average daily insulation irradiation in each region, (Figure, 28). Ma'an and Aqaba (the southern region) have the highest GHI with daily average of 6.7 kwh/m2. Amman governorate, Madaba, Tafilah and Karak (the middle region) have a daily average of GHI 5.5 kwh/m2. Badia, AzZarqa and Al Mafraq (Eastern region) have a daily average of GHI about 6 kwh/m2. The daily average of GHI in northern region (represents cities such as Irbid, Ajlon, Jerash and Salt) is 5 kwh/m2. The western region (represent the Jordan Valley area) has a daily average of GHI 4.5 kwh/m2 (Alrwashdeh et al., 2018).

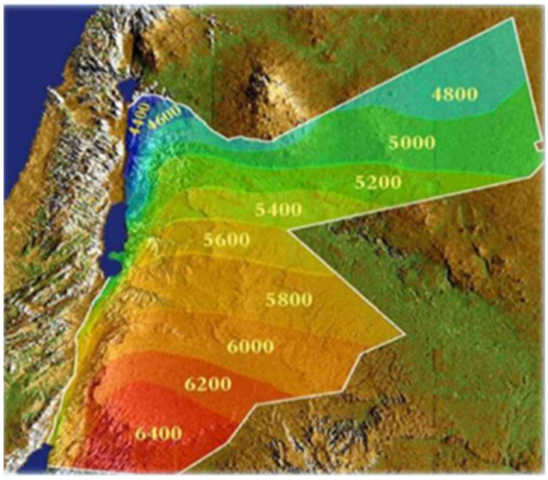

Figure 28: the map of average daily GHI (W/m2) of Jordan. (Alrwashdeh et al., 2018)

Although southern region has the highest both DNI and GHI level, the mid and eastern regions are considered the best places for PV applications. The high efficiency of solar applications in the middle and east of Jordan results from different facts:

1. Their temperature in average is lower than southern region. This temperature is close to the optimum operating temperature of the PV cells. Meaning, higher operating efficiency.

2. Less moving sand due to the stony nature of that area.

3. The middle region is the highest annual daily average diffused irradiation.

4. Although the number of sunny days in the middle region (>= 300) less than the sunny days in the southern region (>=335), the eastern region has the same number of sunny days.

5. Eastern and mid regions have more flat areas where PV systems can be installed easily.

The monthly average daily GHI (ADGHI) in each city of Jordan is shown in (table 3). It illustrates that the highest average of GHI (7610wh/m2/day) can be measured in June in Amman then in Zarqa and Jerash (7580 wh/m2/day). The lowest GHI in Jordan happens in January in all cities, especially in Ajloun where it reaches (3710 wh/m2/day). It is worthy to note that while all cities of Jordan have five months (May, June, July, August, and September) where the ADGHI exceeds 7000 wh/m2/day, Ajloun city hardly reaches only four months. However, Aqaba and Ma'an exceed the level of 7000 wh/m2/day in seven months of the entire year. The lowest ADGHI in all cities except Ajloun is above 4 kwh/m2/day and above 5 kwh/m2/day in both Ma'an and Aqaba (Alrwashdeh, 2018).

All available figures and data prove that Jordan has an excellent potential for solar energy usage as well as solar applications especially PV systems and hence solar pyrolysis. Fortunately, both the government and citizens of Jordan have relied this from early in the last century. Recently, the solar applications have been involved in commercial and industrial applications widely. The optimal PV cell orientation degree (inclination angle) has calculated for fixed PV systems to be 30oC, especially at Hashemite University area in Zarqa (30 KM to north east of Amman) (Alrwashdeh, 2018). Many research are conducted there to apply solar tracking system although still not used commercially there. Figure (1128) shows the potential of PV in kwh/kwp annually. It can be noted from figures that Jordan solar potential, in average, is one of the highest in Middle East countries.

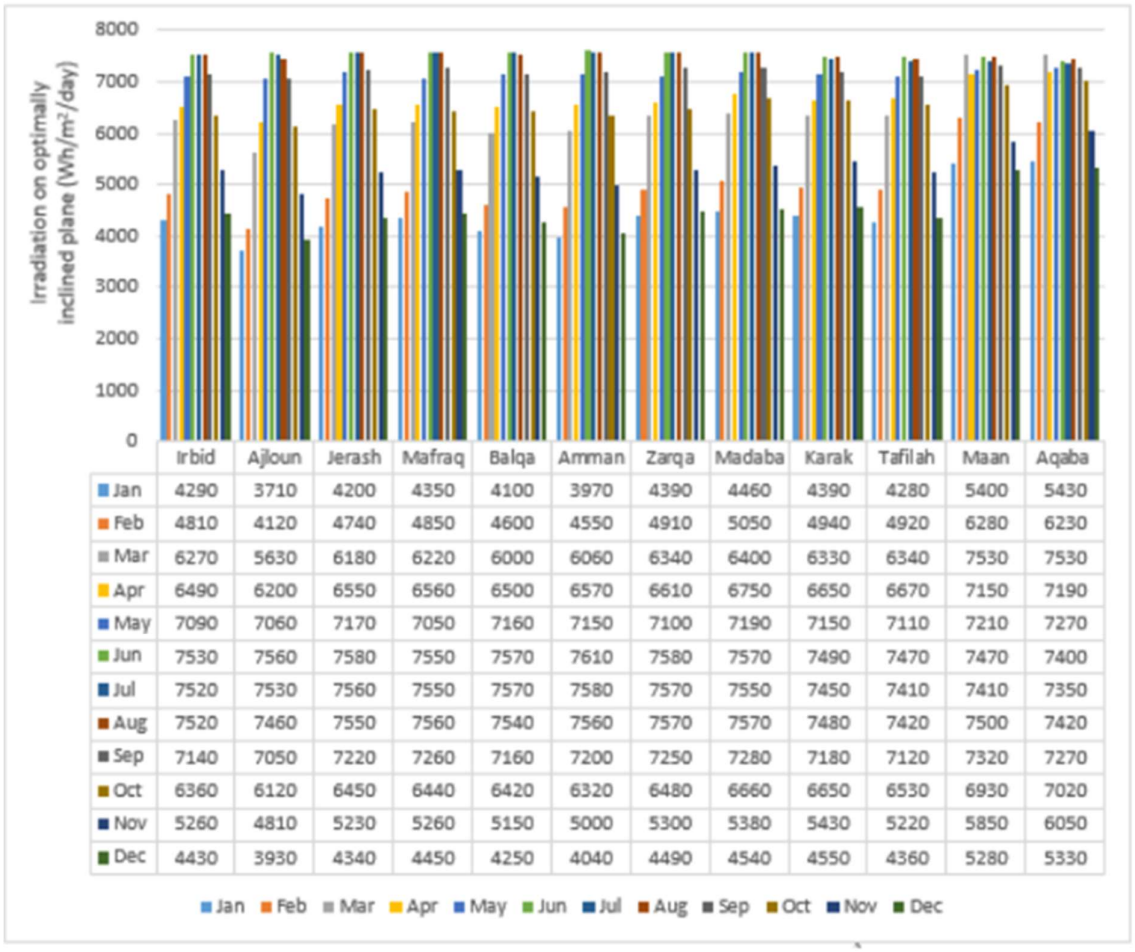

	Irbid	Ajloun	Jerash	Mafraq	Balqa	Amman	Zarqa	Madaba	Karak	Tafilah	Maan	Aqaba
Jan	4290	3710	4200	4350	4100	3970	4390	4460	4390	4280	5400	5430
Feb	4810	4120	4740	4850	4600	4550	4910	5050	4940	4920	6280	6230
Mar	6270	5630	6180	6220	6000	6060	6340	6400	6330	6340	7530	7530
Apr	6490	6200	6550	6560	6500	6570	6610	6750	6650	6670	7150	7190
May	7090	7060	7170	7050	7160	7150	7100	7190	7150	7110	7210	7270
Jun	7530	7560	7580	7550	7570	7610	7580	7570	7490	7470	7470	7400
Jul	7520	7530	7560	7550	7570	7580	7570	7550	7450	7410	7410	7350
Aug	7520	7460	7550	7560	7540	7560	7570	7570	7480	7420	7500	7420
Sep	7140	7050	7220	7260	7160	7200	7250	7280	7180	7120	7320	7270
Oct	6360	6120	6450	6440	6420	6320	6480	6660	6650	6530	6930	7020
Nov	5260	4810	5230	5260	5150	5000	5300	5380	5430	5220	5850	6050
Dec	4430	3930	4340	4450	4250	4040	4490	4540	4550	4360	5280	5330

Table 3: Solar Irradiation on the Optimally Inclined Plane of Jordan Governorates in Kwh/M2/Day. (Alrwashdeh et al., 2018)

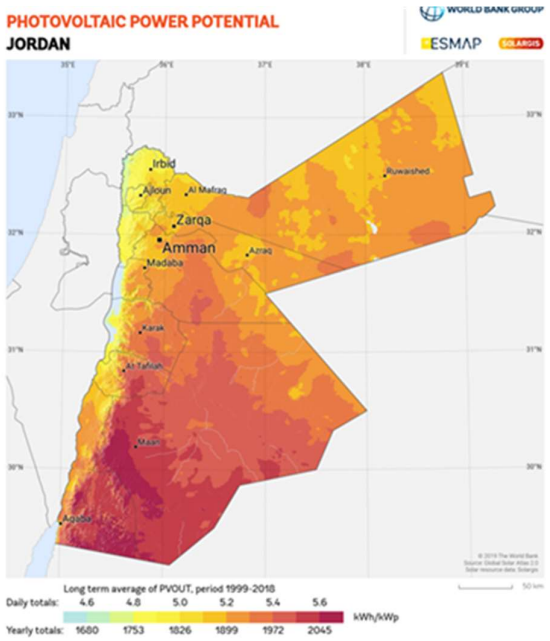

Figure 29: PV potential in Jordan by kwh/kwp. (Alrwashdeh et al., 2018)

The investment in solar energy in Jordan has three shapes (Hrayshat, 2007):

1- Solar water heating

2- Solar thermal power station

3- Photovoltaic

Solar applications for water heating are widely used in Jordan, almost for all purposes; commercially, residentially, and in industry. Research were made in 1995 show that over 25% of houses are using solar thermal water heaters. There is an estimation that about 8% of today Jordan population are using solar heating systems in their houses. The current total number of solar heating systems running in Jordan indicates that about a million family are using solar water heaters in their houses.

An early project utilizing solar energy commercially in Jordan was in Jordan Valley. This project was to evaporate Dead Sea water to produce Potash and other salts. The energy production (energy saving) of this project is calculated to be 46.5 TWH/year (Hrayshat, 2007).

Photovoltaic applications in Jordan could be divided into two category (Abu Hamed and Bressler, 2019); small projects and huge projects. Small projects implemented on top of dwelling roofs and small building such as warship houses (Mosques), banks and universities. Large scale projects include large scale power plants that produce energy in MW. The increase in the awareness of solar energy benefits in terms of economy and environment has led to invest more in Solar and Clean Energy. Fortunately, the law of renewable energy in 2012 and its amendment in 2014 have encouraged the both; private and public sectors to increase their investment in this field. This opens the door for 2030 vision which aims to increase the dependency on all RE including Solar Power by 10% by the end of 2020 (Abu Hamed and Bressler, 2019).

As a reflection of this law, many householders have adopted PV systems to their own dwelling. They use both on-grid system and off-grid system to run their houses. However, the on-grid system is much popular in Jordan.

In 2014, many ministries have started to adopt PV systems in its own projects. Noticeable projects have been made by the Ministry of Water and Irrigation (MWI) to achieve 15% power saving by the end of 2020. Ministry of Endowments, Islamic Affairs and Holy Places (Awqaf)

advised in 2015 that the power of 600000 Mosques in all the country will be transferred into solar energy. However, major projects of solar energy in Jordan are summarized in Table (4) which shows some projects with their power generation capacity.

	Project Info	location	Power Capacity	Status
1	12 Photovoltaic Project direct-offers and Multiple Generation		200MW	Achieved by 2016
2	IPP PV project-direct proposals.	Mafraq	10MW	By 2019 round one was achieved
3	Complete PV Solar Power plant	Azraq	5MW	In operation since April 2015
4	4 PV projects in	Mafraq, Safawi, And Azraq	200MW	4 MOUs were signed for operation in 2017e2018
5	Qweira PV project	Aqaba	103MW	Contract signed and implementation began in December 2015 with operation expected in 2017
6	Solar Plant to produce electricity for Za'tri refugee camp	Mafraq		Contract signed August 2016; implementation scheduled for 2017
7	Solar power plan	Muwaqqar		Achieving financial close; due for completion by 2018

Table 4: illustration of some solar energy projects in Jordan. (Abu Hamed and Bressler, 2019)

5.2 Technologies of harvesting solar energy.

Distribution of solar rays on a particular area is symmetric and uniform. Solar concentrators are used to harvest biggest amount of solar rays in this area by using large surfaces. These surfaces focus the solar rays that fallen over them onto a small surface. This concentrated energy can be either utilized directly to generate electricity, power, and heat energy or can be stored in tanks of molten salts for 24 hour heat production like those in Gemasolar plant in Spain (Candelaria, 2013).

Mirrors and Fresnel lenses are common methods for concentrating solar energy. However, several types of concentrating technologies can be used to capture the solar energy for solar pyrolysis application such as flat plates, heliostat fields, parabolic dishes, linear Fresnel reflectors, compound parabolic concentrators (Kraemer et al., 2011), parabolic troughs (Hotz et al., 2010), box concentrator type (Saxena, Pandey, & Srivastav, 2011), and linear Fresnel lenses (Baral et al., 2015; Bernardo, Davidsson & Karlsson, 2012). These technologies differ in term of design, focal type, achievable temperature, operating characteristics, and reflective materials. Each of these technologies has its own positive and negative impact on biofuel production by solar pyrolysis, and therefore each technology can be used for specific application (Weldekidan, Strezov & Town, 2018).

For instance, from achievable temperature perspective, flat plate collectors can achieve temperature up to 80 °C in normal situation and up to 125 °C if they are combined with evacuated tubes (Weldekidan, Strezov & Town, 2018). Higher temperature can be achieved by linear compound parabolic which is capable to raise up the temperature up to 200 °C (Blanco et al., 1986), while linear Fresnel can obtain temperatures over than 300 °C (Nixon, Dey & Davies, 2010). Medium temperatures that range from 400 °C to 450 °C can be achieved by parabolic trough (Duffie & Beckman, 2013). According to Abu Bakar et al (2015) and others, the highest temperature that can be obtained by solar energy is around 2000 °C which can be achieved by central receiver system or parabolic dish reflector (Nixon, Dey & Davies, 2010; Tsoutsos, Gekas & Marketaki, 2003).

Solar concentrator	**Achievable Temperature (°C)**	**Concentration design**	**Referance**
Flat plate	80 - 125	Open ambient sunlight	Weldekidan, Strezov & Town, (2018)
Linear compound parabolic	200	Focal line	Blanco et al., (1986)
Linear Fresnel	300	Focal line	Nixon, Dey & Davies, (2010)
Parabolic trough	≥ 400	Focal line	Duffie & Beckman, (2013)
Parabolic dish reflector	≤2000	Focal point	Abu Bakar et al (2015)

Table 5: Type of solar collectors, their achievable temperature levels and concentrating design.

Flat plate technology is run without solar concentration. By adding graphite as solar absorbing material to these plates, thermal foam to the bottom of graphite layer as insulator

to minimize heat losses, and transparent bubble wrap on the top of solar plates, flat plate system is able to produce saturated water steam in open ambient sunlight with around 64% efficiency (Ni et al., 2016). Solar parabolic trough is commonly used for industrial purposes whereby solar panels are arranged to reflect solar rays to a receiver. Solar energy that collected by receiver is used to produce steam.

Excluding parabolic dish reflector, most solar collecting systems give linear focus of solar energy. However, focal point type such as parabolic dish is more productive in term of high heat temperature (Weldekidan, Strezov & Town, 2018). Although different types of solar collector can be utilised in solar pyrolysis, some of them are more beneficial for drying process of sludge more than pyrolysis reaction. Following is a view about common solar collectors that can be used in solar pyrolysis reaction.

5.2.1 Parabolic trough concentrator

It is a U-shaped plat which is symmetrically and straight curved in one dimension as a parabola to reflect and concentrate solar energy into a linear tube in the centre (Figure 30 & 31).

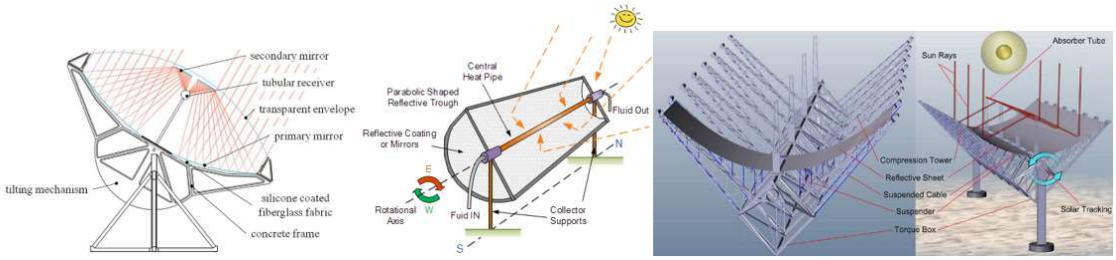

Figure 30: Schemes illustrate parabolic trough concentrator design. (Bader et al., 2009; alternative-energy-tutorials.com; solabolic.com, resp.)

Figure 31: Solar plants use parabolic trough concentrator (energynext.in)

Mirrors or high reflective materials are used to coat the face of parabolic trough from sun side to reflect the solar radiation onto a reactor which is often a tube from a high thermal conductive metal such as copper or evacuated glass (Abid, Ratlamwala & Atikol, 2016). This glass should be able to meet high working temperatures ≥400 °C and high concentration ratio of 30 to 100 (Duffie & Beckman, 2013). Concentration ratio can be defined as the ratio between aperture area which receives concentrated solar energy and the opening are of concentrator. Solar concentration in parabolic can be done through one (Figure 2b) or two stages (figure 2a) (Bader et al., 2009). The reactor should be placed at the line of focal point of parabolic trough. In addition to copper and glass, bimetallic copper-steel can be used efficiently despite of stratification (Flores & Almanza, 2004). According to Lovejoy et al., (1993), parabolic technology is able to provide stagnation temperature up to 600 °C with optical efficiency about 80% and electricity generating rate 354 W/m^2. For pyrolysis of sludge, pyrolysis reactor can be placed either in the focal line for direct heating (Alonso & Romero, 2015) or away from the concentrator and then use heat conveyer or transferring medium (Weldekidan, Strezov & Town, 2018). However, the both methods have technical challenges. Instability and overheating of the reactor are the main risk of direct heating method and complexity of controlling mechanisms for indirect heating method (Nixon, Dey & Davies, 2010).

5.2.2 Linear compound parabolic concentrator (LCPC)

LCPC is a 2D type of Compound Parabolic Collector (CPC) (Antonini et al., 2013). CPC can be described as an ideal collector because it works to collect and focus a large area of sunlight distribution onto a small area with minimal amount of loss (Patel, Brahmbhatt & Panchal, 2018). It is designed with a range of incidence and acceptance angles that able to reflect incident solar radiation on its aperture toward its centre randomly. Due to random reflection, CPC concentrates solar radiation on an area rather than a line or point which results in no forming of image or the light source image. CPCs with smaller concentration ratios don't need to track the sun because of their apertures ability to receive a large ratio of incident diffuse radiation and then concentrate them (Patel, Brahmbhatt & Panchal, 2018). A double-sided absorber or reactor is usually placed in this concentration area which is normally the CPC axis.

The absorber is designed in different shapes such as circular, cylindrical or flat (Gu, Taylor & Rosengarten, 2014).

Although the both CPC an LCPC are non-imaging-type solar energy concentrating collector reflector devices, they have some difference in term of physical design, focus of output energy, and tracking system. LCPC is a linear focus 2D concentrator (Figure 32) that is used generally as stationary collector or a non-tracking solar concentrator (Blanco, Gomez-Leal & Gordon, 1986) whilst CPC is a point focus 3D concentrator (Figure 33) that is used as a solar tracking system (Antonini et al., 2013). The design of CPCs seems like a deep 3D parabola while the common design of LCPC consists of a parabola in the upper section while the bottom section resembles a circle (Figure 32). Thus, focus area of LCPCs extends linearly from edge to edge as a line (Patel, Brahmbhatt & Panchal, 2018).

In the field of solar thermal applications, despite CPCs can achieve high ratios of solar concentration through solar tracking system that can approach the theoretical limits, they are mostly used as static linear concentrators to focus solar light onto tubes at concentration around (~1.5x) (Smestad et al., 1990; Welford & Winston, 1989). While there is no literature about using 3D for pyrolysis of sludge, the ultimate temperature has been achieved by LCPC doesn't exceed 200 °C when concentration ratio is 3 (Weldekidan, Strezov & Town, 2018). Therefore, for sludge pyrolysis process, compound parabolic collectors can be used alone in drying process of sludge but not in the pyrolysis reaction itself which is required 500 to 600 for optimal liquid yield.

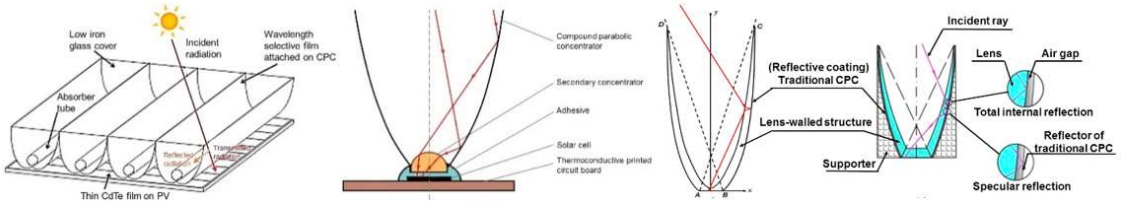

Figure 32: Schematic diagram and cross section of 2D CPC (LCPC). (Tian et al., 2018)

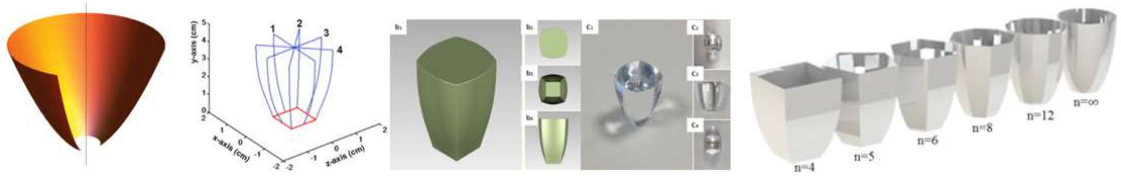

Figure 33: Schematic diagram and design of different types of 3D CPC. (Patel et al., 2018; Tian et al., 2018, resp.)

5.2.3 Linear Fresnel reflectors

Relatively, this type of solar concentrators is the lowest cost among the other types in term of capital cost and maintenance cost (Nixon, Dey & Davies, 2010; Feuermann & Gordon, 1991) because it is made from normal flat mirrors. Practically, long and thin flat mirrors are used to reflect and concentrate sunlight onto a common point or line. The solar reactor or absorber is stationary and placed separately from the mirror field at this common focal point (Figure 34). To enhance the solar energy concentration, a compact linear Fresnel reflector system can be used. In this technology, a rotatable Fresnel linear mirror can be used to track the sun movement and a secondary concentrator such as linear compound parabolic concentrator (LCPC) or parabolic trough concentrator can be combined with linear Fresnels. Secondary reflectors are located at the common focal point of mirrors to increase the total concentration (Wang, 2019). Normal simple linear Fresnels reflector is able to concentrate solar radiation 30 times to achieve 150 °C as operation temperature but, when secondary reflector is integrated with the system, capture efficiency and optical efficiency will improve to 76% and 60% respectively to achieve operational temperature up to 300 °C (Nixon, Dey & Davies, 2010).

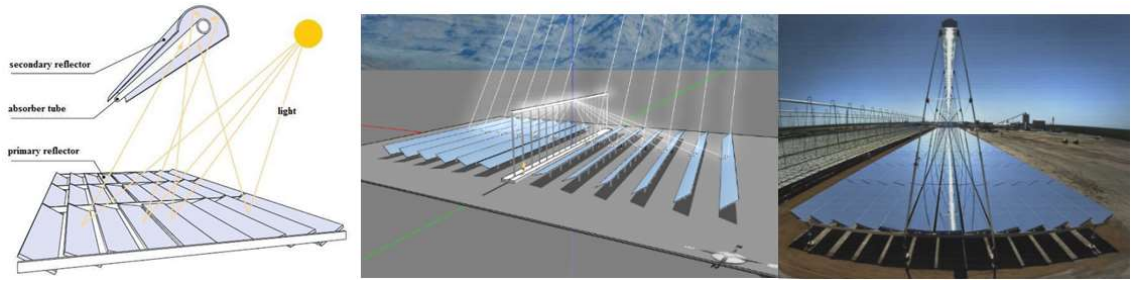

Figure 34: Schematic diagram and design of compact linear Fresnel reflector system. (Gouthamraj, Rani & Satyanarayana 2013; Awesome Inc. theme; fineartamerica.com, resp.)

5.2.4 Parabolic dish reflector

It is a circular coated paraboloid or a coated surface shaped by revolving a half of a parabola around its axis to seem like a dish or satellite antenna (Hafez et al., 2017) (Figure 7). It concentrates incident solar radiation that enters its aperture onto a receiver which is placed at the focal point of reflector (Orosz & Dickes, 2017). For high thermal production, parabolic

dish reflector is the only practical technology that focus solar energy onto a single point rather than linear focal (Pheng et al., 2014). Although it depends on its size, its typical concentration ratio ranges between 500–3000 (Orosz & Dickes, 2017; Tesfay et al., 2014) thus, it is considered the most efficient solar collector (Kalogirou, 2009) and suitable for high temperature production. Its optical efficiency is around 94% (Weldekidan, Strezov & Town, 2018) and its achievable temperature at the reactor reaches 2000 °C (Bakar et al., 2015). In parabolic dish reflector, a two-axis continuous tracking mechanism is required to ensure that solar rays are properly focused onto the focal point throughout the day and hence achieve high performance (Orosz & Dickes, 2017). Parabolic dish reflector works individually as independent generation unit and is rarely connected to other solar collectors in solar field.

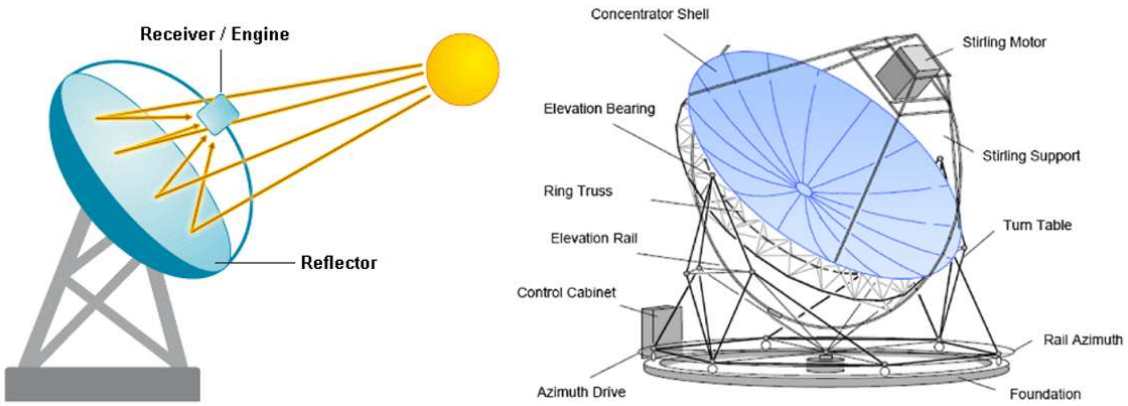

Figure 35: Schematic diagrams illustrate the concept and main parts of parabolic dish reflector. (Shaik Mohasin, 2012; Hafez et al. 2017, resp.)

For pyrolysis of sludge which requires medium to high temperature (450 °C to 900 °C), parabolic dish reflector can be the best solar collector to provide required heat energy. Temperature degrees are simply controlled by using different size of parabolic dish reflector.

5.2.5 Calculating the productivity of solar concentrators

This paper has highlighted the widely used technologies for solar concentration. Following is the mathematical method of calculating productivity and efficiency of the most four common solar concentrators; Linear Compound Parabolic Concentrators (LCPC), Parabolic

Dish Reflectors (PDC), Linear Fresnel Reflector Concentrator (LFR), and Parabolic Trough Concentrator (PTC) (Figure 36).

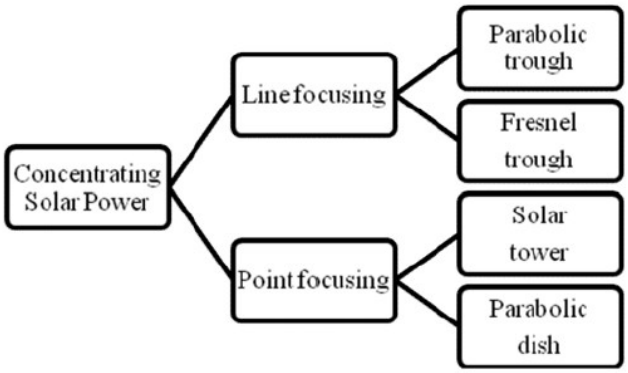

Figure 36: Types of CSP technology

I. Concentrating Solar Power (CSP) general calculation equations

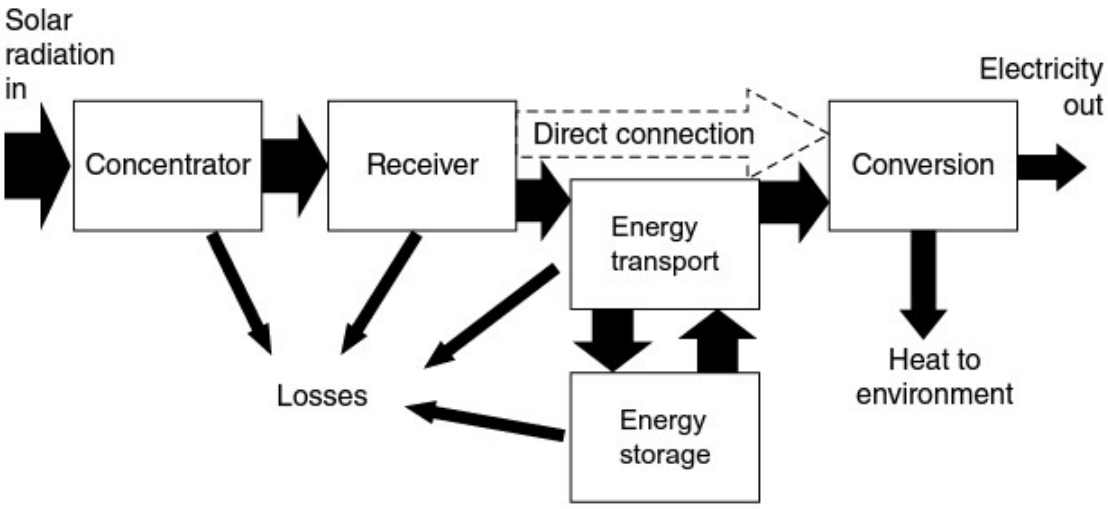

Figure 37: Schematic representation of the component parts of a solar thermal power system

General Terms:

- HTF = heat transfer fluid
- TES = thermal energy storage
- NDI = Normal Directly Irradiation
- C_0 = Optical Concentration ratio
- C_g = geometric concentration ratio

Calculations:

System efficiency η_{system} :

$$\eta_{system} = \eta_{optical} \times \eta_{reciever} \times \eta_{transport} \times \eta_{storage} \times \eta_{conversion}$$

$\eta_{storage}$ is optional, where some power plant or industrial application has no thermal storage unit.

$\eta_{conversion}$ Conversion to any power type or shape. For example to convert to an electric power in Electric-thermal power plant, this value becomes

$$\eta_{conversion} = \eta_{steam\_engine} \times \eta_{turbine} \times \eta_{alternator}$$

Concentrating systems only make use of the Normal Directly Radiated (NDI) component of solar radiation which is the flux density of direct (un-scattered) light from the sun measured on a flat plane perpendicular to the sun's rays.

Insolation flux density or irradiance is the rate of solar radiation energy flow through a unit area of space measured in (W/m^2) (symbol is *G*).

(C_0) is the ratio of irradiance at the receiver surface G_r to the incident solar irradiance *G*:

$$C_0 = \frac{G_r}{G}$$

C_g is the ratio of collector aperture area A_c to receiver area A_r :

$$C_g = \frac{A_c}{A}$$

(CSR) circumsolar ratio is defined by $CSR = \frac{G_{cs}}{G_{cs}+G_s}$

G_s is the solar intensity integrated from just the solar disc out to its limit at 4.65 miliradian (mrad).

G_{cs} is the solar intensity integrated over the annulus from 4.65 mrad to the outer extent of the solar aureole.

Proposed and used sun shape (intensity versus angle) is

$$I_r(\theta) = \begin{cases} \frac{\cos(0.326 \times \theta)}{\cos(0.308 \times \theta)} & 0 \le \theta \le \theta_s \\ \theta^{\gamma} e^{\kappa} & \theta > \theta_s \end{cases}$$

Where

$$\gamma = 2.2 \times CSR^{0.43} \times \ln(0.52 \times CSR) - 0.1$$

$$\kappa = 0.9 \times CSR^{-0.3} \times \ln(13.5 \times CSR)$$

$I_r(\theta)$ is the relative solar intensity, relative to the intensity measured at $\theta = 0^o$

A solar concentrator, whether line focusing or point focusing, needs to be aligned to the direction of the incident solar rays.

Limits on concentration

The solar receiver cannot attain a higher temperature than that of the sun. Using this principle, limits the geometric concentration ratio that can be established. Considering the sun as a black body sphere of radius *r,* a distance *R* from an observer as shown in (Figure 38). At a distance *R* from the sun, all the radiation leaving the surface will be uniformly distributed across a sphere of area $4\pi R^2$. Thus, the irradiance will fall off with distance according to:

$$G = E_0 sin^2(\theta_s) = \sigma \times T_s^4 \times sin^2(\theta_s) = 5.67 \times 10^{-8} \times T_s^4 \times sin^2(\theta_s)$$

σ is the Stefan-Boltzmann constant.

T_s and θ_s are the sun temperature and sun angle respectively

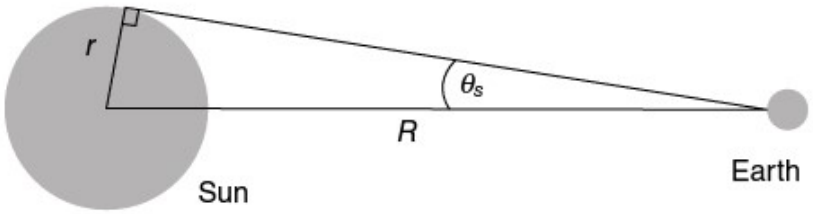

Figure 38: Radiation flux from a spherically symmetric black body falls off as 1/ R2

Thus, any point-focus solar concentrator must has a concentration ratio of no more than

$$C_g = \frac{A_C}{A_R} = \frac{1}{\sin^2(\theta)}$$ For ideal point-focus CSP

Where: A_C = The collector aperture area

A_R = the CSP receiver area

θ = is now generalized to be the acceptance angle (0.27°) which could be more or less than θ_s

More generalization rule considering the spreading angle of insolation radiation by the receiver $\emptyset$

$$C_{g3D} = \frac{A_C}{A_R} = \left(\frac{\sin \emptyset}{\sin \theta}\right)^2$$

Thus, the concentration of radiation can only be achieved by increasing its angular spread$\emptyset$, and this inherently leads to $\emptyset > \theta$

For a line-focus concentrator, then the geometric limitations on acceptance apply only in one direction and $\emptyset = 90$ thus the maximum geometric concertation ratio

$$C_{g2D} = \frac{1}{\sin \theta}$$

So the maximum concentration limit for point focus concentrator is 46250 and for line focus concentrator is 215 only.

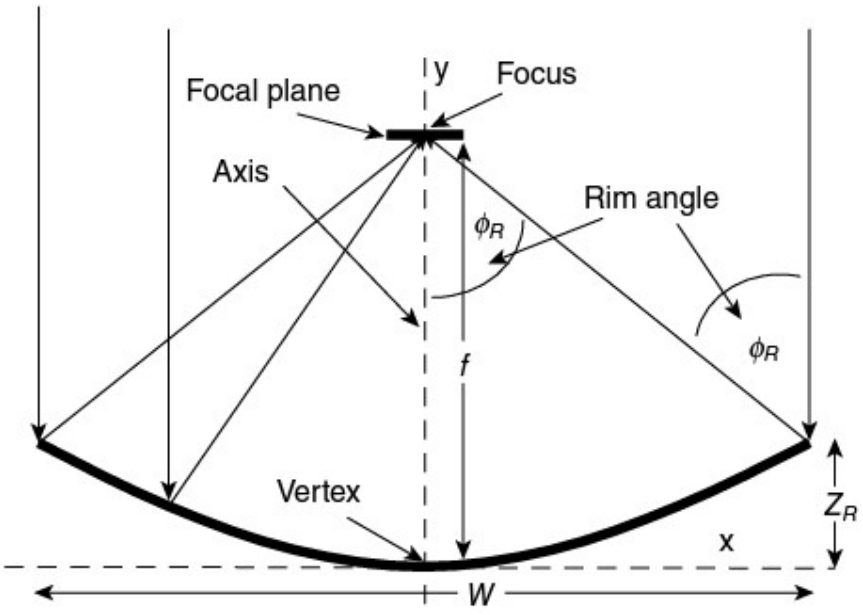

Figure 39: The parabola has the property that, as a reflector, all incident rays parallel to the axis will be reflected to pass through a single point at the focus

For parabolic and paraboloid concentrators:

$\emptyset_R$ is the rim angle calculated as

$$\tan(\emptyset_R) = \frac{W}{2(f - z_R)} = \frac{4fW}{2\left(4f^2 - \left(\frac{W}{2}\right)^2\right)}$$

The width of the receiver (reflected radiation focal spot) d then is $d = \frac{2r \sin \theta_s}{\cos \emptyset_R}$

Where r is the distance from the edge of the receiver to the edge of the collector.

The maximum concentration ratio corresponds to ϕ_R=45°, and gives a maximum concentration ratio for a trough with flat receiver and solar acceptance angle θ_s= 0.266°

$$C_{g,trough,flat,max} = \frac{1}{2 \sin \theta_s} = 108$$

and

$$C_{g,dish,flat,max} = \frac{1}{4 \sin^2 \theta_s} = 11600$$

Thus rim angle for dish and parabolic collectors with flat receivers should be ϕ_R=45°,

<u>Limits for cylindrical and spherical receivers</u>

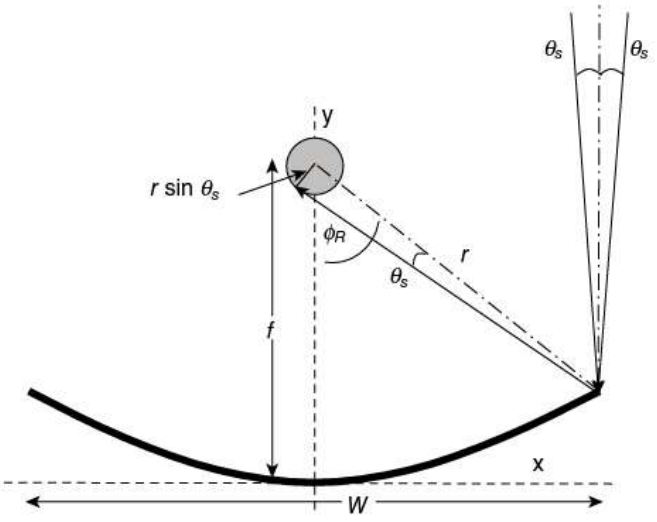

Geometric concentration is

$$C_g = \frac{\sin(\emptyset)}{\pi \sin^2 \theta_s}$$

The maximum angle for this type of receiver is 90° and thus the maximum limit of geometric concentration is

$$C_{g,trough,cyl,max} = \frac{1}{\pi \sin \theta_s} = 68.5$$

and

$$C_{g,dish,sphirical,max} = \frac{1}{4 \sin^2 \theta_s} = 11600$$

Efficiency of optical part of the collector considering all type of error can be described as

$$\eta_{optical} = \frac{\int_{time} \int_{Aperture} G_{incident}(t) dA\, dt}{\int_{time} A_{collector} G_{sol}(t)\, dt}$$

Where

$G_{sol}(t)$ is the time varying NDI,

$G_{incident}(t)$ is the time varying concentrated irradiation at the receiver

$A_{collector}$ is the aperture area of the collector

The total losses of the receiver will be the sum of four losses contributions as

$$\dot{Q}_{loss\_rec} = \dot{Q}_{ref} + \dot{Q}_{rad} + \dot{Q}_{conv} + \dot{Q}_{cond}$$

$\dot{Q}_{ref}$ = reflection losses

$\dot{Q}_{rad}$ = radiative emission losses

$\dot{Q}_{conv}$ = conviction process losses

$\dot{Q}_{cond}$ = conductive process losses

The efficiency of the receiver is

$$\eta_{rec} = \frac{\dot{Q}_{converted}}{\dot{Q}_{input}} = \frac{\dot{Q}_{input} - \dot{Q}_{loss}}{\dot{Q}_{input}}$$

Where

$$\dot{Q}_{input} = \int_{time} \int_{Aperture} G_{incident}(A) dA\, dt$$

Radiation losses:

$$\dot{Q}_{rad} = \sigma A \varepsilon F_{RS}(T_{rec}^4 - T_{env}^4)$$

Where:

σ = Stefen-Boltzman constant

A = Collector aperture area

F_{RS} = is a simplified shape factor between receiver and surroundings.

T_{rec} = receiver temperature in Kalven

T_{env} = environmental temperature in kalven

Reflection losses

$$\dot{Q}_{ref} = (1 - \alpha) A \dot{Q}_{sol}$$

Where α = is the absorptivity of the collector surface

Convection losses is modelled as

$$\dot{Q}_{conv} = hA(T_{rec} - T_{amb})$$

Where

h = is the average convection heat transfer coefficient

A = is the receiver area

Conduction losses

$$\dot{Q}_{cond} = \frac{(T_{rec} - T_{env})}{R_{th}} = kA \frac{(T_{rec} - T_{env})}{L}$$

Where

R_{th} = is the thermal resistance that depends on material conductivity and geometry

A = is the receiver cross sectional area

L = is the thickness of a single homogeneous (insulating) layer

k = is the thermal conductivity

The above calculation is derived from (Lovegrove & Stein, 2012).

II. Thermal linear collector efficiency

The efficiency ŋ of a Parabolic trough collector and linear Fresnel reflector depends on the operating temperature of the collector, the direct normal irradiation Ib and the incidence angle θ i of the solar radiation. The efficiency is defined as the ratio of the thermal power, absorbed by the heat transfer fluid, to the direct normal irradiation on the aperture area (Villamil, Hortúa & Lopez, 2013; Blanco et al., 2000; Wang, Wang & Tang, 2016):

$$\eta = \frac{Q_u}{I_b A_c}$$

$$Q_u = \eta_o I_b A_c - U_c(T_c - T_a)A_a$$

$$\eta_0 = \rho_c(\alpha_c \tau_c)\gamma \cos\theta_i$$

$$U_c = U_{c0} + U_{c1}(T_c - T_a)$$

$$A_a = \frac{A_c}{C}$$

Where

η is the efficiency of the parabolic trough or linear Fresnel

η_o is the optical efficiency

U_c is the solar collector heat transfer loss coefficient that depend on the temperature (W/m^2.°C)

I_b is the direct normal irradiation (W/m^2)

Q_u is the heat received by collector (W)

T_c is the absorber temperature (°C)

T_a is the ambient temperature (°C)

U_{c0} and U_{c1} are constant determined from empirical test (W/m^2.°C)

A_a Total area of the absorber (m^2)

A_c total collector aperture area (m^2)

C is the concentration ratio

ρ_c is the mirror reflectance

α_c is the absorptance of the receiver

τ_c is the transmittance of the receiver (absorber and glass cover)

γ is the intercept efficiency (in most cases it is =1 "assume all reflected ray are intercepted"

ϑ_i is the incidence angle

$cos\ \theta_i$ Varies depends on collector's mirror type and collector direction (East, west, north, or south)

δ is the declination angle (°)

h is the hour angle

then

$$(cos\ \theta_i)_{PT} = \sqrt{1 - \cos^2 \delta \sin^2 h}$$

the incidence angle for Parabolic trough (PT) collector

$$(\cos \theta_i)_{LF} = F(cos\ \theta_i)_{PT}$$

the incidence angle for Linear Fresnel (PT) collector

where

F is a factor empirically evaluated and it is taken equal to 0.7 in some cases.

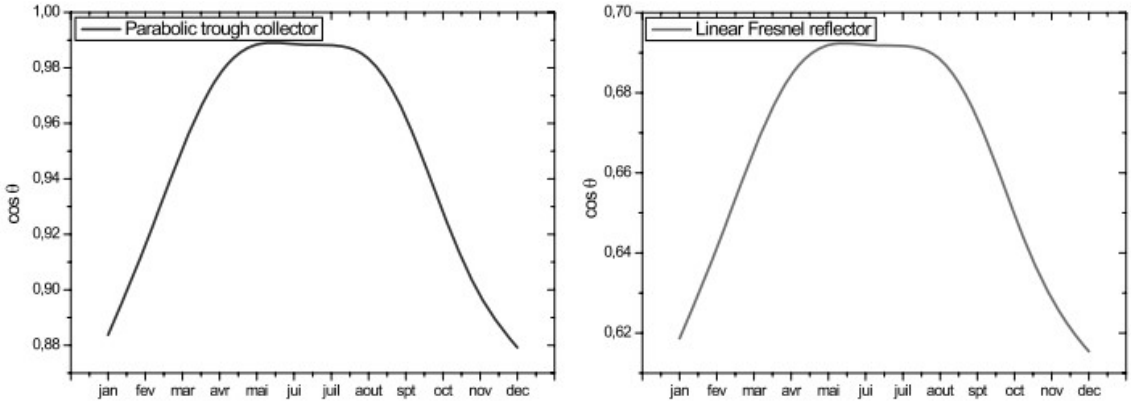

Figure 40: Variation of incidence angle during a typical year For PTC & LFR.

Table (6) below illustrates a compression between these two collectors; parabolic trough and linear Fresnel

	Capacity (MW)	Concen-tration	Peak So. Effic. (%)	Ann. So. Effic. (%)	Capacity so. factor (%)	Temp. out (°C)	Land use per MWh/y (m^2)
Parabolic trough	10 - 200	70-80	21	17-18	25-70	300 - 550	6-8
Linear Fresnel	10 - 200	25-100	20	9-11	25-70	250 - 500	4-6

Table 6: A comparison between parabolic trough and linear Fresnel solar collectors

A comparison study between parabolic trough and Linear Fresnel done in Hassi Rmel region (El Gharbi et al., 2011) located 420 km south of Algiers (Algeria) showed that the calculated annual efficiency of parabolic trough(η_{PT}) is 55.8% while the annual efficiency of Linear Fresnel (η_{LF}) is 47.75%.

III. Linear Fresnel reflector (LFR) technology

Data released thus for (NOVA-1, 2011b) on the Nova-1 technology are:

- Convective thermal loss at coefficient $\mu_0 = 0.056\ W/(m^2K)$
- Radiative thermal loss at coefficient $\mu_1 = 0.000213\ W/(m^2K^2)$
- Power lost $P_{loss} = \mu_0\Delta T + \mu_1\Delta T^2$
- Reference temperature conditions: 40^oC ambient; 100^oC inflow; 270^oC outflow

- Angle-independent optical efficiency $\eta_0 = 0.67$ (for sun in zenith) (with 100% clean primary and secondary reflectors and receiver glass tube)
- No wind assumption stated
- *246.2 kW* per module
- $541 W/m^2$ collected per area of primary reflectors ($502.3 W/m^2$ PE-1)
- $900 W/m^2$ direct normal radiation (DNI) at azimuth angle 0°, zenith angle 30°.

A study was held in 2012 shows that the maximum steam temperature have been reached by using this type of reflectors is $450^o C$.

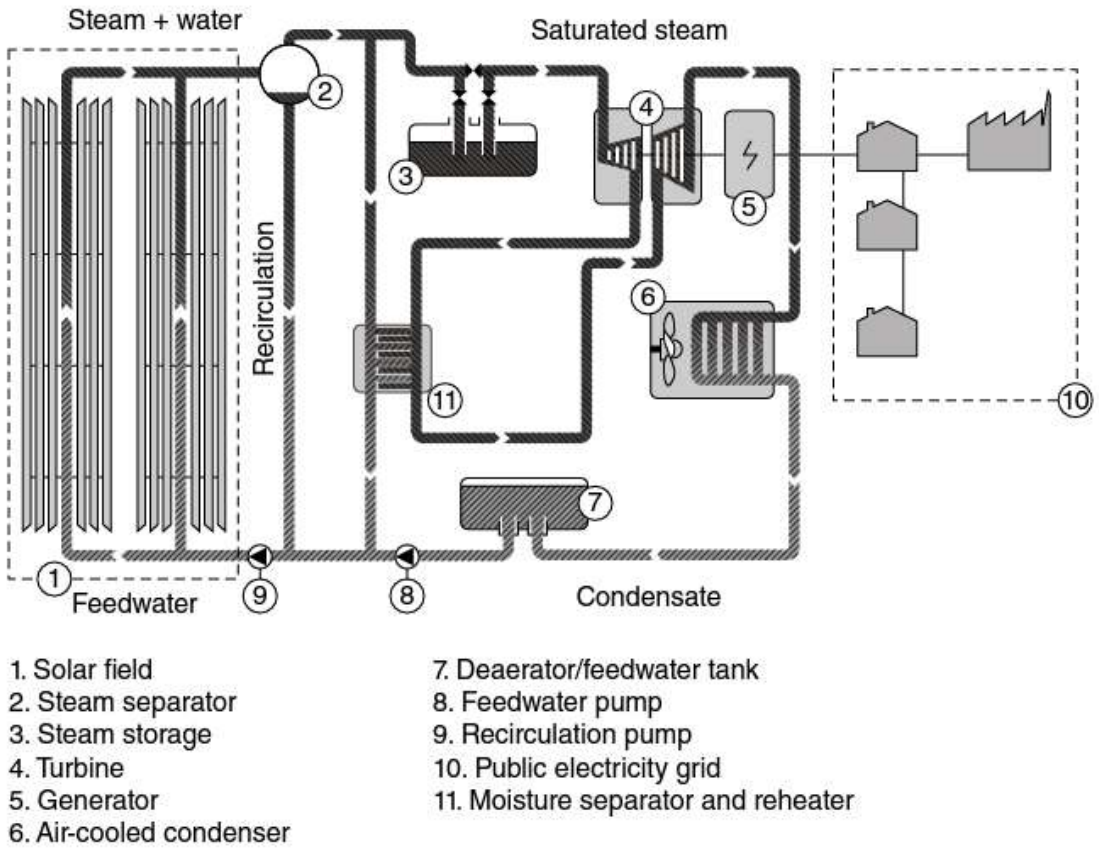

Figure 41: MWe powerplant schematic. The system uses a saturated steam turbine. From Novatec PE-1 brochure (courtesy Novatec Solar GmbH).

ISE thermal Energy loss of hot receiver surface in this reflector is *q'*

$q' = 0.011635.\Delta T^2$ *(W/m²) where* ΔT is the temperature difference in Kalvin between the output fluid temperature and the ambient temperature near the collector.

Novatec Heat losses

$$P_{loss} = \mu_0 \Delta T + \mu_1 \Delta T^2$$

P_{loss} is the heat loss in (W/m^2) of primary reflector

$$\mu_0 = 0.056\ W/(m^2 K)$$

and

$$\mu_1 = 0.000213\ W/(m^2 K^2)$$

Industrial Solar give their loss as simply the thermal loss per m^2 of primary reflector,

$$P_{loss} = 0.00043\ W/(m^2 K^2)$$

Where

- Ambient temperature is supposed to be = 303K
- Optical efficiency = 22.3%
- Sun zenith angle = 5°
- The central reflector is shaded with the sun at zenith and the figure is consequently slightly lower at solar noon

SCHOTTSOLAR and NREL provide another (energy) heat loss as follows with assumption that the output fluid temperature = 500°C (Collares-Pereira, Canavarro & Guerreiro, 2017).

$H_T = 0.141 \times T_{abs} + 6.48 \times 10^{-9} \times T_{abs}^4$ (W/m) (m is the tubular length)

T_{abs} is the fluid output temperature in (°C)

The electricity produced can be calculated on an hourly basis according to

$$q_{el.h} = \left[A_{col} \times DNI \times \eta_{opt} \times \eta_{int} \times K_L \times K_T - T_{htf} \times (H_T + H_P + H_R)\right]^+ \times \eta_S \times \eta_T$$

- A_{col} is the total mirror area of the collector
- T_{htf} is the temperature of the heated fluid (Higher temperature Fluid)

- H_R is the heat loos of the receiver
- H_P the heat losses of the connecting pipes
- η_S is the efficiency of the steam generation
- η_T is the efficiency of the turbine
- $'+'$ means only the positive value of the brackets to be considered

The yearly sum of produced electricity then is

$$Q_{el,year} = \sum_{i=1}^{8760} q_{el.h}$$

Note: the electrical energy generated by the concentrator can be calculated based on (W/m) or (W/m^{2}k^2) from P_{loss} and H_T equations above multiplied by the efficiency of the turbine. Which leads to the final two equations (Collares-Pereira, Canavarro & Guerreiro, 2017).

Example of LFR data and efficiency

According to Lovegrove & Stein (2012) and Collares-Pereira, Canavarro & Guerreiro (2017), industrial LFR reflectors, for example, those made by Industrial Solar (2011) have been developed and provided with a superheated LFR steam generator of 400^{o}C temperature which is used to generate electricity. The data provided by Industrial Solar Company about their LFR concentrator are:

- Thermal loss at 400^{o}C (μ= 0.00043 W/(m^{2}k^2))
- Temperatures of the system (ambient =30^{o}C; inflow = 160^{o}C; outflow = 180^{o}C)
- Angle-independent optical efficiency (100% clean primary and secondary reflectors and receiver glass tube)
- Optical efficiency $\eta_o = 0.635$ (sun in zenith)
- $\eta_{max} = 0.663$ (sun at 5^o transversal zenith angle)
- Mirror reflectivity 95%
- Receiver thermal emittance @380^{o}C = 9%

- Solar absorptance direct = 95%

IV. Parabolic-trough concentrating solar power (CSP) systems

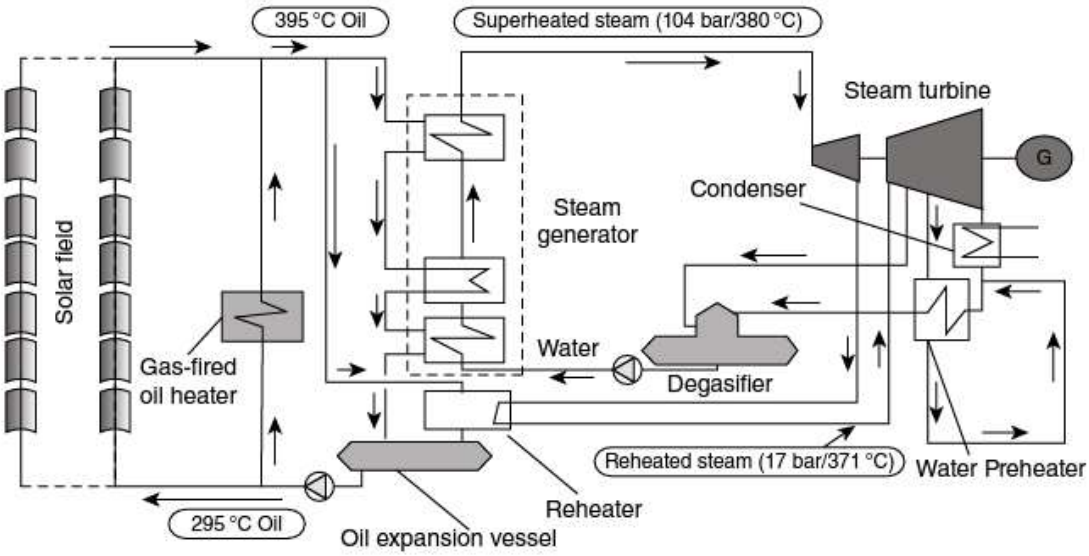

Figure 42: Schematic configuration of a typical SEGS plant using parabolic trough concentrator. (Lovegrove & Stein, 2012)

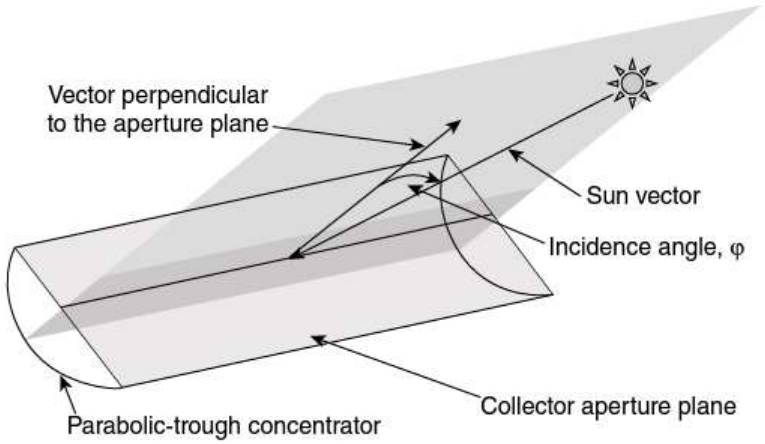

Figure 43: Correct positioning of a parabolic-trough concentrator. (Lovegrove & Stein, 2012)

Commercial PTC designs for solar thermal power plants are 100 m to 150 m long, and have a parabola width of about 6 m, which provides an aperture area of 550 m^2 to 825 m^2 approximately.

The angle defined by the two vectors shown in (Figure 40) is called the incidence angle. As the smaller the incidence angle, the more incident solar flux can be reflected and converted into useful thermal energy in the receiver pipe. The most important PTC parameters are the geometric concentration ratio, acceptance angle, rim angle and peak optical efficiency. These parameters are explained in the following paragraphs. The geometric concentration ratio, C_g, is the ratio between the collector aperture area and the total absorber tube area. This concentration ratio is usually about 25, although theoretically, the maximum is about 70. High concentration ratios are associated with higher working temperatures. The Geometric concentration ratio, C_g, is given by

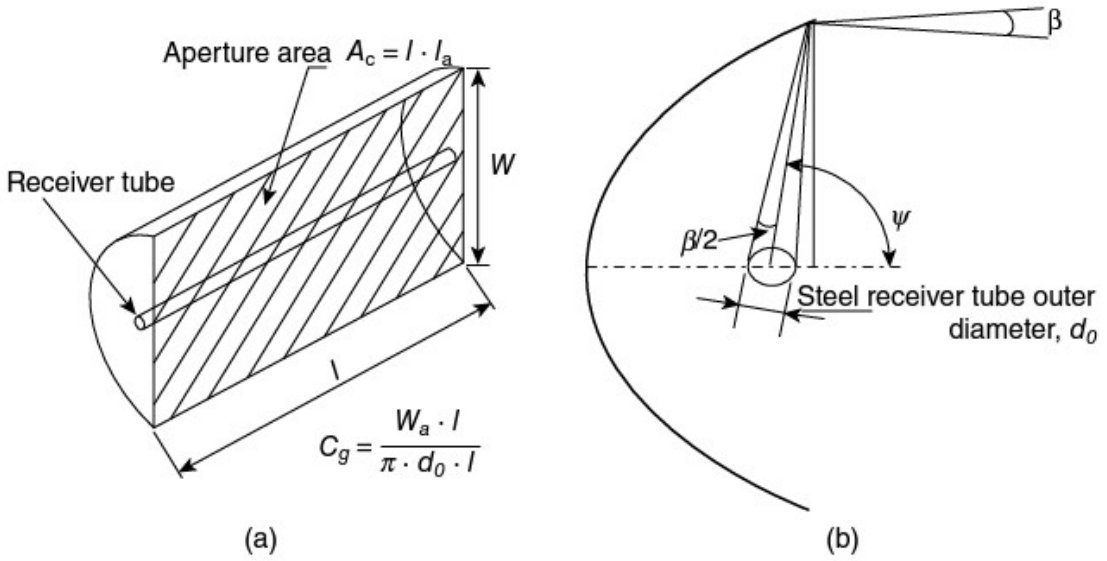

Figure 44: (a) Geometric concentration ratio, Cg , and (b) acceptance angle, β and aperture angle, ψ of a parabolic-trough collector.

$$C_g = \frac{W_a l}{\pi d_o l} = \frac{W}{\pi d_o}$$

Where

- d_o is the outer diameter of the receiver steel pipe
- l is collector length
- W is the parabola width.
- The acceptance angle, β, is the maximum angle that can be formed by two rays on a plane transversal to the collector aperture in such a way that, when they are reflected by the parabolic mirrors, they intercept the absorber pipe. The minimum acceptance angle is 32 ′ (0.53°), which is the average solid angle with which the solar disk is seen from the Earth. Most commercial PTC designs have acceptance angles within the range 1–2°, with geometric concentration ratios of 20 to 30

The rim angle, ψ , which is directly related to the concentrator arc length, can be calculated from as a function of the parabola focal distance, f , and aperture width, W :

$$\tan\psi = \frac{8fW}{W^2 - 16f^2}$$

Optical losses are very important in parabolic-trough collectors because they are about 25% of the total solar flux incident on the PTC aperture plane. Optical losses are associated with the following four parameters:

- Reflectivity, ρ , of the collector reflective surface. Typical reflectivity values of clean silvered glass mirrors are around 0.93.
- Intercept factor, Υ . A fraction of the direct solar radiation reflected by the mirrors does not reach the active surface of the receiver pipe due to either microscopic imperfections of the reflectors, macroscopic errors in the parabolic-trough concentrator shape (e.g., inaccuracies during assembly), mechanical deformation of the PTC, flexible bellows, etc. This optical parameter is typically within the 0.91–0.93 range for high-quality PTCs because γ 1 ≅ 0.97, γ 2 ≅ 0.96 and γ 3 ≅ 0.99 where
  - γ_1 is geometrical errors in the parabolic-trough concentrator shape.
  - γ_2 is shadowing by the flexible bellows
  - γ_3 is the mechanical deformation of the support structure

  And therefore

$$\Upsilon = \gamma_1 \times \gamma_2 \times \gamma_3$$

- Transmissivity of the glass cover, τ. It is typically τ = 0.93, and can be increased up to 0.96 by anti-reflective coatings applied on both sides of the glass cover.
- Absorptivity of the receiver selective coating, α. It is typically 0.95 for receiver pipes with a cermet selective coating, and slightly lower for pipes coated with black nickel or chrome.

The peak optical efficiency of the PTC, $\eta_{\text{opt},0^o}$:

$$\eta_{\text{opt},0^o} = \rho \times \Upsilon \times \tau \times \alpha|_{\varphi=0}$$

$\eta_{\text{opt},0^o}$ is usually in the range 0.74–0.79 for clean, good-quality parabolic trough collectors.

Incidence angle modifier, *K(ϕ),* a modifier used to modify above equation if $\varphi \neq 0$, thus

$$\eta_{\text{ opt},\varphi\neq 0^o} = \eta_{\text{ opt},0^o} \times K(\varphi)$$

K(ϕ), determined by the PTC designer such as in LS-3 PTC power plant by a polynomial function

$$k(\varphi) = \{1 \qquad \varphi = 0\}$$

$$k(\varphi) = \begin{Bmatrix} 1 - 2.23 \times 10^{-4} \times \varphi - 1.1 \times 10^{-4} \times \varphi^2 + 3.186 \times 10^{-6} \times \varphi^3 - 4.855 \times 10^{-8} \times \varphi^4 & 0^o < \varphi < 80^o \\ 0 & 85^o < \varphi < 90^o \end{Bmatrix}$$

Heat losses and energy

- $\dot{Q}_{collector\_ambient}$ is the total thermal losses in a PTC
- $\dot{Q}_{absorber\_ambient}$ is the radiative heat losses from the steel receiver tube
- $\dot{Q}_{absorber\_glass}$ is the convective and conductive heat losses from it to its glass cover
- $\dot{Q}_{sun\_collector}$ is the solar energy f lux incident on the aperture plane
- $\dot{Q}_{collector\_fluid}$ is the useful thermal energy delivered by the PTC

Today's high temperature PTCs are provided with evacuated receiver pipes, thus avoiding convection losses between the steel pipe and its glass cover.

The efficiency of the entire PTC systems is η_{system} calculated as

$$\eta_{system} = \frac{\dot{Q}_{collector\_fluid}}{\dot{Q}_{sun\_collector}}$$

and

$$\dot{Q}_{sun\_collector} = A_c \cdot E_d \cdot \cos(\varphi)$$

$$\dot{Q}_{collector\_fluid} = \dot{m} \cdot (h_{out} - h_{in})$$

Where

- A_c is the collector aperture surface area.

- E_d is the direct solar irradiance (DNI)
- φ is the incidence angle
- $\dot{m}$ is the fluid mass flow through the collector receiver tube
- h_{out} is the fluid specific mass enthalpy at the collector outlet
- h_{in} is the fluid specific mass enthalpy at the collector inlet

Since the fluid mass flow and the inlet and outlet temperatures are not known during the solar field design phase, the expected net thermal output has to be theoretically calculated from the energy balance, and direct solar irradiance, ambient air temperature, incidence angle and PTC optical, thermal and geometrical parameters using

$$\dot{Q}_{collector\_fluid} = A_c \cdot E_d \cdot \cos\varphi \cdot \eta_{opt,0^o} \cdot K(\varphi) \cdot F_e - \dot{Q}_{collector\_ambient}$$

Where

- F_e Soiling factor, which is calculated as the ratio between average PTC mirror reflectivity during real operation and the nominal reflectivity when the PTC is completely clean. Usually, $F_e = 0.978$ and $0.95 < F_e < 1$

Design of parabolic-trough solar fields for CSP plants

A typical parabolic-trough collector field is composed of parallel rows of collectors. Each row is composed of several collectors connected in series. There are three stages in parabolic-trough collector solar field design:

There are three stages in parabolic-trough collector solar field design:

1. Define the design point, which is the set of assumed design values.
    a. Conceder
        i. local weather conditions
        ii. parameters of the PTC design chosen and customer specifications
        iii. Collector orientation
        iv. Design point date (month and day) and time

v. site location (latitude and longitude)
vi. direct solar irradiance and ambient air temperature for the selected date, time and location
vii. total thermal output power to be delivered by the solar field
viii. soiling factor of the solar field
ix. solar field inlet/outlet temperatures
x. solar collector working fluid
xi. Nominal fluid flow rate. The higher the mass flow the smaller the temperature difference that can be provided by a single parabolic-trough collector at design point.

2. Calculate the number of parabolic-trough collectors to be connected in series in each parallel row (n).
    a. Number of PTC that are connected in series in each row is

$$n_{PTC\_row\_series} = \frac{\Delta T_{HTF\ required-ambien}}{\Delta T_{outlet-inlet/collector}}$$

$\Delta T_{HTF\ required-ambient}$ is the difference in temperature between required operating temperature and ambient temperature.

$\Delta T_{outlet-inle\ /collector}$ Temperature difference that can be provided by a single collector at design point at the designed nominal fluid flow rate

3. Calculate the number of parallel rows to be installed in the solar field (N).

$$N = \frac{thermal\ power\ demanded\ by\ the\ industrial\ process\ to\ be\ supplied\ by\ the\ solar\ field}{thermal\ power\ delivered\ by\ a\ single\ row\ of\ collectors\ at\ desi\quad point}$$

N depends also on whether the plant have thermal storage system or not.

Two parameters are essential for calculation of solar field size and rated plant power: the solar multiple and the capacity factor. The solar multiple is the ratio between the solar field

thermal output at design point (the design point is set at noon on a summer day) and the thermal power required to feed the power block at nominal (rated) power. The capacity factor of the solar plant is the ratio between the number of equivalent full-load solar-only operating hours a year and the maximum number of hours of plant operation if it were operated around the clock (365 × 24 = 8,760 hours).

Table (7) illustrates the design specifications of two recent Solar Energy Generating Systems (SEGS) are used in plant built by LUZ International (Lovegrove & Stein, 2012).

	SEGS 8	SEGS 9
Duration service	1989-Present	1990-Present
Net Electric power	80 MW	80 MW
Efficiency in solar mode (%)	37.6	37.6
PTC model	LS3	LS3
Total aperture area (m^2)	464340	483960
Solar field inlet/outlet temperatures (^oC)	293/390	293/390
Synthetic oil (HTF)	M-PV1	M-PV1

Table 7: Specifications of two generation of SEGS; 8 &9. (Lovegrove & Stein, 2012)

V. Parabolic dish concentrating solar power (PDC) systems

Dish concentrators have the highest optical efficiencies, the highest concentration ratios and the highest overall conversion efficiencies of all the CSP technologies.

Omara (2013) designed a solar dish concentrator for water desalination. The system produce a daily average of distillate water of 6.7 L/m2/day for the PDC with preheating of brackish water. In Omara's study, the daily average efficiency of PDC was 68%. However, no information about the size of the plant is available in the reference (Zheng, 2017).

Basic principles:

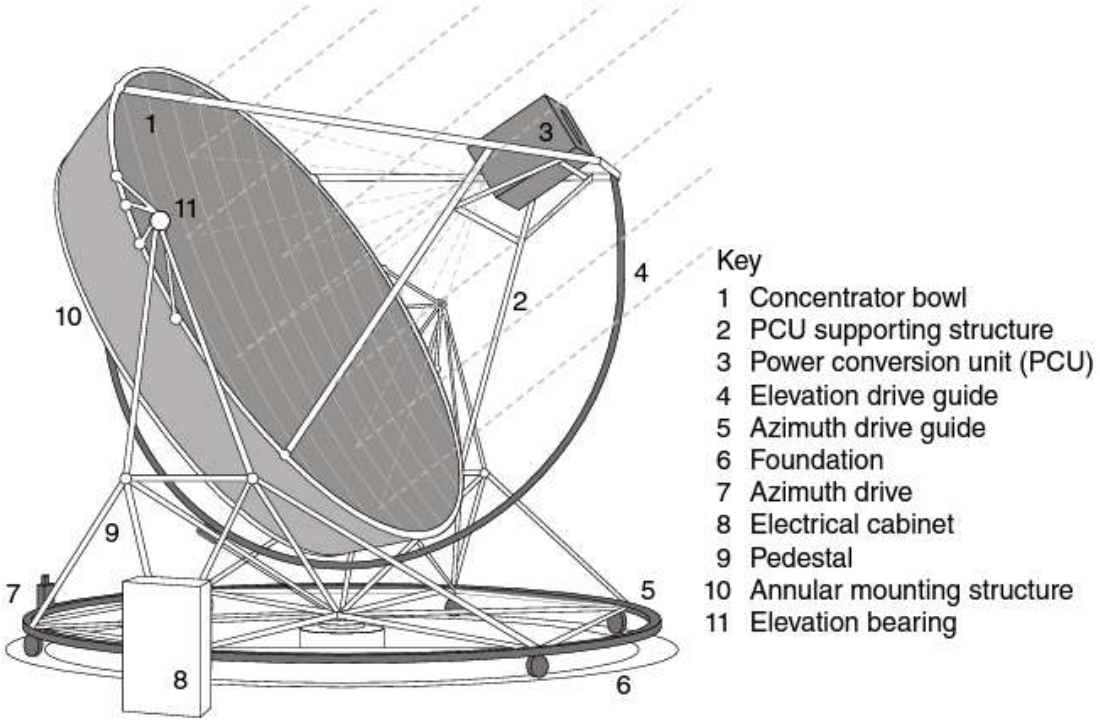

Figure 45: Schematic representation of a dish system. (Lovegrove & Stein, 2012)

A dish system consists of:

1. a parabolic shaped concentrator,
2. tracking system,
3. solar heat exchanger (receiver),
4. an (optional) engine with generator and
5. a system control unit

Figure 46: Steps of design a parabolic solar dish. (Lovegrove & Stein, 2012)

Calculation

Following are the equations of the best design of Parabolic Dish Concentrators (PDC) according to Hafez et al. (2016) and Villamil, Hortúa & Lopez (2013).

The receiver useful output energy to the fluid measured by W/m is

$$Q_{out} = CI\rho K$$

Or, it could be derived by

$$Q_{optical} = A_{collc}\alpha_c\tau_v\rho SI$$

Where

C = is the concentration ratio of the solar dish

I = direct solar radiation on the solar dish, W/m^2

ρ = reflectivity of the concentrator

K = the thermal conductivity coefficient of the receiver, W/(m.K)

$$K = \alpha_c\tau_v * U_L$$

α_c = the absorptance of the material of the receiver.

τ_v = the transmittance of the glass cover of the receiver pipes

S = the shape factor

$$C = \frac{A_{collector}}{A_{rec}}$$

Where

$A_{collector}$ is the area of the dish collector (concentrator) and A_{rec} is the area of the point receiver.

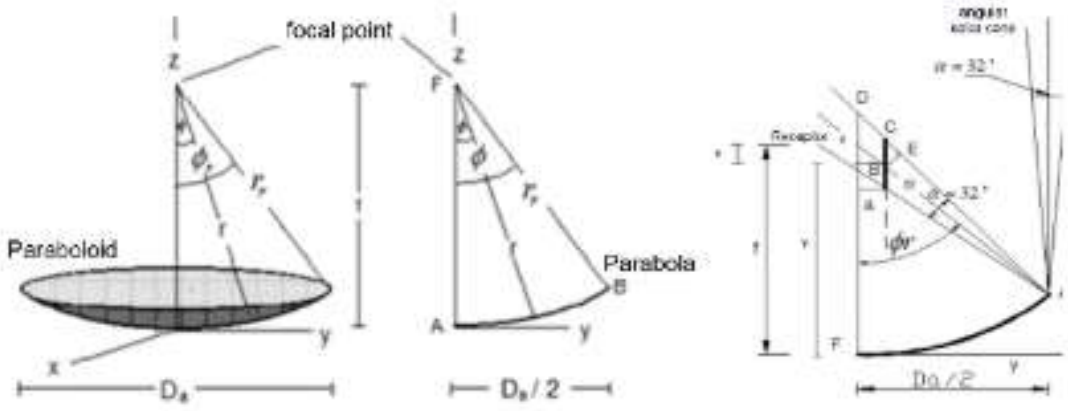

Figure 47: Geometry and dimension of the solar collector parabolic dish (Hafez et al., 2016)

The usable energy output of the receiver is (Villamil, Hortúa & Lopez, 2013)

$$Q_{out} = Q_{opt} - Q_{loss}$$

Q_{out} = is the usable energy from the receiver,

Q_{opt} = total optical energy reach the receiver

Q_{loss} = Energy losses by the system and fluid

U_L = the receiver fluid coefficient of heat losses

$$U_L = \left[\frac{1}{h_c + h_r}\right]^{-1} \ (W/m^2.K)$$

h_c = receiver fluid convection coefficient

$$h_c = \frac{k_{fluid}}{D_{rec}} \times N$$

k_{fluid} = thermal coefficient of the receiver fluid (HTF)

D_{rec} = diameter of the receiver.

N = Nusslet number.

h_r = receiver fluid radiation coefficient

$$h_r = 4\sigma\epsilon_r T_{fluid}^3$$

σ = Stefen-Boltzman constant

ϵ_r = Emissivity del receiver

T_{fluid} = average temperature of the fluid running inside the receivers pipe.

then

$$Q_{loss} = A_{rec}U_L\left(T_{recfluidout} - T_{amb}\right)$$

System instantaneous efficiency can be calculated for each dish as follows:

$$\eta_{dish-insta} = \frac{Q_{out}}{A_{coll} \times I}$$

To calculate the collector area

$$A_{coll} = \frac{\pi {D_a}^2}{4}$$

D_a = is the dish apparatus diameter (Figure, 47)

$\emptyset$ = is the rim angle, from the first section, optimum rim angle is 90° for the dish type and 45° for linear type. However it could be changed according to the design, location and shape. It will be much better if it is very close to 90°. Thus,

$$\emptyset = 2 \times \tan^{-1}\left(\frac{D_a}{4f}\right)$$

and

$$r_r = \frac{2f}{1 + \cos\emptyset}$$

r_r = is the receiver distance (focal point) from the edge of the dish (m)

f = is the distance from any point of the dish surface to the focal point (receiver)

Now to calculate the area of the receiver (A_{rec})

$$A_{rec} = 2\pi ah$$

h = is the contact surface of the receiver cylinder

$$h = \frac{2 \times R_r}{\cos(\alpha - \emptyset)}$$

$$\alpha = 90 + \frac{\theta_{sun}}{2}$$ (All are measured in degrees)

a = is the height of the receiver shape (it is considered to be almost cylindrical in this case)

θ_{sun} = the sun angle as it is seen by a circular dish in radian. It depends on the location and it's too small (0.266° to 0.53°) according to (Villamil, Hortúa & Lopez, 2013). It can be obtained from solar and geometry data.

R_r = is the receiver (receptor) radius

$$R_r = (r_r - c) \times \sin(\frac{\theta_{sun}}{2})$$

c = is a hypotenuse distance between the focus and the dish boarders (edge)

$$c = \frac{a}{\sin(\emptyset)}$$

Optimal focal length

$$f_{optim} = \frac{D_a}{4 \times \tan\left(\frac{\emptyset}{2}\right)}$$

Shape factor (*S*)

$$S = \frac{A_a - A_t}{\mathrm{A}_a}$$

A_t = is the fraction of the concentrator (collector) aperture area, which is not shadowed by receptor at noon.

$$A_t = A_a - A_{receptor\ base}$$

Dish optical efficiency is calculated by

$$\eta_{opt} = \alpha_c \tau_v \rho S$$

Average temperature of the receiver fluid can be estimated by

$$T_{recfluidout} = \frac{T_{amb} + T_{sun} \times \left[\left(1 - \eta_{opt}\right) \times \frac{\eta_{opt} \times C_{max}}{46311 \times \epsilon_r}\right]}{2}$$

VI. Linear compound parabolic concentrators (LCPC) and compound parabolic concentrator (CPC)

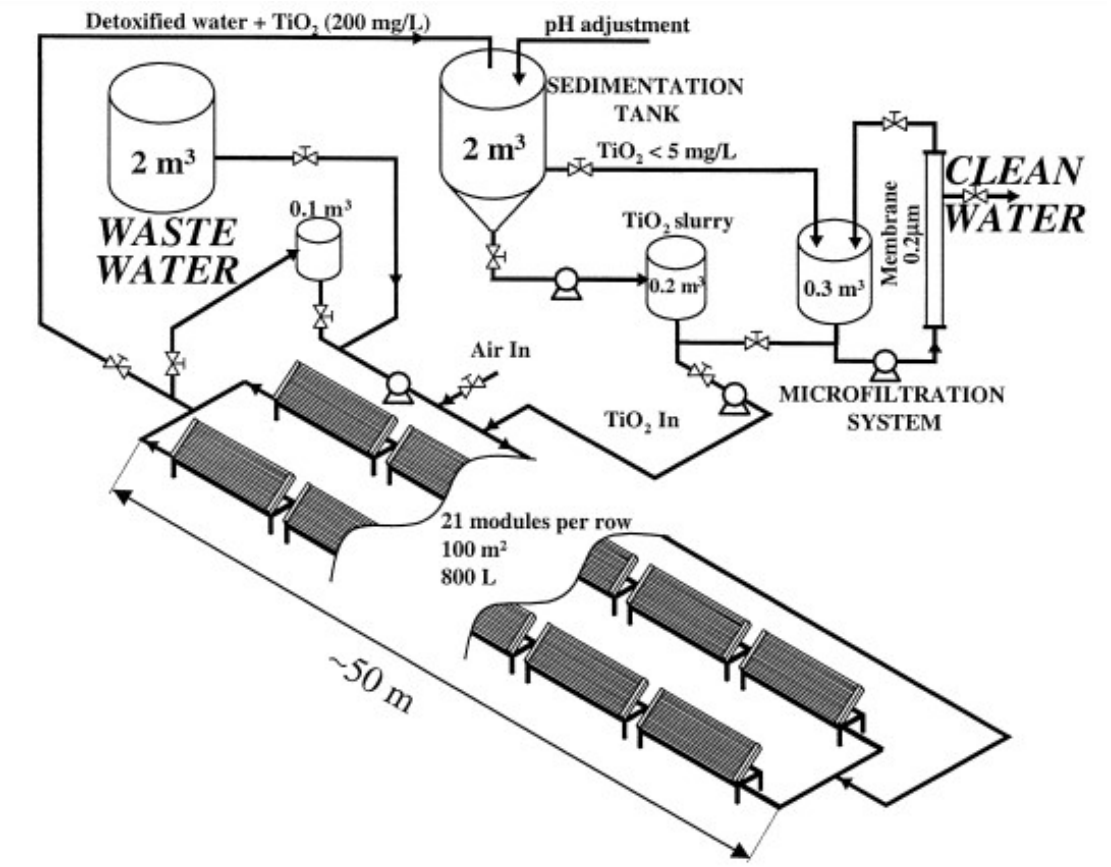

Figure 48: Isometric drawing of solar detoxification demonstration plant. (Blanco et al., 2000)

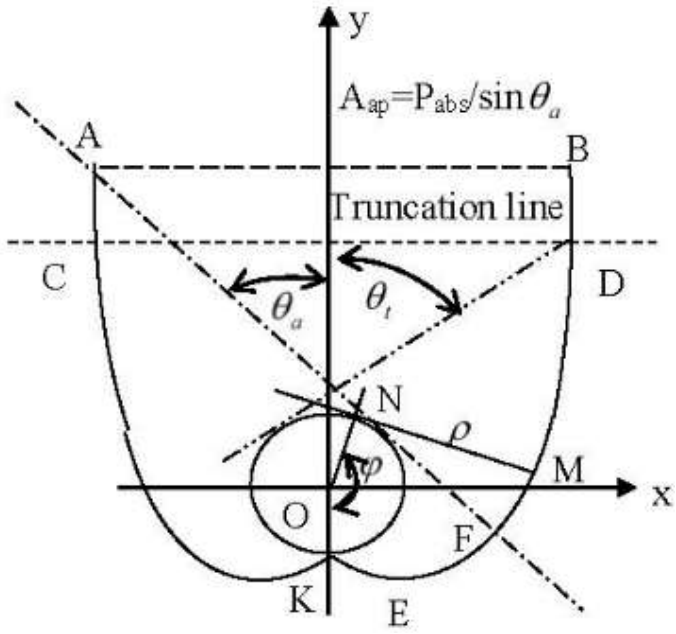

Figure 49: Geometry of a tubular absorber ideal solar concentrator. (Wang, Wang & Tang, 2016)

LCPC & CPC have been studied by Umair, Akisawa & Ueda, (2014) and Oommen & Jayaraman, (2001). According to their study, following are the governing equations of LCPC & CPC

The CPC cover temperature is given by:

$$(M_c Cp_c)\frac{dT_c}{dt} = Q_c + [(h_{Rr} + h_{rc})(T_{ab} - T_c)] - \left[h_{Rs}\left(T_c - T_{sky}\right)\right] - [h_{ca}(T_c - T_{air})]$$

where

Q_c = is the energy absorbed by the cover

M_c = is the mass of the cover

Cp_c= is the specific of the cover heat (J/kg·K)

h_{Rr} = is the radiation heat transfer coefficient between the receiver and the cover (W/m^2·K)

h_{rc} = is the convective heat transfer coefficient between the cover and the receiver (W/m^2·K)

T_{ab} = is the temperature of the absorber (K)

T_c = is the temperature of the cover (K)

h_{Rs} = is the radiation heat transfer coefficient between the cover and the sky (W/m^2·K)

T_{sky} = temperature of the sky (K)

h_{ca} = is the convective heat transfer coefficient from the cover due to wind (W/m^2·K)

T_{air} = is the temperature of the air (ambient temperature) (K)

And

$$Q_c = A_c I_{bm} cos\theta_i \left(\alpha_c + \alpha_c \tau_c \rho_{ab} \rho_{cpc}^{nr}\right)\frac{A_c}{A_{ab}}$$

Where:

A_c = is the total area of the cover (m^2)

A_{ab} = is the total area of the absorber (m^2)

I_{bm} = is the direct normal solar irradiation beam (W/m^2)

θ_i = is the angle of incidence (º)

α_c = is the absorptance of the cover.

τ_c = is the transmittance of the cover.

ρ_{cpc}^{nr} = is the average number of reflections of the compound parabolic concentrator

ρ_{ab} = is the reflectance of the absorber

The CPC absorber temperature is given by

$$(M_{ab}Cp_{cu})\frac{dT_{ab}}{dt} = Q_{ab} - [(h_{Rr} + h_{rc})(T_{ab} - T_c)]$$

M_{ab} = is the mass of the absorber (Kg)

Cp_{cu} = copper specific heat ((J/kg·K)

Q_{ab} = is the energy of the absorber (W)

$$Q_{ab} = A_{ab}\left(FI_{bm}\cos\theta_i\,\tau_{cpc}\tau_c\alpha_{ab} + I_{diff}\tau_{cpc}\tau_{diff}\alpha_{ab}\right)$$

F = is the control factor for whether the radiation is accepted by the CPC (1 or 0

I_{diff} = is the geometric insolation-diffused irradiation (W/m2)

τ_{diff} = transmittance of the diffuser.

$$\left(\beta - \theta_{cpc}\right) \le \tan^{-1}(\tan\theta_z\cos\gamma_s) \le \left(\beta + \theta_{cpc}\right)$$

β = is the tilt angle (°)

θ_{cpc} = is the half sun acceptance angle (°)

θ_z = is the zenith angle (°)

γ_s = is the solar azimuth angle (°)

Then the useful system energy $Q_{usefull}$

$$Q_{usefull} = Q_{ab} - Q_{loss}$$

And the lost energy

$$Q_{loss} = A_{ab}F^1U_L(T_{av} - T_a)$$

Where:

F^1 = is the heat transfer factor of the fluid

U_L = is the heat loss coefficient of the fluid

T_{av} = average temperature of the fluid

T_a = is the ambient (air temperature)

System instantaneous efficiency η_i then [11]is

$$\eta_i = \frac{\dot{m}Cp_{HTF}(T_{fuid\ out} - T_{fluid\ in})}{I_{eff} \times A_c}$$

$$I_{eff} = I_{bm}\cos\theta_i + \left(\frac{I_{diff}}{CR}\right)$$

CR = is the CPC concentration ration

$$CR = \frac{A_c}{A_{ab}}$$

I_{eff} = is the effective irradiation (W)

$\dot{m}$ = is the mass flow rate (kg/s)

Cp_w = is the specific heat of heated fluid.

$$\eta_i = \frac{m\left[Cp_{HTF}\left(T_{fuid\ out} - T_{fluid\ in}\right) + L\right]}{I_{eff} \times A_c \times t}$$

m = is the mass of the condensate fluid inside the CPC pipes

L = is the latent heat of vaporization of water

t = is the condensation time in seconds

Design of Compound Parabolic Solar Concentrators is shown by (Wang, Wang & Tang, 2016). They used All-Glass Evacuated Solar Tube as Receiver. However, for water heating system, at 100o C and normal pressure, the instantaneous efficiency of this system is calculated to be 28%.

5.3 Arrangement and installation of solar harvesting system

Despite most studies on solar pyrolysis of sludge are at pilot scale, there are different trials around the world to build facilities use the actual solar input for thermochemical processes at industrial scale (Yadav & Banerjee, 2016). These days, there are solar plants in Spain,

Germany, Australia, and the US. In these facilities, different ways have been used to install the solar system; a typical horizontal on-axis solar arrangement (Hinkley, McNaughton & Neumann, 2010), a horizontal off-axis solar arrangement (Institute of Solar Research in Germany DLR, 2015), a vertical axis solar arrangement (Rodriguez, Canadas & Zarza, 2014), and a beam down solar arrangement which known as tower top arrangement (Epstein et al. 2008). For typical horizontal on-axis solar systems (Figure 50), losses in the incoming solar energy experienced because of the experimental platform that sets between concentrator and heliostat. The arrangement off-axis solar systems (Figure 51) has been set up to address this issue. However, this arrangement cannot achieve the maximum optical performance because of the non-symmetricity of the beam from the focal plane. However, horizontal axis design results in losses in melted materials, therefore a vertical axis arrangement (Figure 52) has been developed to make the focus horizontally (Yadav & Banerjee, 2016).

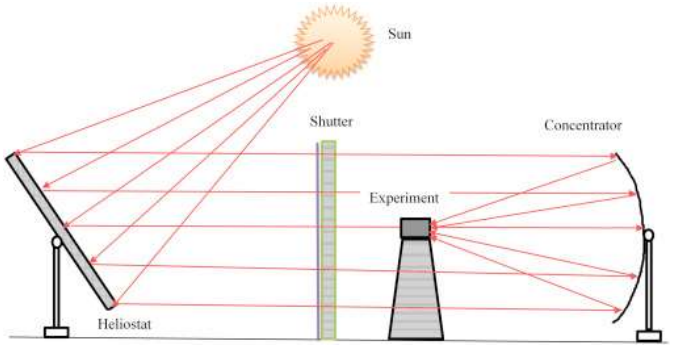

Figure 50: Schematic of typical horizontal on-axis solar design. (Hinkley, McNaughton & Neumann, 2010)

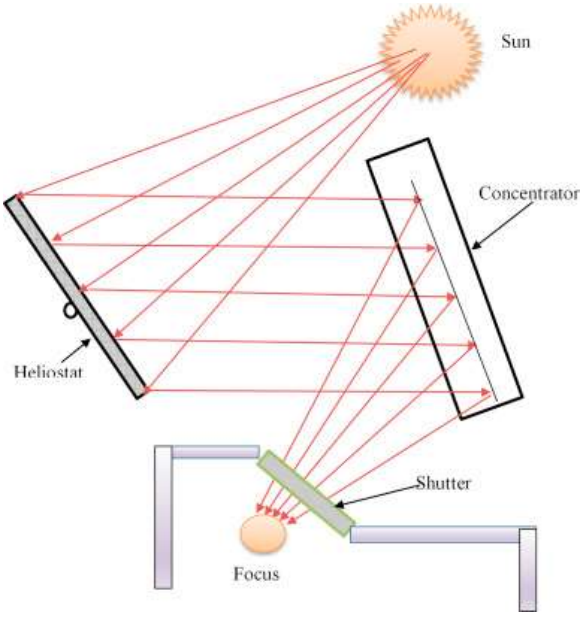

Figure 51: Schematic of horizontal off-axis solar design. (Institute of Solar Research in Germany DLR, 2015)

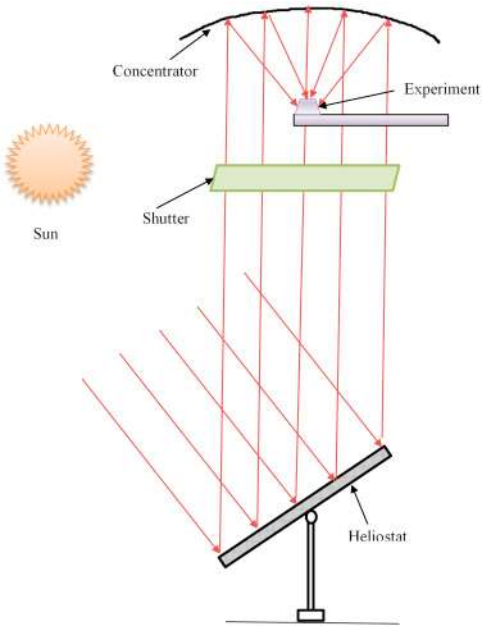

Figure 52: Schematic of vertical axis solar design. (Rodriguez, Canadas & Zarza, 2014)

For commercial production, the solar thermochemical plant should use high concentration system. Therefore, tower top arrangement which operates with receivers located on top of a tower is the typical arrangement (Yadav & Banerjee, 2016). The heliostat in this arrangement receives the solar radiation and then reflect them to a tower mounted hyperboloid reflector. The reflector redirects the solar radiation to a reactor located on the ground. This arrangement especially a beam down system (down faced reflector) (Figure 53) is desirable (Epstein et al. 2008) due to its advantages such as achieving high temperature, ease of instalment, operation and maintenance of solar reactor and other auxiliary equipment because of their location on the ground rather than on tower. Financially, this arrangement results also in considerable savings in the costs required for the tower building (no need for high tower), and the heat transport system (compact arrangement) (Yadav & Banerjee, 2016). However, this arrangement requires an array of secondary collectors to concentrate and then to recover the lost magnification as well as a well-supported huge hyperboloid reflector which located almost half height of a tower top (Vant-Hull, 2014).

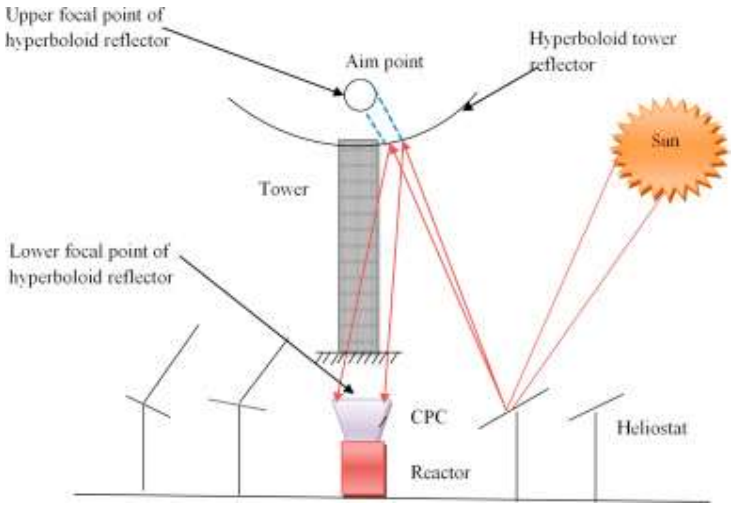

Figure 53: Schematic of beam down solar arrangement. (Epstein et al. 2008)

The secondary concentrator is more recommended to be used for solar thermochemical processes which operating above 725 Co because this will decrease the thermal radiation losses from the receiver more than the optical losses (Segal & Epstein, 1999). Segal & Epstein (1999) found that the density of optimum heliostat field is about 35% and this relies on the net energy absorbed in receiver.

5.4 Coating materials

Coating material of the both reflector and receiver affect the efficiency of solar concentrating system. The achievable temperature will be maximized with proper reflective filming of solar collector such as parabolic dish collector (Kaygusuz, 2001). Silver is the most preferable colour to coat solar collectors particularly parabolic dish collector which is the best candidate for solar thermochemical processes. For instance, silvered polymer films or stretched aluminium silvered polymer, silver coated glass (Weldekidan, Strezov & Town, 2018), and anodized sheet of aluminium (Auti et al., 2015). Plain aluminium also has been gotten attention as a reflector coating because it offers 85% reflectivity and low cost (Kumar, Pachauri & Chauhan, 2015). Although the trend in current studies is to use long-term solar reflective materials that withstand with outdoor applications such as anodized aluminium sheets or polished stainless protective polymer coating (DiGrazia, Gee & Jorgensen, 2009;

Fend, Jorgensen & Küster, 2000). In comparison to glass mirror reflectors, polymer reflectors offer great flexibility in term of system design due to its low weight and cost (Kennedy & Terwilliger, 2005).

Matte Black is the colour used widely for coating materials of receiver or reactor in solar thermal applications (Weldekidan, Strezov & Town, 2018). Materials that used for black coating should be able to endure operation conditions such as high temperatures. In addition, they should be stable chemically and manufactured easily with low cost (Kennedy, 2002). Cobalt oxide (Co_3O_4) is presented as a durable, hardly degraded, and effective black coating material for solar thermal reactors. Its high sunlight absorbing efficiency which reaches 88.2% makes it a preferable choice for high solar absorption in high-temperature solar harvesting systems (Weldekidan, Strezov & Town, 2018). Furthermore, oxide nanoparticles showed reasonable performance as a black coating material for solar absorbing (Moon et al., 2015).

In addition to black coating materials, reactor in solar systems can be also enveloped or covered by a glass tube to achieve higher temperature and to maintain this high temperature for longer time (Weldekidan, Strezov & Town, 2018).

5.5 Thermal Storage Systems

The limited hours of sun appearance during the day is one of the main challenges of solar systems. Therefore, different systems of thermal storage are used to overcome this issue. The common three thermal storage methods are latent, sensible, and composite (Wang, 2019). Thermal storage by chemical reaction is used in a limited scale due to its complexity, safety requirements, and low overall efficiency. Nowadays, thermal storage by using phase-change materials (PCMs) has received high attention and development as a superior thermal storage system. Regular PCMs divided into organic and inorganic. Inorganic PCMs in actual applications have many problems such as phase separation and PMC super-cooling while organic PCMs have low thermal conductivity. Therefore, they are severely restricted in solar thermal storage. For solar thermal storage, new types of PCMs such as composite phase-

change materials, functional thermal fluid, and shaped PCMs seem as promising candidates (Wang, 2019).

Practically, molten inorganic salts such as carbonates of sodium, lithium, and potassium can simultaneously, absorb, store and transfer solar energy. The molten salt can be also a mixture of different salts such as sodium nitrate, calcium nitrate, and potassium nitrate. The most common mixture contains 40% potassium-nitrate and 60% sodium nitrate (saltpetre) (Mancini, 2011). In comparison to other heat transfer liquids, molten salts are non-toxic and non-flammable. According to present working projects, molten salts are able to make solar pyrolysis feasible by keeping the solar pyrolysis unit runs continuously, round the clock (Adinberg, Epstein & Karni, 2004). Ability of molten salts to retain thermal energy from the sun is supposed to grant solar pyrolysis unit an annual efficiency of 99% (Biello, 2009; Mancini, 2011).

Thermal storage system consists of two insulated storage tanks; a relatively cold tank and hot tank. Because the melting point of salt is 131 °C, the temperature in the cold tank should be 288 °C to keep the salt liquid. Heat resistant pumps are used to pump the liquid salt from the cold tank through tubes to the focal point of the solar collector. The concentrated solar irradiance heats the molten salt to 566 °C or higher. Molten salt then carry on in to reach the hot storage tank. The well insulated tank is able to store usefully thermal energy for up to a week (Ehrlich & Geller, 2017; Xiang, 2017; Xiang & Zhang, 2017). During the night time, the hot molten salt is pumped to the solar dryer and pyrolysis reactor to provide them by the required temperature to start up the reaction.

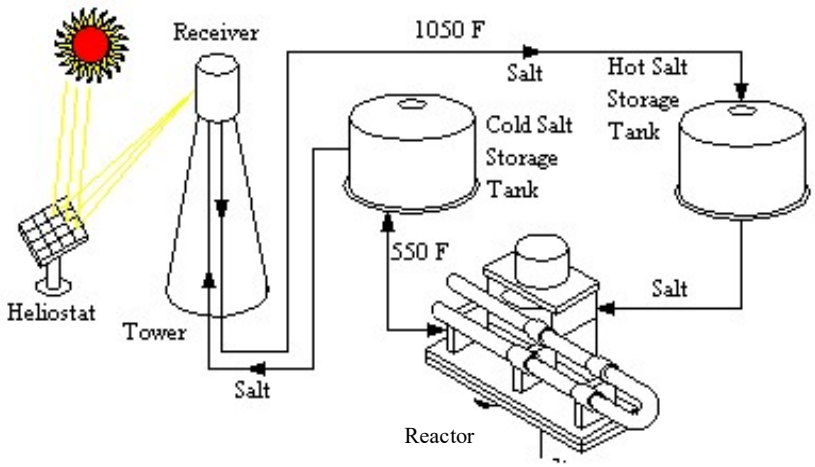

Figure 54: Schematic of molten salt technology for thermal storage. (Mancini, 2011).

The volumetric capacity of these tanks depends on the size of the unit and its requirements. For example, the stored energy in a circular tank of about 12m radius and 9.1m height can generate heat energy equivalent to 100-megawatt of electrical energy for four hours (Mancini, 2011).

Molten salts are able to sustain temperature up to 600° C (Xiang, 2017). Furthermore, involving these molten alkali carbonate salts in solar pyrolysis could also enhance the solar transients' stability, increase the pyrolysis rate by 74%, and lessen the time rates of reaction (Hathaway, Davidson & Kittelson, 2011).

This concept has been applied in many solar stations around the world. The Gemasolar station in Spain (Figure 55) has utilised molten salts since 2010. This solar plant is run 24 hours a day and during cloudy days by storing solar thermal energy using molten salts at more than 500 ◦C (Abiven, 2012). In the same concept, molten salt technology is used in the Solana Generating Station in the U.S. and the María Elena plant in the northern Chilean region of Antofagasta (Marca Chile).

Figure 55: The Gemasolar plant in Spain. (endalldisease.com; masdar.ae, resp.)

There are research have done currently to develop devices are able to collect and store the heat from solar energy. These devices are known nanoantennas (nantennas). Nantennas are electromagnetic collectors capable to collect and absorb the both solar and background infra-red (heat) energy at specific wavelengths. This absorbed energy can be used later in the night time or cloudy weather (Rhodes, 2009; Gorman, 2010).

5.6 Solar Reactor of sludge

Although there are a few literatures about solar pyrolysis of sludge, the same design of solar reactor of biomass can be used for sludge (Zadik & Israel, 2011). In solar thermochemical biofuel production, sludge is placed in a solar reactor which can be heated either directly or indirectly by using solar energy from the solar collector.

In all solar collector systems, solar thermal reactor is exposed directly to the concentrated solar radiation by placing it in the focal point or line of solar system. The essential difference between direct and indirect reactors is the way of sludge heating. For directly heated reactors, sludge absorbs heat directly from solar radiation (Figure 56a). To increase the efficiency of energy transfer to sludge by direct solar radiation, the reactor should be transparent. It is usually made from fused quartz or borosilicate glass (Alonso & Romero, 2015), therefore, the solar reactor surfaces should be cleaned continually at all-time to maintain the continuous passage of the concentrated solar rays and hence heating of sludge (Piatkowski & Steinfeld, 2011; Melchior et al., 2009). In term of the method of processing sludge, any traditional pyrolysis technique can be used for solar pyrolysis such as fluidized bed reactor, fixed bed reactor, super critical water reactor, or vacuum pyrolysis reactor (Zadik & Israel, 2011).

For indirect heating reactors (Figure 56b), clean walls are not a problem because the reactor has opaque walls and usually coated by matte black. They are practically made from metals that have high thermal conductivity such as copper (K: 423 W/m.K), pure silver (K: 418 W/m.K), and aluminium (K: 215 W/m.K). To improve the performance of reactors, they are enveloped by evacuated tube to prevent the losses in radiative heat (Weldekidan, Strezov & Town, 2018). Opaque walls of reactor absorb the heat first and then transfer it to sludge by conduction (Tesfay, Kahsay & Nydal, 2014) or conviction via heat transferring fluid (HTF) (Asmelash et al., 2014). Despite HTF is normally mineral or synthetic conducting oil, molten salts (Xiang, 2017) and other intermediate fluids such as liquid metals and gasses can be used as HTF as well to improve the conditions of heat transfer (Adinberg, Epstein & Karni, 2004). Conducting oils might be less suitable for pyrolysis of sludge due to their lower heat capacity in comparison to others. However, indirect heating reactors are usually less efficient than direct ones because the efficiency of heat transmission is influenced by the material of the both absorber and conductive (Piatkowski & Steinfeld, 2011). Heat transfer efficiency is also

affected by packing density of feedstock, feedstock' particles size, physical properties of feedstock' particles and reactants, and their flexibility of movement inside the reactor (Adinberg, Epstein & Karni, 2004). Previous variables, in addition to its requirement to maximum operating temperature and its resistance to radiative absorbance and thermal shocks are considered as some drawbacks of indirect heating reactors (Piatkowski & Steinfeld, 2011).

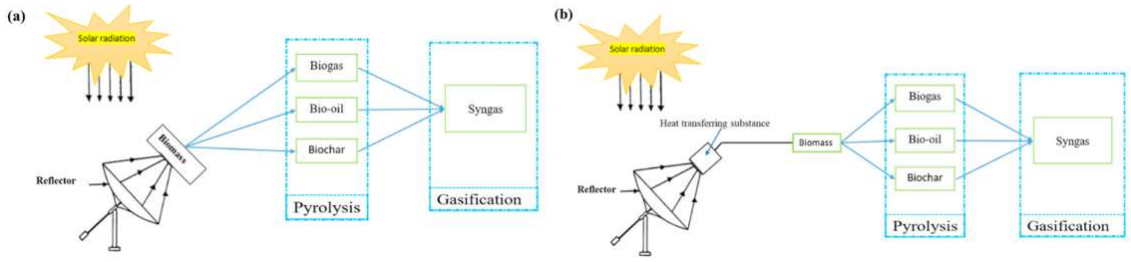

Figure 56: diagram of (a) direct heating solar reactor, (b) indirect heating solar reactor. (Weldekidan, Strezov & Town, 2018)

5.7 The process of solar pyrolysis of sludge

As mentioned before, due to the shortage of literatures about solar pyrolysis of sludge, sludge might be treated as a solar pyrolysis of biomass due to its organic and carbonaceous content. However, solar pyrolysis to convert biomass into biofuel is still also an emerging technology although it has started from 1980s (Zeng et al., 2015).

Previous literatures about solar pyrolysis of biomass demonstrate that liquid yield is more affected by reaction temperature and heating rates than type of biomass. The highest liquid yield by solar pyrolysis of biomass was obtained at 465 °C by using a parabolic trough to process orange peel. This temperature is almost similar to that of optimal liquid yield of pyrolysis of sludge (Morales et al., 2014). However, most experiments were done at temperatures range from 450-2000°C with heating rates range from 5-450°C/s (Weldekidan, Strezov & Town, 2018).

Zeng et al. (2015) used argon as sweep gas in his laboratory scale experiment that demonstrates that sweep gases have minor effect on products of solar pyrolysis in comparison to reaction temperature which is with heating rate the most significant parameters in the process where the higher temperature and heating rates result in lower

liquid yield. Meanwhile, when the temperature increases, the Lower Heating Value (LHV) increases as well. Applying pressure has negligible effect on the product distribution but may affect LHV.

Experimental tests (Zeng et al., 2015) and Computational Fluid Dynamics (CFD) (Soria et al., 2017) indicate that fast pyrolysis which means fast heating rate produces more volatiles because it improves the decomposition of intra-particle tar and the char profile uniformity. Therefore, similarly to the temperature, the higher heating rates the higher gaseous yield (Zeng et al., 2016). Different types of catalysts can be utilised in solar pyrolysis. Although their impact is small when compared to the temperature and heating rate, they can improve the distribution of pyrolysis product. For instance, H-beta can increase the liquid and gas yield whilst TiO2 produces high yield of Isopropane which is gas-like product (Zeaiter et al., 2015). Joardder et al. (2014) found that the optimum liquid yields (50 wt% of the dry date seed as feedstock) can be achieved when size volume of reactor feedstock is about 0.2 cm^3. In term of emissions, studies indicate that solar pyrolysis is environmentally safer than fossil fuel pyrolysis because it significantly reduces CO^2 emission. Co^2 is one of gaseous products of pyrolysis that can be used for further energy recovery and hence reduce fuel cost by 32.4% (Joardder et al. 2014).

6. Sludge drying process

As the huge production of sludge is a current global problem, dewatering or drying this sludge to reduce its volume may be the main problem in sludge disposal. Sewage sludge contains initially about 98% water which means only 2% dry mass. Water treatment processes such as settling, coagulation, flocculation and aerobic and anaerobic digestion result in sludge with approximately 75% water content. Drying processes aim to produce sludge with at least 90% of dry mass (Flaga, 2005). Drying of sludge is considered the main challenge in sludge disposal process due to the complexity of chemical and physical composition of sludge (Flaga, 2005; Jorand et al., 1995; Li & Ganczarczyk, 1990; Li, Ganczarczyk & Jenkins, 1986). Namely, municipality sludge from wastewater treatment facilities is widely complex and considered the most difficult sludge to dewater (Vaxelaire & Cézac, 2004; Neyens & Baeyens, 2003). Its dewater-ability is highly influenced by different parameters such as particles size, cationic salts, extracellular polymeric substances, conditioning, and filamentous bacteria (Mikkelsen & Keiding, 2002). Moreover, moisture distribution and the binding energy are also other parameter of dewatering the sludge. However, obtaining a significant dried sludge in a short time is impossible without using one of drying process (Flaga, 2005). This chapter is to give an overview about thermo-drying methods of sludge, challenges of thermal drying of sludge and a novel design for a solar drying unit.

6.1 Overview of drying sludge

Huge production of sewage sludge is one of current environmental problem. Interestingly, water represents most of sludge volume therefore, drying process is highly required to obtain high dry solids (DS) concentration in sludge. Drying process of sludge passes mainly through three stages: thickening, dewatering and then drying. Thickening process can obtain approximately only 6% of total dry solid concentration while further dewatering can obtain 32% of total dry solid concentration and the rest which is approximately 62% of total dry solid concentration can be achieved by thermal drying to get 90% of dry solid content in sludge (Figure, 57 & 58) (Flaga, 2005). Nowadays, mechanical dewatering and drying of sludge by centrifuges technologies, pressure belts or pressure filters may be not sufficient to meet both

the present high production and the new environmental regulations. Therefore, utilizing heat energy is presented as an optimal solution. Conductive and convective drying as well as combined drying are the most common techniques for relatively fast thermal drying.

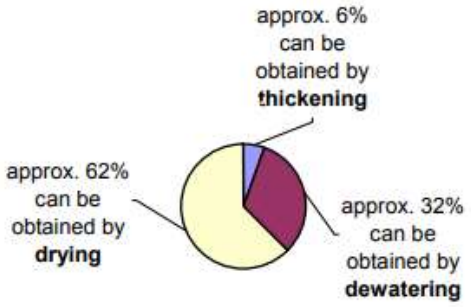

Figure 57: the total possible DS concentration which can be achieved by drying, dewatering, and thickening processes. (Flaga, 2005)

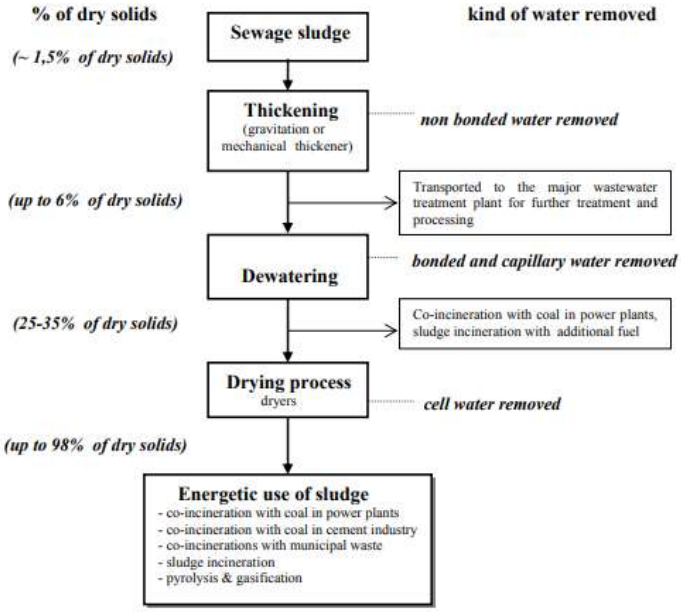

Figure 58: water removal processes of sludge and their DS productivity and utilization. (Flaga, 2007)

However, drying of sludge aims to reduce the water content of sludge. Practically, this is much difficult because the water molecules within sludge have not the same behaviour during dewatering and drying process. This is because of their different properties in term of enthalpy, entropy, vapour pressure, density, and viscosity (Vesilind, 1994; Katsiris & Kouzeli-Katsiri, 1987). Drying sludge is correlated with the type of water in sludge (Flaga, 2005).

Water content of sludge can be divided into three main types based on its proximity to the solid during drying process: free water, free capillary water, and bound water which is intercellular water (adsorbed) or intracellular water (absorbed). Free water is not influenced by solid particles and the estimation of its amount in sludge depends on the method of measurement because it is considered as an operationally defined value (Lee & Hsu, 1995; Colin & Gazbar, 1995). Free water in activated sludge can be also defined as the water between pores that is subjected to gravity force and can be removed partially by thickening or gravity settling (Flaga, 2005) or totally by mechanical stress by applying moderate pressure (5×10^4 Pa) for 30 minutes (Smollen, 1986) or high pressure (over 28 MPa) (Lee, 1994). It includes void water that is not influenced by capillary force and water that non-associated with sludge solid particles (Vaxelaire & Cézac, 2004). Free capillary water or interstitial water that trapped inside interstitial spaces of particles due to adhesion and cohesion forces which can be removed by mechanical methods such as centrifugal forces (Flaga, 2005).

On the other hand and as a result of the presence of the solid, properties of bound water are modified and the estimation of its amount in sludge depends on the amount of free water because its amount is the complement of the whole water content (Vaxelaire & Cézac, 2004). Bound water can be defined as the water that remains in the sludge due to chemical bonding (flaga, 2005) and remains unfrozen below −20°C (Wu, Huang & Lee, 1998; Colin & Gazbar, 1995) or the water that has binding energy surpasses 1 kJ kg−1 (Herwijn, 1996). Bound water includes half-bound water which is bound physically inside sludge' flakes, hydration water, vicinal or surface water on the surface of solid particles (colloids) due to the surface tension on the border of phases, intercellular water due to the crystal lattice form of molecules of constant phase of sludge, biological intracellular water which is a part of living organisms cells that present in sludge (Flaga, 2005; Vaxelaire & Cézac, 2004; Vesilind & Hsu, 1997) as well as osmostic water, and trapped water within polymer network (Mikkelsen & Keiding, 2002). Due to chemical bonding, bound water can be partially removed by adding polymers and apply mechanical dewatering method. Polyelectrolytes are also used to remove chemical bonding in bound water because of their ability to change the surface tension. The only way to remove intracellular bound water is by breaking the sludge particle walls either by freezing, heating, or electroinduced forces (Flaga, 2007).

However, different techniques are used to measure water distribution within sludge and hence best dewatering method such as vacuum drying (Kopp & Dichtl, 2001), dilatometric test (Wu, Huang & Lee, 1998), drying at atmospheric pressure (Chu & Lee, 1999), centrifugal settling test (Yen & Lee, 2001), expression test (Chu & Lee, 1999), filtration test (Lee, 1996), Differential Thermal Analysis (DTA) (Katsiris & Kouzeli-Katsiri, 1987), Differential Scanning Calorimetry (DSC) (Erdincler & Vesilind, 2000), Combined Thermal Gravimetry Analysis (TGA) and differential thermal analysis (TGA/DTA) (Chu & Lee, 1999), water vapour sorption (Vaxelaire, 2001), nuclear magnetic resonance (Carberry & Prestowitz, 1985).

Practically, the water distribution or bound water content within sludge is not the only factor influences sludge drying. Other parameters such as floc structure, particle size, layer thickness, and surface characteristics act simultaneously during the sludge solid-liquid separation (Mikkelsen & Keiding, 2002). Therefore, only few techniques already took place in commercial scale of sludge drying application. Modern thermal drying facilities can produce dried sludge granules of 1-4mm consist of 2-10% of water and less than 1% of dust (Flaga, 2005).

In the same economic concept, achieving dried sludge with 90% of DS consumes energy and hence more costs. Energy consumption depends strongly on the water content of sludge and drying techniques. Although mechanical methods consume about 30 times lower energy than thermal methods (Kowalik P., 1998), their ability in water removal still limited up to 75% (Flaga, 2007). However, mechanical dewatering of sludge by mechanical techniques such as chamber press or belt press before drying can reduce energy consumption and costs. Energy consumption during mechanical dewatering is estimated by 17-34 kWh/m^3 of water removed from sludge, while approximately 850 kWh/m^3 of water removed is required during thermal drying at 300 °C (Kowalik, 1998). The optimal water content of sludge before drying process should not exceed 65% but it is still acceptable until 88% (Flaga, 2005). According to Flaga (2005), when the initial water content of sludge is 75%, then 100 litter of fuel oil is required to evaporate 1 ton of water. In other words, to obtain one ton of dried sludge with 35% DS, then approximately 120 litter of fuel oil or 30kWh of electric energy is required if the initial water content of sludge is 75%. For thermal utilization purposes such as pyrolysis (Figure 59), the water content of sludge should be less than 10%, therefore, the energy required to obtain one ton of dried sludge with 95% DS is approximately 300 litter of fuel oil or 50kWh of electric

energy. The cost will drop about 50% if biogas from sewage treatment plant is available for use. Moreover, heat recovery from products of thermochemical reaction such as biogas or bio-char can diminish the amounts of energy consumption for drying. However, different technical solutions have been offered to obtain completely dried sludge. These solutions vary in term of type of dryer, characteristic of sludge, technique of heat recovery, delivery method of heating factors such as gases and steam.

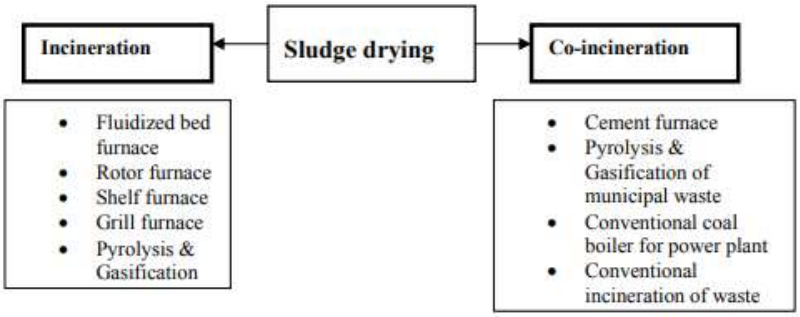

Figure 59: sludge thermal utilization methods. (Flaga, 2007)

Moisture content of sludge influences also the nett surplus energy value of thermochemical reactions. High water content of sludge may result in false low calorific values and hence prevents autothermal reaction of sludge without additional auxiliary fuel. The maximum value of water content to achieve auto-thermochemical reaction is 50% (Flaga, 2007). The energy balance of thermal treatment of sludge shows that more than 50% of obtained energy is already consumed to achieve dried sludge with 45% DS and the rest of obtained energy is partially lost as heat losses at the drying installation as well as drying air enthalpy at the drier outlet (Flaga, 2007; Kowalik P., 1998).

Apart from that, drying sludge before thermochemical treatment is important in term of odours. According to Flaga (2007), sludge with water content >15% causes odours spreading.

Drying curves are considered as a graphical representation of phases that the sludge passes by during the drying process. Operating conditions as well as method of drying affect the number of these phases that change from one type of sludge to another (Bennamoun et al 2013; Bennamoun, Belhamri & Mohamed, 2009). Drying curves are typically used to illustrate the relation between the moisture content of the sludge (Kg/Kg) and drying time (h) (Figure 60a & 60b) or to plot the drying rate (Kg/h m^2) versus drying time (h) (Figure 61a) or moisture

content (Kg/Kg) (Figure 61b). Drying curves is also known as Krischer's curve (Kemp et al., 2001). These curves give information about the variation of sludge behaviour during drying (Bennamoun, Arlabosse & Léonard, 2013). Different stages of drying can be seen in the drying curves: transient early stage (transient period) which occurs during the heating up of the sludge; constant rate period in which free water of sludge is removed; finally, falling rate period, in which bound water within the solid matrix is removed. These curves also demonstrate the critical moisture content at the changing point of drying period from a constant rate to a falling rate. Practically, the unit (kg s^{-1} m^{-2}) is widely used during the graphical representation to describe the evaporated flow per product surface (Bennamoun, Crine & Léonard, 2013; Deng et al., 2011)

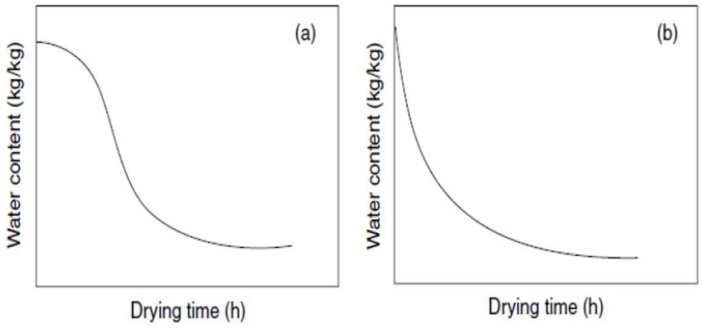

Figure 60: Typical drying curves: (a) with a lag period, and, (b) without a lag period. (Wah, 2015)

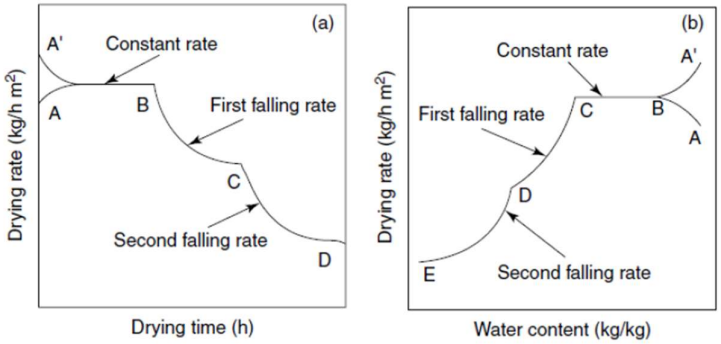

Figure 61: Typical drying rate curves, drying rate versus: (a) drying time, (b) water content. (Wah, 2015)

6.1.1 Thermal drying of sludge

Thermal drying of sludge is the most preferable drying technique due to many reasons. It is the only way to remove biologically and chemically intercellular bound water from the sludge

and hence the only way to obtain 90% or higher of dry solid concentration (Flaga, 2005). Removing biologically bound water means also hygienic sludge clear of pathogenic organisms which makes it usable for fertilization and soil conditioning of high market value. Moreover, thermal drying of sludge improves sludge structure and increases its calorific value for further use and for further thermal treatment without additional heat energy or fuel (Arlabosse et al., 2012).

Practically, there are three methods are widely applied in thermal drying: conductive drying (indirect dryers), convective drying (direct dryers), and solar drying. Combination of these methods are also common in hybrid or combined dryers (Figure 62). However, each method has different features. For example, three phases can be distinguished during convective drying: readjustment phase, phase of fixed drying rate and phase of falling or descending drying rate. Drying kinetic of convective drying is affected by several parameters such as operating conditions and the nature of sludge or its origin. Three phenomena can be observed during convective drying: skin formation, shrinkage, and cracks phenomenon (Bennamoun, Arlabosse & Léonard, 2013). During conductive drying, sludge passes through three phases as well: pasty or sticky phase, rugged or lumpy phase and finally granular phase. First phase is given a special focus due its negative impacts on both drying process performance and dryer itself. Present solar drying occurs by exposing the sludge to sun rays. Therefore, the solar drying productivity of dried sludge depends entirely on climatic conditions such as air temperature and solar radiation which are the main factors in this process. However, only limited studies about solar drying are available and almost none of them has used concentrated solar energy for sludge drying purposes (Bennamoun, Arlabosse & Léonard, 2013). Finally, drying by super-heated steam and fry drying are other methods have been used for sludge drying.

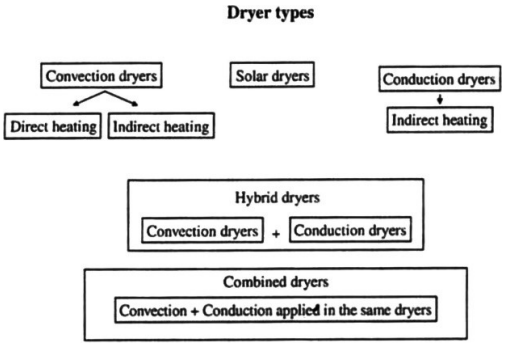

Figure 62: Classification of sludge thermal dryers based on heating method. (Arlabosse et al., 2012)

Thermal drying is essentially a kind of mass and heat exchange between sludge and air. Heat exchange which can be achieved by one of methods mentioned above (conduction, convection, and radiation) motivates diffusion. Diffusion results in moving the moisture mass from higher concentration area to lower concentration area by evaporation from the surface of sludge to the air during the connection with the heated factor. Evaporation rate differs depending on the sludge properties, thickness as well as the contact area between dried material and drying medium. However, evaporation rate in the first phase of drying is highest because the water content of sludge is greatest and then it stables steady for a while before it diminishes. Wider contact area makes drying process shorter by increasing the moisture evaporation rate. Granulation is one of common methods to expand the contact area between sludge and drying medium at economic level.

Drying process of sludge passes through three phases. A very short preliminary drying phase where the temperature of sludge is rising up to a certain and constant value. Follow that essential drying phase which is the longest phase because the water evaporates with a constant speed regardless the type of sludge. The evaporation occurs from the surface of the sludge particles that have been totally covered with water. This water is gradually replaced by internal water from inside of sludge particles. During this phase, the temperature of sludge remains constant at about 85°C. The great difference between the water amount on the surface of particles and the water amount inside particles (not bonded water) results in longer time of this phase. When the difference diminishes and the moister content of sludge reaches critical value, the temperature of sludge begins increase as starting point of final phase of drying. In this phase, evaporation from particles surface becomes faster than water replacement from inside of the particles. Evaporation rate then decreases until balanced hydration is achieved. Balanced hydration depends on air humidity and drying temperature. From economic perspective, drying process should be fast to meet huge production and huge demand on dried sludge as well. The speed of drying process depends on: moisture content of sludge, drying temperature, air humidity, contact area which includes the thickness of sludge layer, mixing process of sludge during drying, time of retention in dryer, drying rate, the contact method between sludge and the heating factor.

In addition to that, the physical status of sludge is also important parameter in drying process. While drying process of sludge is progressing, three physical phases can be observed:

wet phase, sticky phase and granular phase respectively (Li et al., 2014). In wet phase, sludge is flow-able and easily spreads onto surfaces especially those in indirect dryers. After that, when moisture content reduces with evaporation, sludge becomes like plastic and forms a skin layer on the exposed contact surfaces. This is known as sticky phase of sludge, wherein the drying ratio of sludge drops (Peeters et al., 2013; Kudra, 2003). After adhesion and cohesion of sludge bulks reaches the peak, high drying results in almost disappearance of the contact between sludge components and heating surfaces, therefore, sludge peels from contact surfaces and then fritters into small pieces similar to granules.

In the same concept of thermal drying, there are several studies investigated the impact of fry drying on sludge. Silva et al. (2005) reported the first experiment of fry drying of sludge by using used and fresh oil separately to fry cylindrical pieces of sludge (12 mm radius and 40 mm height) at temperature ranges from 180-215°C in a 5L normal fry pan. They achieved dried sludge with ≤5% moisture content after 10 minutes frying time at 180°C. They found also that the heating value of sludge improves more with longer frying time as a result of oil incorporation and lower moisture content (Tunçal, Jangam & Güneş, 2011). Ayol & Durak (2013) found that using fry drying technology by using waste engine oil to fry circular cakes of sludge with diameter ranges from 1-3 cm for 2-20 minutes in temperature ranges from 100-180°C can be an efficiently fast alternative process for drying municipal sludge. Different studies have been launched in this field to investigate the impact of fry drying technique by using different types of sludge, different oils, different frying temperature, and different frying processes which resulted in positive impact of fry drying of sludge. (Peregrina et al., 2006; Romdhana et al., 2009; Ohm et al., 2009; Park, Lim & Lee, 2010; Ohm et al., 2010). Interestingly, mixing raw sludge with a substantial amount of fat or oil before drying process in indirect dryers may give positive results in “sludge flakes” production. This theory will be investigated in this study.

However, thermal drying by present techniques is not cheap as well as not sustainable due to its high energy demand which depends mainly on fossil fuel. Global trend toward sustainable sources nominates the sun to play important role in the next generation of thermal drying and disposal of sludge. Feasibility of involving concentrated solar energy to achieve thermal drying of sludge by conduction and convection with a little frying to produce “sludge flakes” will be investigated in this study as well.

6.2 Challenges of drying sludge

Different studies have been involved to investigate some phenomena during thermal drying of sludge such as cracks (Léonard et al., 2002), crust phenomenon (Vaxelaire et al., 2000), shrinkage phenomenon, and sticky phase (Peeters et al., 2013). Classical drying curve shows some of these phenomena through describing the development of the evaporation flux versus the average moisture content of sludge. As shown in (Figure 63), four phases can be seen during drying process. First phase appears after a short period of heating and increasing the temperature of sludge. The second when the temperature of sludge reaches a constant rate where free water evaporates at the surface of sludge. The third phase is known as a period of falling rate where drying boundary is progressing. Above this boundary only bound water is found whilst below it only free water that is removed as vapour. Drying boundary affects negatively heat and mass transfer resistance. Resistance increases during the progressing of drying boundary into the sludge and thus decreases the evaporation flux. Fourth phase is a second period of falling rate occurs in activated sludge and other hygroscopic materials because of slow evaporation of bound water (Vaxelaire & Cézac, 2004).

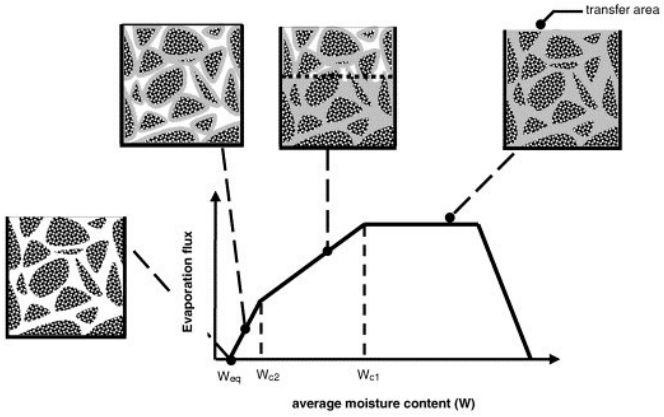

Figure 63: Classical drying curve. (Vaxelaire & Cézac, 2004)

Where: W_{C1}: water content of sludge at 1st transition point. (kg_{H2O} kg_{DS}^{-1}).

W_{C2}: water content of sludge at 2nd transition point. (kg_{H2O} kg_{DS}^{-1}).

W_{eq}: water content at the thermodynamic equilibrium. (kg_{H2O} kg_{DS}^{-1}).

First transition point (W_{C1}) is the point of transition from a period during drying process that is controlled by external variables (such as temperature, air velocity, and relative humidity)

to a period controlled by the transfer properties of the sludge (Vaxelaire & Cézac, 2004). The equilibrium moisture content (W_{eq}) demonstrates the moisture content of sludge at the thermodynamic equilibrium by identifying the intracellular or internal water. Combination of operational conditions such as air humidity and temperature with the development of sludge' equilibrium moisture content is known as sorption isotherms (Vaxelaire, 2001). In activated sludge, sample size, sample mass, sample thickness and transfer surface area of the sample affect the evaporation flux (g water s^{-1} m^{-2}). It can be noticed that during the drying process, the size of a sample of activated sludge widely decreases and thus the transfer surface area decreases as well due to the shrinkage phenomenon. However, thick layer of sludge can be used to limit this phenomenon (Vaxelaire & Cézac, 2004).

In early attempt to measure the binding energy correlating with drying process of sludge, it is found that it is affected by the amount required of residual moisture content. For example, adsorpted water such as hydrogen bonding or solvatation, and physiochemical adsorption can be removed by 170 kJ kg^{-1} whilst chemically attached water by molecular bonding requires about 280 kJ kg^{-1} to be removed (Vaxelaire & Cézac, 2004).

6.2.1 Sticky phase

Sticky phase of sludge is a negative phenomenon occurs during drying process. This phenomenon results in higher torque requirements in drying machines such as sludge paddle dryers (Komline-Sanderson, 2008; Arlabosse, Chavez, & Lecomte, 2004) and decanter centrifuges (Peeters et al., 2013; Peeters et al., 2012) which consumes more energy, reduces significantly dryer capacity, decreases the dryer efficiency and then high potentially that sludge build-up on equipment surfaces results in breakdown or damaging of dryer (Peeters, Dewil & Smets, 2012; Peeters, 2010).

Sticky phase is a kind of changing the consistence of sludge from liquid phase to sticky rubbery phase similar to a paste form that literally glues and clings to dryer walls and surfaces when it is partially dried. Partially dried means that the sticky phase occurs in a specific dryness region but its exact location depends on the sludge characteristics. The range of DS content of sludge where sticky phase characters appear differs based on both sludge organic

content such as polysaccharides and proteins (Li et al., 2014) and dryness of sludge (Figure 64). More organic content of sludge means appearance of sticky phase in earlier stage of drying due to the formation of "biopolymer matrix" as a combination of biopolymers and microorganisms in the sludge (Kudra, 2003); Peeters, Dewil & Smets, 2014). However, this sticky phase occurs for municipal sludge during drying at stage when its dry solid content (DS) becomes more than 25% up to 65% (Peeters, Dewil & Smets, 2014; Li et al., 2014) and for normal municipal sludge from 44% up to 65% (Flaga, 2007). Li et al., (2014) stated that there are two stages of stickiness: adhesion and cohesion and they significantly arise in the sludge at temperature of 120°C when its water content ranges from 30-60%. Raising up the heating temperature only results in a small movement to the location of sticky range.

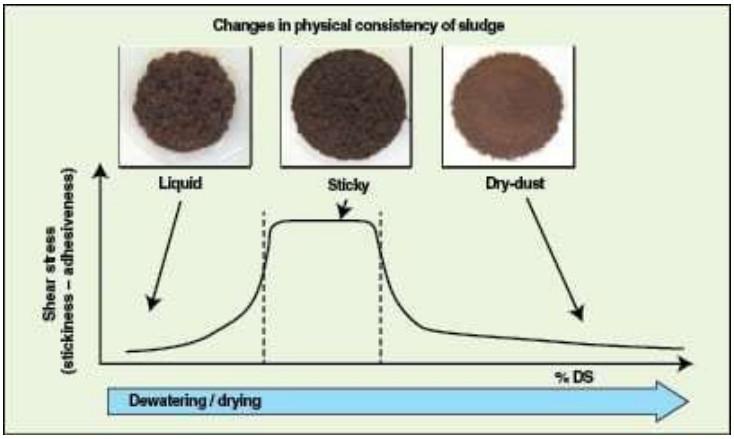

Figure 64: Physical consistency of sludge during drying. (Peeters, Dewil & Smets, 2014)

Different methods can be used to cope with this issue or to mitigate it. Right now, there are three control strategies have been practically used in sludge drying plants (Peeters, Dewil & Smets, 2014). One of them targets the formation of biopolymer matrix during drying whilst the other two strategies targets the dry solid contents (%DS) of sludge at the entrance of dryer by either decreasing or increasing its percentage. As shown in (Figure 65), the first method depends on increasing the %DS in sludge by back-mixing of totally dried (≥90% DS) sludge with mechanically dewatered raw sludge before thermal drying process in dryer (Strand & Alsaker, 2009; Léonard et al., 2008). This well-established technique increases the DS content in the blended sludge beyond the sticky phase to form a crumbly mixture of sludge easier to handle in the drier. Practically, to avoid sticky phase, dewatered sludge with 20-35% DS is

mixed with previously dried sludge with 90-95% DS to get sludge with 65-75% DS at the dryer entrance (Flaga, 2005).

Second method aims to postpone the timing and place of sticky phase during thermal drying of sludge in flash dryer by reducing its %DS after mechanical dewatering and at the beginning stage of thermal drying process (Peeters, Dewil & Smets, 2012; Peeters, 2010). Therefore, combined of flash-drying and mechanical dewatering systems are involved in this technique. As a result, sticky phase of sludge appears at less critical places causing no operational problems in the dryer.

The third method based on using chemical additives into the raw sludge feed stream of dryer before drying such as polyaluminium chloride (PACl) (Peeters et al., 2013) and lime (Li, Zou & Li, 2012). These additives can completely eliminate or at least mitigate the stickiness of sludge (Peeters et al., 2013; Peeters et al., 2012; Li, Zou & Li, 2012). Practically in Monsanto wastewater treatment plant in Antwerp that uses a combined centrifuge dryer system, adding about 20 L of PACl are sufficient to address sticky phase in a volumetric flow rate of seven m^3 of raw sludge (Peeters, Dewil & Smets, 2014). In this technique, PACl super aluminium structures associate with the bound hydration water that acts as a lubrication or aquaplaning and then directs sticky biopolymers to the non-sticky dryness range (Peeters et al., 2013).

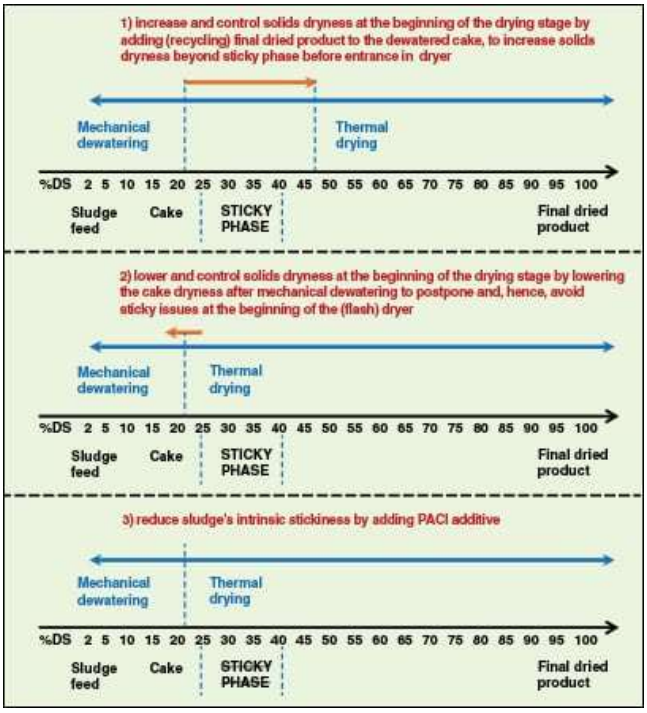

Figure 65: strategies to practically overcome sticky phase issue during sludge drying. (Peeters, Dewil & Smets, 2014)

6.2.2 Vapours removal

In present technologies, vapours that are produced as a result of drying process should undergo further treatment rather than direct release to the atmosphere. These vapours may contain dry solid particles that should be separated by bag filters or de-dusting cyclone-type devices. Moreover, heat content of these vapours can be recovered rather than causing extra heat for ambient. Direct vapour condensation systems such as spray devices or indirect coolants such as membrane heat exchangers can be used to cool and condense these vapours. After condensation, dry air should be deodorized by using fire method or biological filters while condensate water should be sent to wastewater treatment plant (Flaga, 2005).

6.2.3 Sludge storage

Dried sludge requires specific storage systems because it has a high possibility of rewetting (Arlabosse et al. 2011). These systems should be appropriate for adjustment of the quality of sludge, preventing sludge getting dump by adsorbing the moist again, as well as preventing self-ignition. Therefore, totally isolated systems are required to storage dry sludge. Practically, dried sludge is stored in isolated silos with a cover of inert gas such as gaseous nitrogen (Flaga, 2005).

6.3 Present thermal techniques for drying sludge

Dewatering of sludge is very important step before thermal drying. Dewatering process reduces the initial free water content of sludge. Mechanical techniques such as compression, filtration, or centrifugation are the most common used dewatering methods (Bennamoun, Arlabosse & Léonard, 2013). The electro-osmotic dewatering by applying dense electrical current or high electrical voltage was presented as an alternative dewatering method by (Mahmoud et al., 2010; Citeau et al., 2012; Tuan, Mika & Pirjo, 2012). However, more efficient dewatering process results in shorter drying time, less energy consumption and hence lower drying cost.

Dried sludge is obtained in current thermal drying technologies by subjecting sludge continuously for heating source under temperature ranges from 140-450 °C. The resident time of sludge in dryer, which may extend at least to 30 minutes, depends on the drying method and drying temperature. The classification of drying methods is based on the heat supplying method to the sludge. However, there are four groups of dryers (Flaga, 2005): convective dryers, contact dryers, mixed of convection-conduction dryers, and infrared dryers. Solar dryers can be also considered as a group of dryers (Bennamoun, 2012). In convective dryers, sludge is subjected for a direct contact with hot medium such as hot air. Pneumatic or flash dryers, fluidized bed dryers, and drum or rotary dryers represent such kind of dryers while “tray and layer” concept such as paddle dryers, disc dryers, hollow flight dryers, and multi-shelf dryers represents contact dryer where a conductive surface separates the heating factor and the sludge which has a direct contact with the hot surface. High frequency currents or infrared radiation are used in infrared dryers. Practically, fluidized and drum dryers are more efficient when they are used for granulated sludge (Urbaniak & Hillebrand, 2004). In comparison to direct dryers (convective dryers), indirect dryers (conductive dryers) are safer in term of pollution by volatile compounds, dust production, and gas emissions and high risk of dust explosions. They are also cheaper in term of capital cost of the drying facility due to the necessity for expensive equipment for deodorization, air protection, and dried sludge recirculation in convective dryers. In opposite, indirect dryers are less efficient from economic perspective due to their long retention time of sludge and their limited drying efficiency (Flaga, 2005).

However, the basic concept of convective, conductive, and solar dryers that have currently used in industrial scale are represented in (Figures 66), (Figures 67), and (Figures 68) respectively. Nevertheless, as mentioned before, drying methods can be combined to produce hybrid or combined dryers. Following is a brief about these three main methods and their present applications:

6.3.1 Convective drying

The sludge is subjected to a direct contact with heating medium which is usually hot air or steam. The heating medium goes through the sludge to heat up the water content into the

sludge and then causes water evaporation. Convective heating can be applied directly, indirectly via heat exchangers as well as a combination of directly and indirectly (Arlabosse et al., 2011). For industrial scale, biogas, biomass, solid waste (through incineration), and fossil fuel are the main source of heat. Electricity resistances can be used as a source of heat in small semi industrial convective dryers (Léonard et al., 2008). The efficiency of convective dryers depends on the contact surface between the sludge and the heating medium. Practically, granulation and extrusion are the common methods that are used to maximize the area of the contact surface and hence increase the evaporation rate. Shrinkage and crakes are the most common phenomenon of this method. Figure (66) shows examples of the most used convective dryers on industrial scale: (a) belt dryer, (b) flash dryer, (c) fluidized bed dryer, and (d) rotary dryer.

Despite they change based on the dryer type, the specific energy (Cp) consumption of convective dryers varies from (700 - 1400) kW.h per one ton of evaporated water and the specific drying rate varies from (0.2 to 30) $kg.m^{-2}.h^{-1}$ for a flash dryer and a belt dryer respectively (Arlabosse et al., 2011).

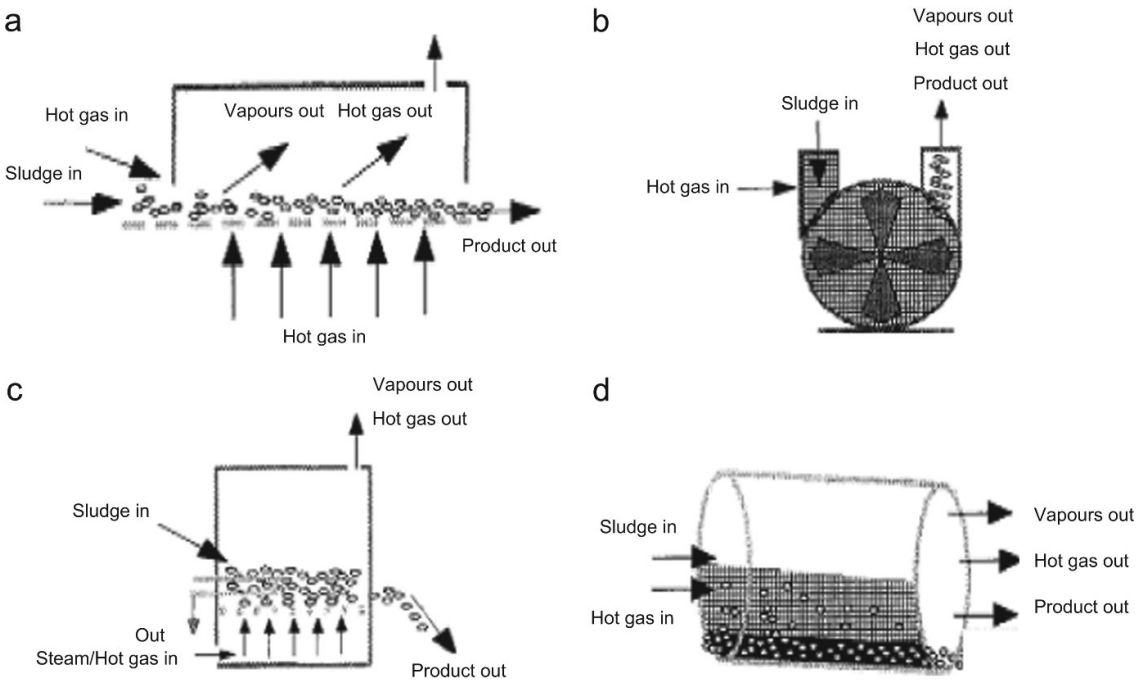

Figure 66: Examples of convective heating dryers of sludge industrially (types of convective dryers). (Bennamoun, Arlabosse & Léonard, 2013)

6.3.2 Conductive drying

In conductive drying the sludge is heated indirectly because there is a surface separates the sludge and heating medium. The surface of dryer is heated up first and then this surface transfers the heat to the sludge. Fossil fuel, biomass, biogas, and solid waste (through incineration) are used to heat up saturated steam at (0.85 MPa) or thermal oil which are used generally as heating fluid. Figure (67) shows the three main types of conductive dryers: (a) disc dryers, (b) paddle dryers, and (c) thin film dryers (Bennamoun, Arlabosse & Léonard, 2013; Yan et al., 2009).

All conductive dryers use the rotor design which is decisive for sludge conveying (Bennamoun, Arlabosse & Léonard, 2013). Rotary design helps also to renew the contact between the sludge and the heated walls of dryer. This contact maintains the heat transfer coefficient at the highest level between heated walls of dryer and the sludge. As mentioned before, the sludge during conductive drying passes through three distinguishable phases: pasty, lumpy and granular phase, respectively. These phases results in variations of the torque of dryer. Sticky phase is the most challenging phenomena of conductive drying method (Deng et al., 2009; Kudra, 2003; Ferrasse, Arlabosse & Lecomte, 2002).

Operating conditions such as stirrer speed, air temperature, vacuum rate (in partial vacuum drying) as well as the initial input mass of the sludge and the distance between heated walls of dryer and the agitator influence the rate of evaporated water (Yan et al., 2009; Ferrasse, Arlabosse & Lecomte, 2002) .

Differently from convective drying, conductive drying has many advantages such as odour and steam confinement, no pollution due to the absence of heat carrying medium and hence reduction of explosion or fire risks, and Low concentration of volatile organic compound (VOC).

The specific energy (Cp) consumption per ton of evaporated water in conductive dryers varies from (800 to 955 kW.h) to give higher specific drying rate than convective dryers which varies from (7 to 35 $kg.m^{-2}.h^{-1}$) (Arlabosse et al., 2011).

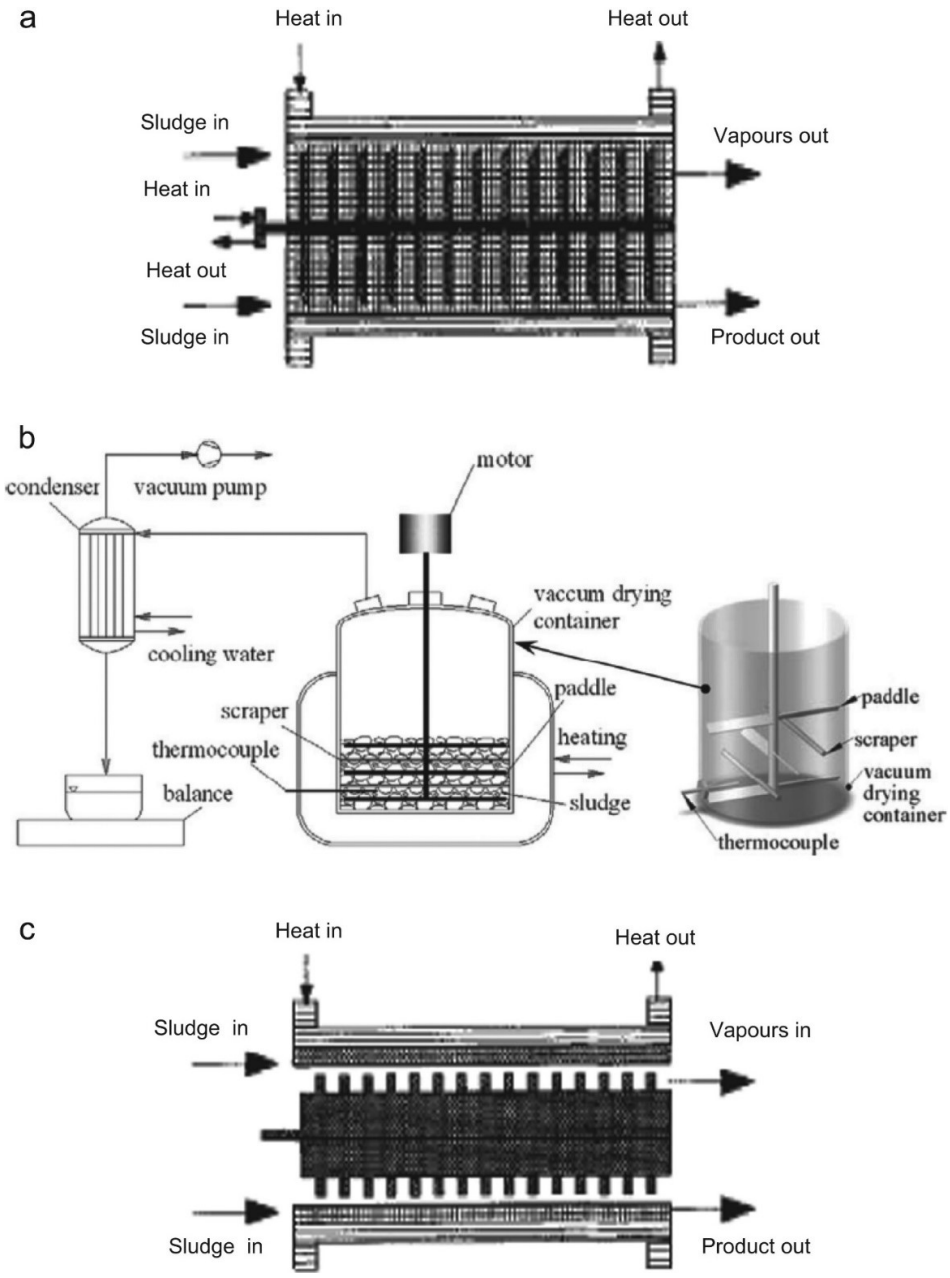

Figure 67: Methods of conductive heating of sludge industrially (types of conductive dryers). (Bennamoun, Arlabosse & Léonard, 2013)

6.3.3 Solar drying

Current solar drying units are able to reduce the moisture content of sludge up to a range typically between 20–30% and can serve as an alternative to thermal drying units for medium-size WWTP (up to 50,000 population equivalent) (Tunçal & Uslu, 2014). These units can be

classified into three main types: closed greenhouses, open greenhouses, and solar dryers integrated with a heated floor.

The most modern solar dryers use the greenhouse concept combined with a heated floor. They performed in closed or open greenhouse tunnels. In these dryers, the sludge is located in deep bed (40 to 80 cm height) inside a quartz or transparent dome. Solar radiations are used to heat the surface of dome. For more efficiency, solar harvesters can be used to concentrate the solar radiations on the dome. The vapour and humidified air are evacuated from inside the dome by ventilation. The sludge need to continuous spread, aerate, turn and convey to avoid crust formation (Bennamoun, 2012). Special sludge-mixing systems are used to mix fresh sludge with partially dried sludge and to spread it, turn it, and aerate it (Tunçal & Uslu, 2014). Other solutions such as using heat pump to inject hot fluid underneath the floor are utilised to maximize the heat and mass transfer. Figure (68) illustrates a modified design of solar dryer (Bennamoun, 2012) that used in Turkey for sludge solar drying (Salihoglu, Pinarli & Salihoglu, 2007).

Solar drying has a specific character because it entirely depends on the changes of climatic conditions particularly solar radiations, weather temperature and humidity, and the air velocity (Bennamoun, 2012; Roux et al., 2010; Slim, Zoughaib & Clodic, 2008; Seginer & Bux, 2006; Seginer & Bux, 2005). Therefore, the highest drying rate and shortest drying time can be obtained in summer where the favourable climatic conditions is available. Winter and night affect negatively the solar drying.

Most available studies in this field focus on the comparison between covered and open solar dryers, pathogen and odour reduction as well as the impact of the humidity and the temperature of both the sludge and the heated air (Salihoglu, Pinarli & Salihoglu, 2007; Mathioudakis et al., 2009; Zhao et al., 2009).

However, in the most favourable climate conditions, studies indicate that to evaporate a ton of water by this process, (30 to 200) kW h is needed. This energy will increase to 1000 kW h if chemical deodorization is applied (Arlabosse et al., 2011). Moreover, the partial drying of sludge (range from 48-80% of dry solids content) is not applied due to the unfavourable physical properties of sludge such as sticky phase. The most convenient drying is when the

dry solids content ranges from 80-97%. This research is to present a solar drying unit that likely to achieve this percent of DS in a short time and relatively low energy.

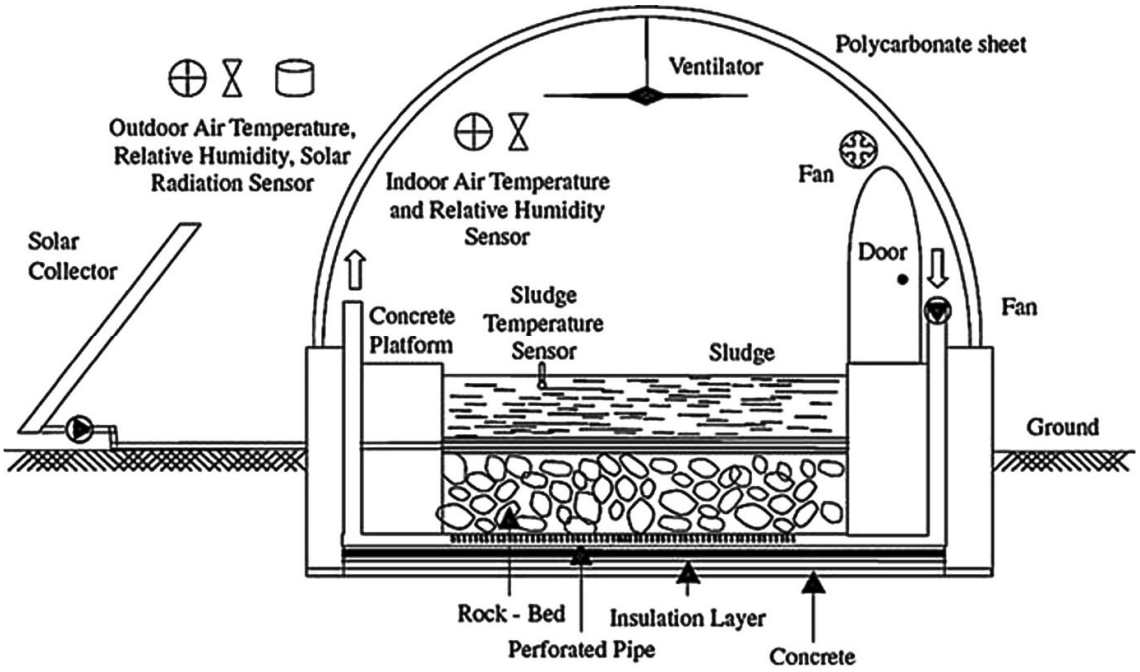

Figure 68: one of developed techniques in solar drying of sludge (developed solar dryer). (Bennamoun, 2012)

6.3.4 Present drying equipment

Different types of dryer are used in sludge drying industry (Chen, Lock Yue & Mujumdar, 2002; Bennamoun, Arlabosse & Léonard, 2013). Generally, they apply the same principles of drying - mentioned above - with some differences in the movement of the drying solids and the drying air in continuous dryers and some differences with lodging time in batch dryers. However, for calculation purposes, the fundamental principles of heat and mass balances are the same. Present drying equipment (Figure 69) include Tray dryers, Tunnel dryers, Roller or Drum dryers, Fluidized Bed dryers, Spray dryers, Pneumatic dryers, Rotary dryers, Trough dryers, Bin dryers, Belt dryers, Vacuum dryers. Tray dryers where the sludge is thinly spread out on fixed trays and heated up by air current, conduction from the tray itself or by radiation. Tunnel dryers is a hot tunnel or compartment where the sludge is spread out on a movable trays that are heated up by passing through this tunnel. Roller (Drum) dryers can be regarded conduction dryers because the sludge is spread over the surface of a hot rotating drum. The sludge remains on the drum surface until it is scraped off. During rotation the drying takes

place. Fluidized bed dryers are mostly convective dryers because they use hot upward-flowing air current to heat up the suspended sludge against gravity. Spray dryers have a large body (can reach to 10 m diameter and 20 m high). However, drying by spray dryers are rapid because they are used for liquid or fine solids in slurry. In these dryers, hot air current moves counter-flow or in parallel of solids that are sprayed as a fine droplet dispersion into its stream. When particles become dry, they can settle without sticking or even touching the dryer walls because of its large body.

Pneumatic dryers use the balance between velocity of particles and turbulence of air stream for drying. In these dryers, the sludge passes rapidly through a hot air stream until it reaches the balance point. At this point, sludge becomes suspended until it is totally dried. Practically, classifying devices are used to separate dry materials. A rotating or fixed horizontal inclined cylinder is used in rotary dryers where sludge is contained and heated in it by hot air flow through it or by conduction from its hot walls. If dryer is stationary, a screw or paddles are used to stir and convey the sludge through the cylinder. In bin dryers, hot air is blown vertically upwards into a perforated bin from the bottom. The air passes through the sludge which is contained in this bin and so drying it.

In trough dryers, a hot air current is blown through a conveyor belt made from mesh and shaped like a trough. Because of the continuous movement of the conveyor, the sludge is continually turned over and hence fresh surfaces are exposed to the hot air until total dry. Belt dryers use the same concept of trough dryers but they use often a horizontal straight solid belt. The sludge is spread as thin layers on the belt and hot air is blown over it. Like trough dryers, the belt is moving but in some designs it is stationary and the sludge is transported by scrapers.

Two types of vacuum dryers are used; batch vacuum dryers and roller vacuum dryers. Batch vacuum dryers are basically similar to tray dryers except they run under a vacuum and they heated by conduction or radiation. In these dryers, vacuum pumps that installed in a large cabinet deal only with non-condensable gases because the production of water vapour is generally condensed. The design of roller vacuum dryers is similar to roller dryers but consists of an evacuated chamber.

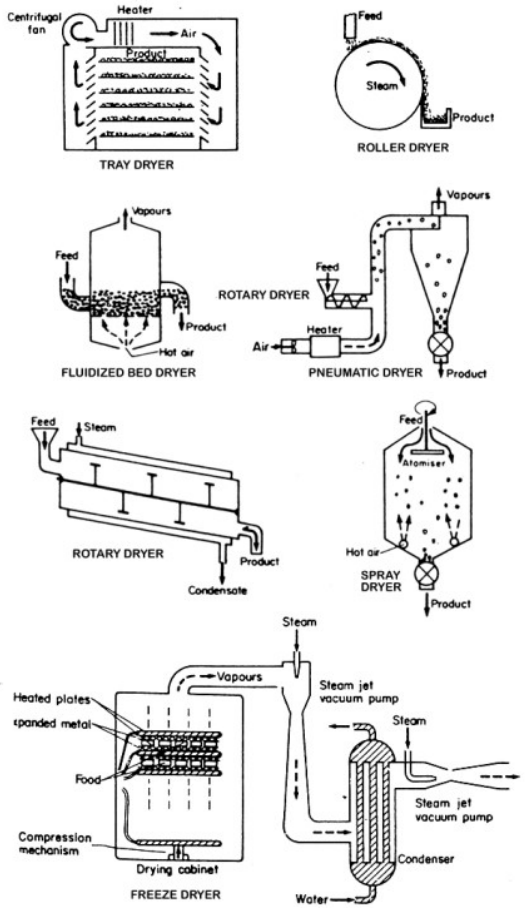

Figure 69: some types of widely used dryers. (nzifst.org.nz)

6.4 Calculation of drying theory

The high moisture content of sludge prevents any direct use of it in thermochemical processes such as pyrolysis which requires moisture content <10 wt%. Although dewatering sludge mechanically is able to remove its free water content, sludge still requires drying. Drying implies the removal of moisture content of sludge mainly its bond water. Drying is usually accomplished by evaporation of water content which achieved by supplying the sludge with the latent heat of vaporization. Therefore, designing of drying unit must take in consideration two main process-controlling factors; providing the sludge with the necessary latent heat of vaporization which includes heat source and heat transfer method, and disposal of water vapour to improve the separation process efficiency. Drying processes are included into three major groups; contact drying, vacuum drying, and freeze drying. In contact drying,

the sample is heated directly by heated surface or heated medium (air) under atmospheric pressure. The water vapour finds its way away from dryer with heated air. Vacuum drying works to reduce the pressure in the dryer by vacuum which increase vaporization of water. The sample can be heated only by conduction or radiation. Sublimation is the main concept in freeze drying where the water vapour (under suitable pressures and temperatures) is sublimed off frozen sample.

This study aims to design a solar dryers that involves the first two techniques; direct and indirect heating to achieve optimal dry sludge. Industrially, freeze drying is not used for sludge drying, therefore, it is out of this study scope.

Achieving optimal design of dryer requires basic acknowledge of drying theory or behaviour of water under temperature and pressure. The state of pure water at any time, in general, is either liquid, solid or vapour. This state depends on two variables; temperature and pressure (Figure 70). Phase diagram for water gives the state of the water under these variables.

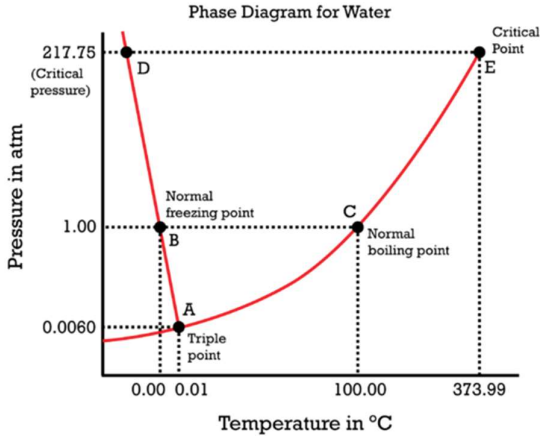

Figure 70: phase diagram for water (Earle & Earle, 2004)

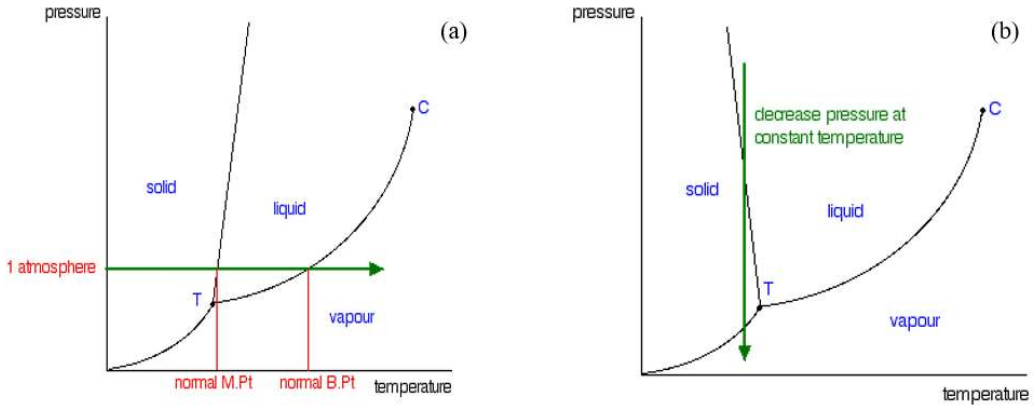

Figure 71: State of water during (a) heating under fixed pressure, (B) reducing pressure under fixed temperature. (Earle & Earle, 2004)

Red lines in the diagram indicates to the possibility of the two states exist side by side. At 0.0098oC and 0.60 kPa (point A on the diagram), all three stats of water can be found together. Heating water under a constant pressure will change its conditions horizontally across the diagram and boundaries and hence its state (Figure 71a). The same will occur for the water state if pressure is reduced under a constant temperature (Figure 71b).

The line AE in Figure (70) which is known as the vapour pressure/temperature curve represents the conditions of liquid and water vapour coexist in equilibrium. The vapour pressure in turn indicates to the tendency of water molecules to escape in gaseous form from the liquid. The vapour pressure/temperature curve for water can be enlarged as shown in Figure (72). Boiling occurs when the water molecules get energy enough to overcome the total water surface pressure or in different words when the vapour pressure of the water caused by water molecules is equal to the pressure on the water surface caused by atmospheric or ambient pressure. In normal atmospheric pressure, the boiling point is 100oC. Any change in atmospheric pressures up or down requires corresponding change in water boiling temperatures above or below 100oC respectively.

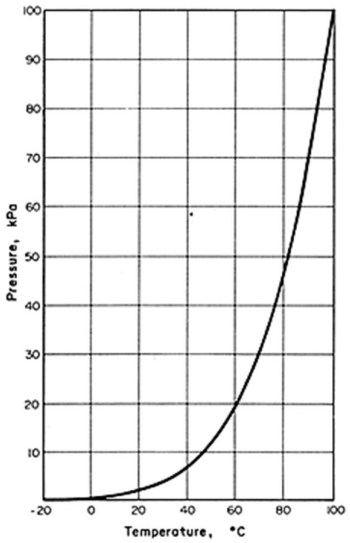

Figure 72: Enlargement of The vapour pressure/temperature curve (Earle & Earle, 2004)

6.4.1 Heat energy required for vaporization

The heat energy must be supplied to the sludge to vaporize its water content. The quantity of energy required to vaporize a unit of liquid water is known by the latent heat of

vaporization. It is measured by KJ energy per Kg water (KJ/Kg). The heat energy required can be easily calculated by using values of the latent heat of vaporization of water illustrated in Table (8) below. However, at atmospheric pressure and 100oC, the latent heat of vaporization of water is 2257kJkg-1 and the specific heat capacity of water is 4.186 kJkg-1oC -1 (Earle & Earle, 2004).

Temperature (°C)	Pressure(Absolute) (kPa)	Enthalpy (sat. vap.) (kJ kg^{-1})	Latent heat (kJ kg^{-1})	Specific volume (m^3 kg^{-1})
		Temperature Table		
0	0.611	2501	2501	206
1	0.66	2503	2499	193
2	0.71	2505	2497	180
4	0.81	2509	2492	157
6	0.93	2512	2487	138
8	1.07	2516	2483	121
10	1.23	2520	2478	106
12	1.40	2523	2473	93.9
14	1.60	2527	2468	82.8
16	1.82	2531	2464	73.3
18	2.06	2534	2459	65.0
20	2.34	2538	2454	57.8
22	2.65	2542	2449	51.4
24	2.99	2545	2445	45.9
26	3.36	2549	2440	40.0
28	3.78	2553	2435	36.6
30	4.25	2556	2431	32.9
40	7.38	2574	2407	19.5
50	12.3	2592	2383	12.0
60	19.9	2610	2359	7.67
70	31.2	2627	2334	5.04
80	47.4	2644	2309	3.41
90	70.1	2660	2283	2.36
100	101.4	2676	2257	1.67
105	120.8	2684	2244	1.42
110	143.3	2692	2230	1.21
115	169.1	2699	2217	1.04
120	198.5	2706	2203	0.892
125	232.1	2714	2189	0.771
130	270.1	2721	2174	0.669
135	313.0	2727	2160	0.582
140	361.3	2734	2145	0.509
150	475.8	2747	2114	0.393
160	617.8	2758	2083	0.307
180	1002	2778	2015	0.194
200	1554	2793	1941	0.127
		Pressure Table		
7.0	1.0	2514	2485	129
9.7	1.2	2519	2479	109
12.0	1.4	2523	2473	93.9
14.0	1.6	2527	2468	82.8
15.8	1.8	2531	2464	74.0
17.5	2.0	2534	2460	67.0
21.1	2.5	2540	2452	54.3
24.1	3.0	2546	2445	45.7
29.0	4.0	2554	2433	34.8
32.9	5.0	2562	2424	28.2
40.3	7.5	2575	2406	19.2
45.8	10.0	2585	2393	14.7
60.1	20.0	2610	2358	7.65
75.9	40.0	2637	2319	3.99
93.5	80.0	2666	2274	2.09
99.6	100	2676	2258	1.69
102.3	119	2680	2251	1.55
104.8	120	2684	2244	1.43
107.1	130	2687	2238	1.33
109.3	140	2690	2232	1.24
111.4	150	2694	2227	1.16
113.3	160	2696	2221	1.09
115.2	170	2699	2216	1.03
116.9	180	2702	2211	0.978
118.6	190	2704	2207	0.929
120.2	200	2707	2202	0.886
127.4	250	2717	2182	0.719
133.6	300	2725	2164	0.606
138.9	350	2732	2148	0.524
143.6	400	2739	2134	0.463
147.9	450	2744	2121	0.414
151.6	500	2749	2109	0.375
167.8	750	2766	2057	0.256
179.9	1000	2778	2015	0.194

Table 8: values of the latent heat of vaporization of water, (Steam table of saturated steam). (Keenan et al., 1969)

In sludge drying systems, steam is practically used as a heat source to heat air or surfaces that are used for drying. Steam gives up, by condensation, its latent heat of vaporization to the sludge to convert its moisture content to vapour. However, the latent heat of vaporization is affected by pressure wherein lower surface pressure results in slightly higher latent heat of vaporization (Table 9). Therefore, one unit of steam is practically not enough to evaporate one unit of sludge moisture content due to the difference in surface pressure and transferring losses (Earle & Earle, 2004).

Absolute pressure (kPa)	Latent heat of vaporization (kJ kg^{-1})	Saturation temperature (°C)
1	2485	7
2	2460	18
5	2424	33
10	2393	46
20	2358	60
50	2305	81
100	2258	99.6
101.35 (1 atm)	2257	100
110	2251	102
120	2244	105
200	2202	120
500	2109	152

Table 9: the latent heat & saturation temperature of water (Singh, 2014)

This formula below is used to calculate the energy required for drying,

Heat energy required to dry raw sludge (Q)

Q = *heat energy to raise its temperature to 100°C+ latent heat to remove (evaporate) water*

*= ΔT °C * specific heat capacity of sludge (kJkg^{-1}°C^{-1}) * mass of sludge (Kg) + moisture content of sludge %wt (Kg_{water}/Kg_{sludge})* mass of sludge (Kg)* the latent heat of vaporization of water at 100°C ($kJkg^{-1}_{water}$).*

$$\boldsymbol{Q = m\, c\, \Delta T + moisture\ content\ \%wt \times m\, \Delta H_{vap}}$$

Q = heat energy (Joules, KJ)

m = mass of the sludge (kg)

c = specific heat (KJ/kg·K)

ΔT = change in temperature (Kelvins, K)

ΔH_{vap} = *the latent heat of vaporization of water at 100°C (kJ/kg$_{water}$)*

6.4.2 Rates of heat transfer during drying

The amount of heat energy that can be transferred to the water content of sludge to provide it with latent heat of vaporisation determine the rates of drying. Heat transfer can be accompanied with mass transfer (water vapour) under some circumstances which limits the determination of drying rates (Earle & Earle, 2004). Determining the heat transfer mechanism; conduction, convection, and radiation in drying process is important because very often one method of them predominates and likely governs the overall process. For instance, air drying and roller dryer. The rate of heat transfer from gas to liquid by using air drying is given by this formula:

$$\boldsymbol{q = h_s A\,(T_a - T_s)}$$

q = *the heat transfer rate (J/s) or (Watt)*

h_s = *the surface heat transfer coefficient ($Jm^{-2}\,s^{-1}{}^{o}C^{-1}$)*

A = *the area of heat flow (m^2)*

T_a = *the air temperature (°C)*

T_s = *the temperature of sludge surface which is drying (°C).*

For roller dryer, the area of heat flow is bigger because the sludge is spread over the dryer surface (rotating heated drum). The heat transfers from the drum to the sludge by conduction. The heat transfer formula is

$$\boldsymbol{q = U A\,(T_d - T_s)}$$

U = *the overall heat-transfer coefficient*

T_d = *the drum surface temperature (close to the steam temperature)*

T_s = *the surface temperature of the sludge (close or slightly above the boiling point of water)*

A = the area of real drying surface.

Practically, the conductivity of the sludge layer and of the drum material are used to estimate the value of U. Based on the quality of conduction conditions, values of U vary from 60 ($Jm^{-2}\ s^{-1}\ ^oC^{-1}$) to as maximum as 1800 ($Jm^{-2}\ s^{-1}{}^oC^{-1}$) (Earle & Earle, 2004).

However, if heat is transferred by radiation, the temperature of sludge surface likely to be higher than the ambient air temperature.

After a while as drying proceeds, the surface layers become dry. These layers take place as heat conductors to lower layers. Because of their poor conductivity, drying process progressively becomes slower.

6.4.3 Efficiency of dryer

Efficiency of dryer is used as a description for its performance. Dryer efficiency is basically the ratio of the minimum quantity of energy needed to the quantity of energy that actually consumed. The minimum quantity of heat energy required to remove water from the sludge is that required to supply its water content with the latent heat of vaporisation. For dryers that use air drying, the heat balance over the air can be used to measure their efficiency by assuming the dryer as an isothermal (adiabatic) system. The efficiency can be given as:

$$\eta = \frac{T_1 - T_2}{T_1 - T_a}$$

η = *dryer efficiency*

T_1 = *the temperature of inlet air into dryer*

T_2 = *the temperature of outlet air from dryer*

T_a = *the ambient air temperature*

Despite practically two or more of drying mechanisms may be involved in the dryer to increase the drying efficiency, following are an experimental overall thermal efficiencies of common dryers that use different drying mechanisms (Earle & Earle, 2004):

Spray dryers 20-50% (convection),

Radiant dryers 30-40% (radiation),

Drum dryers 35-80% (conduction)

Attention should be paid to that energy can vaporise water content of sludge but a method must be used to dispose this moisture and non-condensable gases such as vacuum systems or a current of dry air.

6.4.4 Mass transfer during drying

As the difference between inlet and outlet temperatures and heat-transfer coefficient are the main factors affect the rate of heat transfer, the difference in pressure or concentration and mass-transfer coefficient affecting the rate of mass transfer. The mass-transfer rate is proportional to the pressure or concentration difference and to the mass-transfer coefficient.

Mass transfer can be driven from the equation q = UA ΔT to find

$$\frac{\boldsymbol{d_w}}{\mathbf{d}_{\boldsymbol{t}}} = \boldsymbol{kg'A\,\Delta Y}$$

dw/dt = the mass of water being transferred from sludge in time (kgs^{-1})

A = the area where mass transfer takes place (m^2)

kg' = the mass transfer coefficient ($kgm^{-2}\ s^{-1}$)

ΔY = the difference of humidity ($kgkg^{-1}$)

The mass rate of water vapour can be calculated by:

$$\boldsymbol{G_v = \frac{kg'\,A\,M_w\,(P_w - P)}{RT}}$$

then

$$\boldsymbol{G_v = kg'\,A\,\rho_A\,(Y_w - Y)}$$

G_v = dw/dt = the mass rate of vaporisation

M_w = *the molecular weight of water*

P_w = *the vapour pressure of water at wet bulb temperature* (T_w)

R = *the universal gas constant*

T = *the absolute temperature*

ρ_A = *the density of air at its mean partial pressure*

Y =*the humidity of the dry air stream*

Y_w = *the humidity of saturated air at wet bulb temperature* (T_w).

The heat transfer rate that required to achieve this mass transfer rate of vaporisation is given by:

$$= \boldsymbol{kg'\, A\, \rho_A\, (Y_w - Y)\, \lambda}$$

Which can be given at equilibrium as:

$$\boldsymbol{Y - Y_w = -h_c\, \frac{T - T_w}{kg'\rho_A\, \lambda}}$$

h_c = *the heat transfer coefficient*

T = *the temperature of dry air stream*

T_w = *the wet bulb temperature*

λ = *the latent heat of vaporisation of a unit mass of water.*

Mass transfer formula is not easily to be applied directly due to changes in the nature of mass movement as drying proceeds (Earle & Earle, 2004). The first stage of mass movement when moisture is transferred from the sludge surface to the ambient. As drying proceeds, the second stage when moisture from deeper layers is transferred to the surface of sludge and then to the air. Therefore, the relationships of water diffusion through the sludge as well as the relationships between the wet sludge surface and the ambient air are required for mass transfer calculations. Practically, heat and mass transfer are considered simultaneously. As air is a major heat and mass transfer medium, more focus will be given to the relationships between it and its moisture content (humidity).

6.4.5 Psychrometry of air and Psychrometric Chart

Psychrometry of air is the relationships between it and its correlating moisture including its temperature and its humidity. Psychrometry of air illustrates its capacity for moisture removal. These relationships are represented graphically by psychrometric chart which represents the psychrometric processes of air including air properties such as wet bulb temperature, dry bulb temperature, humidity, and dew point (Figure 73).

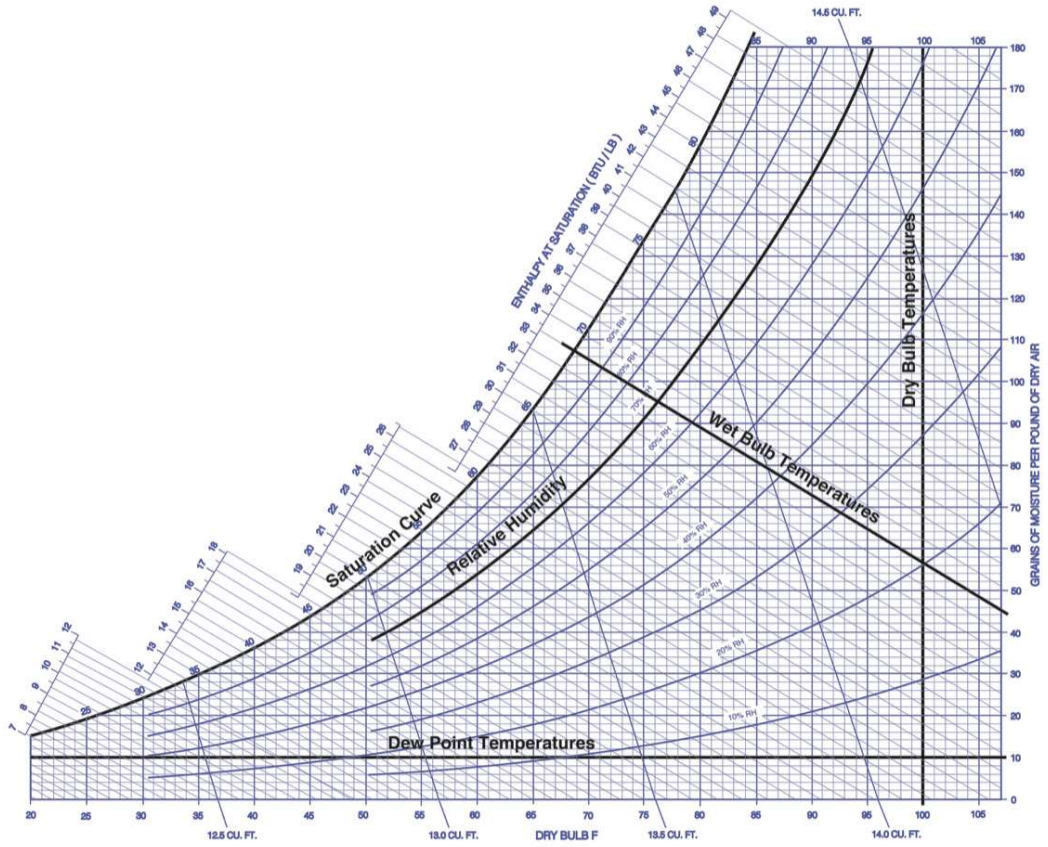

Figure 73: typical psychrometric chart. (Technical Bulletin 3 of Desert aire, 2019)

Typical psychrometric chart shows Dry Bulb temperatures (the ordinary temperature of dry air) as vertical lines and Dew Point temperatures as horizontal lines. The straight diagonal lines that sloping downward from left to right represent Wet Bulb temperatures (the temperature of a water surface when air stream passing over it).

When the wet sludge exposed to a dry hot air stream, the temperature of air decreases below the dry-bulb temperature because the air loses its heat to the surface water in the sludge. The heat transfer continues until the dry-bulb temperature becomes equal to wet-bulb temperature. The rate of heat transfer from dry hot air proceeds until becomes just equal to the rate of heat transfer required for evaporation of water into the air stream. These rates can be expressed mathematically by:

$$\boldsymbol{h_c A\,(T_a - T_s) = \lambda\, kg'\, A\,(Y_s - Y_a)}$$

where

T_a = *actual temperature,* T_s = *saturation temperature*

Y_a = *actual humidity,* Y_s = *saturation humidity*

h_c = *the heat transfer coefficient*

kg' = *the mass transfer coefficient*

λ = *the latent heat of evaporation of water.*

Therefore,

$$\frac{\boldsymbol{h_c}}{\boldsymbol{kg'}} = \boldsymbol{\lambda}\,\frac{\boldsymbol{(Y_s - Y_a)}}{\boldsymbol{(T_a - T_s)}}$$

The bold black curve that forming the top edge of the chart represents the Saturation Curve. Saturation curve represents the conditions (temperature and pressure) wherein air is completely saturated with moisture. Air in such conditions that fall on this curve being not able to absorb any additional moisture. At saturation curve when air is saturated, both temperatures; the dry-bulb and the wet-bulb are identical. Moreover, at any temperature falls on the saturation curve, the partial pressure of the water vapour in the air is equal to the saturation vapour pressure of water. Partial pressure is the pressure exerted by the molecular concentration (the present number of moles) of a particular gas among a gaseous mixture, such as wet air (air with water vapour), into the total volume of the system. Thus, the total pressure of a mixture of gases is the sum of partial pressures of its constituents.

The water content of air is known by humidity (Y). Humidity is the mass of water associated with the unit mass of dry air. This can be expressed mathematically as:

$$\boldsymbol{Y = \frac{moles\ of\ water\ vapour}{moles\ of\ dry\ air}}$$

$$\boldsymbol{Y = \frac{P_w}{P - P_w}}$$

P_w = the partial pressure of the water in air vapour

P = the total pressure

$$\boldsymbol{Percentage\ humidity\ = \frac{Humidity\ of\ air}{Humidity\ of\ saturated\ air}\ \times 100}$$

$$\boldsymbol{Percentage\ humidity = \frac{Y}{Y_0} \times 100}$$

The relative humidity is the ratio of the partial pressure of water vapour in the air to the partial pressure of saturated water vapour at the same temperature. The decreasing in the relative humidity of the air results in the increasing of the difference between the dry-bulb temperature and the wet-bulb temperature. Relative humidity is given by:

$$\boldsymbol{RH = \frac{p}{p_s}}$$

RH = the relative humidity

p = the partial pressure of the water vapour in the air

p_s = the partial pressure of saturated water vapour at the same temperature

RH is commonly expressed as a percentage.

$$\boldsymbol{RH = \frac{Partial\ pressure\ of\ water\ vapour\ in\ air}{Vapour\ pressure\ of\ water\ at\ the\ same\ temperature} \times 100}$$

$$\boldsymbol{RH = \frac{p}{p_s} \times 100}$$

In saturated air at a given temperature and pressure, the air will be in equilibrium with water vapour, thus, $p = p_s$ and hence RH = 100%.

The humidity can be calculated by:

$$\boldsymbol{Y = \frac{18\, p_w}{29\,(P - p_w)}}$$

Y = the humidity

P_w = the partial pressure of the water in air vapour

P = the total pressure

In air systems at room temperature, p_w is very small, therefore, the humidity will be approximately:

$$\boldsymbol{Y \approx \frac{18\, p_w}{29\, P}}$$

Two kinds of humidity are used widely; relative humidity and absolute humidity because of the difference in nature of air and water. Volume of air is represented by:

$$\boldsymbol{v = K\, \frac{T}{P}}$$

v *= Volume, K = Constant, T = Temperature, P = Pressure.*

However, the volume of a unit mass of dry air with its associated water vapour is known as humid volume (m^3 /kg). At atmospheric pressure and ideal conditions, humid volume is given by:

$$\boldsymbol{Humid\ volume} = \frac{22.4}{29} \times \frac{T}{273} + \frac{22.4\, Y}{18} \times \frac{T}{273}$$

Air has a compressible nature, therefore, volume of air increases as its temperature increases and decreases as the pressure increases. In opposite, water is not compressible and will occupy almost the same volume regardless its conditions. In psychrometric chart, the extended curved lines that come under the saturation curve represent the Relative Humidity.

Relative humidity is expressed as a percentage represents the amount of air volume that displaced by moisture in comparison to the total air volume. The absolute humidity represents the mass of water vapour that associated with the unit mass of dry air (kg_{water}/ $kg_{dry\ air}$). However, the difference in the values between them does not exceed commonly 8 per cent (Chakraverty & Singh, 2014).

Therefore, changes in the air volume do not affect the moisture volume, thus, changes in relative humidity do not affect the actual water content. In other words, absolute humidity concentration is the point of water vaporization regardless of the relative humidity of air. This is represented in the constant Dew Point Temperature which is the temperature where p = ps at a particular moisture content. Below the dew-point, water vapour will condense out as a fog or droplets.

In term of energy, psychrometric chart shows sensible (heating or cooling) energy and latent (heat or cooling) energy. Sensible heat and sensible cooling occur by adding and removing heat respectively with keeping the moisture constant. Latent heat (humidification) occurs by adding moisture without any change in the dry bulb temperature. In opposite, latent cooling (dehumidification) occurs by removing of moisture without any change in the dry bulb temperature. The enthalpy change of moist air can be calculated be multiplying the mass of dry air by both the difference of temperature and by the humid heat of moist air (c_s) and given as (KJ^{o}C/kg).

When a stream of wet sludge is in contact with the wet air, they, in the end, reach a point where the temperature of the heat lost by humid air and the temperature of the heat of evaporation that gained by water are equal. This case is known by adiabatic saturation condition. The change in total enthalpy for isothermal system adiabatically saturated can be given by:

$$\Delta H = c_s\,(T_a - T_s) + \lambda(Y_s - Y_a) = 0$$

$$c_s = \frac{-\lambda\,(Y_s - Y_a)}{T_a - T_s}$$

$$c_s = \frac{-h_c}{kg'}$$

ΔH is given by (kJ/kg dry air)

c_s *= the humid heat of the air.*

T_a *= actual temperature,* T_s *= saturation temperature*

Y_a *= actual humidity,* Y_s *= saturation humidity*

h_c *= the heat transfer coefficient*

kg' *= the mass transfer coefficient*

λ *= the latent heat of evaporation of water.*

For drying systems working in normal conditions, the ratio above is known as the Lewis number and practically is widely used numerically as:

$$\frac{h_c}{c_s\, kg'} = 1$$

When the Lewis number = 1, this indicates that the adiabatic saturation line and the wet bulb line are identical.

6.4.6 Air drying

The water content of sludge is a mix of free and bond water. Many forces their intensity vary from weak to very strong chemical bonds are involved. Free water has weak bonds and hence easier to be removed. In the first drying stage, the water content of sludge behaves as a free surface water. The rate of drying in this stage is known by constant rate drying. Dry solid content and water content of sludge can be given by:

$$w = W\, x\, \frac{X}{(1 + X)}$$

- w *= the mass of dry solid content of sludge*
- x *= the moisture content of the sludge on a dry basis*
- W *= the original mass of the wet sludge being dried*
- X *= the mass of associated moisture content for the original mass.*

Then water content of the sludge starts vaporising constantly with a constant rate drying as:

$$\boldsymbol{X(dw/dt\,) = w\,(dX/dt\,) = 1}$$

After a while of constant drying rate, the water then vaporises more slowly.

6.4.7 Drying time

Time of drying process is an important factor in dryer design. Calculating the drying time is not simple because it vary as long as drying process proceeds and the moisture content of the sludge is lower. A simplified approach can be used such as assuming that relative humidity of the drying air and its temperature are constant. Therefore, the time of the constant rate period, which is needed to reduce the water content of sludge to the critical point wherein drying rate falls, can be calculated by:

$$\boldsymbol{t = \frac{w(X_0 - X_c)}{(\frac{d_w}{d_t})_{constant}}}$$

Where

$$\boldsymbol{(dw/dt\,)_{constant} = kg'\,A\,(Y_s - Y_a)}$$

- *Xc = the final moisture content of sludge on a dry basis (critical content).*
- *Xo = the initial moisture content of sludge on a dry basis.*
- *w = the dry solid content of sludge.*
- $\boldsymbol{(\frac{d_w}{d_t})_{constant}}$ *= the constant drying rate.*
- *kg′ = the mass transfer coefficient*
- *A = the area where mass transfer takes place (m2)*

By using factor *f* to reduce the drying rate at different moisture levels, the equations above can be given as:

$$\boldsymbol{t = \frac{w(X_0 - X_f)}{f(\frac{wd_x}{d_t})_{constant}}}$$

$$t = \frac{w(X_0 - X_f)}{f\, kg'\, A\, (Y_s - Y_a)}$$

- *Xf = the final water content of sludge*
- *f = the ratio of the actual drying rate of sludge to the maximum drying rate of sludge.*

As mentioned before, three rates can be noticed during the drying process; constant rate, first falling-rate, and second falling-rate (Figure 74). Each one of these rates takes a period of time.

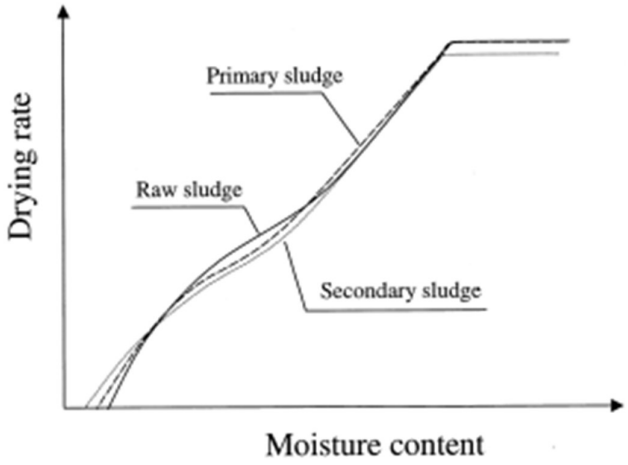

Figure 74: typical drying rate curve of sludge. (Chen, Lock Yue & Mujumdar, 2002)

The rate of drying during the constant rate period can be calculated, for most design proposes, by this equation:

$$W = \frac{dw}{dt} = \frac{h\, A\, \Delta T}{\lambda} = k'\, A\, (P_s - P_w)$$

Where

- *W = the rate of losing of water,*
- *h = the heat transfer coefficient from air to the wet surface,*
- *ΔT = the temperature difference between the air and the surface,*
- *λ = the latent heat of vaporisation per unit mass,*
- *kg' = the mass transfer coefficient for diffusion from the wet surface through the air,*

- *A = the area of interface for heat and mass transfer, and*
- *$(P_s - P_w)$ = the difference between the vapour pressure of water at the surface and the partial pressure in the air.*

The equation shows that P_w needs to be as minimum to get high drying rate. P_w can easily reach a value equal to the value of saturated air when the temperature of sludge surface is greater than the temperature of the air stream. In this case, the value of W will be zero because the air capacity to absorb moisture is zero. This will result in forming mist and hence probably redepositing water on the sludge surface.

It may be preferable to use the values of T, h, and A to determine the rate of drying to avoid the influence of the conditions inside the solid. h depends on the speed and the direction of air flow. It is practically calculated as

$$h = C\,G'^{0.8}$$

Where

G' = the mass rate of flow air (kg/s m^2)

The high air temperature may result in the sludge temperature rising above the wet bulb temperature. This is due to passing a considerable amount of the heat to the sludge by radiation which increases the heat transfer coefficient.

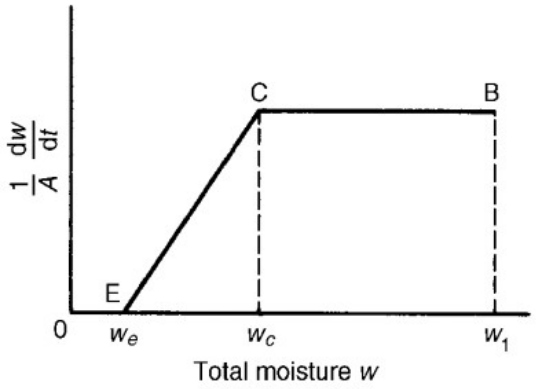

Figure 75: estimating the time for drying by using a rate of drying curve (University of Babylon)

In order to measure the rate of drying of the sludge with presence of hot air, it is better to use the simplest drying curve (Figure 75); where

- $\boldsymbol{w}$ = *the total moisture,*
- $\boldsymbol{w_e}$ *is the equilibrium moisture content (point E),*
- $(\boldsymbol{w - w_e})$ = *the free moisture content,*
- $\boldsymbol{w_c}$ = *the critical moisture content (point C)*

Based on the rate of drying curve, the time of drying can be divided into two stages; constant-rate period and falling-rate period. During the constant rate of drying from the initial moisture content $\boldsymbol{w_1}$ to the point of critical moisture content $\boldsymbol{w_c}$, the time of drying $\boldsymbol{t_c}$ is calculated by

$$\boldsymbol{t_c = \frac{w_1 - w_c}{R_c\, A}}$$

Where

- $\boldsymbol{R_c}$ = *the rate of drying per unit area in the constant rate period,*
- $\boldsymbol{A}$ = *the area of exposed surface.*

During falling-rate period, the rate of drying is proportional to the free moisture content given by $(\boldsymbol{w - w_e})$. Therefore, the rate of drying is

$$\boldsymbol{-\left(\frac{1}{A}\right)\frac{dw}{dt} = m\,(w - w_e) = m\,f}$$

Then

$$\boldsymbol{t_f = \frac{1}{m\,A}\ln\left(\frac{f_c}{f}\right)}$$

Thus, the total time of drying will be

$$\boldsymbol{t_c = \frac{(w_1 - w_c)}{m\,A\,f_c}}$$

Thus,

$$\boldsymbol{t_{total} = \frac{(w_1 - w_c)}{m\,A\,f_c} + \frac{1}{m\,A}\,ln\left(\frac{f_c}{f}\right)}$$

$$t_{total} = \frac{1}{m\,A}\left[\frac{(f_1 - f_c)}{f_c} + ln\left(\frac{f_c}{f}\right)\right]$$

7. Design of solar pyrolysis system

7.1 Overview

Different processes involve pyrolysis (Baso, 2013). Basically, pyrolysis process works to break down large and complex molecules of hydrocarbon into simpler and smaller molecules by rapid heating rate to pyrolysis temperature (350 ^{o}C to 600 ^{o}C) in absence of oxygen (Figure 76) to produce gas, liquid, and solid. This process is done technically by using a chamber known as pyrolysor or pyrolysis reactor. This reactor contains “fluidized bed” that is fed with almost totally dry feedstock. The initial products of pyrolysis are vapours and solids. The solid product is char which in turn leaves chamber partly with vapours and the rest remains in the chamber. Vapours both condensable and non-condensable are released through the chamber to be cooled and hence separate char. Later, condensable vapours are condensed to produce pyrolysis oil or bio-oil while solid char are collected for several uses.

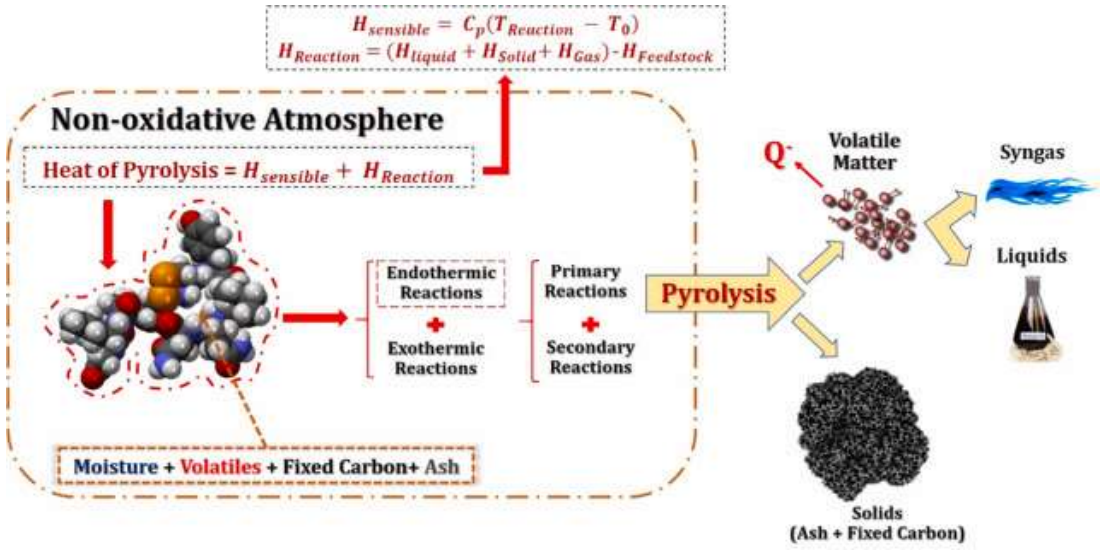

Figure 76: Pasic concept of Pyrolysis: breaking down thermally large and complex molecules into smaller ones. (Campuzano, Brown & Martínez, 2019)

To produce bio-oil, typical pyrolysis operation is by subjecting feed material to rapid heating rate until intermediate pyrolysis temperature reached and then immediate quenching to prevent any further reactions among feed molecules.

To facilitate the pyrolysis process, many factors need to be taken into consideration. These factors affect pyrolysis products as well. For instance, moisture content, feeding speed, particle size and other physical structure of pyrolysis feedstock have an impact on pyrolysis process and pyrolysis yield. Interestingly, smaller size of feed material gives a higher liquid yield.

Therefore, the both solar and conventional pyrolysis systems have the same concept. The main difference is the source of energy. Depending on the source of energy, pyrolysis unit requires supplementary equipment to achieve that.

The shortcomings of conventional fossil fuel-based pyrolysis are a great motivation forward developing a sustainable pyrolysis system. These drawbacks include diminishing the sources of heat energy that is required to heat the reactor, prominent global warming due to the extensive heat energy required to start up the pyrolysis reaction, the complication of pyrolysis units that have electrical heaters, the high cost of these systems as well as the potential environmental pollution because of the huge amount of CO_2 production. Since the current heating systems are external biomass and fossil fuel heating system (generates huge amount of CO2 and causes air pollution) and internal electrical heating system (very complex and expensive option), therefore, solar pyrolysis is presented as a solution to eliminate these issues. Solar assisted pyrolysis that based on combination of solar and sludge heating system can be very effective because it is more eco-friendly system and more energy efficient. Solar assisted pyrolysis uses the solar energy as an external heating source to heat up the feed material into the reactor. The products of solar pyrolysis contain huge amount of heat energy that can be used also either to heat up directly the feed material into the reactor or to generate the electricity needed for continuous heating of the reactor (Figure 77). Unlike fluidize system, using a control valve to control the feed supply is recommended because it relieves a controlled fixed bed pyrolysis (Joardder et al. 2014).

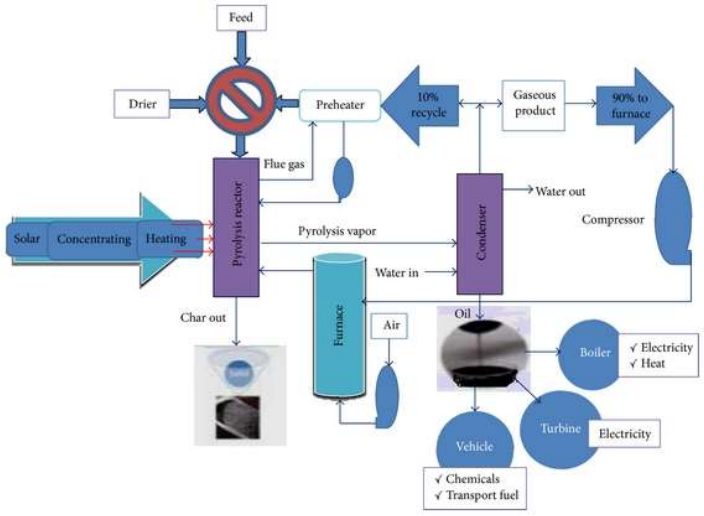

Figure 77: a conceptual design for a solar assisted pyrolysis system. (Joardder et al. 2014)

Joardder 2014 presented one of the most reasonable desian for commertial solar-powerd - pyrolysrs systems. This design is shown in Figure (78) where two parabolic solar concentrator were used to focus the solar energy over a stainless steel fixed bed reactor. Both parabolic solar heater and biomass heating system were used to heat up the reactor. The heater was surrounded by asbestoses to reduce heat loss. Nitrogen gas was used to maintain the inert atmosphere inside the reactor. A liquid condenser was used to condensate the gaseous products of pyrolysis into bio-oil by using ice-cooled liquid collectors.

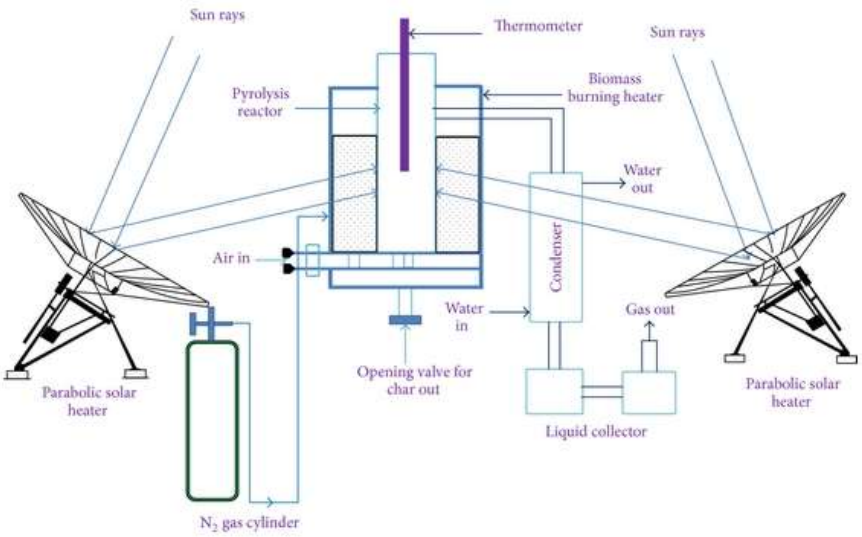

Figure 78: a schematic diagram of solar assisted pyrolysis system using a fixed bed reactor. (Joardder et al. 2014)

The main units in the traditional pyrolysis plant are grinder, heater, reactor and condenser. For sludge pyrolysis, the dryer is the first main unit followed by a solar collector, reactor and condenser respectively. Unlike other organics, grinder is not important in the sludge pyrolysis unit presented in this study because the product will be similar to “flakes” which are brittle and can be easily broken into fine particles. Design of pyrolyzer afficts type of pyrolysis as well as the distribution of pyrolysis products. Therefore, the final required product should be taken into account in the tentative design criteria of pyrolyzer (Basu, 2013).

This chapter gives an overview of the main units in solar pyrolysis system and a suggested design to obtain the optimal yield.

7.1.1 Practical applications

Many studies have been held to study solar pyrolysis. Interestingly, most of them were on a laboratory scale (Yadav & Banerjee, 2016). However, solar pyrolysis started indoor in laboratory environment with solar simulators as a radiation source and elliptic or parabolic mirrors as concentrators (Yadav & Banerjee, 2016; Zeng et al., 2017). Mercury-xenon arc lamps, xenon lamp, and carbon arcs were used as powerful light sources to produce artificial solar energy (Figure 79) (Authier et al., 2009; Boutin, Ferrer & Lédé, 2002; Tabatabaie-Raissi & Antal, 1986; Hopkins et al, 1984). For instance, Arribas et al. (2017) used a high flux solar simulator by using 7 kW xenon short-arc lamp to analyse sewage sludge, wheat straw, and algae. Two kinds of mirrors were used in this system: one flat mirror and two ellipsoidal mirrors. One of the ellipsoid mirror hosted the arc discharge while the flat mirror used to reflect and concentrate emitted radiation on the second ellipsoid mirror. The reactor was made from stainless steel. This design gave 5800 kW/m2 as a maximum flux at the focal plane. Interestingly, solar simulated pyrolysis of sludge produced as maximum as 74 vol% syngas in a different range of temperatures.

Figure 79: High Flux Solar Simulator (HFSS) to produce artificial solar energy in Germany. (Institute of solar research DLR)

As a sequent result of solar research, Zeng et al., (2015) used a series of heliostat mirrors to reflect and redirect the solar radiation continuously to a parabolic solar dish collector which focuses solar radiation on the reactor at the focal point. The parabolic solar dish of Zeng et al. was downward facing dish with 1.5 kW maximum power and 15000 W/m^2 flux density. The reactor was a pellet located at the focal point of the dish and was designed with inlets for argon entrance as a sweep gas and outlets for reaction products. The pellet was surrounded and insulated by a transparent graphite crucible. A shutter was used to control the temperature and heating rate in the reactor by applying Proportional Integral Derivative (PID) Controller which modifies the incident solar radiation.

This system was modified by Zeng et al. (2015) by using a 2m diameter downward facing parabolic mirror with 0.85m focal length and adding a sensor to detect the sun and then adjust the system to achieve maximum concentration. In term of reactor, it was made from transparent Pyrex and argon was used as a sweep gas to wash its walls and hence pass the radiation. Later in (2015) also, Zeng et al. modified the previous system to a system works in direct normal irradiance by using a solar dish that is able to concentrate 1 kW/m^2 of flux intensity of direct normal solar radiation to 15,000 kW/m^2. A solar blind optical pyrometer was added to the system to measure the reaction temperature. The reactor was a 6L balloon made from transparent Pyrex and was heating directly from the solar dish. The process was optimized by using Box-Behnken design.

Zeaiter et al. (2015) in an experiment on scrape tyres as a feedstock, approved that Fresnel lens can be used efficiently as solar collector for pyrolysis process. They used Fresnel lens with solar tracking system to maximize the reaction temperature to 850°C with 1500 W/m^2 solar

intensity from simulated radiation. Catalysts such as Metal oxide particles (Weimer et al., 2008), TiO_2, HUSY, and H-beta (Zeaiter et al., 2015) were used to improve pyrolysis product distribution. Excluding TiO_2, catalysts relatively have positive impact on quantity of liquid yield.

Linear Mirrors were used also in a design of solar system. They were used to concentrate solar radiation on the reactor which placed at 5m from the set of mirrors. The reactor was rectangular and hollow from steel. Their system was able to raise the temperature to 500°C within 90 min (Grassmann et al., 2015).

In the same concept, different types of direct and indirect heating solar reactor were designed. The term “Direct heating” in solar pyrolysis is usually used to describe a solar system where the feedstock in the reactor absorbs the heat required for the reaction directly from the sun after it has been concentrated by a solar collector and focused on the reactor (Zadik & Israel, 2011). Therefore, the reactor should be transparent or comprised inside a transparent shell or has an opening to allow concentrated sun radiation reaches the feedstock (Weimer et al., 2008). Indirect heating systems usually use heat transfer fluid (HTF) that absorbs the heat from solar collector and then transfer it to the reactor through the heat exchanger. Thus, the reactor can be opaque and may be away from the solar collector. Despite gases can be used as HTF, liquid materials are commonly used namely molten salts and heat conducting or mineral oils (Jakahi, 1984; Xiang, 2017).

Figure (80) shows a diagram and schematic diagram of a solar system for pyrolysis of sludge has been designed by Zadik & Israel (2011). This design is more about how to assemble different parts together to create a solar system rather than specifying a design for every single part. Their design describes a self-sustainable combination of a solar tower, a thermo-regulated sensor, a control unit, solar thermal reactor, and sludge drying unit.

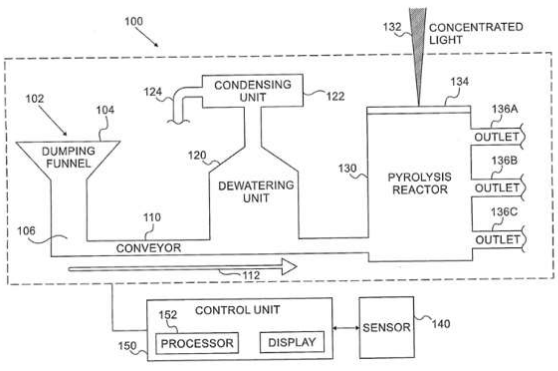

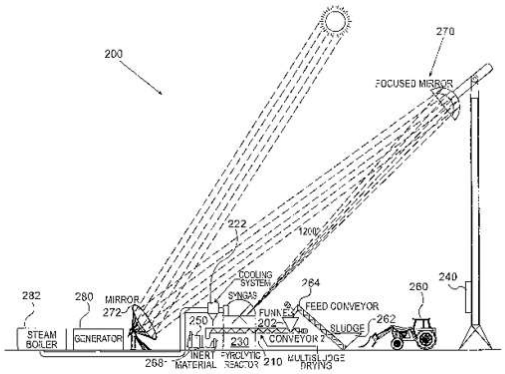

Figure 80: Diagram and schematic diagram of solar system for sludge pyrolysis. (Zadik & Israel, 2011)

According to (Zadik & Israel, 2011), two solar collectors (preferably parabolic dishes or heliostats mirrors) can be used. First one to collect and reflect solar radiation to the second collector. Second one is downward facing collector located over a tower to collect the concentrated radiation from the first collector and focus it on the reactor to generate temperature about 1200°C. Solar collector system is provided with a sun tracking device and a sensor to measure sunlight radiation received and then solar energy generated by the system and hence feasibility of operating the unit. The unit is operated and shut down via control unit based on the output data from solar sensor. The reactor that can be fluidized bed reactor, fixed bed reactors, super critical water reactor, or vacuum pyrolysis reactor is exposed directly to concentrated sunlight, and thus it is comprised of two shells: outer one is transparent from quartz for protection and minimizing heat lost whilst inner one is the reaction shell. This solar thermal reactor that can run selectively by solar energy is equipped with one inlet for sludge feeding, outlets for discharging pyrolysis products, and sensors. These sensors that can be Resistance Temperature Detectors (RTD), thermocouples, solid temperature sensors (thermistor) measure the temperature inside the reactor and hence determine the rate of sludge entry by sending output data to the control unit. Sludge that is carried to the reactor via a helical screw conveyor can be also companied with a stream of inert gas through the inlet while the outlet is also covered by a transparent shell for more transmission of the solar radiation.

Dewatering unit can be a vacuum less evaporation unit equipped with a sensor for sensing the moisture content of the sludge and providing output data to the control unit. A spiral press conveyor or hot air blower can be used to achieve more drying of sludge. The acceptable moisture content of sludge to be able to send to the reactor according to Zadik & Israel (2011) system ranges from (40%-60%) of initial weight. The control unit, in turn, comprises a processor to process the output data received from different sensors and a display unit to display all measured data such as real working time, amount of sunlight received, amount of solar energy concentrated by mirrors, amount of solar energy consumed by the reactor, rate of sludge inters and leaves the dewatering unit to the reactor, amount and rate of production. Therefore, the control unit should be configured to run based on several variables such as the

real time of sun shining, internal heat, the dewatering unit, rate of initial dewatering, sludge feed rate, rate of pyrolysis, temperature, time of residence, and rate of product discharge.

The reactor can be heated directly via concentrated solar energy or indirectly via heat carriers such as hot sand, ceramics, synthetic fluids, or molten salts. Indirect heating can be employed to heat solar reactors during night time which gives more opportunity to run the solar pyrolysis facility for 24 hours per day.

7.2 Design of solar pyrolysis dryer

Drying process is considered as one of most important steps in sludge management specifically thermochemical treatment processes. The most efficient dryer should take into consideration different factors such as energy consumption, resident time, properties and the moisture content of outputs. The water content of sludge affect the calorific value of sludge and its auto-thermal combustion and hence the required amount of energy for reaction. To achieve auto-thermal reaction without auxiliary energy, the moisture content of sludge should be less than 50%.

Preparing of sludge mixture

However, to produce Sludge Flakes with 10% output moisture content, the moisture content of input sludge should be high enough to make the spreading process over the dryer walls easy and without -auxiliary energy. To moderate the moisture content of sludge up to reasonable percent, the feed raw sludge can be also mixed with hot bio-char generated from pyrolysis reaction (5% of initial mass) as well as a percent of dry sludge (7-10% of initial mass) to achieve high heat transfer, fast drying, and to overcome sludge sticky phase as well.

To solve spreading issue, sludge of reasonable moisture content (about 75%) can be also mixed with used frying oils, used mineral oils, grease or animal fat from a meat processing plants as a pre-preparation step for drying. Experimental results of this study show that mixing a mass of raw sludge with waste mineral oil (5-7% of the initial mass of raw sludge) has significant impact in term of spreading as well as results in producing Sludge Flakes (Figure

81). Furthermore, experiments of drying oily sludge (mixture of raw sludge and waste mineral oil) also demonstrate that the oil does not involve in the structure of dry sludge or even in its final mass DS (Figure 82). However, despite the mixture is easier to spread and results in sludge flakes, its drying time is longer than raw sludge Figure (82). The experiment was done by using a Moisture Analyser KERN & Sohn GmbH, TYPE DBS 60-3, SN WB17AH0888. A 1mm layer of this mixture was subjected to a relatively high temperature (200 °C). The process was, to some extent, like a semi-fry process. With the progress in drying process, the sludge layer shrunk from 95mm diameter to 67mm diameter but it remained interconnected as a complete unit unlike raw sludge. It was exactly like a flake. Figure (83) illustrates a comparession between the final product of drying raw sludge and oily sludge.

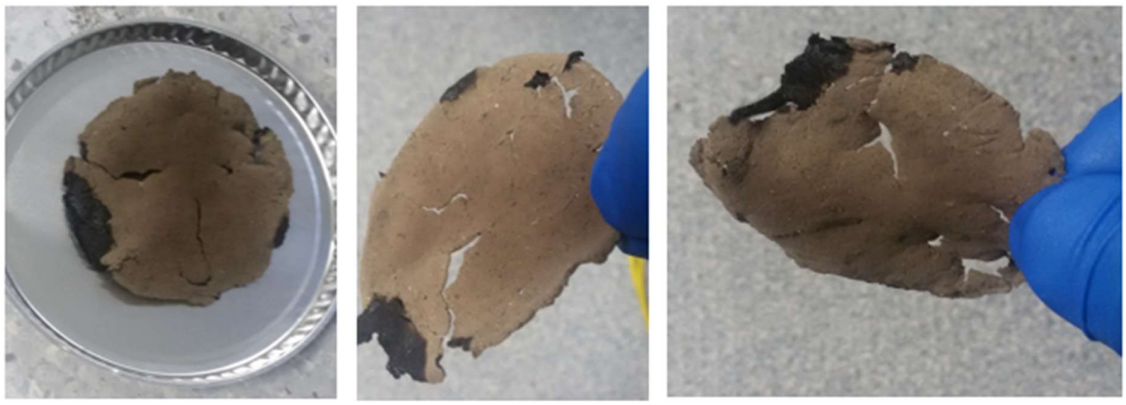

Figure 81: Sludge Flakes as a result of drying oily sludge.

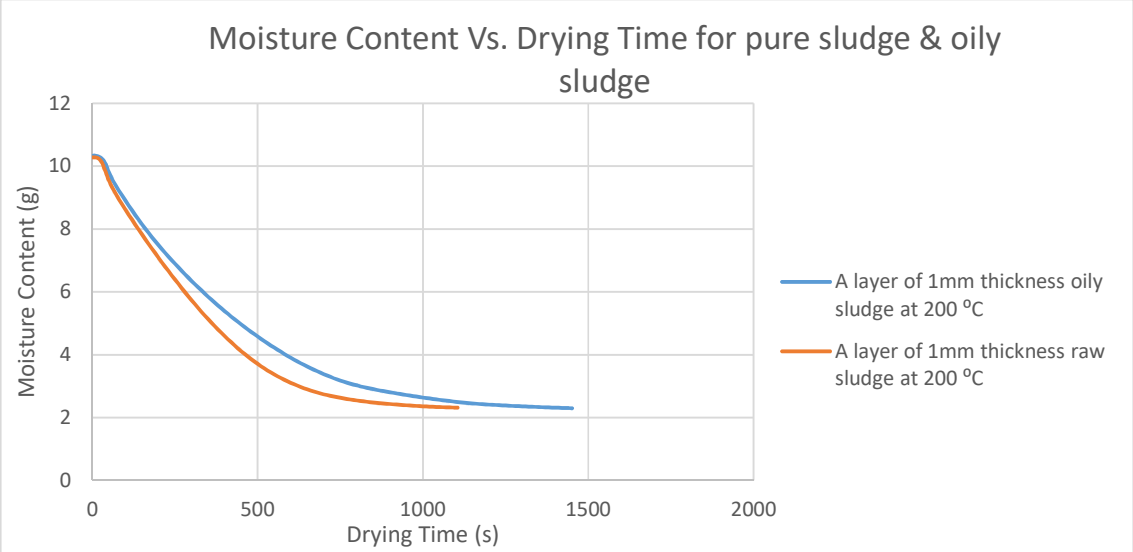

Figure 82: comparison of drying time and final mass for 1 mm layer of raw sludge and oily sludge.

Figure 83: results of drying raw sludge and oily sludge

Frying sludge was presented as drying process by Ohm et al. (2009), Romdhana et al. (2009), Wu et al. (2012), Chang et al. (2013), and Chae et al. (2016). Using used frying oil as a feed material for pyrolysis process was experimented by Billaud, Gornay & Coniglio (2007). The biofuel from pyrolysis process of waste cooking oil fried sludge was studied by Wu et al. (2020). However, all studies indicate that mixing sludge with oils or grease more likely to result in positive impact on the drying process as well as the liquid yield of pyrolysis. Moreover, oily mixture helps to avoid the sticky phase and crust phenomenon of sludge.

Preparing of dryer

Many experiments had been done to find out how to achive the best performance of the dryer. Despite many parameters can affect the dryer efficiency, two main parameters were examined to find out the drying time and then the productivity; operating temperature and the thickness of sludge layer. Experiments show that a layer of 2mm raw sludge needs 4537 seconds (1:15:37) to be dry at 120 °C while the same layer needs 2973 seconds (00:49:33) and 1878 seconds (00:31:18) to be dry at 150 °C and 200 °C respectively. In other words, higher temperature results in shorter drying time. Means that, at 200 °C the dryer can do one run every half hour approximately. According to letreatures in sloar energy, such temperatures (200°) can be obtaind by using Solar Parabolic Trough Concentrator which is able to provide stagnation temperature up to 600 °C with optical efficiency about 80%.

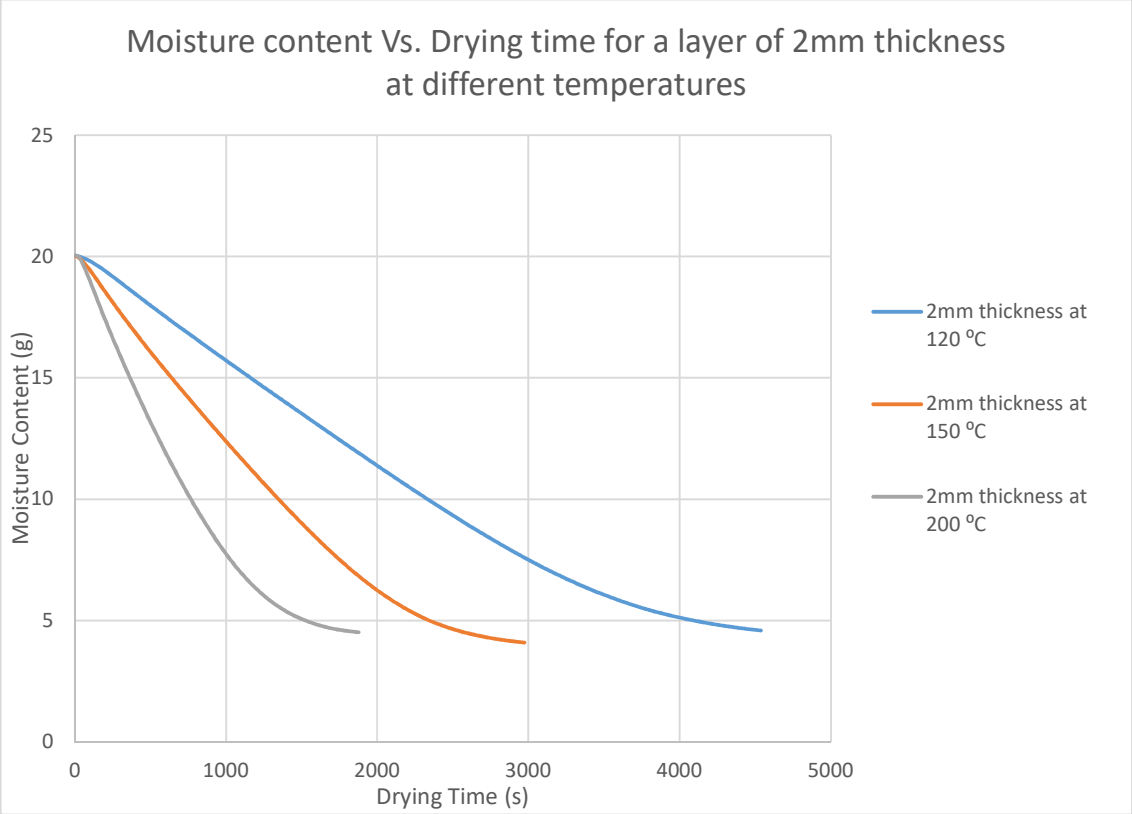

Figure 84: Drying time for a layer of 2mm thickness at different temperatures

Determining the perfect thickness of sludge layer was very challenging. The main difficulty was spreading process. Raw sludge is very sticky and can easily stick on the inlet tube walls as well as dryer walls. Stickness of sludge is highly required in such design of rotating dryers to produce sludge flakes. Adding oil to the sludge can ease spreading process but it also reduces the sludge stickness. Experiments had been done to measure the proper amount of oil to be added to the sludge with maintain its stickness. Therefore, experiments show that a layer of 1mm thickness is the best in term of drying time but it is also challenging in term of its oil content and spreading process. 2mm and 3mm layers are not efficient from time perspective. The best and easiest experimental thickness was 1mm (Figure 85). The oil content of 1mm layer does not highly affect the stickness character of sludge. The best oil content was measured to be 5-7% of the initial mass of raw sludge. The thickness of 1mm meets also the target productivity of this study.

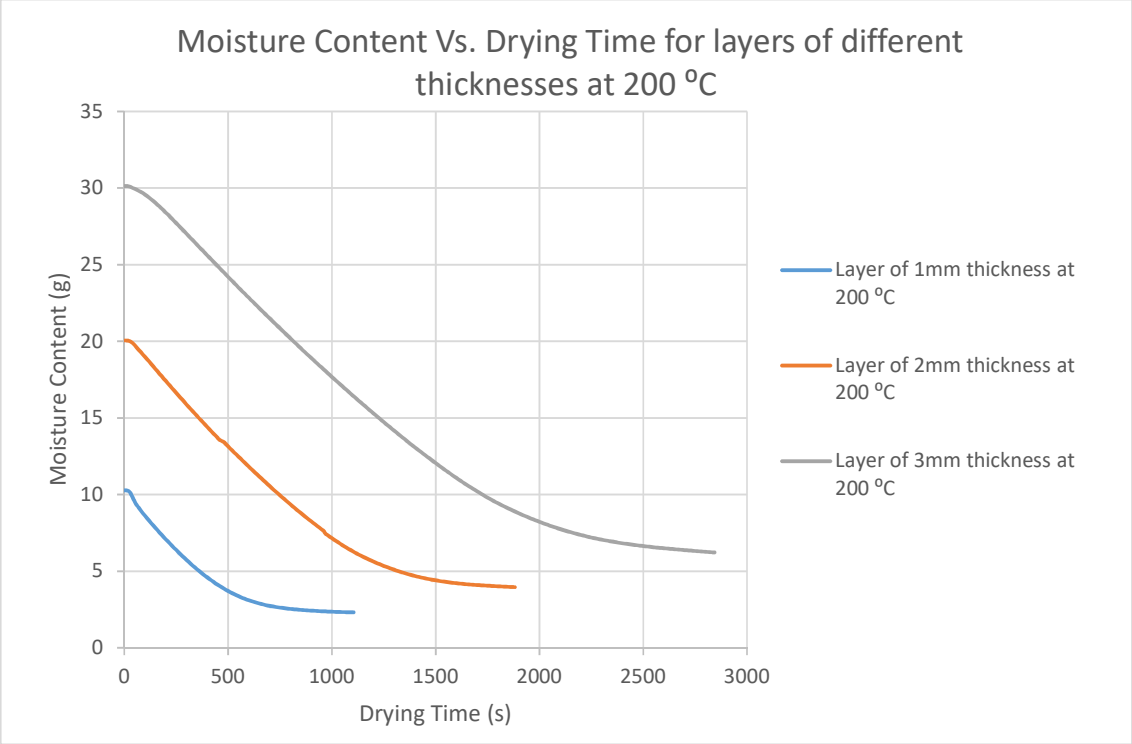

Figure 85: Drying time for sludge layers of different thicknesses.

To accelerate the drying process, the heat energy results from the pyrolysis reaction is conveyed by air and then blown in the dryer. Heat exchanger and air pump is used for this purpose.

For design purposes, drying process to produce Sludge Flakes was modelled via Solidwork designing program (Figure 84) based on parameters have been taken from laboratory analysis for a specific municipal sludge sample from Hamilton Wastewater Treatment Plant. The dryer is a metal tube (copper) with 100cm diameter 100cm length. The thickness of its wall is 1.5 mm.

Due to the stickness of sludge, a screw convoyer is used inside the inlet tube to carry the sludge from the hopper (mixer) and to spread it over the dryer wall. The screw convoyer with a special design shows great performance in this regard because it works as a mixer, convoyer, and spreader and achieves uniform pre-heating for the inlet sludge.

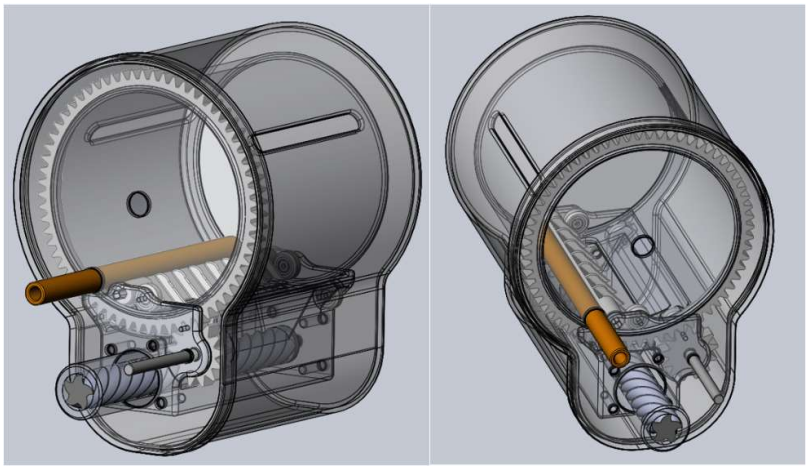

Figure 86: Using Solidwork program to designing & model a novel solar dryer for Sludge Flakes production

Design of the inlet screw convoyer

Design of screw convoyer depends on parameters such us the nature of the feedstock material and the feedstock flow rate and it should include four main physical characteristics; the length of the convoyer, inside and outside diameter of the convoyer shaft, the distance between adjacent fins (the pitch), and the clearance as shown in Figure (87).

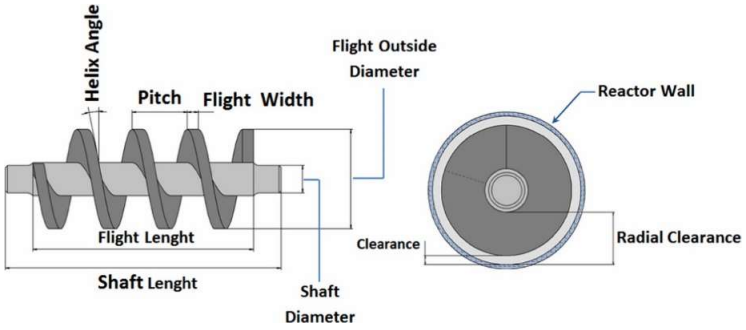

Figure 87: the main dimentional charactaristice in the convoyer design

The standard flight is when the pitch-diameter ratio equal to 1.0. According to Bortolamasi and Fottner (2001), the minimum distance between adjacent flights must be ≥ 0.5 the screw diameter (d_{screw}) and the maximum pitch must be equal to the screw diameter (d_{screw}). In compare to outside diameter of the screw, Evstratov et al. (2015) stated that the pitch must not be more than 1.5 and not less than 0.9 of the outside diameter.

Recognizing the feedstock characteristics are the first step in screw convoyer design. Feedstock with abrasive charactaristics needs to be given special consideration during the designing of screw convoyer. Convoing sticky materials such of sludge is complicated and increase torque requirements due to their tendency to jam and arch. However, screw convoyers run with a load factor ranges between 15 - 45%. The recommended load factor for sticky material is 15% (Figure 88)

Auger capacities

Load factor	Load	Feedstock characteristics
15%		Abrasive
30%		Moderately abrasive
45%		Non-abrasive

Figure 88: suggested load factor of screw convoyer based on the feedstock charactarastics. (Campuzano, Brown & Martínez, 2019)

In term of flighting characteristics, Figure (89) below shows of flight characteristics and geometries according to the manual of screw conveyor components and design of Conveyor Engineering and Manufacturing Co. (2012).

Standard flight: Augers with a pitch-to-diameter ratio equal to 1. It has been widely used to convey a wide variety of feedstock.

Ribbon flight: It is used for conveying sticky, gummy or viscous substances, or where the material tends to stick to the flight at the shaft.

Cut flight: It is used for conveying light, fine, granular or flaky materials. This kind of flight offers an efficient mixing action of dry material especially at high speeds.

Cut and folded flight: It is used to create a lifting motion in the feedstock that helps to promote agitation and aeration while mixing.

Sectional flight with paddles: It is used to mix material while being conveyed. Peddles can be fixed (welded in place) or adjustable to provide different degrees of mixing.

Shaftless: Similar to ribbon augers, it used to convey sticky, gummy or viscous substances. It is also used with stringy products that would typically wrap around the auger shaft. This type of flight has been implemented in the Spirajoule

Paddle: It is used for improving mixing or stirring. Paddles could be fixed or adjustable to provide different degrees of radial and axial mixing patterns.

Interrupted flight: It is also used for conveying sticky, gummy or viscous substances, or when the material tends to stick to the flight at the shaft. It is similar to ribbon flight but offers better throughput and flow consistency than ribbon auger.

Short pitch: It has a pitch-to-diameter radio less than 1 and is meanly used in incline or feeding applications.

Figure 89: Flight and pitch types, characteristics, and geometries and their applications

Therefore, the recommended type for sludge is a screw convoyer combined between shaftless and interrupted flight screw convoyer. This means that the convoyer needs to have a relatively big shaft diameter, small flight outside diameter, and long pitch.

However, the material in this study is known as wet oily sludge (abrasive). The maximum capacity of the screw convoyer is 15%. The required is to calculate the size, speed, and charactaristics of the auger convoyer.

Sludge density is 1020 kg/m^3.

Area of drayer wall ($2\pi r.h$) = 2*3.14*0.5*1 = 3.14 m^2

Volume of sludge on drayer wall in one round = 3.14 m^2 * 0.001 m = 0.00314 m^3

Mass of sludge on drayer wall = Density * Volume = 1400 kg/m^3 * 0.00314 m^3 = 4.396 Kg.

According to the experiments: a layer of 1mm sludge needs 0.5h to be dried.

The capacity of the drayer per one hour is: 4.396 Kg / 0.5h = 8.792 Kg/h

The design of the screw must meet the drayer capacity or greater.

$$Q=60\times(\frac{\pi}{4})\times D^2\times S\times N\times\alpha\times\rho\times C$$

With

Q = screw capacity in kg/h

D = screw diameter in m

S = screw pitch in m

N = screw speed in rpm

α = loading ratio

ρ = material loose density in kg/m^3

C = inclination correction factor

Therefore, according to the engineering manual guideline

Q_{screw} = 60 * (3.14/4) * $(0.05)^2$ * (1.5* 0.05) * 7 * 0.15 * 1020 * 1 = 9.273 Kg/h

Q_{screw} (9.458 Kg/h) is ≥ Q_{drayer} (8.792 Kg/h)

The convoyer design should be as following:

Screw diameter 5 cm, screw pitch 1.5 diameter (4.5 cm), screw speed is 5 rpm, loading factor is 15%, and flight outside diameter is 10 cm.

Pitch	Pitch length S
Standard	S=D
Short	S=2/3*D
Half	S=D/2
Long	D=1.5*D

Figure 90: the common pitch scales based on the characteristics of the material to be conveyed according to the diameter of the screw. (Engineering resources for powder processing industry)

Material	Min loading ratio	Max loading ratio
Not free flowing	0.12	0.15
Average flowability	0.25	0.30
Free flowing	0.4	0.45

Figure 91: Maximum and minimum loading factor of the screw based on the flow properties of the material. (Engineering resources for powder processing industry)

Inclination in °	Correction factor C
0	1
5	0.9
10	0.8
15	0.7
20	0.65

Figure 92: inclination and correction factor of the screw convoyer. (Engineering resources for powder processing industry)

Screw diameter in m	15%	30%A	30%B	45%
0.1	69	139	69	190
0.15	66	132	66	182
0.23	62	122	62	170
0.25	60	118	60	165
0.30	58	111	58	157
0.36	56	104	56	148
0.41	53	97	53	140
0.46	50	90	50	131
0.51	47	82	47	122
0.61	42	68	42	105

Figure 93: Some reference maximum screw speed as given in the manual guidline of engineering resources for powder processing industry

The tube (dryer) rotates horizontally around the x-axis between a couple of sliding parabolic trough concentrators to heat up the dryer evenly and uniformly (Figure 82). These two concentrators of 7 m^2 each are able to track the sun and focus the solar energy linearly over the dryer wall in a focal line of 100 cm tall. The rotating tube is located inside a case of transparent quartz which is provided by a vacuum pump to maximize the drying process. Air pump or (air blower) is also used to blow the hot air coming from the heat exchanger (products of pyrolysis reaction and air) into the rotating tube. Therefore, drying process occurs thermally; directly and indirectly by convection (hot air), conduction (metal wall of dryer), and solar radiation (sun rays passing through quartz case).

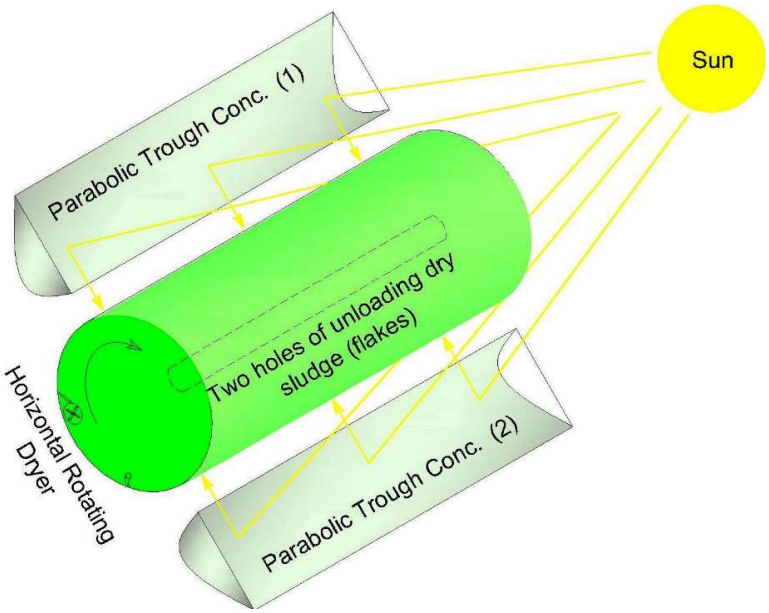

Figure 94: Conceptual design of solar dryer to produce Sludge Flakes

Design of Parabolic Trough Concentrator

Although the maximum geometric concentration ratio, C_g, is about 25 and 70 practically and theoretically respectivally, it (C_g) can be given by

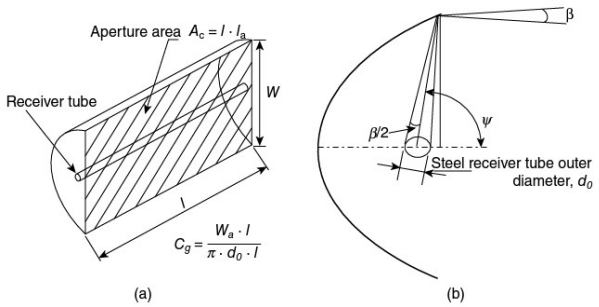

$$C_g = \frac{W_a l}{\pi d_o l} = \frac{W}{\pi d_o}$$

Where

- d_o the outer diameter of the receiver steel pipe (0.002 m)
- l collector length (1m)
- W_a the width of parabola aparature
- β the acceptance angle. The minimum acceptance angle is 32’ (0.53°). Most commercial PTC designs have acceptance angles within the range 1–2°, with geometric concentration ratios of 20 to 30

Therefore,

$$C_g = \frac{W_a l}{\pi d_o l}$$

Since the focal area will be a line on the dryer wall, then d_o can be considered 0.45 m, and the geometric concentration ratios 5. Therefore, W_a = 7.065 m

Area of parabolic trough is

$$\text{AreaParabola} = \frac{4}{3}\,\text{a} \times \text{b}$$

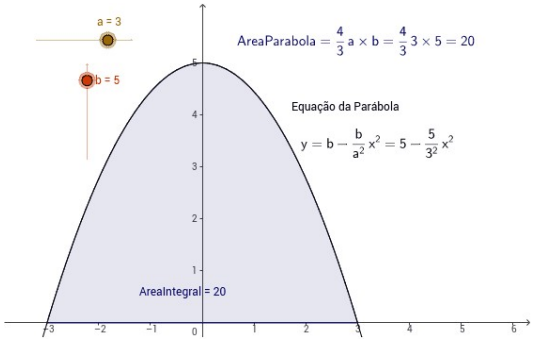

Where,

a: ½ of W_a

b: the depth of the parabola

Therefore, the area of parabolic trough (A_p) is

A_p = (4/3) * (1.413/2) * (1.5) = 7.065 m^2

Two parabolic troughs are used for the dryer, then the total area = 7.065 * 2 = 14.13 m^2, which is enough to suplly the system with heat energy required for drying.

The rim angle, ψ, can be calculated as a function of the parabola focal distance, f , and aperture width, W :

$$\tan\psi = \frac{8fW}{W^2 - 16f^2}$$

$$\tan\psi = \frac{8 * 2 * 7.065}{7.065^2 - 16 * 2^2}$$

$$\tan\psi = \frac{113.04}{-14.0858}$$

$$\tan\psi = -8.025$$

Therefore ψ = -82.896952891°

Reflectivity, ρ , of the collector reflective surface which is clean silvered glass mirror is around 0.93. This is also affected by optical losses which forms about 25% of the total solar flux incident on the PTC aperture plane.

Transmissivity of the glass cover (quartiz case), τ. It is typically τ = 0.93, and can be increased up to 0.96 by anti-reflective coatings applied on both sides of the case.

The peak optical efficiency of the PTC, $\eta_{opt,0^o}$ is usually in the range 0.74–0.79 for clean, good-quality parabolic trough collectors.

Heat losses and energy

The efficiency of the entire PTC systems is η_{system} calculated as

$$\eta_{system} = \frac{\dot{Q}_{collector\_fluid}}{\dot{Q}_{sun\_collector}}$$

and

$$\dot{Q}_{sun\_collector} = A_c \cdot E_d \cdot \cos(\varphi)$$

$$\dot{Q}_{collector\_fluid} = \dot{m} \cdot (h_{out} - h_{in})$$

Where

- $\dot{Q}_{sun\_collector}$ is the solar energy f lux incident on the aperture plane
- $\dot{Q}_{collector\_fluid}$ is the useful thermal energy delivered by the PTC
- A_c is the collector aperture surface area.
- E_d is the direct solar irradiance (NDI) (average for Jordan is $(2045 + 2922)/2$
- φ is the incidence angle (average 35°)
- $\dot{m}$ is the sludge mass flow through the collector receiver tube = the capacity of the drayer = 8.792 Kg/h = 0.0024422 Kg/s
- h_{out} is the sludge specific mass enthalpy at the collector outlet KJ/Kg = [(0.29090926 KJ/s + 0.248744904 KJ/s) / (0.0024422 Kg/s)] = 220.971 KJ/Kg
- h_{in} is the fluid specific mass enthalpy at the collector inlet KJ/Kg = [(1.195517508 KJ/s)/ (0.0024422 Kg/s)] = 489.52482 KJ/Kg

$$\dot{Q}_{sun\_collector} = A_c \cdot E_d \cdot \cos(\varphi)$$

$$\dot{Q}_{sun\_collector} = (7.065 * 1)m2 * 2483.5\ kwh/m2 * \cos(35)$$

$$\dot{Q}_{sun\_collector} = 14373.62381\ \text{Kwh} \div 3600\ \text{s} = 3.9927 \frac{\text{KJ}}{\text{s}}$$

$$\dot{Q}_{sun\_collector} = 3.9927 \frac{\text{KJ}}{\text{s}} \div 0.0024422 \frac{Kg}{s}$$

$$\dot{Q}_{sun\_collector} = 0.009751 \frac{\text{KJ}}{\text{Kg}}$$

$$\dot{Q}_{collector\_fluid} = \dot{m} \cdot (h_{out} - h_{in})$$

$$\dot{Q}_{collector\_fluid} = 0.0024422 \frac{\text{Kg}}{\text{s}} * \left(489.52482 \frac{KJ}{Kg} - 220.971 \frac{KJ}{Kg}\right)$$

$$\dot{Q}_{collector\_fluid} = 0.0024422 \frac{\text{Kg}}{\text{s}} * \left(268.55382 \frac{KJ}{Kg}\right)$$

$$\dot{Q}_{collector\_fluid} = 0.6558622 \frac{\text{KJ}}{\text{Kg}}$$

Therefore,

$$\eta_{system} = \frac{\dot{Q}_{collector\_fluid}}{\dot{Q}_{sun\_collector}}$$

$$\eta_{system} = \frac{0.6558622\ KJ/Kg}{0.009751\ KJ/Kg}$$

$$\eta_{system} = 80.26$$

The efficiency ŋ of a parabolic trough collector which is the ratio of the thermal power absorbed by the heat transfer fluid to the direct normal irradiation on the aperture area can be also calculated by:

$$ŋ = \frac{Q_u}{I_b A_c}$$

$$Q_u = ŋ_o I_b A_c - U_c(T_c - T_a)A_a$$

$$ŋ_0 = \rho_c(\alpha_c \tau_c)\gamma \cos\theta_i$$

$$U_c = U_{c0} + U_{c1}(T_c - T_a)$$

$$A_a = \frac{A_c}{C}$$

Where

ŋ the efficiency of the parabolic trough

ŋ$_o$ the optical efficiency

U$_c$ the solar collector heat transfer loss coefficient that depend on the temperature (W/m^2. °C)

I$_b$ the direct normal irradiation (W/m^2)

Q$_u$ the heat received by collector (W)

T_c the absorber temperature (°C)

T_a the ambient temperature (°C)

U_{c0} and U_{c1} are constant determined from empirical test (W/m^2.°C)

A_a Total area of the absorber (m^2)

A_c total collector aperture area (m^2)

C the concentration ratio

ρ_c the mirror reflectance

α_c the absorptance of the receiver

τ_c the transmittance of the receiver (absorber and glass cover)

γ the intercept efficiency (in most cases it is =1 "assume all reflected ray are intercepted"

ϑ_i the incidence angle

$cos\ \theta_i$ Varies depends on collector's mirror type and collector direction (East, west, north, or south)

δ the declination angle (°)

h the hour angle

then

$$(cos\ \theta_i)_{PT} = \sqrt{1 - \cos^2 \delta \sin^2 h}$$

the incidence angle for Parabolic trough (PT) collector

$$(\cos \theta_i)_{LF} = F(cos\ \theta_i)_{PT}$$

the incidence angle for Linear Fresnel (PT) collector

where

F is a factor empirically evaluated and it is taken equal to 0.7 in some cases.

Therefore,

$$A_a = \frac{A_c}{C}$$

$$A_a = \frac{7.065\ \text{m2}}{5}$$

$$A_a = 1.413 \text{ m}^2$$

$$U_c = U_{c0} + U_{c1}(T_c - T_a)$$

$$U_c = U_{c0} + U_{c1}(200 - 27)$$

Empirically,

U_{c0} = 1.967 (W/m^2.°C) And

U_{c1} = 0.021 (W/m^2.°C)

$$U_c = 1.967 \ + 0.021(200 - 27)$$

$$U_c = 5.6 \ \text{W/m2 °C}$$

The mirror reflectance (ρ_c) ranging from 99.8% up to 99.999%. For this design, the mirror reflectance is 99.9%

The absorptance of the receiver (α_c) typically for selective coatings is higher than 96%.

The transmittance of the receiver (τ_c) is 93%.

The intercept efficiency (γ) in most cases is =1

The daily average of the incidence angle (ϑ_i) is 45°

Therefore,

$$\eta_0 = \rho_c(\alpha_c\tau_c)\gamma \cos\theta_i$$

$$\eta_0 = 0.999(0.96 * 0.93) * 1 * \cos 45$$

$$\eta_0 = 0.631 = 63.1\%$$

$$Q_u = \eta_o I_b A_c - U_c(T_c - T_a)A_a$$

The average direct normal irradiation DNI (W/m^2) (I_b) for Jordan is 2483.5 KW/m^2 = 2483000 W/ m^2.

$$Q_u = 0.631 * 2483.5 * 7.065 - 5.6(200 - 27) * 1.413$$

$$Q_u = 11071.48 - 1368.91$$

$$Q_u = 9702.57 \ KW$$

$$\eta = \frac{Q_u}{I_b A_c}$$

$$\eta = \frac{9702.57}{2483.5 * 7.065}$$

$$\eta = 0.80268 = 55.3\%$$

Heat transfer to the drying system (dryer)

Although all types of heat transfer are applied in this design; conduction, convection, and radiation from direct sun rays, the most transfer of heat in this design occurs through conduction process, therefore,

$$Q = \frac{kA(T_{Hot} - T_{Cold})t}{d}$$

Where

Q: Heat transferred which should be ≤ the heat received by collector. Heat received by the collector is 9702570 W

K: Thermal Conductivity (for copper 0.99 (cal/sec)/(cm2 ˚C/cm)). Note that 1 (cal/sec)/(cm2 ˚C/cm) = 419 W/m K. Then K = 414.81 W/m K.

T_{HOT}: Hot temperature (200 ˚C = 473 K)

T_{COLD}: Cold Temperature (27 ˚C = 200 K)

t: Time Second (one second)

D: The thickness of the material (0.15 cm = 0.0015 m)

A: Area of surface (the area subjected to focal line of parabolic trough concentrator = 0.45 * 1= 0.45 m^2).

Therefore,

Q= 414.81 W/m^2 * 0.45 m^2 * 173 K * (1) (sec) / 0.0015 m

$Q_{transfered\ to\ the\ dryer}$ = 21528639 (W/m^2)

The heat received by collector (Q_u) = 68548657.05 W/m^2

Total energy required for the drying system (dryer) is 1399.34841 W/ m^2

Therefore, the heat transfer is sufficient to dry the inlet sludge.

However, inside the rotating tube (dryer), the tube of mixture inlet is fixed very close to the tube walls from inside (Figure 83). To achieve the best performance, the inlet tube should be fixed 2.5 mm away from the wall of dryer. A spreading scrapper is attached to the inlet tube on the opposite direction of the dryer rotation to ensure getting the best uniform spreading of sludge mixture over the dryer walls and hence uniform layer of sludge. The scrapper is movable to control the thickness of sludge layer as desired up to 3 mm.

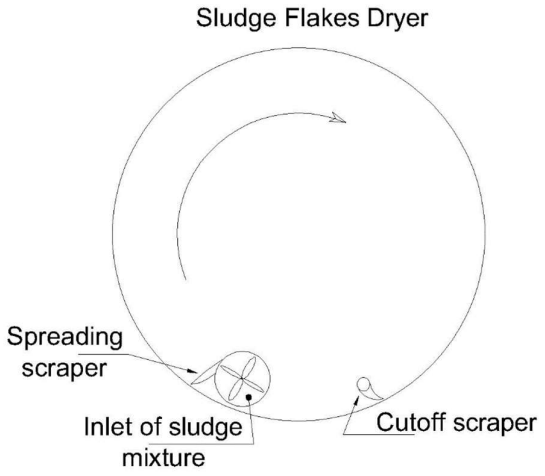

Figure 95: schematic diagram of solar dryer to produce sludge flakes.

On the opposite side of the inlet tube, a scraper is fixed inside the dryer (Figure 83). This is to scrap the dry layer of sludge flakes after every complete rotation and to ensure that dryer wall is clean for the next layer. In addition to the nature structure of dry sludge, the scraper has been designed to remove the dry layer in small pieces rather than one layer.

The rotating tube (dryer) has two linear holes for unloading (Figure 83). These two holes allow the dry layer of sludge, which is removed by the scraper, to find its way to the reactor.

When the sludge flakes drop from the dryer holes, a parabolic trough will collect them and drive them to a tube which is opened from the top along the holes of dryer (Figure 84). Sludge flakes in this tube are taken to the reactor by a screw feeder (Figure 81). Inert gas is blown in the feeding tube of reactor before leaving the quartz case of dryer as shown in the schematic diagram (Figure 85 & 86).

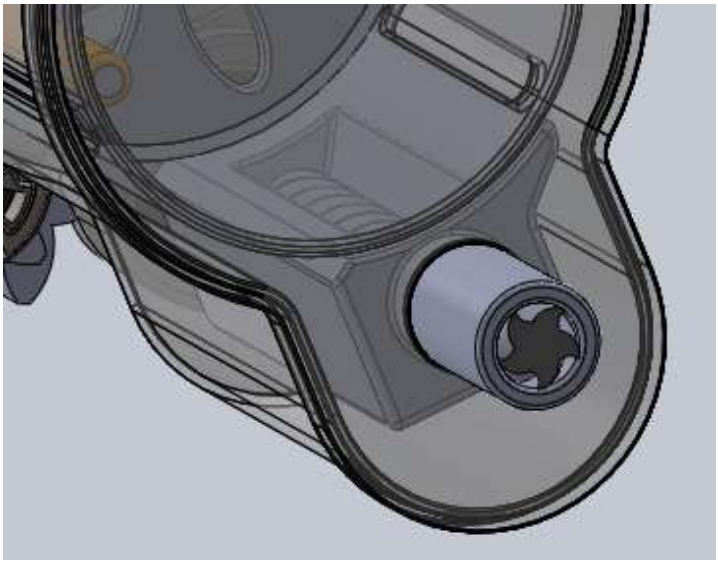

Figure 96: a parabolic trough to collect the sludge flakes and to lead them to the screw feeder of reactor

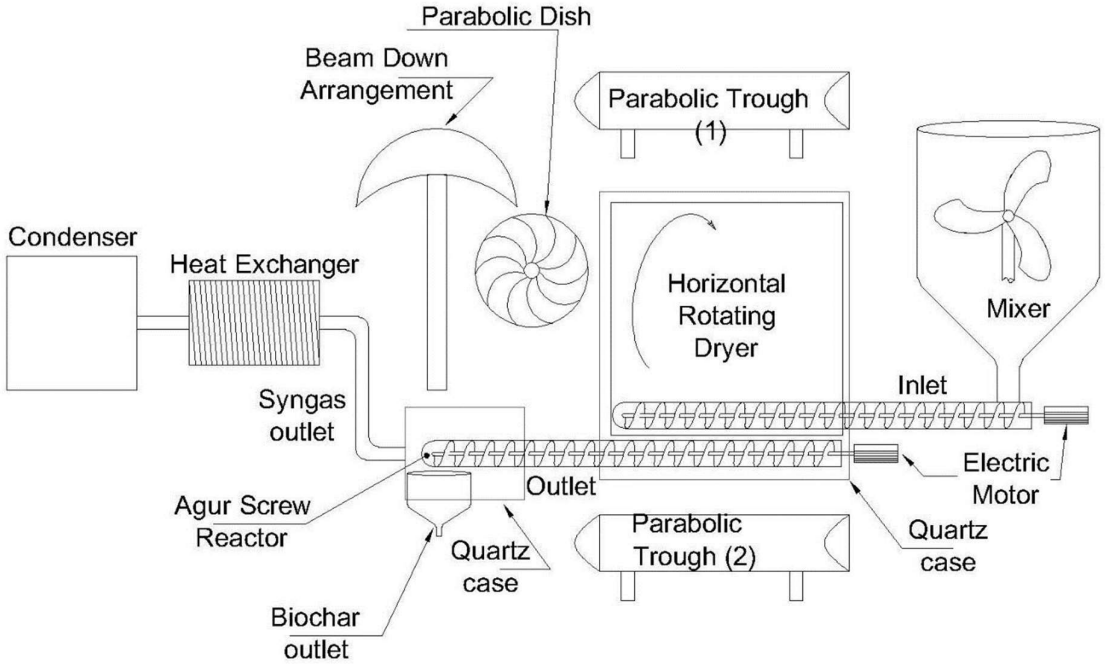

Figure 97: schematic diagram of proposed design for the solar pyrolysis unit.

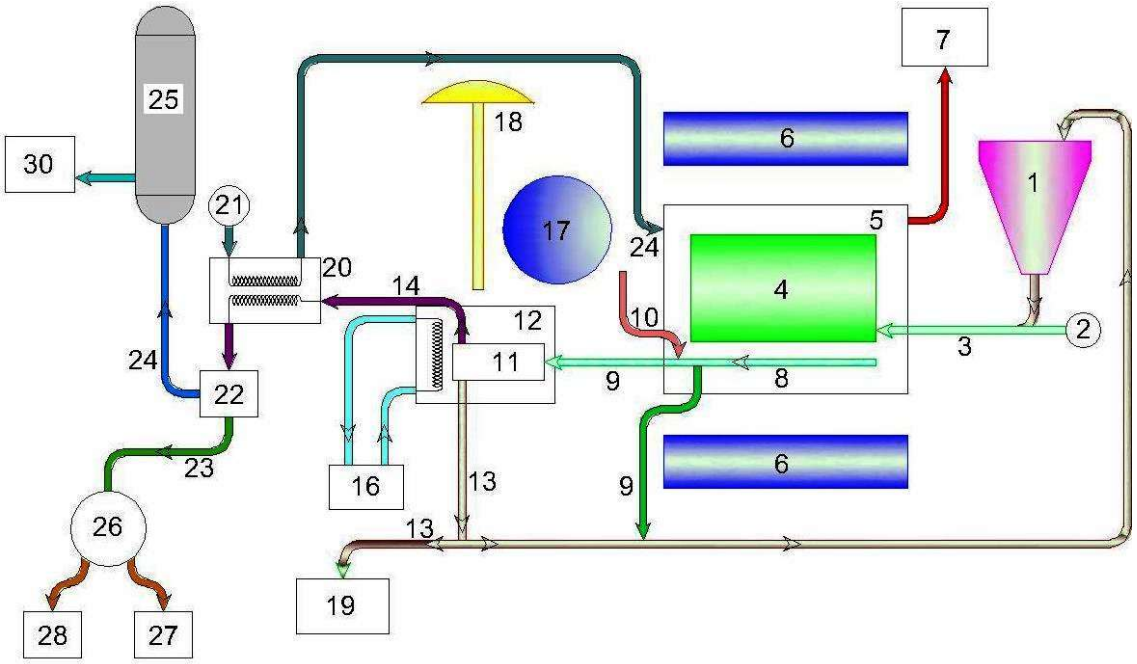

1. Mixer
2. Electric motor
3. Screw feeder
4. Rotating dryer
5. Quartz case
6. Parabolic trough concentrator
7. Vacuum pump
8. Tube contains screw shaft
9. Dry sludge outlet
10. Inert gas inlet
11. Auger (screw) reactor
12. Quartz case
13. Char outlet
14. pyro gas and liquid mixture outlet
15. Molten salt
16. Heat storage system
17. Parabolic dish concentrator
18. Beam down arrangement for solar concentration
19. Biochar storage tank
20. Heat exchanger
21. Air blower
22. Condenser
23. Liquid Yeild outlet
24. Syn gas outlet
25. Syn gas storage tank
26. Oil and water separator
27. Heavy oil tank
28. Water Tank
29. Hot air inlet
30. Syn gas outlet for further treatment to produce Syn diesel.

Figure 98: schematic diagram shows the general design and main parts of solar pyrolysis unit.

Results of thermochemical decomposition of Hamilton City sludge

As mentioned before, pyrolysis is a thermal decomposition of material in an inert ambient. The results of this thermochemical reaction are volitaile matters, syngas, vapour, liquids of bio-oil and tar, and solids of fixed carbon and ash as shown in Figure (99). These components vary from sludge to another and it is very important to measure these component for our samples from Hamilton Wastewater Treatment Facility. Three samples were run in the lab by using Simultaneous Thermal Analyser STA 8000 from PerkinElmer which is known also as TGA device. The samples were dry sludge with 10% moisture content in powder form. The

conditions of the experemints were: initial temperature was 30 ̊C, final temperature 700 ̊C, Argun is the inert gas, heating rate 10 ̊C per minute, resident time is 10 seconds and then oxygen was allowed to measure the ash content.

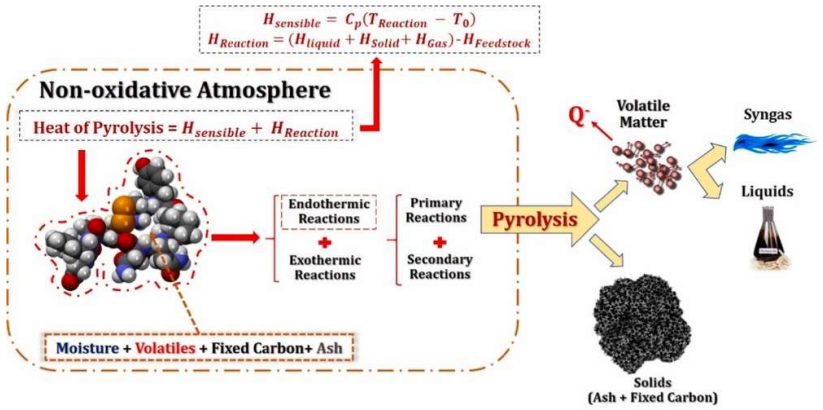

Figure 99: Schematic diagram illustrates pyrolysis process and its main four products. (Campuzano, Brown & Martínez, 2019).

The conditions of the experemints were: initial temperature 30 ̊C, final temperature 700 ̊C, Argun is the inert gas, heating rate 10 ̊C per minute, resident time at 700 ̊C was 10 seconds before oxygen was intered for complete compostion to measure the ash content of Hamilton sludge. Results show that water content evaporates at the first step. In the average of three samples, the water vapour is about 10%, the volatile organic solids content of Hamilton sludge (dry basis) is about 40%, fixed carbon content (dry basis) is 20%, and ash content (dry basis) is 40% as shown in Figure (100).

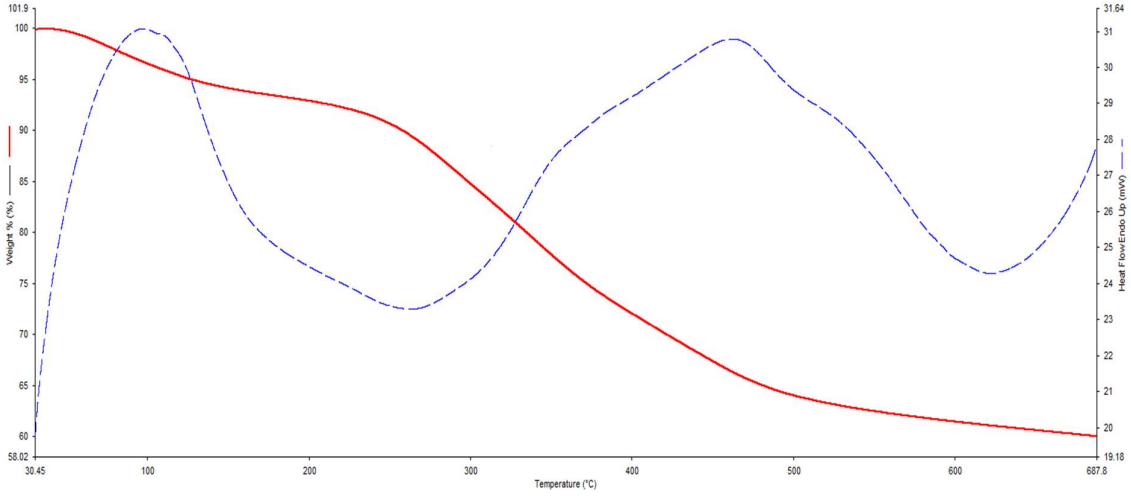

Figure 100: experemintal results of Hamilton sludge decompostion

Pyrolysis device has been modelled based on the solar intensity and the ambient temperature of Hamilton City in NZ. Results from previous calculations were taken in consideration. The both solar intensity and ambient temperature were measured for every hour per day of 365 days a year. The parameters that are taken in consideration in this model are Correction (days) -8, Daylight hours adjustment 1, Peak adjust (MJ/m^2) 0.75, Peak mean adjust (MJ/m^2) 0.1, Total adjust (MJ/m^2) 4, Total mean adjust (MJ/m^2) 2, Peak sunlight (time) 12, Gaussian spread correction 0.205, and Cloud cover correction is 0.3. In term of PTC, total rea is 7.2 m^2, efficiency is 80%.

Raw data show that daylight hours are about 9 hours in short days (winter) and about 17 hours in long days (summer) (Figer 101).

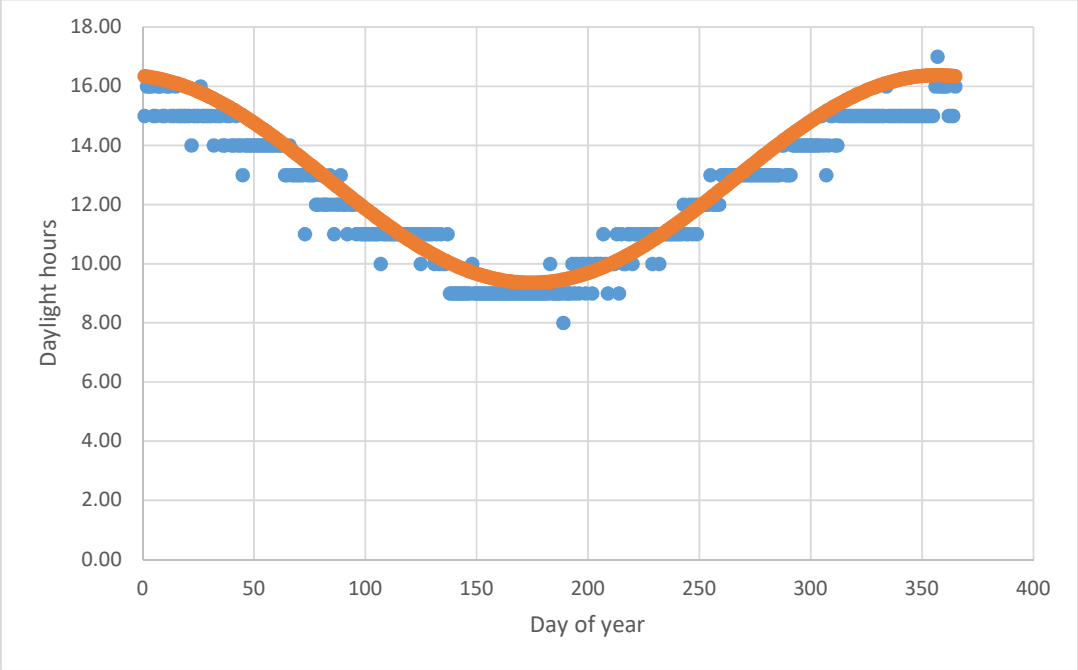

Figure 101: hours of daily sun appearance during a year.

It also show that the maximum energy can be received in summer days higher than other seasons (Figure 101). During the daytime the maximum energy can be received in the midday (Figure 102) and it can be as maximum about 2 MJ/m^2 daily and it is at highest at 12:00 pm of everyday.

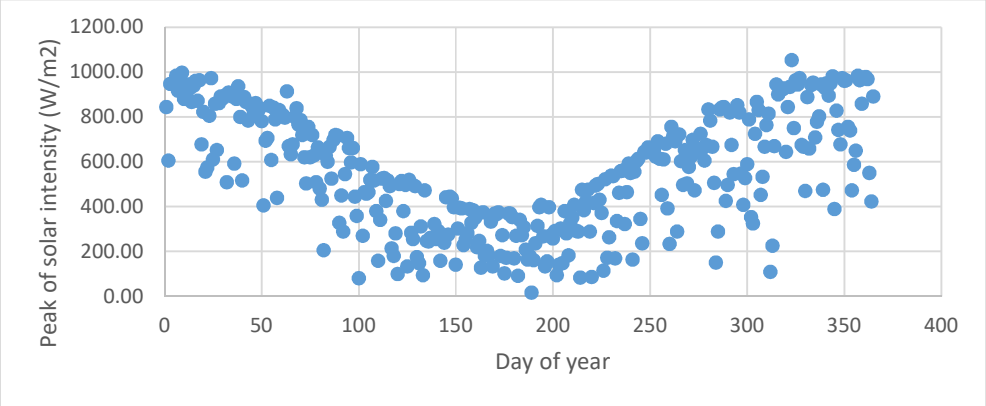

Figure 102: the peak of solar intensity during the year days.

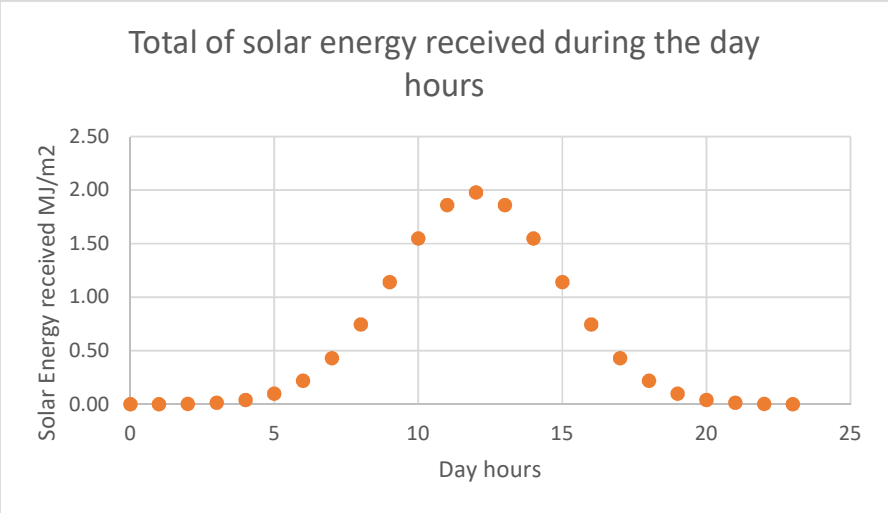

Figure 103: Amount of total solar energy received during the day

The zenith of daily solar energy (Figure 104) and the solar incedince angle (Figure 105) are positive indicator about the possibility of solar pyrolysis at - small scales- especially in sunny days. However, the average of solar energy received daily as shown in figure (106) indicates to the necessity of employing heat recovery from pyrolysis reaction and burning of pyrolysis gases to achieve higher productivity. Using such kind of energy recovery will be very useful to increase the productivity especially during winter and cloudy days.

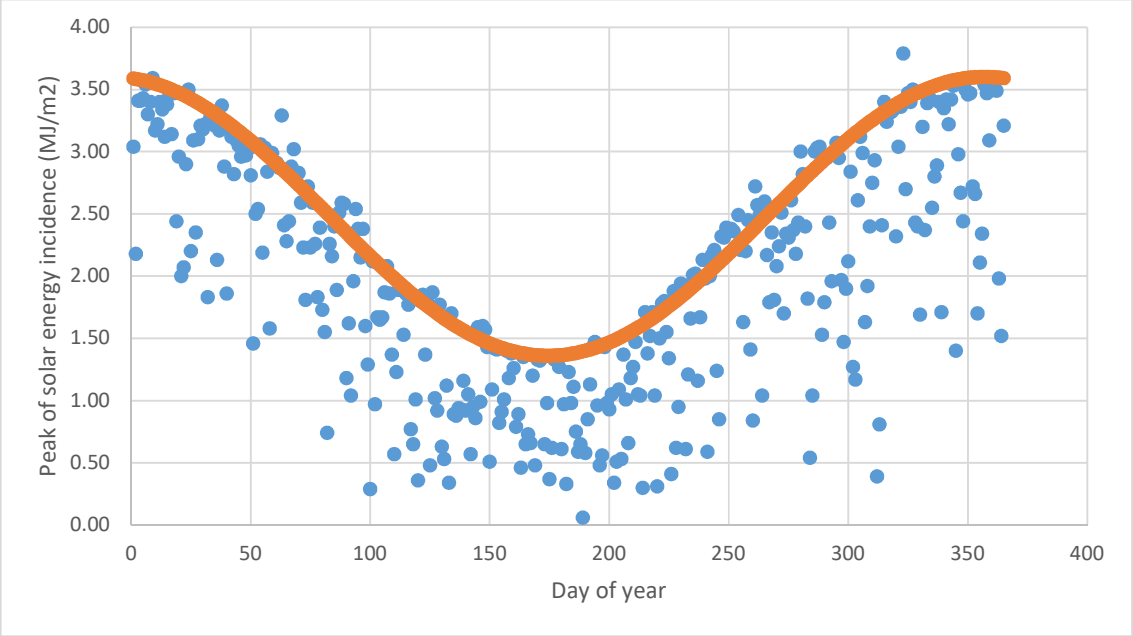

Figure 104: zenith of daily solar energy during a year

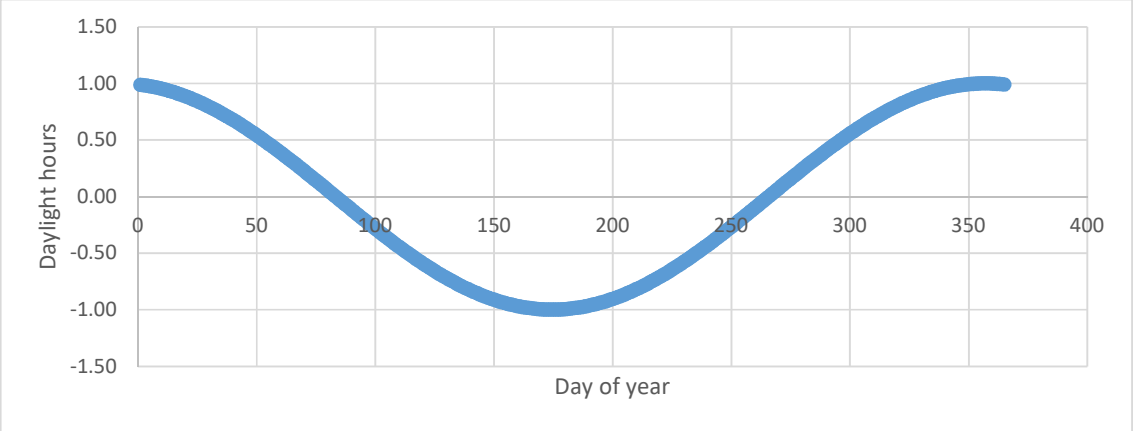

Figure 105: angle of daily solar incedince during a year

Despite the average of daily solar intensity in NZ is encouraging, the productivity of solar pyrolysis device can be considered zero in some days of winter as shown in figure 106. However, New Zealand is not on of Sunbelt countries, which could give this project higher potentials in countries of Midlle East such of Jordan.

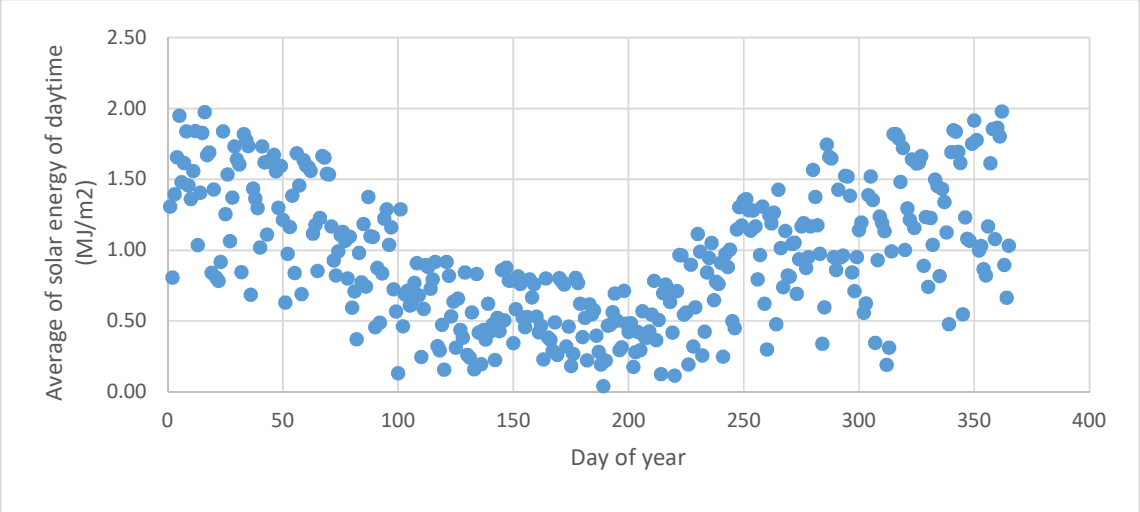

Figure 106: average of daily solar intensity in a year

A couple of parabolic trough solar concentrators with 7.2 m^2 total concentrating area were considered to increase the solar incedince over the dryer ten times. The concentrator efficiency is considered as 80%. Results show that total heat energy collected from the sun can exceed 25 MJ in summer days as shown in Figure (107). In winter days it can be less than 5 MJ but it is still sufficient in most days to start up the pyrolysis reaction. However, the peak of heat energy received by dryer from the sun light is shown in Figure (108).

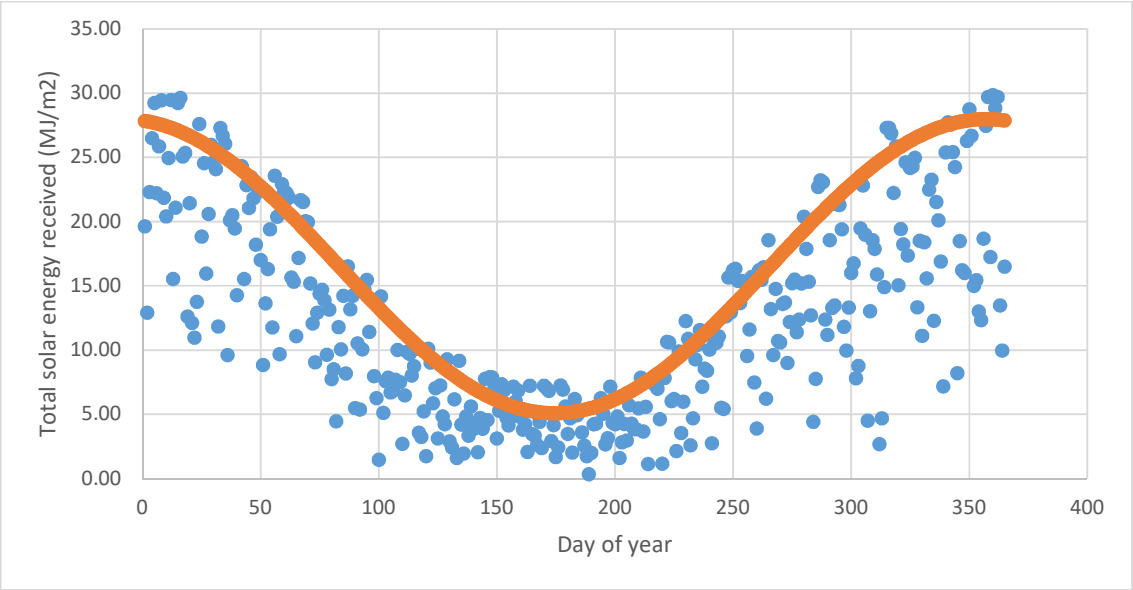

Figure 107: average of total daily solar energy incedince over the dryer from Parabolic Trough Solar collector.

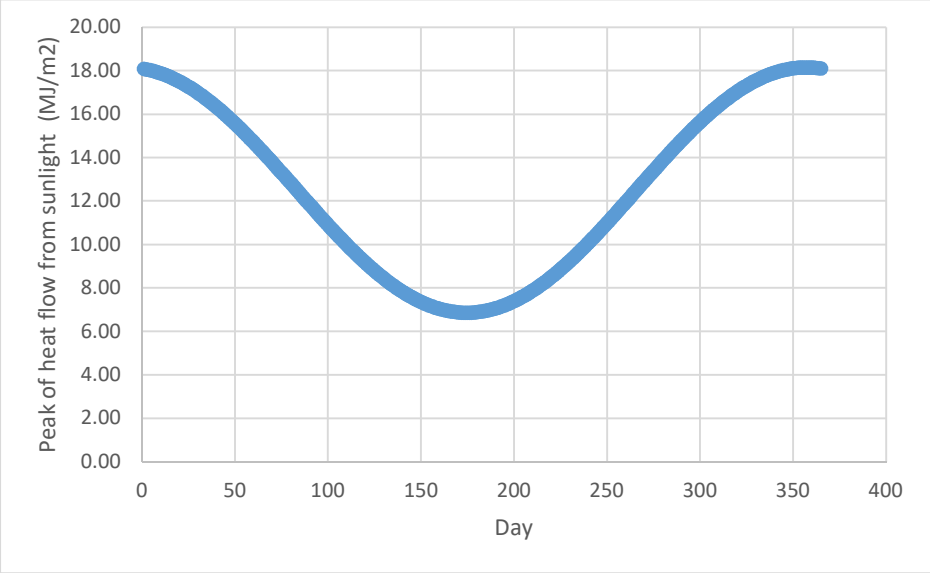

Figure 108: the peak of heat flow (MJ) for dryer from concentrated sunlight

However, these raw data were modled to calculate the productivity of the solar dryer as well as the solar pyrolyser. Depending on formulas of drying theory, air moisture holding capacity, and sludge and air enthalipy, results show that dryer is able to produce a reasonable amount of dry sludge (0% of moisture content) by direct solar energy from collectors which can exceed 50 Kg per day as shown in Figure (109) below. Heat recovery from pyrolysis reaction and burning the gaseus production of pyrolysis result in maximizing the productivity of dryer as the heat energy gained will increase as well (Figure 110).

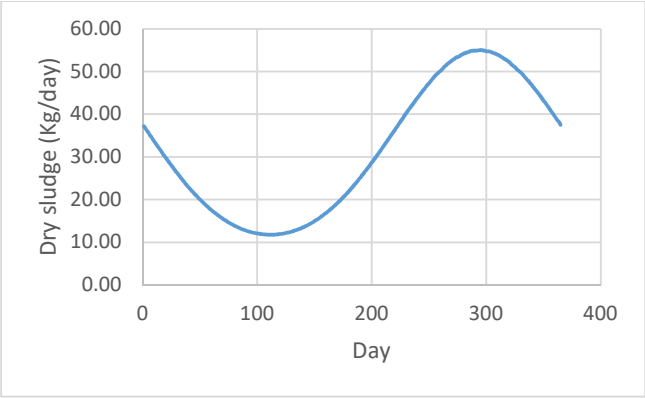

Figure 109: daily production of the dryer by direct concentrated solar energy from the parabolic trough concentrator.

Figure (110) below shows the total heat energy that flow into the dryer. The total heat flow is the summation of concentrated sunlight, heat recovery from hot air, and burning of gaseus products of pyrolysis.

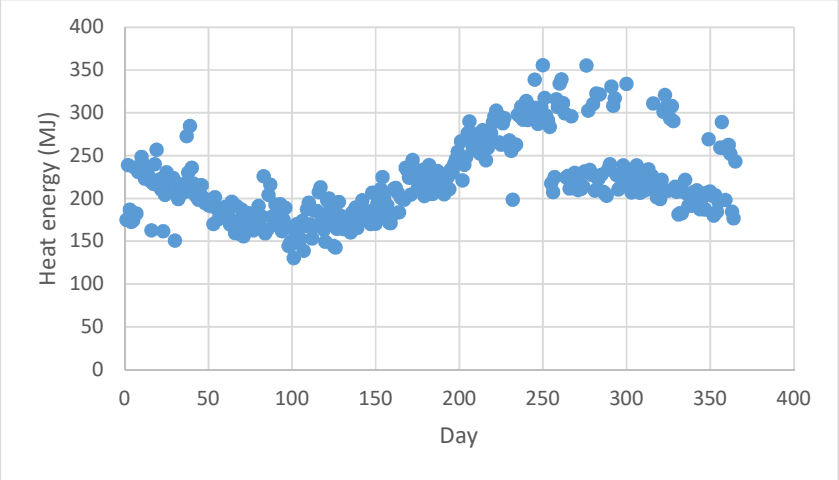

Figure 110: total daily heat energy flows into the dryer from sunlight, heat recovery and burning of pyrolysis gases.

More heat flow into the dryer will result in more productivity of dry sludge. The total hourly and daily production is shown in figures (111 and 112) respectively.

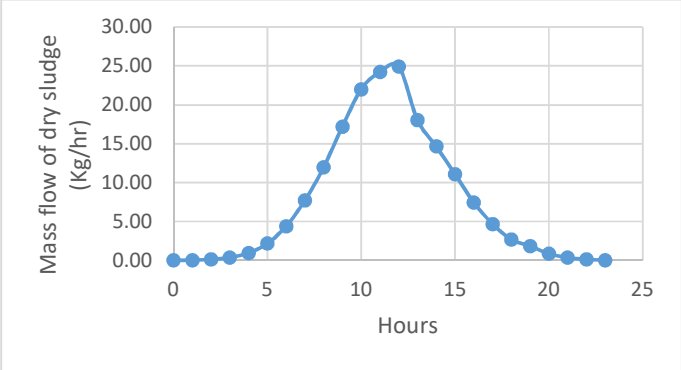

Figure 111: hourly mass flow of dry sludge at the outlet of the dryer

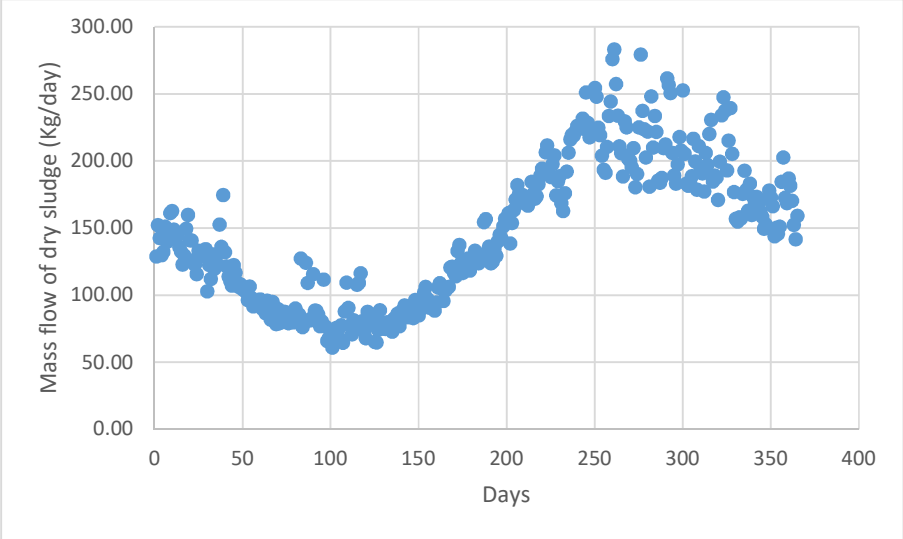

Figure 112: total daily production of dry sludge from the solar dryer.

A comparision between results in figure (109) and figure (112) shows that solar energy is required to start up the pyrolysis process but, in the meantime, exploiting the heat energy that results from pyrolysis reaction can increase the productivity several times. For example, the maximum daily production of dryer by solar energy was about 55 Kg per day while the maximum daily production of dryer by exploiting the sources of heat energy from pyrolysis itself is about 260 Kg per day. However, results show also that solar pyrolysis can be run in winter or cloudy days as the minimum production of dryer is more than 50 Kg per day (Figure 112) which is technically sufficient to run the device in term of dry sludge availability.

7.3 Design of solar pyrolysis reactor

In addition to operating parameters such as pyrolysis temperature, heating rate, lodging time, and chemical and physical features of pyrolysis feedstock, the design of pyrolysor itself affects pyrolysis product yield (Basu, 2013). Based on pyrolysor design, pyrolysis process can be determined mainly as fast pyrolysis or slow pyrolysis. The fast process is widely used to produce bio-oil within seconds. Particularly, yields of fast pyrolysis is around 60% bio-oil, 20% biochar and 20% syngas. Whilst slow pyrolysis requires several hours to produce mainly biochar. However, to increase the pyrolysis liquid yield, important features need to be implemented in the design of the reactor; flexibility for high heating rate, able to withstand for high temperature, able to achieve quick disposal of solid products and fast passing of produced vapours as the residence time of these vapours in the reactor should be less than 3 seconds (Basu, 2013).

The type of reactor affects significantly pyrolysis in term of heat transfer, residence time, mixing process, and the efficiency of the reaction. According to Basu (2013), there are seven types of Pyrolyzer; fixed or removing bed, bubbling fluidized bed, circulating fluidized bed (CFB), ultra-rapid reactor, rotating cone, ablative reactor, and vacuum reactor. Although each reactor has its own characters and usages, the best performance reactors are batch or semi batch reactors, continuous flow reactors such as fixed-bed reactor, fluidized bed, auger reactor (screw reactor) (Campuzano, Brown & Martínez, 2019) and Conical Spouted Bed Reactor (CSBR) (Sharuddin, et al., 2016). Other thermal technologies were developed by using

different concept of pyrolysers such as microwave-assisted technology and fry technology but they are out of this study scope.

However, the reactors used for solar thermochemical processes divided broadly into two groups; directly heated reactors (Figure 87) and indirectly heated reactors (Figure 88). The reactants in directly heated reactors are directly exposed to the concentrated solar radiation whilst those in indirectly heated reactors are exposed to the concentrated solar radiation through an opaque surface such as quartz or glass which is heated first and then transfers the heat to the reactants (Yadav & Banerjee, 2016).

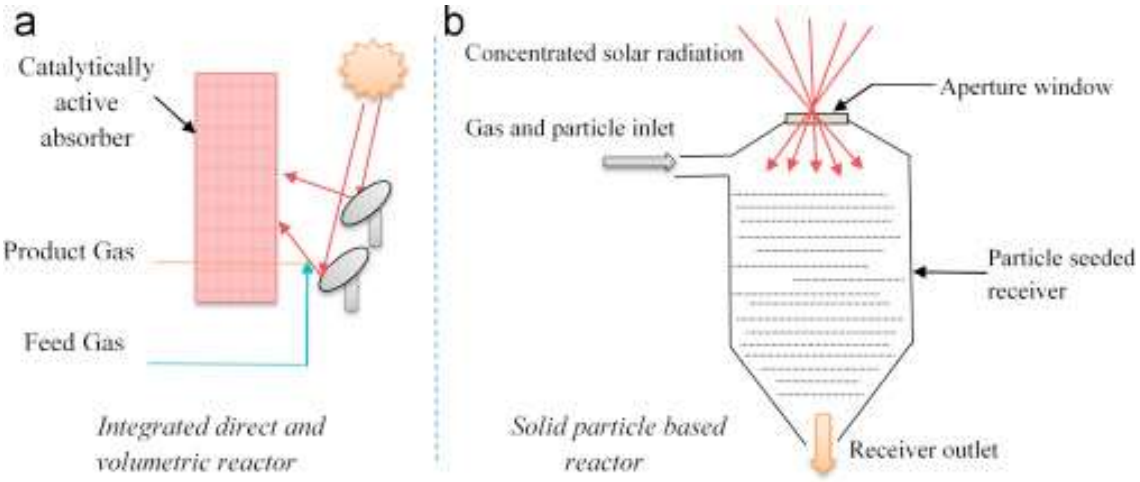

Figure 113: directly heated solar reactors. (Yadav & Banerjee, 2016)

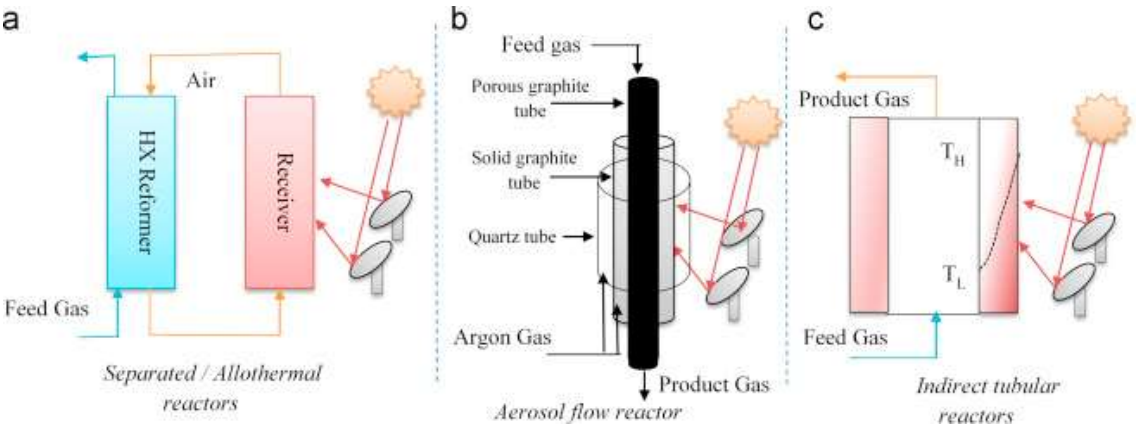

Figure 114: indirectly heated solar reactors. (Yadav & Banerjee, 2016)

For purpose of pyrolysis, indirectly heated solar reactors are more desirable to avoid gas emissions. Since reactor is a pillar of pyrolysis unit, thus its design is the vital part in all

pyrolysis systems. Although obtaining uniform heating throughout whole surface of the reactor for solar and solar assisted heating systems (both continuous and intermitted solar assisted heating) is challenging, design of solar reactor is simpler and easier than those of conventional reactors of pyrolysis. However, to achieve uniform heating for the reactor surfaces, Joardder et al. (2014) reported that using a rotating reactor exposed to a continuous solar heating from sliding solar concentrator (Figure 89) will result in evenly heated up reactor as well as raising up the feed material temperature evenly to the optimum temperature.

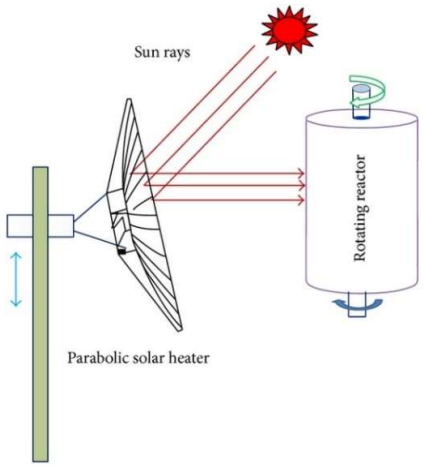

Figure 115: design of continuous solar heating system using rotating reactor to obtain complete solar pyrolysis. (Joardder et al. 2014)

In the current design of this study, the solar reactor is a small-diameter rotating metal tube firmly surrounded by a transparent quartz tube of bigger diameter (Figure 90). The reactor is designed to rotate horizontally. The reactor of 12 mm diameter metal tube is designed from inside to be a screw reactor. Dry sludge flows through the reactor with a velocity of about 0.257 cm/s.

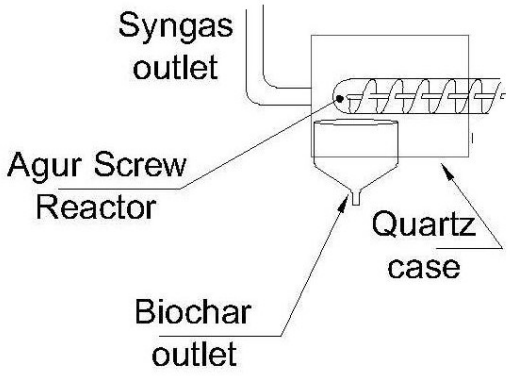

Figure 116: Conceptual design of the proposed solar reactor

The reactor receives the concentrated solar radiation from a beam down solar arrangement by using a couple of parabolic dishes; 200 cm dish to receive the solar radiation and to reflect it to a 20 cm dish which in turn focuses the solar radiation above the reactor. The small diameter of the reactor is to achieve uniform heating and the screw design to achieve optimal reaction for the whole feed material. The length of the reactor tube depends on the required rate of heating to obtain the maximum liquid yield. The transparent quartz tube that works as a greenhouse assists to keep the heat energy of the reactor as long as possible.

The general design of the present solar pyrolysis reactor is shown in Figure (91). It shows the general conceptual design of the proposed solar pyrolysis reactor by this study.

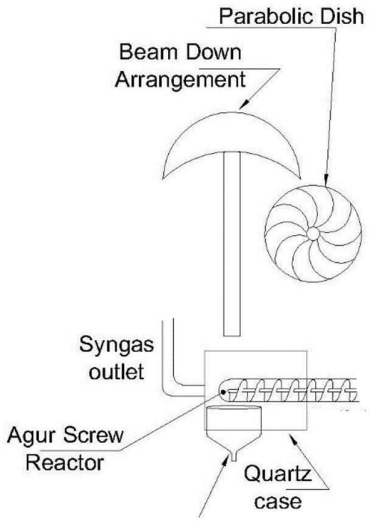

Figure 117: the general conceptual design of the proposed solar pyrolysis reactor.

However, this design was modelled through Solidwork. The productivity of the reactor is counted only for eight hours of day time (the theoretical results are shown below). The ability of molten salts to store and carry heat energy is employed in this design to heat solar reactor during night time, which gives more opportunity to run the solar pyrolysis unit for 24 hours per day.

As mentioned before, results of thermochemical decompositionof Hamilton City sludge show that water content evaporates at the first step. In the average, the water vapour is about 10%, the volatile organic solids content of Hamilton sludge (dry basis) is about 40%, fixed carbon content (dry basis) is 20%, and ash content (dry basis) is 40%.

Design of auger screw reactor

The design of the outlet screw convoyer (screw reactor) is similar to the inlet wet sludge screw convoyer with taking two main differences in consideration. The first one is the nature of dry sludge which is granular and to some extent can be dusty. Therefore, the recommended load factor for dry sludge is 45%.

The second one is the amount of heat energy that involves in the pyrolysis reaction. Yang et al. (2013) stated that determining the amount of heat required for pyrolysis reaction plays essential role in designing reactor and its quantity is known as the enthalpy for pyrolysis. Therefore, the reactor design should take into account the capability of the screw reactor to receive the heat supply and its size. However, previous studies show that the enthalpy of required for pyrolysis at 550 °C in single-screw reactor ranges from 1.1–1.6 MJ/kg for biomass (Yang et al. 2013) and around 1.9 MJ/kg for waste tires (Daugaard & Brown, 2003; Martínez, et al. 2013).

Therefore, the design of screw reactor should meet the flow rate of dry sludge from the dryer (size), nature of dry sludge, and amount of heat energy required for pyrolysis.

Capacity of dryer is 8.792 Kg/h of wet sludge.

Moisture content of inlet sludge is 75% and outlet dry sludge is 10%.

Productivity of dryer = 8.792 Kg/h – (8.792 Kg/h * 65%) = 3.0772 Kg/h of dry sludge.

By applying the equation of screw convoyer design according to the engineering manual guideline

$$Q = 60 \times (\frac{\pi}{4}) \times D^2 \times S \times N \times \alpha \times \rho \times C$$

With

Q = screw capacity in kg/h

D = screw diameter in m = 0.04 m

S = screw pitch in m= 1.2 * d_{screw} = 1.2 * 0.04 =

N = screw speed in rpm= 2.5 rpm

α = loading ratio = 30%

ρ = material loose density in kg/m^3 = 1400 Kg/m^3

C = inclination correction factor = 1

The pitch depth is 1 cm to achieve the best interaction with the direct heat supply from the solar concentrator through the reactor tube wall.

The results are

Q = 60 * (3.14/4) * (0.04^2) * (1.2 *0.04) * 2.5 * 0.30 * 1400 * 1 = 3.798 Kg/h

$Q_{screw} \geq Q_{dryer}$ *then the design is acceptable from size perspective.*

From enthalpy perspective,

The heat required for sludge pyrolysis is around 0.2668 KJ/s

The total capacity of convoyer = 3.798 Kg/h * (1h/ 3600 s) = 0.001055 Kg/s

The total heat required = (0.2668 KJ/s) / (0.001055 Kg/s) = 252.891 KJ/Kg = 0. 252891 MJ/Kg

Then, the enthalpy of the screw reactor is acceptable as it does not exceed the recorded average for other biomass (1.1 – 1.6 MJ/Kg).

Design of Parabolic Dish Concentrator

Parabolic dish concentrates sunrays in a focal point. The focal opoint (circle) should not exceed the diameter of the screw reactor. For the best efficiency, the diameter of the focal point should be smaller than the diameter of the reactor. Since the reactor is cylindrical, the surface area of a cylinder is (2πr). Only half this area is exposed to the concentrated sunrays. Then

$$A_{rec} = A_{small\ dish} = \pi . b^2 + \frac{\pi}{6} . \frac{b}{a^2} . \left[(b^2 + 4a^2)^{\frac{3}{2}} - b^3 \right]$$

$$A_{rec} = \pi * 0.1^2 + \frac{\pi}{6} . \frac{0.1}{0.04^2} . \left[(0.1^2 + 4 * 0.04^2)^{\frac{3}{2}} - 0.1^3 \right]$$

$$A_{rec} = 0.06283 \text{ m}^2$$

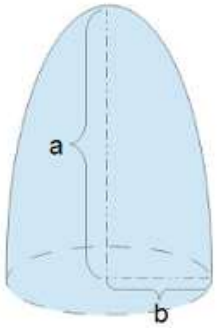

Theoritically, $A_{collector}$ should be ≥ 1.4 m^2 to provide the sufficient heat energy for the pyrolysis reaction in the reactor without losses.

The area of parabolic dish can be calculated through this formula, where a= 50cm and b= 100cm.

$$A_{collector} = \pi . b^2 + \frac{\pi}{6} . \frac{b}{a^2} . \left[(b^2 + 4a^2)^{\frac{3}{2}} - b^3 \right]$$

$$A_{collector} = \pi * 1^2 + \frac{\pi}{6} * \frac{1}{0.5^2} * \left[(1^2 + 4 * 0.5^2)^{\frac{3}{2}} - 1^3 \right]$$

$$3.1415+2.1[2.83 - 1]$$

$$A_{collector} = 6.97413 \text{ m}^2$$

Concentration ratio

$$C = \frac{A_{collector}}{A_{rec}}$$

$$C = \frac{3.2632}{0.06283}$$

$$C = 111$$

Parabolic dish is a point focusing concentrator. The highest concentration ratio can be achieved by this dish is theoretically 2000 with an efficiency up to 40% (Joardder et al. 2017).

The small parabolic dish (20 cm diameter) concentrates the solar rays over the reactor as a point of 5 mm diameter (area = 2πr).

Therefore,

$$C = \frac{0.067421}{0.0157}$$

$$C = 4.3$$

$$Q_{out} = CI\rho K$$

Where

C = is the concentration ratio of the solar dish = 111

I = direct solar radiation on the solar dish, W/m^2 = the average direct normal solar

irradiation DNI (W/m^2) of Jordan = 2483.5 KW/m^2 = 2483000 W/ m^2.

ρ = reflectivity of the concentrator = 0.93

K = the thermal conductivity coefficient of the receiver, W/(m.K) = The thermal conductivity coefficient (K) of *copper* = 414.81 W/m K, then

$$Q_{out} = (111) * 2483000 * 0.93 * 414.81$$

$$Q_{out} = 288612746.5 \text{ W}$$

The usable energy output of the receiver is

$$Q_{out} = Q_{opt} - Q_{loss}$$

Q_{out} = is the usable energy from the receiver,

Q_{opt} = total optical energy reach the receiver

Q_{loss} = Energy losses by the system

But

$$Q_{loss} = A_{rec} U_L \left(T_{rec.sludgeout} - T_{amb}\right)$$

U_L = the sludge coefficient of heat losses of 441 W/m^2.K

$$Q_{loss} = 0.06283 * \ 441 * (833 - 300)$$

$$Q_{loss} = 0.06283 * \ 441 * (533)$$

$$Q_{loss} = 14768.38 \text{ W}$$

Therefore,

$$Q_{opt} = 288627514.88 \text{ W}$$

System instantaneous efficiency can be calculated for each dish as follows:

$$\eta_{dish-instan} = \frac{Q_{out}}{A_{coll} \times I}$$

Where, A_{coll} is the collector area

$$A_{coll} = \frac{\pi {D_a}^2}{4}$$

D_a = is the dish apparatus diameter.

$$A_{main\ coll} = \frac{\pi\,(2)^2}{4} = 3.1415\ \text{m}^2$$

$$A_{secondary\ coll} = \frac{\pi\,(0.2)^2}{4} = 0.03142\ \text{m}^2$$

Therefore,

$$\eta_{dish-insta} = \frac{Q_{out}}{A_{coll} \times I}$$

$$\eta_{dish-instan} = \frac{288612746.5}{3.1415 \times 2483000} = 79.93\%$$

For the parabolic dish collectors, the optimum rim angle is 90°. However, it will be much better if it is very close to 90°. Thus, to calcolate the rim angle (∅) from the first section,

$$\emptyset = 2 \times \tan^{-1}\left(\frac{2}{4f}\right)$$

f = is the distance from any point of the dish surface to the focal point (receiver) (m). Therefore,

$$\emptyset = 2 \times \tan^{-1}\left(\frac{2}{4 * 1.5}\right)$$

$$\emptyset = 2 \times \tan^{-1}\left(\frac{2}{6}\right) = 2 * \ 18.434948823$$

$$\emptyset = \ 36.87$$

And

$$r_r = \frac{2f}{1 + \cos\emptyset}$$

r_r = is the receiver distance (focal point) from the edge of the dish (m)

$$r_r = \frac{2 * 1.5}{1 + \cos 36.87}$$

$$r_r = \frac{3}{1+0.801} = 2.863 \text{ m}$$

Now to calculate the area of the receiver (A_{rec}) which is a screw reactor (cylindrical tube)

$$A_{rec} = 2\pi ah$$

a = is the height of the cylindrical receiver

h = is the contact surface of the receiver cylinder

a can be found by this equation,

$$c = \frac{a}{\sin(\emptyset)}$$

Where, c = is a hypotenuse distance between the focus and the dish boarders (edge) =1.566 m

$$1.566 = \frac{a}{\sin(36.87)}$$

a = 0.9996023809 m

Therefore, the receiver (receptor) radius (R_r) is,

$$R_r = (r_r - c) \times \sin(\frac{\theta_{sun}}{2})$$

$$R_r = (2.863 - 1.566) \times \sin(\frac{\theta_{sun}}{2})$$

θ_{sun} = the sun angle as it is seen by a circular dish in radian. It depends on the location and it's too small (0.266° to 0.53°) according to (Villamil, Hortúa & Lopez, 2013). It can be obtained from solar and geometry data. For Jordan, θ is around 0.511°. Therefore,

$$R_r = (1.803 - 1.666) \times \sin(\frac{0.511}{2})$$

$$R_r = 0.0129319742 \text{ m} = 12.932 \text{ mm}$$

Then,

$$h = \frac{2 \times R_r}{\cos(\alpha - \emptyset)}$$

$$\alpha = 90 + \frac{\theta_{sun}}{2}$$

$$\alpha = 90 + \frac{0.511}{2} = 90.2555^{\circ}$$

Therefore,

$$h = \frac{2 \times 0.0129319742}{\cos(90.2555 - 36.87)} = 0.04336483 \text{ m}$$

Then, the area of the receiver is

$$A_{rec} = 2\pi ah$$

$$A_{rec} = 2\pi * 0.9996023809 * 0.04336483$$

$$A_{rec} = 0.27236 \text{ m}^2$$

Optimal focal length

$$f_{optim} = \frac{D_a}{4 \times \tan\left(\frac{\emptyset}{2}\right)}$$

$$f_{optim} = \frac{2}{4 \times \tan\left(\frac{36.87}{2}\right)}$$

$$f_{optim} = 1.5$$

Shape factor (*S*)

$$S = \frac{A_a - A_t}{\mathrm{A}_a}$$

A_t = is the fraction of the concentrator (collector) aperture area, which is not shadowed by receptor at noon.

$$A_t = A_a - A_{receptor\ base}$$

$$A_t = 2\pi\,(1-0.7)^2$$

$$A_t = 0.56547$$

$$S = \frac{6.283 - 0.56547}{6.283}$$

$$S = 0.91$$

Dish optical efficiency is calculated by

$$\eta_{opt} = \alpha_c \tau_v \rho S$$

α_c : the absorptance of the collector = 0.96

τ_c : the transmittance = 0.47

ρ : reflectivity of the concentrator = 0.93

$$\eta_{opt} = 0.96 * 0.47 * 0.93 * 0.91$$

$$\eta_{opt} = 0.3819 = 38.19\%$$

Average temperature of the sludge inside the reactor (receiver) can be estimated by

$$T_{recsludgeout} = \frac{T_{amb} + T_{sun} \times \left[\left(1-\eta_{opt}\right) \times \frac{\eta_{opt} \times C_{max}}{46311 \times \epsilon_r}\right]}{2}$$

Where,

ϵ_r = Emissivity of the receiver. The receiver is made from copper heated and covered with thick oxide layer with emissivity of 0.78

$$T_{recsludgeout} = \frac{27 + 1570000 \times \left[(1 - 0.3819) \times \frac{0.3819 \times 111}{46311 \times 0.78}\right]}{2}$$

$$T_{recsludgeout} = 582.91\,^{\circ}\text{C}$$

Heat transfer through reactor wall

$$Q = m.C_A.\Delta T$$

Where

Q: Heat transferred

M: mass flow rate of dry sludge

C_A: Specific Heat of dry sludge

ΔT: Difference in temperature

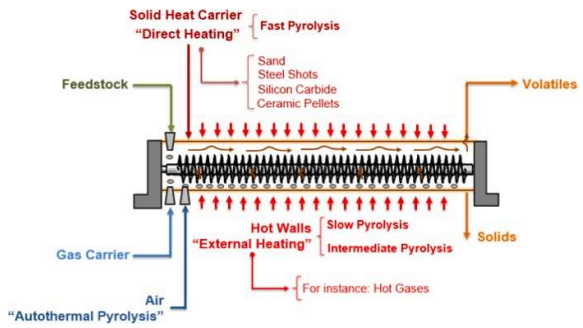

Although all types of heat transfer are applied in this design; conduction, convection, and radiation from direct sun rays, the most transfer of heat in this design occurs through conduction process, therefore,

$$Q = \frac{K.A(T_{ho} - T_{cold})t}{d}$$

Where

Q: Heat transferred

K: Thermal Conductivity of copper = 0.99 (cal/sec)/(cm2 C/cm) or 385 W/m K.

T_{HOT}: Hot temperature = 582.91 ˚C

T_{COLD}: Cold Temperature = 200 ˚C

T: Time second

D: The thickness of the material (m)

A: Area of surface (m^2) = area of the receiver = 0.27236 m^2

$$Q = \frac{K.A(T_{hot} - T_{cold})t}{d}$$

$$Q = \frac{385 * 0.27236\ (582.91 - 200) * 1}{0.0015}$$

$$Q = 26767736.31\ \text{W}$$

The amount of heat energy provided by the parabolic dish collector is generaly sufficient for the pyrolysis reaction.

However, pyrolysis process has been modelled to determine the feasibility of solar pyrolysis. The raw data and parameters used for solar pyrolyser are the same as the dryer. From the calculations above, the area of parabolic solar collector dish were considered as 2 m^2 and its

concentration efficiency is 90%. Results show that solar pyrolyser can process more than 30Kg of dry sludge in the sunny hours. Figure (118) below shows the consumption of the pyrolyser from dry sludge in one of summer sunny days. Interestingly, the heat energy received from solar collector dish is sufficient to decombust this amount of dry sludge. However, the pyrolyser receives the whole amount of dry sludge produced by dryer (Figure 119). The modelling process aims to determine whether the heat energy provided by the solar concentrator is sufficient to run the pyrolysis reaction or not. Empirically, thermochemical combustion of Hamilton sludge shows that it contains 30% of light volatiles, 14% of heavy volatiles, 16% of very heavy volatiles, 23% fixed carbon, and 17% ash.

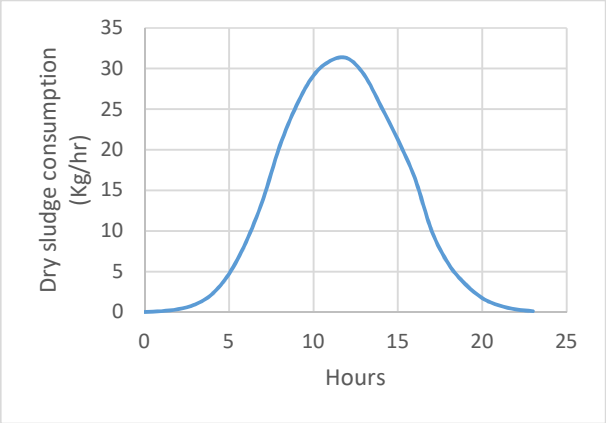

Figure 118: mass flow of dry sludge into the solar pyrolyser during a sunny summer day

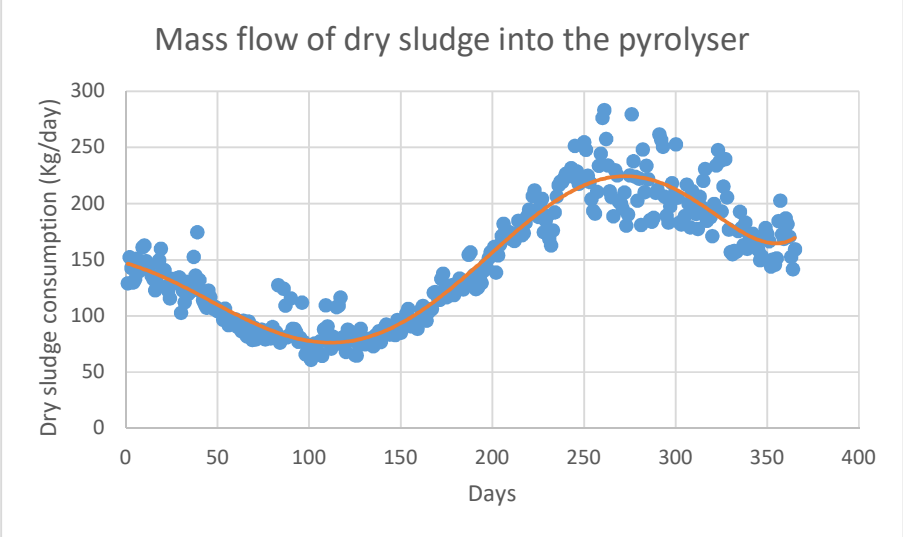

Figure 119: total daily mass flow of dry sludge into the pyrolyser

Three sources of heat energy are used for pyrolysis; heat that flows in the reactor with dried sludge (Figure 120), heat flow for pyrolysis from sunlight through concentrator (Figure 121), and heat flow for pyrolysis from burning pyrolysis gases (Figure 122). As shown in these figures, heat flow from burning pyrolysis gases is several times bigger than heat energy from the sun. However, solar energy is needed to start up the reaction. Sustainability of solar pyrolysis depends on the result of subtracting heat energy required for the reaction from total heat energy provided. Positive surplus indicates to the possibility of the pyrolysis reaction.

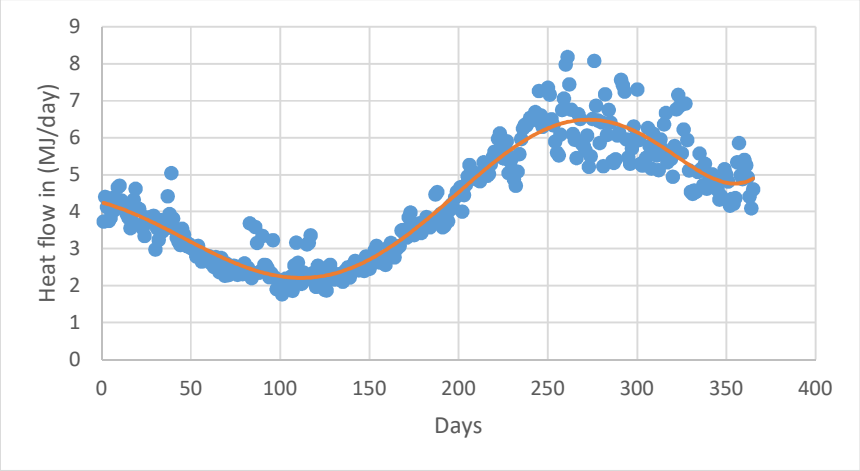

Figure 120: total daily heat flow in of dried sludge for pyrolysis

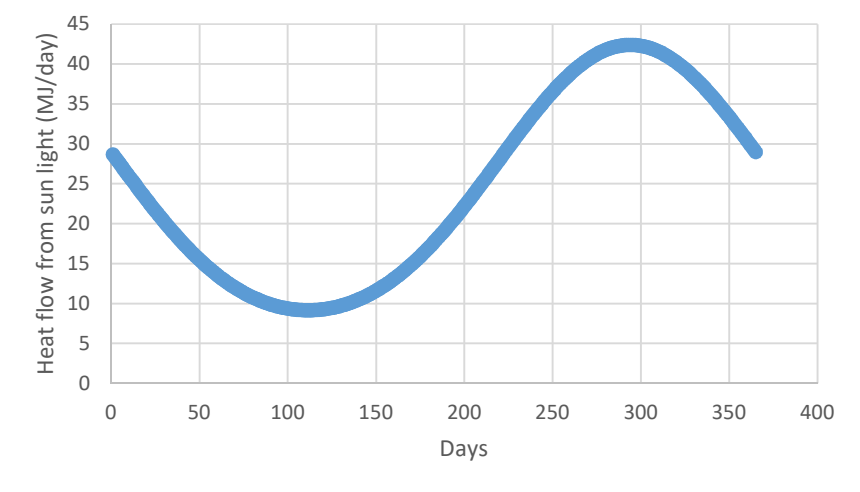

Figure 121: total daily heat flow for pyrolysis from sunlight

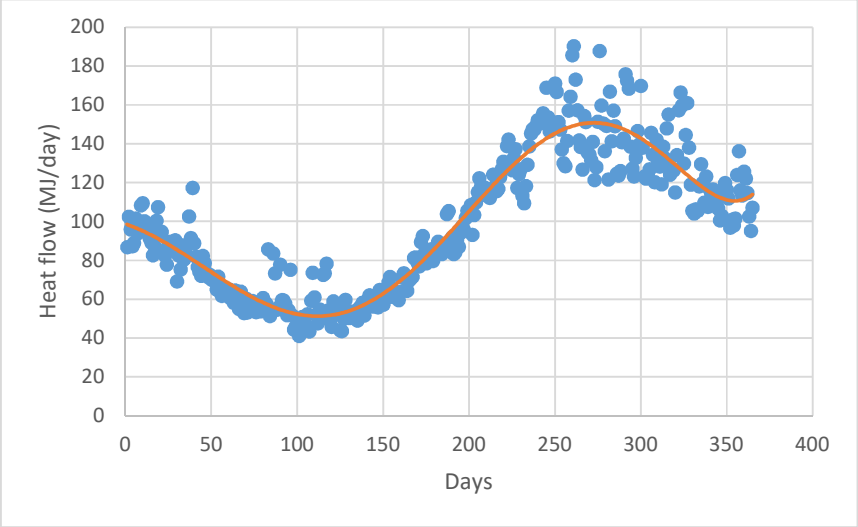

Figure 122: total daily heat flow for pyrolysis from burning pyrolysis gases

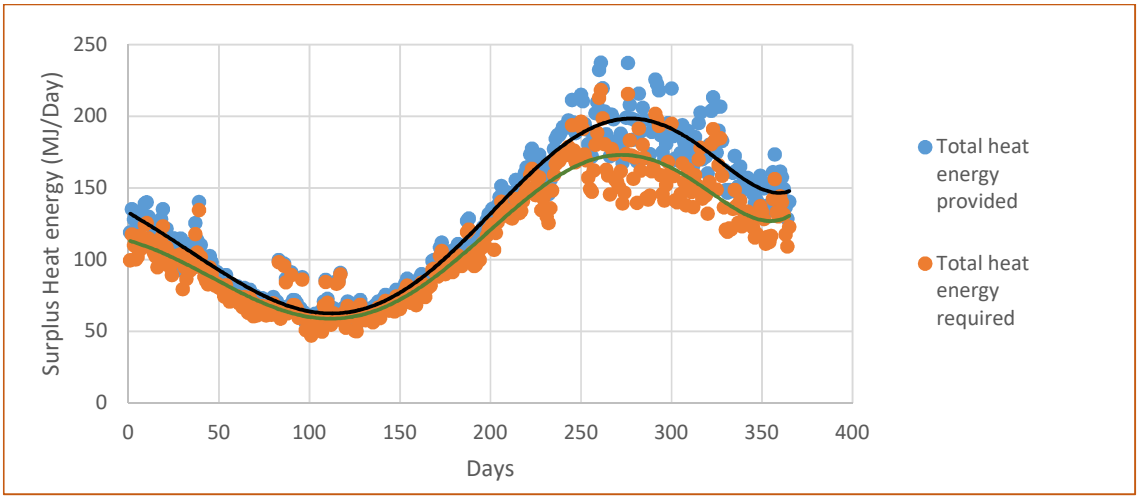

Figure 123: the surplus of heat energy for solar pyrolysis device

For the solar pyrolyser in this study, the surplus of heat energy indicates clearly to the feasibility of solar pyrolysis although it has a small mergine in winter days (Figure 123) . In summer days where the sun shines long hours without cloud and the ambient temperatures are relatively high, it can be seen that the mergine surplus is larger than winter days.

However, although the surplus of heat energy is encouraging, the solar pyrolysis is more challenging. When the thermal mass component of the equipment is taken in consideration to account for the heat required to heat up the equipment material and a heat loss component, the total surplus could be challenging. Figure (124) shows that surplus of heat

energy in one of the summer sunny days. It can be seen that the surplus is positive when sun is clear during thew daytime and it moves to be negative during the night-time. In other words, the system receives energy during the daytime and looses energy during the night time and cloudy days. When surplus is negative, the reaction is not possible. This concludes that the solar pyrolyser can't run for more than ten hours daily which reduces the final productivity. Heat storage systems such as molten salts can be useful to maintain the positive surplus of heat energy and hence the productivity. However, such kind of these system might be not possible at this stage because of the small mergine of surplus unless a separate solar collecting system is provided to heat up the molten salts. Increasing the collecting area of the parabolic dish can be another solution but it is also not feasible from practical perspective because of the cost and the limited area that could be available specifically for householders.

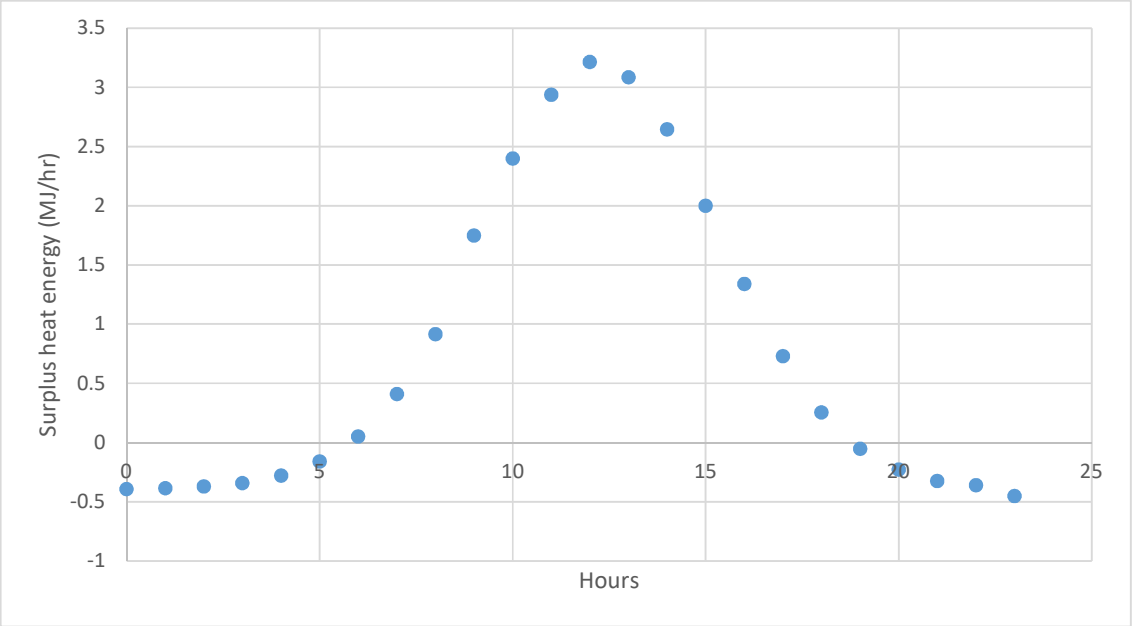

Figure 124: the total surplus of heat energy for one of summer sunny days.

8. The novel design of this study

The novelty of this design is represented in the merging process of available literatures in different arts (MSW, Sludge, Pyrolysis, Harvesting of solar energy, and Drying theory) to build up a pyrolysis unit that runs entirely by solar energy. This design merges waste disposal technologies with technologies of harvesting solar energy as a renewable source of energy to

produce a sustainable solution for global waste issue. Since the municipalities are responsible about waste disposal, then the best waste management practice is likely to be reducing the volume of waste collected from householders. Therefore, this study can be an initial trial to set the cornerstone for the final goal which is producing a household solar pyrolysis units exactly similar to ovens, refrigerators, and washing machines. This in turn, will result in lower volume of waste to be collected, lower municipal spending on waste disposal, and lower environmental consequences. Furthermore, this will change the social understanding about the “waste”. The waste will be a benefit for individuals which will change their behaviours against unwanted items “waste”. This unit can be a sustainable solution in solid waste management specifically for those countries on the Sun Belt.

The merging process was challenged mainly by the nature of solid waste and the moisture content of solid waste, among others. To overcome the nature of solid waste, this study has focused on sewage sludge as a part of municipal solid waste. The chemical structure of sludge is complex which makes sludge processing very complicated in comparison to other sloid waste processing. Successful processing of sludge at small scale indicates to the feasibility of processing other types of municipal solid waste in a household unit.

The main challenge in sludge processing is its high moisture content. The merging process of available literatures led to a novel idea to produce a novel product; “Sludge Flakes”. Producing sludge flakes requires spreading of a relatively high moisture content sludge over a very hot surface to make thin layers. Structure of sludge in addition to other phenomena during sludge drying such as skin formation, sticky phase, shrinkage, and cracks phenomenon led to produce a novel mixture. This mixture contains wet sludge, dry sludge, hot biochar, and finally grease, fat, or waste oil. This mixture is easier to spread, easier to scrape and faster to dry because the final product will be a layer of almost semi-fried sludge.

Drying process of this novel mixture requires a dryer with a novel design. This study demonstrates a novel conceptual design for a rotating solar dryer. The dryer is a drum rotates inside a quartz shell. The quartz shell is located between two parabolic trough solar concentrators. The dryer consists of inlet tube contains a screw convoyer. A linear spreader is fixed on the exit hole of the tube. A linear scraper is fixed also on the body of dryer which has linear holes to drop the final dry sludge. When dry sludge falls from the linear holes, finds its way to the solar reactor via screw conveyer.

Interestingly, a simple change by replacing the spreader and scraper with a rotating cylindrical net contains blades like grinders will make this dryer suitable for all different kinds of organic municipal solid wastes such as bread, fruit peels, vegetables, etc. It can be also developed to be used like a grinder for other kinds of municipal solid wastes such as plastic, tyres, papers and cardboard.

Employing technologies of harvesting solar energy to provide the pyrolysis unit with heat energy and electricity to be operated completely by solar energy is also one of this study novelties. Different kinds of solar concentrators as well as solar photovoltaic systems (PV) were used in this design.

9. Potential economic value of solar pyrolysis products

Products of pyrolysis mainly bio-oil and biochar make it one of the most efficient Waste-to-Energy thermochemical conversion processes (Campuzano, Brown & Martínez, 2019). Using solar energy as a heat source rather than current sources such as fusel fuel makes pyrolysis more attractive environmentally and more valuable economically. The oil prices outlook indicates that oil prices will volatile to be around 180 US$ per barrel in 2030 (Oxford Economics, 2010) which with other factors such as reducing production cost and finding economic uses for pyrolysis products result in potential bloom in value creation of solar pyrolysis products (Haruthaithanasan et al., 2016).

The available reviews show that solar pyrolysis products can have a reasonable calorific value making them useful as a fuel source. For example, the biochar combustion value is over 1800 Kcal, thus it can be used as a low calorific value fuel in different industrial application. According to Xiuguang (2016), the market price of biochar is about 90 US$/ton. This in turn, could cover about 18% of the production cost of bio-oil (Rogers & Brammer, 2012). Other saving such as sludge transport cost and sludge disposal cost should be taken in consideration.

Other products of solar pyrolysis (oil and gases; methane, hydrogen, etc.) are more valuable and have economic benefits. The normal price of Hydrogen is about 15 US$/Kg but it sometimes jumps to more than 26 US$/kg. The energy content of a kilogram of hydrogen is about the same energy content as a gallon of gasoline (Brown, 2015; McKinney et al. 2015).

Yadav & Banerjee (2016) have evaluated the hydrogen production cost by different solar methods. The results are encouraging. The market prices for pyrolysis oil depend significantly on its quality and hence its energy content. Pyrolysis oil prices range from 0.3-0.75 US$/litter (Indiamart.com; Alibaba.com) which are also encouraging. Finally, solar pyrolysis ash has broad application prospects as a raw material for the production of ceramsite and lightweight building materials.

However, the sludge in the current design of this study does not need to be tempered or dehydrated as a pre-treatment condition which minimizes the total cost of pyrolysis process. Furthermore, this design of the solar system is able to treat various sewage sludge without using other chemical additives that used as modifiers such as CaO. Avoiding these additives will improve the calorific value of the sludge (Xiuguang, 2016). The relatively small area needed for solar pyrolysis facility is also unmatched by other technologies.

The table (10) below demonstrates the productivity of our small sludge solar pyrolysis plant.

Productivity		
Working time of plant (hr)		8
Fraction oil content in volatile solids		0.6
Oil density (Kg/m3)		850
Average Wet sludge consumption (Kg/day)	Mass flow of sludge (Kg/h) * Working hours	587.85
Average Dry sludge production (Kg/day)	Wet sludge consumption (Kg/day) * (1-moisture content wet base) + Moisture content flow of dry base *3600 * working hours	146.96
Average Volatile solids (Kg/day)	Volatile solids (Kg/s) * 3600 * Working hours	44.09
Average Oil production (L/day)	(Oil production (Kg/day) / Oil density (Kg/m3)) * 1000 (L/m3)	51.87
Average Char production (Kg/day)	(Fixed Carbone content + Ash content) * Dry sludge production (Kg/day)	31.7829
Average Gas production (Kg/day)	(1- Oil fraction) * Dry sludge production (Kg/day)	58.785

Table 10: productivity of the small sludge solar pyrolysis unit of this this study.

10. Results and Conclusion

The huge volume of solid waste generated every year is a global issue. Three reasons have associated with this issue; environmental, economical, and social. Technology can offer an optimal solution able to cover theses three reason by producing a household solar pyrolysis device.

Sludge, as a part of municipal solid waste, has a specific consideration in solid waste management. There is a very limited number of literature on the integration of solar system with sludge pyrolysis. Current studies show various degrees of success at a pilot scale. This study gives clear indication about the feasibility of manufacturing a household solar pyrolysis device due to its sustainability, low energy consumption, low operating cost, and its relatively low equipment investment.

This device is designed to treat sludge although it is able to treat different types of municipal solid wastes. The main part in this device is the dryer. This study investigated the possibility of drying sludge instantly to produce Sludge Flakes. Results show that the efficient drying process of sludge depends on the mixing process of sludge with other components. The mixture consists of wet sludge, dry sludge, hot smashed char, and waste oil, fat, or grease. The best formula for the mixture (percentage of each component) to produce Sludge Flakes needs further study. However, results are promising. Despite mixing sludge with other municipal solid wastes (mainly biomass) is out of this study scope, it can result in perfect mixture to produce flakes.

However, this research illustrated that the average daily production of this dryer per 8 sunny working hours was around 51.87 litters of bio-oil, 31.78 Kg bio-char, and 58.785 Kg syngas. The dryer can be run over 24 hours a day by using thermal energy storage tanks. Samples of Hamilton Wastewater Treatment Facility was used with 30% of light volatiles, 14% heavy volatiles, 16% very heavy volatiles, 23% Fixed Carbon Content, and 17% of Ash Content all on dry basis. Two Parabolic Trough Concentrators (PTC) of 7.2 m^2 total area and 80% efficiency were used. A beam down solar arrangement of two Parabolic Dish Concentrators with 90% concentrating efficiency were used also to provide an Auger solar reactor with the energy required; 2m^2 and 0.4m^2 reflecting area. The reactor is a tube from copper with 12mm

diameter. The best results were measured when the average mass flow into the reactor is 21 kg/hr. Four normal photovoltaic cells (fifteen square foots each) of Linear Fresnel Concentrators (LFC) were also used to provide the unit by 880 Watts electricity.

Heat energy is the vital player in pyrolysis process through all its stages (drying, reaction, and condensing). Solar energy can be employed successfully to provide this device with direct heat energy by solar harvesting technologies. Furthermore, solar energy can be also employed to generate the electric energy needed to operate the device. Therefore, the utilization rate of solar energy is almost 100% which makes the investment cost is relatively low.

The current design aims to maximize the bio-oil yield by applying fast pyrolysis reaction. The daily yield (8 working hours) of this small device was 51.87L bio-oil (0.5$/L), 31.7829Kg char (0.1$/Kg), and 58.785Kg gas (15$/Kg). All volatile solids and 60% of pyrolysis gases were burnt to increase the productivity. The rest is 23.514Kg gases. According to the market price, the total income will be about 381.82329 US$ per day. However, the market prices of the yield generated from solar pyrolysis of sludge and other residual biomass and waste can be a new source of income for families especially those in rural areas and developing countries. This device will induce them to clean their area as a source of income which could result in low poverty and clean environment, among goals of the Millennium Development.

11. Recommendation

This study is to investigate the feasibility of manufacturing a household solar pyrolysis device. Such kind of work can not be done totally at one stage. It can be the fundamental work further study. For example, further research are needed to find the best formula for the sludge mixture to produce sludge flakes. Most components of present mixture are sludge-based materials. Mixing sludge with other biomass wastes may give perfect results. This device is designed basically to treat sludge. Further research are needed to develop it to be suitable for all kinds of solid wastes.

Furthermore, this study was done in New Zealand which is not one of the Sunbelt countries. Although the figures show that solar pyrolysis of sludge has high potential in Jordan and

Middle East countries in term of plenty of solar energy and sunny days, further studies need to be done there. Moreover, more experiments are needed to find out the impact of different metals and different types of coating materials on the productivity of this device. However, although solar pyrolysis can be described as an affordable eco-friendly technology that can be used directly by householders as a source of energy, its viability and feasibility in Middle East still need further study. However, with few fully sunny days per year, difficult situation (Covid19 Ara), and limited financial sources, this study can be a cornerstone for further research to achieve the final goal; household solar pyrolysis device.

Commercializing “the household solar pyrolysis device” as well as its products will be very helpful in term of waste management. This device more likely will induce people to adopt “self society cleaning vision” to achieve benefits and clean their area.

12. References

1. Abbas-Abadi, M., Haghighi, M. &Yeganeh, H. (2013). Evaluation of pyrolysis product of virgin high density polyethylene degradation using different process parameters in a stirred reactor. Fuel Processing Technology, 109, 90–95.
2. Abdelrassoul, R. A. (1998). Potential for economic solar desalination in the Middle East. Renewable Energy, 14(1), pp. 345–349. doi: https://doi.org/10.1016/S0960-1481(98)00088-3.
3. Abed, F. M., Al-douri, Y. and Al-shahery, G. M. Y. (2014). Review on the energy and renewable energy status in Iraq : The outlooks. Renewable and Sustainable Energy Reviews. Elsevier, 39, pp. 816–827. doi: 10.1016/j.rser.2014.07.026.
4. Abid, M., Ratlamwala, T. A. H., & Atikol, U. (2016). Performance assessment of parabolic dish and parabolic trough solar thermal power plant using nanofluids and molten salts. International Journal of Energy Research, 40(4), 550-563.
5. Abiven, K. (2012, March 18). Thermosolar power station in Spain works at night. Retrieved from https://phys.org/news/2012-03-thermosolar-power-station-spain-night.html
6. Abu Hamed, T. and Bressler, L. (2019). Energy security in Israel and Jordan : The role of renewable energy sources. Renewable Energy. Elsevier Ltd, 135, pp. 378–389. doi: 10.1016/j.renene.2018.12.036.
7. Adinberg, R., Epstein, M., & Karni, J. (2004). Solar Gasification of Biomass: A Molten Salt Pyrolysis Study. ASME. Journal of Solar Energy Engineering, 126(3), 850–857. https://doi.org/10.1115/1.1753577
8. Agrawal, R., & Singh, N. R. (2010). Solar energy to biofuels. Annual review of chemical and biomolecular engineering, 1, 343-364.
9. Aguado, J., Serrano, D. P., & Escola, J. M. (2008). Fuels from waste plastics by thermal and catalytic processes: a review. Industrial & Engineering Chemistry Research, 47(21), 7982-7992.
10. Ahmad, I., Al-Hamadani, N. and Ibrahim, K. (1983). Solar radiation maps for Iraq. Solar Energy. Pergamon, 31(1), pp. 29–44. doi: 10.1016/0038-092X(83)90031-2.
11. Alibaba, (2020). Pyrolysis oil prices per ton. Retrieved On Thursday 16/07/2020 from https://www.alibaba.com/showroom/pyrolysis+oil+price+per+ton.html?fsb=y&IndexArea=product_en&CatId=&SearchText=pyrolysis+oil+price+per+ton&isGalleryList=G
12. Aljaradin, M. (2014). Solid waste management in Jordan. International Journal of Academic Research in Business and Social Sciences, 4(11), 2222-6990.
13. Almasoud, A. H. and Gandayh, H. M. (2015). Future of solar energy in Saudi Arabia. Journal of King Saud University - Engineering Sciences. King Saud University, 27(2), pp. 153–157. doi: 10.1016/j.jksues.2014.03.007.
14. Alonso, E., & Romero, M. (2015). Review of experimental investigation on directly irradiated particles solar reactors. Renewable and sustainable energy reviews, 41, 53-67.
15. Alrwashdeh, S. (2018). Comparison among solar panel arrays production with a different Amman –Jordan. International Journal of Mechanical Engineering and Technology (IJMET), 9(6), pp. 420–429. doi: IJMET_09_06_047.
16. Alrwashdeh, S. et al. (2018). Solar radiation map of Jordan governorates. International Journal of Engineering & Technology, 7(3), p. 1664. doi: 10.14419/ijet.v7i3.15557.

17. Alternative Energy Tutorials (2019). Parabolic Trough Reflector. Retrieved from http://www.alternative-energy-tutorials.com/solar-hot-water/parabolic-trough-reflector.html

18. Alvarez, E. A., Mochon, M. C., Sánchez, J. J., & Rodríguez, M. T. (2002). Heavy metal extractable forms in sludge from wastewater treatment plants. Chemosphere, 47(7), 765-775.

19. Alvarez, J., Amutio, M., Lopez, G., Bilbao, J., & Olazar, M. (2015). Fast co-pyrolysis of sewage sludge and lignocellulosic biomass in a conical spouted bed reactor. Fuel, 159, 810-818.

20. Alvarez, J., Lopez, G., Amutio, M., Artetxe, M., Barbarias, I., Arregi, A., Bilbao, J. & Olazar, M. (2016). Characterization of the bio-oil obtained by fast pyrolysis of sewage sludge in a conical spouted bed reactor. Fuel Processing Technology, 149, 169-175.

21. Amasuomo, E., & Baird, J. (2016). The Concept of Waste and Waste Management. Journal of Management and Sustainability, 6(4), 88-96. https://doi.org/10.5539/jms.v6n4p88

22. American Veterinary Medical Association AVMA (2019). Definitions: What is Waste? Retrieved from https://www.avma.org/PracticeManagement/Administration/Pages/Definitions-What-is-Waste.aspx

23. Antonini, A., Stefancich, M., Coventry, J., & Parretta, A. (2013). Modelling of compound parabolic concentrators for photovoltaic applications. International Journal of Optics and Applications, 3(4), 40-52.

24. Aramideh, S., Xiong, Q., Kong, S. C., & Brown, R. C. (2015). Numerical simulation of biomass fast pyrolysis in an auger reactor. Fuel, 156, 234-242.

25. Arena, U. (2012). Process and technological aspects of municipal solid waste gasification. A review. Waste management, 32(4), 625-639.

26. Arlabosse, P., Chavez, S., & Lecomte, D. (2004). Method for thermal design of paddle dryers: Application to municipal sewage sludge. Drying Technology, 22(10), 2375-2393.

27. Arlabosse, P., Ferrasse, J. H., Lecomte, D., Crine, M., Dumont, Y., & Léonard, A. (2011). Efficient sludge thermal processing: From drying to thermal valorization. Modern Drying Technology: Volume 4: Energy Savings, 4, 295-329.

28. Arribas, L., Arconada, N., González-Fernández, C., Löhrl, C., González-Aguilar, J., Kaltschmitt, M., & Romero, M. (2017). Solar-driven pyrolysis and gasification of low-grade carbonaceous materials. International Journal of Hydrogen Energy, 42(19), 13598-13606.

29. Asmelash, H., Bayray, M., Kimambo, C. Z. M., Gebray, P., & Sebbit, A. M. (2014). Performance test of Parabolic Trough Solar Cooker for indoor cooking. Momona Ethiopian Journal of Science, 6(2), 39-54.

30. Asmelash, H., Kebedom, A., Bayray, M., & Mustofa, A. (2014). Performance Investigation of Offset Parabolic Solar Cooker for Rural Appplications. International Journal of Engineering Research & Technology, 3(12), 2278-0181.

31. Auta, H. S., Emenike, C. U., & Fauziah, S. H. (2017). Distribution and importance of microplastics in the marine environment: a review of the sources, fate, effects, and potential solutions. Environment international, 102, 165-176.

32. Authier, O., Ferrer, M., Mauviel, G., Khalfi, A. E., & Lédé, J. (2009). Wood fast pyrolysis: comparison of Lagrangian and Eulerian modeling approaches with experimental measurements. Industrial & engineering chemistry research, 48(10), 4796-4809.

33. Auti, A. B., Pangavane, D. R., Singh, T. P., Sapre, M., & Warke, A. S. (2015). Study on Reflector Material Optimization of a Parabolic Solar Concentrator. In Power Electronics and Renewable Energy Systems (pp. 275-284). Springer, New Delhi.

34. Awesome Inc. theme (2017, July 15). Modeling linear Fresnel reflectors in Energy3D. Retrieved from http://molecularworkbench.blogspot.com/2017/07/modeling-linear-fresnel-reflectors-in.html

35. Ayol, A., & Durak, G. (2013). Fate and effects of fry-drying application on municipal dewatered sludge. Drying technology, 31(3), 350-358.

36. Ayoub, M. H. et al. (2013). Renewable Energy in Lebanon. 2013 25th International Conference on Microelectronics (ICM). IEEE, pp. 1–4. doi: 10.1109/ICM.2013.6734950.

37. Bader, R., Haueter, P., Pedretti, A., & Steinfeld, A. (2009). Optical design of a novel two-stage solar trough concentrator based on pneumatic polymeric structures. Journal of Solar Energy Engineering, 131(3), 031007.

38. Bakar, R. A., Froome, C., Sup, B. A., Zainudin, M. F., Ali, T. Z. S., & Bakar, R. A. (2015). 2nd international conference on sustainable energy engineering and application (icseea) 2014 sustainable energy for green mobility effect of rim angle to the flux distribution diameter in solar parabolic dish collector. Energy Procedia, 68, 45-52.

39. Balat, M., Balat, M., Kırtay, E., & Balat, H. (2009). Main routes for the thermo-conversion of biomass into fuels and chemicals. Part 1: Pyrolysis systems. Energy Conversion and Management, 50(12), 3147-3157.

40. Baral, S., Kim, D., Yun, E., & Kim, K. (2015). Experimental and thermoeconomic analysis of small-scale solar organic Rankine cycle (SORC) system. Entropy, 17(4), 2039-2061.

41. Barnes, S. J. (2019). Understanding plastics pollution: The role of economic development and technological research. Environmental pollution, 249, 812-821.

42. Barneto, A. G., Carmona, J. A., Alfonso, J. E. M., & Blanco, J. D. (2009). Kinetic models based in biomass components for the combustion and pyrolysis of sewage sludge and its compost. Journal of Analytical and Applied Pyrolysis, 86(1), 108-114.

43. Basu, P. (2018). Biomass gasification, pyrolysis and torrefaction: practical design and theory. Academic press.

44. Bennamoun, L. (2012). Solar drying of wastewater sludge: A review. Renewable and Sustainable Energy Reviews, 16(1), 1061-1073.

45. Bennamoun, L., Arlabosse, P., & Léonard, A. (2013). Review on fundamental aspect of application of drying process to wastewater sludge. Renewable and Sustainable Energy Reviews, 28, 29-43.

46. Bennamoun, L., Belhamri, A., & Mohamed, A. A. (2009). Application of diffusion model to predict drying kinetics changes under variable conditions: experimental and simulation study. Fluid Dyn. Mater. Process., 5, 177-191.

47. Bennamoun, L., Crine, M., & Léonard, A. (2013). Convective drying of wastewater sludge: Introduction of shrinkage effect in mathematical modeling. Drying Technology, 31(6), 643-654.

48. Bennamoun, L., Kahlerras, L., Michel, F., Courard, L., Salmon, T., Fraikin, L., ... & Léonard, A. (2013). Determination of moisture diffusivity during drying of mortar cement: experimental and modeling study. International Journal of Energy Engineering, 3(1), 1-6.

49. Bernardo, L. R., Davidsson, H., & Karlsson, B. (2012). Retrofitting domestic hot water heaters for solar water heating systems in single-family houses in a cold climate: A theoretical analysis. Energies, 5(10), 4110-4131.

50. Bhatia, S. C. (Ed.). (2014). Advanced renewable energy systems,(Part 1 and 2). CRC Press.

51. Bianchini, A., Bonfiglioli, L., Pellegrini, M., & Saccani, C. (2015). Sewage sludge drying process integration with a waste-to-energy power plant. Waste Management, 42, 159-165.

52. Bielinskas, V. (2012). Efficiency of solar energy harvesting. Construction21 international. Retrieved from https://www.construction21.org/articles/h/efficiency-of-solar-energy-harvesting.html

53. Biello, D. (2009). How to use solar energy at night? Molten salts can store the sun's heat during the day and provide power at night. SCIENTIFIC AMERICAN, A DIVISION OF NATURE AMERICA, INC. Scientific American, a Division of Springer Nature America, Inc. Retrieved from https://www.scientificamerican.com/article/how-to-use-solar-energy-at-night/

54. Billaud, F., Gornay, J., & Coniglio, L. (2007). Pyrolysis of secondary raw material from used frying oils. arXiv preprint arXiv:0709.4340.

55. Blanco, J., Malato, S., Fernández, P., Vidal, A., Morales, A., Trincado, P., ... & Brunotte, M. (2000). Compound parabolic concentrator technology development to commercial solar detoxification applications. Solar Energy, 67(4-6), 317-330. doi: https://doi.org/10.1016/S0038-092X(00)00078-5.

56. Blanco, M. E., Gomez-Leal, E., & Gordon, J. M. (1986). Asymmetric CPC solar collectors with tubular receiver: geometric characteristics and optimal configurations. Solar energy, 37(1), 49-54.

57. Bortolamasi, M., & Fottner, J. (2001). Design and sizing of screw feeders. In Partec 2001.

58. Boucher, P. S., & Van Eeden, J. J. (1994). Investigation of inorganic materials derived from water purification processes for ceramic applications: Report to the water research commission. WRC.

59. Boutin, O., Ferrer, M., & Lédé, J. (2002). Flash pyrolysis of cellulose pellets submitted to a concentrated radiation: experiments and modelling. Chemical Engineering Science, 57(1), 15-25.

60. Brassard, P., Godbout, S., & Raghavan, V. (2017). Pyrolysis in auger reactors for biochar and bio-oil production: A review. Biosystems engineering, 161, 80-92.

61. Bridgwater, A. V. (2012). Review of fast pyrolysis of biomass and product upgrading. Biomass and bioenergy, 38, 68-94.

62. Bridgwater, J. (2012). Mixing of powders and granular materials by mechanical means—a perspective. Particuology, 10(4), 397-427.

63. Brown, E. G. (2015). Joint Agency Staff Report on Assembly Bill 8: Assessment of Time and Cost Needed to Attain 100 Hydrogen Refueling Stations in California. California Energy Commission: Sacramento, CA, USA.

64. Brown, J. N. (2009). Development of a lab-scale auger reactor for biomass fast pyrolysis and process optimization using response surface methodology.

65. Brunner, P. H., & Rechberger, H. (2015). Waste to energy–key element for sustainable waste management. Waste management, 37, 3-12. https://doi.org/10.1016/j.wasman.2014.02.003

66. Caballero, B. M., De Marco, I., Adrados, A., López-Urionabarrenechea, A., Solar, J., & Gastelu, N. (2016). Possibilities and limits of pyrolysis for recycling plastic rich waste streams rejected from phones recycling plants. Waste management, 57, 226-234.

67. Campuzano, F., Brown, R. C., & Martínez, J. D. (2019). Auger reactors for pyrolysis of biomass and wastes. Renewable and Sustainable Energy Reviews, 102, 372-409.

68. Candelaria, M. (2013). Mirrors vs Fresnel Lenses for Concentrating Solar Power. Solar novus today: delivering today's global technology news, today. 18 November 2013. Retrieved from https://www.solarnovus.com/mirrors-vs-fresnel-lenses-for-concentrating-solar-power_N7202.html

69. Carberry, J. B., & Prestowitz, R. A. (1985). Flocculation effects on bound water in sludges as measured by nuclear magnetic resonance spectroscopy. Appl. Environ. Microbiol., 49(2), 365-369.

70. Chae, J. S., Choi, S. A., Kim, Y. H., Oh, S. C., Ryu, C. K., & Ohm, T. I. (2016). Experimental study of fry-drying and melting system for industrial wastewater sludge. Journal of hazardous materials, 313, 78-84.

71. Chakraverty, A., & Singh, R. P. (2014). Postharvest technology and food process engineering. CRC Press.

72. Chan, W. P., & Wang, J. Y. (2016). Comprehensive characterisation of sewage sludge for thermochemical conversion processes–based on Singapore survey. Waste management, 54, 131-142.

73. Chan, W. P., & Wang, J. Y. (2016). Comprehensive characterisation of sewage sludge for thermochemical conversion processes–based on Singapore survey. Waste management, 54, 131-142.

74. Chandler, A. J., Eighmy, T. T., Hjelmar, O., Kosson, D. S., Sawell, S. E., Vehlow, J., … Sloot, H. A., & Hartlén, J. (1997). Municipal solid waste incinerator residues (Vol. 67). Amsterdam: Elsevier.

75. Chang, F. C., Ko, C. H., Wu, J. Y., Wang, H. P., & Chen, W. S. (2013). Resource recovery of organic sludge as refuse derived fuel by fry-drying process. Bioresource technology, 141, 240-244.

76. Chen, D., Yin, L., Wang, H., & He, P. (2014). Pyrolysis technologies for municipal solid waste: a review. Waste management, 34(12), 2466-2486.

77. Chen, G. B., Li, J. W., Lin, H. T., Wu, F. H., & Chao, Y. C. (2018). A study of the production and combustion characteristics of pyrolytic oil from sewage sludge using the taguchi method. Energies, 11(9), 2260.

78. Chen, G., Lock Yue, P., & Mujumdar, A. S. (2002). Sludge dewatering and drying. Drying Technology, 20(4-5), 883-916.

79. Chen, H., Chen, D., & Hong, L. (2015). Influences of activation agent impregnated sewage sludge pyrolysis on emission characteristics of volatile combustion and De-NOx performance of activated char. Applied energy, 156, 767-775.

80. Chen, H., Yan, S. H., Ye, Z. L., Meng, H. J., & Zhu, Y. G. (2012). Utilization of urban sewage sludge: Chinese perspectives. Environmental Science and Pollution Research, 19(5), 1454-1463.

81. Chen, T., Zhang, Y., Wang, H., Lu, W., Zhou, Z., Zhang, Y., & Ren, L. (2014). Influence of pyrolysis temperature on characteristics and heavy metal adsorptive performance of biochar derived from municipal sewage sludge. Bioresource technology, 164, 47-54.

82. Chen, W. H., Peng, J., & Bi, X. T. (2015). A state-of-the-art review of biomass torrefaction, densification and applications. Renewable and Sustainable Energy Reviews, 44, 847-866.

83. Chintala, V. (2018). Production, upgradation and utilization of solar assisted pyrolysis fuels from biomass–A technical review. Renewable and Sustainable Energy Reviews, 90, 120-130.

84. Chu, C. P., & Lee, D. J. (1999). Moisture distribution in sludge: effects of polymer conditioning. Journal of Environmental Engineering, 125(4), 340-345.

85. Cieślik, B. M., Namieśnik, J., & Konieczka, P. (2015). Review of sewage sludge management: standards, regulations and analytical methods. Journal of Cleaner Production, 90, 1-15.

86. Citeau, M., Olivier, J., Mahmoud, A., Vaxelaire, J., Larue, O., & Vorobiev, E. (2012). Pressurised electro-osmotic dewatering of activated and anaerobically digested sludges: electrical variables analysis. Water research, 46(14), 4405-4416.

87. Colin, F., & Gazbar, S. (1995). Distribution of water in sludges in relation to their mechanical dewatering. Water Research, 29(8), 2000-2005.

88. Collares-Pereira, M., Canavarro, D., & Guerreiro, L. L. (2017). Linear Fresnel reflector (LFR) plants using superheated steam, molten salts, and other heat transfer fluids. In Advances in Concentrating Solar Thermal Research and Technology (pp. 339-352). Woodhead Publishing.

89. Cronshaw, I. (2015). World Energy Outlook 2014 projections to 2040: natural gas and coal trade, and the role of China. Australian Journal of Agricultural and Resource Economics, 59(4), 571-585.

90. Czajczynska, D., Anguilano, L., Ghazal, H., Krzyzynska, R., Reynolds, A. J., & Spencer, N. (2017). Potential of pyrolysis processes in the waste management sector. Therm Sci Eng Prog 2017; 3: 171e97.

91. Czernik, S., & Bridgwater, A. V. (2004). Overview of applications of biomass fast pyrolysis oil. Energy & fuels, 18(2), 590-598.

92. Daradki, A. (2008). The Jordanian experience in the management of solid waste, Corporation for Environmental Protection. Arabic Report.

93. Daud, Z., Awang, H., Nasir, N., Ridzuan, M. B., & Ahmad, Z. (2015). Suspended solid, color, COD and oil and grease removal from biodiesel wastewater by coagulation and flocculation processes. Procedia-Social and Behavioral Sciences, 195, 2407-2411.Retrieved on : 8th march, 2019.Retrieved from :https://ac.els-cdn.com/S1877042815037131/1-s2.0-S1877042815037131-main.pdf?_tid=a2b31bdd-7cab-43ec-8785-ff0f7e4835cc&acdnat=1552639830_b3ca1452409b0aa99904b565e4dc6391

94. Daugaard, D. E., & Brown, R. C. (2003). Enthalpy for pyrolysis for several types of biomass. Energy & fuels, 17(4), 934-939.

95. Demirbas, A. (2011). Waste management, waste resource facilities and waste conversion processes. Energy Conversion & Management, 52(2), 1280-1287. https://doi.org/10.1016/j.enconman.2010.09.025

96. Deng, W. Y., Yan, J. H., Li, X. D., Wang, F., Lu, S. Y., Chi, Y., & Cen, K. F. (2009). Measurement and simulation of the contact drying of sewage sludge in a Nara-type paddle dryer. Chemical Engineering Science, 64(24), 5117-5124.

97. Deng, W., Li, X., Yan, J., Wang, F., Chi, Y., & Cen, K. (2011). Moisture distribution in sludges based on different testing methods. Journal of Environmental Sciences, 23(5), 875-880.

98. Desert aire: Technical Bulletin 3, (2019). Optimizing solutions through superior dehumidification technology: Dehumidification and the Psychrometric Chart. Retrieved from https://www.desert-aire.com/resources/application-notes/dehumidification-and-psychrometric-chart

99. DiGrazia, M., Gee, R., & Jorgensen, G. (2009, January). ReflecTech® mirror film attributes and durability for CSP applications. In ASME 2009 3rd International Conference on Energy Sustainability collocated with the Heat Transfer and InterPACK09 Conferences (pp. 677-682). American Society of Mechanical Engineers, NY.

100. Dijkema, G. P. J., Reuter, M. A., & Verhoef, E. V. (2000). A new paradigm for waste management. Waste Management, 20(8), 633-638. https://doi.org/10.1016/S0956-053X(00)00052-0

101. Ding, H. H., Chang, S., & Liu, Y. (2017). Biological hydrolysis pretreatment on secondary sludge: Enhancement of anaerobic digestion and mechanism study. Bioresource technology, 244, 989-995.

102. Ding, H. S., & Jiang, H. (2013). Self-heating co-pyrolysis of excessive activated sludge with waste biomass: energy balance and sludge reduction. Bioresource technology, 133, 16-22.

103. Dixon, N., & Jones, D. R. V. (2005). Engineering properties of municipal solid waste. Geotextiles & Geomembranes, 23(3), 205-233. https://doi.org/10.1016/j.geotexmem.2004.11.002

104. Dominguez, A., Menéndez, J. A., & Pis, J. J. (2006). Hydrogen rich fuel gas production from the pyrolysis of wet sewage sludge at high temperature. Journal of analytical and applied pyrolysis, 77(2), 127-132.

105. Duffie, J. A., & Beckman, W. A. (2013). Solar engineering of thermal processes. John Wiley & Sons.

106. Earle, R. L. & Earle, M.D. (2004). Unit operation in food processing. The New Zealand Institute of Food Science and Technology (Inc.). Retrieved from https://nzifst.org.nz/resources/unitoperations/drying1.htm

107. Ehrlich, R., & Geller, H. A. (2017). Renewable energy: a first course. CRC press.

108. El Gharbi, N., Derbal, H., Bouaichaoui, S., & Said, N. (2011). A comparative study between parabolic trough collector and linear Fresnel reflector technologies. Energy Procedia, 6, 565-572.

109. El Mghouchi, Y., El Bouardi, A., Choulli, Z., & Ajzoul, T. (2014). New model to estimate and evaluate the solar radiation. International Journal of Sustainable Built Environment, 3(2), 225-234.

110. Elliott, D. C., Beckman, D., Bridgwater, A. V., Diebold, J. P., Gevert, S. B., & Solantausta, Y. (1991). Developments in direct thermochemical liquefaction of biomass: 1983-1990. Energy & Fuels, 5(3), 399-410.

111. El-Naqa, A. (2005). Environmental impact assessment using rapid impact assessment matrix (RIAM) for Russeifa landfill, Jordan. Environmental Geology, 47(5), 632-639.

112. Elordi, G., Olazar, M., Aguado, R., Lopez, G., Arabiourrutia, M. & Bilbao, J. (2007). Catalytic pyrolysis of high density polyethylene in a conical spouted bed reactor. Journal of Analytical and Applied Pyrolysis, 79, 450–455.

113. Elordi, G., Olazar, M., Lopez, G., Amutio, M., Artetxe, M., Aguado, R., et al. (2009). Catalytic pyrolysis of HDPE in continuous mode over zeolite catalysts in a conical spouted bed reactor. Journal of Analytical and Applied Pyrolysis, 85, 345–351.

114. EnergyNext (2013). India's first CSP plant commissioned under JNNSM. Retrieved from http://www.energynext.in/2013/06/indias-first-csp-plant-commissioned-under-jnnsm/

115. Engineering ToolBox, (2003). Moisture Holding Capacity of Air. Retrieved from https://www.engineeringtoolbox.com/moisture-holding-capacity-air-d_281.html

116. Engineering ToolBox, (2004). Enthalpy of Moist Air. Retrieved from https://www.engineeringtoolbox.com/enthalpy-moist-air-d_683.html

117. Epstein, M., Olalde, G., Santén, S., Steinfeld, A., & Wieckert, C. (2008). Towards the industrial solar carbothermal production of zinc. Journal of Solar Energy Engineering, 130(1).

118. Erdincler, A., & Vesilind, P. A. (2000). Effect of sludge cell disruption on compactibility of biological sludges. Water Science and Technology, 42(9), 119-126.

119. Etier, I., Al, A. and Ababne, M. (2010). Analysis of solar radiation in Jordan. Jordan Journal of Mechanical and Industrial Engineering, 4(6), pp. 733–738.

120. European Commission, (2018). ANNEX 1 of the Commission Decision on the Annual Action Programme 2016 (part 2) and 2017 (part 1) in favour of the Hashemite Kingdom of Jordan. Initial Action Document for the Support to the implementation of the National Solid Waste Management Strategy (NSWMS). Retrieved from https://ec.europa.eu/neighbourhood-enlargement/sites/near/files/c_2016_6629_jordan_aap_2016_part_2_aap_2017_part_1_annex_1.pdf

121. Evstratov, V. A., Rud, A. V., & Belousov, K. Y. (2015). Process modelling vertical screw transport of bulk material flow. Procedia engineering, 129, 397-402.

122. Fend, T., Jorgensen, G., & Küster, H. (2000). Applicability of highly reflective aluminium coil for solar concentrators. Solar Energy, 68(4), 361-370.

123. Fernández-Gonzalez, J. M., Grindlay, A. L., Serrano-Bernardo, F., Rodríguez-Rojas, M. I., & Zamorano, M. (2017). Economic and environmental review of Waste-to-Energy systems for municipal solid waste management in medium and small municipalities. Waste Management, 67, 360-374.

124. Ferrasse, J. H., Arlabosse, P., & Lecomte, D. (2002). Heat, momentum, and mass transfer measurements in indirect agitated sludge dryer. Drying technology, 20(4-5), 749-769.

125. Feuermann, D., & Gordon, J. M. (1991). Analysis of a two-stage linear Fresnel reflector solar concentrator. Journal of solar energy engineering, 113(4), 272-279.

126. Fine Art America (2019). Compact Linear Fresnel Reflector Wood Print. Retrieved from https://fineartamerica.com/featured/compact-linear-fresnel-reflector-us-department-of-energy.html?product=wood-print

127. Fischer, M., & Tamme, R. (1991). Solar Fuels and Chemicals, Solar Hydrogen. In Solar Power Plants (pp. 336-366). Springer, Berlin, Heidelberg.

128. Flaga, A. (2005, March). Sludge drying. In Proceedings of Polish-Swedish seminars, Integration and optimization of urban sanitation systems. Cracow March (pp. 17-18).

129. Flaga, A. (2007). The aspects of sludge thermal utilization. Institute of Heat Engineering and Air Protection, Cracow University of Technology, Kraków, Poland, 9-18.

130. Flores, V., & Almanza, R. (2004). Direct steam generation in parabolic trough concentrators with bimetallic receivers. Energy, 29(5-6), 645-651.

131. Fogler, H. (2010). Elements of chemical reaction engineering. 4th ed. New Jersey: Pearson Education Inc.

132. Font, R., Fullana, A., Conesa, J. A., & Llavador, F. (2001). Analysis of the pyrolysis and combustion of different sewage sludges by TG. Journal of Analytical and Applied Pyrolysis, 58, 927-941.

133. Fonts, I., Gea, G., Azuara, M., Ábrego, J., & Arauzo, J. (2012). Sewage sludge pyrolysis for liquid production: a review. Renewable and sustainable energy reviews, 16(5), 2781-2805.

134. Fonts, I., Gea, G., Azuara, M., Ábrego, J., & Arauzo, J. (2012). Sewage sludge pyrolysis for liquid production: a review. Renewable and sustainable energy reviews, 16(5), 2781-2805.

135. Fonts, I., Juan, A., Gea, G., Murillo, M. B., & Sánchez, J. L. (2008). Sewage sludge pyrolysis in fluidized bed, 1: influence of operational conditions on the product distribution. Industrial & Engineering Chemistry Research, 47(15), 5376-5385.

136. Fullerton, D. & Raub, A. (2004). Addressing the Economics of Waste: Economic analysis of solid waste management policies. The Organisation for Economic Co-operation and Development (OECD). Retrieved from https://www.oecd-ilibrary.org/environment/addressing-the-economics-of-waste/economic-analysis-of-solid-waste-management-policies_9789264106192-4-en

137. Funke, A., Henrich, E., Dahmen, N., & Sauer, J. (2017). Dimensional Analysis of Auger-Type Fast Pyrolysis Reactors. Energy Technology, 5(1), 119-129.

138. Fytili, D., & Zabaniotou, A. (2008). Utilization of sewage sludge in EU application of old and new methods—a review. Renewable and sustainable energy reviews, 12(1), 116-140.

139. Gao, N., Li, J., Qi, B., Li, A., Duan, Y., & Wang, Z. (2014). Thermal analysis and products distribution of dried sewage sludge pyrolysis. Journal of analytical and applied pyrolysis, 105, 43-48.

140. Gao, N., Quan, C., Liu, B., Li, Z., Wu, C., & Li, A. (2017). Continuous pyrolysis of sewage sludge in a screw-feeding reactor: products characterization and ecological risk assessment of heavy metals. Energy & Fuels, 31(5), 5063-5072.

141. Garcia-Nunez, J. A., Pelaez-Samaniego, M. R., Garcia-Perez, M. E., Fonts, I., Abrego, J., Westerhof, R. J. M., & Garcia-Perez, M. (2017). Historical developments of pyrolysis reactors: a review. Energy & fuels, 31(6), 5751-5775.

142. Garfoth, A., Lin, Y., Sharratt, P. & Dwyer J. (1998). Production of hydrocarbons by catalytic degradation of high density polyethylene in a laboratory fluidizedbed reactor. Applied Catalysis A: General, 169, 331–342.

143. Global Climate and Energy Project (GCEP), (2018). Exergy Flow Charts. Stanford University. Retrieved from http://gcep.stanford.edu/research/exergycharts.html

144. Global Solar Atlas (n. d.). Available at: https://globalsolaratlas.info/download/middle-east-and-north-africa (Accessed: 5 April 2020).

145. Goldemberg, J. (2000). United Nations Development Programme, United Nations, Department of Economic and Social Affairs and World Energy Council. World energy assessment: energy and the challenge of sustainability.

146. Gollakota, A. R. K., Kishore, N., & Gu, S. (2018). A review on hydrothermal liquefaction of biomass. Renewable and Sustainable Energy Reviews, 81, 1378-1392.

147. Gollakota, A. R., Reddy, M., Subramanyam, M. D., & Kishore, N. (2016). A review on the upgradation techniques of pyrolysis oil. Renewable and Sustainable Energy Reviews, 58, 1543-1568.

148. Gouthamraj, K., Rani, K., & Satyanarayana, G. (2013). Design and Analysis of Rooftop Linear Fresnel Reflector Solar Concentrator.

149. Gradus, R. H., Nillesen, P. H., Dijkgraaf, E., & Van Koppen, R. J. (2017). A cost-effectiveness analysis for incineration or recycling of Dutch household plastic waste. Ecological Economics, 135, 22-28.

150. Grassmann, H., Boaro, M., Citossi, M., Cobal, M., Ersettis, E., Kapllaj, E., & Pizzariello, A. (2015). Solar biomass pyrolysis with the linear mirror II. Smart Grid and Renewable Energy, 6(07), 179.

151. Grilli, M. G., Bildstein, K. L., & Lambertucci, S. A. (2019). Nature's clean-up crew: Quantifying ecosystem services offered by a migratory avian scavenger on a continental scale. Ecosystem Services, 39, 100990.

152. Grüter, H., Matter, M., Oehlmann, K. H., & Hicks, M. D. (1990). Drying of sewage sludge–An important step in waste disposal. Water Science and Technology, 22(12), 57-63.

153. Grüter, H., Matter, M., Oehlmann, K. H., & Hicks, M. D. (1990). Drying of sewage sludge–An important step in waste disposal. Water Science and Technology, 22(12), 57-63.

154. Gu, X., Taylor, R. A., & Rosengarten, G. (2014). Analysis of a new compound parabolic concentrator-based solar collector designed for methanol reforming. Journal of Solar Energy Engineering, 136(4), 041012.

155. Hafez, A. Z., Soliman, A., El-Metwally, K. A., & Ismail, I. M. (2017). Design analysis factors and specifications of solar dish technologies for different systems and applications. Renewable and Sustainable Energy Reviews, 67, 1019-1036.

156. Hafez, A. Z., Soliman, A., El-Metwally, K. A., & Ismail, I. M. (2016). Solar parabolic dish Stirling engine system design, simulation, and thermal analysis. Energy Conversion and Management, 126, 60-75.

157. Han, R., Zhao, C., Liu, J., Chen, A., & Wang, H. (2015). Thermal characterization and syngas production from the pyrolysis of biophysical dried and traditional thermal dried sewage sludge. Bioresource technology, 198, 276-282.

158. Harrison, E. Z., Oakes, S. R., Hysell, M., & Hay, A. (2006). Organic chemicals in sewage sludge. Science of the total environment, 367(2-3), 481-497.

159. Haruthaithanasan, M., Sae-Tun, O., Lichaikul, N., Ma, S., Thongmanivong, S. & Chanthavong, H. (2016). The role of biochar production in sustainable development in Thailand, Lao PDR and Cambodia. In Bruckman, V., Varol, E., Uzun, B., & Liu, J. (2016). Biochar: A Regional Supply Chain Approach in View of Climate Change Mitigation, pp 197-288. Cambridge University Press. Retrieved from https://www.cambridge.org/core/books/biochar/biochar-production/E5F22B717DFB662E4E03F120E540E556/core-reader

160. Hathaway, B. J., Davidson, J. H., & Kittelson, D. B. (2011). Solar gasification of biomass: kinetics of pyrolysis and steam gasification in molten salt. ASME. Journal of solar energy engineering, 133(2), 021011. https://doi.org/10.1115/1.4003680

161. Hemeda, S., Aboukarima, A. and El-Bakhshawan, M. (2015). Performance evaluation of a solar powered lighting system provided with automatic control for agricultural applications. Agricultural Engineering and Country Challenges, pp. 33–50. Available at: https://www.researchgate.net/publication/324784046_PERFORMANCE_EVALUATION_OF_A_SOLAR_POWERED_LIGHTING_SYSTEM_PROVIDED_WITH_AUTOMATIC_CONTROL_FOR_AGRICULTURAL_APPLICATIONS.

162. Hertwich, E. G., & Zhang, X. (2009). Concentrating-solar biomass gasification process for a 3rd generation biofuel. Environmental science & technology, 43(11), 4207-4212.

163. Herwijn, A. J. M. (1996). Fundamental aspects of sludge characterization.

164. Hinkley, J., McNaughton, R., & Neumann, A. (2010, December). Development of a high flux solar furnace facility at CSIRO for Australian research and industry. In Solar2010, 48th AuSES Annu. Conf., Canberra, ACT, Australia (pp. 1-9).

165. Hoffman, V., & Marmsjö, A. (2014). Combustion of sludge in Fortum's plants with possible phosphorus recycling.

166. Hoornweg, D., & Bhada-Tata, P. (2012). What a waste: a global review of solid waste management (Vol. 15, p. 116). World Bank, Washington, DC.

167. Hopkins, M. W., Antal Jr, M. J., & Kay, J. G. (1984). Radiant flash pyrolysis of biomass using a xenon flashtube. Journal of applied polymer science, 29(6), 2163-2175.

168. Hopkins, M. W., Dejenga, C., & Antal Jr, M. J. (1984). The flash pyrolysis of cellulosic materials using concentrated visible light. Solar energy, 32(4), 547-551.

169. Horton, A. A., Walton, A., Spurgeon, D. J., Lahive, E., & Svendsen, C. (2017). Microplastics in freshwater and terrestrial environments: evaluating the current understanding to identify the knowledge gaps and future research priorities. Science of the Total Environment, 586, 127-141.

170. Hotz, N., Zimmerman, R., Weinmueller, C., Lee, M. T., Grigoropoulos, C. P., Rosengarten, G., & Poulikakos, D. (2010). Exergetic analysis and optimization of a solar-powered reformed methanol fuel cell micro-powerplant. Journal of Power Sources, 195(6), 1676-1687.

171. Hrayshat, E. S. (2007). Analysis of renewable energy situation in Jordan. Renewable and Sustainable Energy Reviews, 11(Jordan, like most developing countries, has problems, constraints, and difficulties that mandate increasing renewable energy (RE) technology utilization. The most effective argument, in favour of the adoption of RE technologies in Jordan, is that Jordan's), pp. 1873–1887. doi: 10.1016/j.rser.2006.01.003.

172. Hu, M., Gao, L., Chen, Z., Ma, C., Zhou, Y., Chen, J., ... & Guo, D. (2016). Syngas production by catalytic in-situ steam co-gasification of wet sewage sludge and pine sawdust. Energy Conversion and Management, 111, 409-416.

173. Huang, Y. F., Shih, C. H., Chiueh, P. T., & Lo, S. L. (2015). Microwave co-pyrolysis of sewage sludge and rice straw. Energy, 87, 638-644.

174. Indiamart, (2020). Pyrolysis Oil. Retrived from https://dir.indiamart.com/impcat/pyrolysis-oil.html (On Thursday 16/07/2020).

175. Inguanzo, M., Domınguez, A., Menéndez, J. A., Blanco, C. G., & Pis, J. J. (2002). On the pyrolysis of sewage sludge: the influence of pyrolysis conditions on solid, liquid and gas fractions. Journal of Analytical and Applied Pyrolysis, 63(1), 209-222.

176. Institute of Solar Research - Deutsche Luft-Reederei (DLR). German Aerospace Center (DLR). Laboratory tests at the Institute's Xenon-High-Flux Solar Simulator. Cologne, Germany. INDUSOL. DLR 2015. Retrieved from https://www.dlr.de/sf/en/desktopdefault.aspx/tabid-9315/16078_read-41174/gallery-1/216_read-2/

177. International Energy Agency (IEA) Bioenergy/Task 34 (2017). Pyrolysis reactors, direct thermochemical liquifaction. Retrieved from http://task34.ieabioenergy.com/pyrolysis-reactors/

178. International Energy Agency IEA, (2011). Solar energy perspective.

179. Ischia, M., Dal Maschio, R., Grigiante, M., & Baratieri, M. (2011). Clay–sewage sludge co-pyrolysis. A TG–MS and Py–GC study on potential advantages afforded by the presence of clay in the pyrolysis of wastewater sewage sludge. Waste management, 31(1), 71-77.

180. Islam, M. S., & Tanaka, M. (2004). Impacts of pollution on coastal and marine ecosystems including coastal and marine fisheries and approach for management: a review and synthesis. Marine pollution bulletin, 48(7-8), 624-649.

181. Jaffer, M. (2011). Use of solar energy in the Middle East, course work PH240. Available at: http://large.stanford.edu/courses/2011/ph240/jaffer1/ (Accessed: 29 March 2020).

182. Jahirul, M. I., Rasul, M. G., Chowdhury, A. A., & Ashwath, N. (2012). Biofuels production through biomass pyrolysis—a technological review. Energies, 5(12), 4952-5001.

183. Jakahi, D. Y. (1984). Apparatus for storing solar energy in synthetic fuels. Patent No. 4455153. Patent Application No. 6/71,983. Mililani Town, HI

184. Jin, B., Wilén, B. M., & Lant, P. (2004). Impacts of morphological, physical and chemical properties of sludge flocs on dewaterability of activated sludge. Chemical Engineering Journal, 98(1-2), 115-126.

185. Jin, J., Li, Y., Zhang, J., Wu, S., Cao, Y., Liang, P., ... & Christie, P. (2016). Influence of pyrolysis temperature on properties and environmental safety of heavy metals in biochars derived from municipal sewage sludge. Journal of hazardous materials, 320, 417-426.

186. Joardder, M. U. H., Halder, P. K., Rahim, M. A., & Masud, M. H. (2017). Solar Pyrolysis: Converting Waste Into Asset Using Solar Energy. In Clean Energy for Sustainable Development (pp. 213-235). Academic Press.

187. Joardder, M. U., Halder, P. K., Rahim, A., & Paul, N. (2014). Solar assisted fast pyrolysis: a novel approach of renewable energy production. Journal of engineering, 2014.

188. Jorand, F., Zartarian, F., Thomas, F., Block, J. C., Bottero, J. Y., Villemin, G., ... & Manem, J. (1995). Chemical and structural (2D) linkage between bacteria within activated sludge flocs. Water research, 29(7), 1639-1647.

189. Jordan Green Building Council GBC (2016). Your Guide to Waste Management in Jordan: Waste Sorting Informative booklet. The Hashemite Kingdom of Jordan. ISBN: 978-9957-8751-0-7. (2016/8/3569). Retrieved from http://library.fes.de/pdf-files/bueros/amman/12729.pdf

190. Kabir, G., & Hameed, B. H. (2017). Recent progress on catalytic pyrolysis of lignocellulosic biomass to high-grade bio-oil and bio-chemicals. Renewable and Sustainable Energy Reviews, 70, 945-967.

191. Kalogirou, S. (2009). Solar energy collectors. In a Solar energy engineering: processes and systems (1est edition) (pp. 121-217). Retrieved from https://www.sciencedirect.com/science/article/pii/B9780123745019000030

192. Kaminsky, W. & Kim, J. (1999). Pyrolysis of mixed plastics into aromatics. Journal of Analytical and Applied Pyrolysis, 51, 127–134.

193. Kapoor, L., Mekala, A., & Bose, D. (2016, November). Auger reactor for biomass fast pyrolysis: Design and operation. In 2016 21st Century Energy Needs-Materials, Systems and Applications (ICTFCEN) (pp. 1-6). IEEE.

194. Katsiris, N., & Kouzeli-Katsiri, A. (1987). Bound water content of biological sludges in relation to filtration and dewatering. Water Research, 21(11), 1319-1327.

195. Kaygusuz, K. (2001). Renewable energy: Power for a sustainable future. Energy exploration & exploitation, 19(6), 603-626.

196. Kaza, S., Yao, L., Bhada-Tata, P., & Van Woerden, F. (2018). World Bank Group. World Bank Report "What a Waste 2.0: A global Snapshot of Solid Waste Management to 2050". World Bank Publications. Retrieved from

https://openknowledge.worldbank.org/handle/10986/30317?deliveryName=DM5107&locale-attribute=en

197. Keenan, J. H., Keyes, F. G., Hill, P. G., & Moore, J. G. (1969). Steam tables (International edition-metric units). John Wiley, New York

198. Kelessidis, A., & Stasinakis, A. S. (2012). Comparative study of the methods used for treatment and final disposal of sewage sludge in European countries. Waste management, 32(6), 1186-1195.

199. Kemp, I. C., Fyhr, B. C., Laurent, S., Roques, M. A., Groenewold, C. E., Tsotsas, E., ... & Kind, M. (2001). Methods for processing experimental drying kinetics data. Drying technology, 19(1), 15-34.

200. Kennedy, C. & Terwilliger, K. (2005). Optical durability of candidate solar reflectors. Transactions of the ASME. Journal of Solar Energy Engineering, 127, pp. 262-269

201. Kennedy, C. E. (2002). Review of mid-to high-temperature solar selective absorber materials (No. NREL/TP-520-31267). National Renewable Energy Lab., Golden, CO.(US).

202. Khan, A. A., De Jong, W., Jansens, P. J., & Spliethoff, H. (2009). Biomass combustion in fluidized bed boilers: Potential problems and remedies. Fuel processing technology, 90(1), 21-50.

203. Kim, Y., & Parker, W. (2008). A technical and economic evaluation of the pyrolysis of sewage sludge for the production of bio-oil. Bioresource technology, 99(5), 1409-1416.

204. Kingston, T. A. (2013). Granular mixing visualization and quantification in a double screw mixer.

205. Kirubakaran, V., Sivaramakrishnan, V., Nalini, R., Sekar, T., Premalatha, M., & Subramanian, P. (2009). A review on gasification of biomass. Renewable and Sustainable Energy Reviews, 13(1), 179-186.

206. Kishimoto, A., Oka, T., Yoshida, K., & Nakanishi, J. (2001). Cost effectiveness of reducing dioxin emissions from municipal solid waste incinerators in Japan.

207. Komline-Sanderson, (2008). Komline-Sanderson Paddle Dryer. Drying Technology for Biosolids, Sludges and By-products. Retrieved from http://www.komline.com/wp-content/uploads/KS-SDB_080714.pdf

208. Kopp, J., & Dichtl, N. (2001). Influence of the free water content on the dewaterability of sewage sludges. Water Science and Technology, 44(10), 177-183.

209. Kowalik P., 1998. Energetic use of sewage sludge in the sewage treatment plant in Swarzewo. Materials of the VII Conf. Nauk.-Techn. on "Sewage sludge in practice" under red. J.B. Bienia, Częstochowa 1998.

210. Kraemer, D., Poudel, B., Feng, H. P., Caylor, J. C., Yu, B., Yan, X., ... & McEnaney, K. (2011). High-performance flat-panel solar thermoelectric generators with high thermal concentration. Nature materials, 10(7), 532.

211. Kudra, T. (2003). Sticky region in drying—definition and identification. Drying Technology, 21(8), 1457-1469.

212. Kumar, A., Pachauri, R. K., & Chauhan, Y. K. (2015, March). Analysis and performance improvement of solar PV system by solar irradiation tracking. In 2015 International Conference on Energy Economics and Environment (ICEEE) (pp. 1-6). IEEE.

213. Lamb, G., Pogson, S., & Schliebs, D. (2012). Waste definitions and classifications: Report on issues, opportunities and information gaps. Revision 02. Hyder Consulting Pty Ltd for

Department of Sustainability, Environment, Water, Population and Communities. Sydney, Australia. ABN 76 104 485 289. Retrieved from http://www.environment.gov.au/system/files/resources/d05aa2d3-be01-44f3-904b-04dd09e9b0a1/files/waste-classification-gaps-part1.pdf

214. Lay, M. (2020). Personal communication, lecturer.

215. Lee, D. J. (1994). Measurement of bound water in waste activated sludge: use of the centrifugal settling method. Journal of Chemical Technology & Biotechnology: International Research in Process, Environmental AND Clean Technology, 61(2), 139-144.

216. Lee, D. J. (1996). Moisture distribution and removal efficiency of waste activated sludges. Water science and technology, 33(12), 269-272.

217. Lee, D. J., & Hsu, Y. H. (1995). Measurement of bound water in sludges: a comparative study. Water Environment Research, 67(3), 310-317.

218. Lee, I. S., Parameswaran, P., & Rittmann, B. E. (2011). Effects of solids retention time on methanogenesis in anaerobic digestion of thickened mixed sludge. Bioresource technology, 102(22), 10266-10272.

219. Lee, Y. E., Kim, I. T., & Yoo, Y. S. (2018). Stabilization of high-organic-content water treatment sludge by pyrolysis. Energies, 11(12), 3292.

220. Lehto, J., Oasmaa, A., Solantausta, Y., Kytö, M., & Chiaramonti, D. (2014). Review of fuel oil quality and combustion of fast pyrolysis bio-oils from lignocellulosic biomass. Applied Energy, 116, 178-190.

221. Lenntech BV. Water treatment solution. Calculating the daily sludge production of a sewer wastewater treatment plant. Retrieved from https://www.lenntech.com/wwtp/calculate-daily-sludge-production.htm#ixzz5z7NfJL00

222. Léonard, A., Blacher, S., Marchot, P., & Crine, M. (2002). Use of X-ray microtomography to follow the convective heat drying of wastewater sludges. Drying Technology, 20(4-5), 1053-1069.

223. Léonard, A., Meneses, E., Le Trong, E., Salmon, T., Marchot, P., Toye, D., & Crine, M. (2008). Influence of back mixing on the convective drying of residual sludges in a fixed bed. Water Research, 42(10-11), 2671-2677.

224. Lewis, N. S., & Nocera, D. G. (2006). Powering the planet: Chemical challenges in solar energy utilization. Proceedings of the National Academy of Sciences, 103(43), 15729-15735.

225. Li, B., Wang, F., Chi, Y., & Yan, J. H. (2014). Adhesion and cohesion characteristics of sewage sludge during drying. Drying technology, 32(13), 1598-1607.

226. Li, D. H., & Ganczarczyk, J. (1990) Structure of Activated Sludge Flocs. Biotechnn]. Bioeng, 11, 127.

227. Li, D. H., Ganczarczyk, J. J., & Jenkins, D. (1986). Physical characteristics of activated sludge flocs. Critical Reviews in Environmental Science and Technology, 17(1), 53-87.

228. Li, H., Jiang, L. B., Li, C. Z., Liang, J., Yuan, X. Z., Xiao, Z. H., ... & Wang, H. (2015). Co-pelletization of sewage sludge and biomass: The energy input and properties of pellets. Fuel processing technology, 132, 55-61.

229. Li, H., Zou, S., & Li, C. (2012). Liming pretreatment reduces sludge build-up on the dryer wall during thermal drying. Drying Technology, 30(14), 1563-1569.

230. Lin, K. H., Lai, N., Zeng, J. Y., & Chiang, H. L. (2017). Temperature influence on product distribution and characteristics of derived residue and oil in wet sludge pyrolysis using microwave heating. Science of The Total Environment, 584, 1248-1255.

231. Liu, G. & Wang, J., 2017. Enhanced removal of total nitrogen and total phosphorus by applying intermittent aeration to the Modified Ludzack-Ettinger (MLE) process. Journal of Cleaner Production, Volume 166, pp. 163-171.

232. Lofrano, G. & Brown, J., 2010. Wastewater management through the ages: A history of mankind. Science of the Total Environment, 26 July, 408(22), pp. 5254-5264.

233. Longo, S., Katsou, E., Malamis, S., Frison, N., Renzi, D., & Fatone, F. (2015). Recovery of volatile fatty acids from fermentation of sewage sludge in municipal wastewater treatment plants. Bioresource technology, 175, 436-444.

234. Lovegrove, K., & Stein, W. (Eds.). (2012). Concentrating solar power technology: principles, developments and applications. Elsevier.

235. Lovejoy, D., Johansson, T., Kelly, H., Reddy, A., Williams, R., (1993). Renewable energy-sources for fuels and electricity. Natural Resource Forum, Vol. 17, No. 3, pp. 244-245. The boulevard, Langford lane, Kidlington, Oxford, OXON, England. OX5 1GB: Butterworth-Heinemann LTD.

236. Lu, T., Yuan, H. R., Zhou, S. G., Huang, H. Y., Noriyuki, K., & Chen, Y. (2012). On the pyrolysis of sewage sludge: the influence of pyrolysis temperature on biochar, liquid and gas fractions. In Advanced Materials Research (Vol. 518, pp. 3412-3420). Trans Tech Publications.

237. Ma, R., Sun, S., Geng, H., Fang, L., Zhang, P., & Zhang, X. (2018). Study on the characteristics of microwave pyrolysis of high-ash sludge, including the products, yields, and energy recovery efficiencies. Energy, 144, 515-525.

238. Magdziarz, A., Dalai, A. K., & Koziński, J. A. (2016). Chemical composition, character and reactivity of renewable fuel ashes. Fuel, 176, 135-145.

239. Mahmoud, A., Olivier, J., Vaxelaire, J., & Hoadley, A. F. (2010). Electrical field: A historical review of its application and contributions in wastewater sludge dewatering. Water research, 44(8), 2381-2407.

240. Malkow, T. (2004). Novel and innovative pyrolysis and gasification technologies for energy efficient and environmentally sound MSW disposal. Waste management, 24(1), 53-79.

241. Mancini, T. (2011). Advantages of using molten salt. Sandia National Laboratories, Albuquerque.

242. Marca Chile, (n.d.). Here comes the sun Chile greenlights enormous 400-megawatt solar project. Retrieved from https://www.marcachile.cl/web/this-is-chile.html?p=8861

243. Marmur, B. L. (2015). The effects of scale on granular mixing in a double screw pyrolyzer.

244. Marmur, B. L., & Heindel, T. J. (2016). Effect of particle size, density, and concentration on granular mixing in a double screw pyrolyzer. Powder Technology, 302, 222-235.

245. Marrero, T. W., McAuley, B. P., Sutterlin, W. R., Morris, J. S., & Manahan, S. E. (2004). Fate of heavy metals and radioactive metals in gasification of sewage sludge. Waste Management, 24(2), 193-198.

246. Martínez, J. D., Murillo, R., García, T., & Veses, A. (2013). Demonstration of the waste tire pyrolysis process on pilot scale in a continuous auger reactor. Journal of hazardous materials, 261, 637-645.

247. Martínez, J. D., Veses, A., Mastral, A. M., Murillo, R., Navarro, M. V., Puy, N., ... & García, T. (2014). Co-pyrolysis of biomass with waste tyres: Upgrading of liquid bio-fuel. Fuel Processing Technology, 119, 263-271.

248. Mas'ud, A. A. et al. (2018). Solar energy potentials and benefits in the gulf cooperation council countries: A review of substantial issues. Energies, 11(2), pp. 1–20. doi: 10.3390/en11020372.

249. Masdar a mubadala company (n.d.). Project of Gemasolar Station. Retrieved from https://masdar.ae/en/masdar-clean-energy/projects/gemasolar

250. Mathioudakis, V. L., Kapagiannidis, A. G., Athanasoulia, E., Diamantis, V. I., Melidis, P., & Aivasidis, A. (2009). Extended dewatering of sewage sludge in solar drying plants. Desalination, 248(1-3), 733-739.

251. McDougall, F. R., White, P. R., Franke, M., & Hindle, P. (2008). Integrated solid waste management: a life cycle inventory. John Wiley & Sons.

252. McKinney, J., Bond, E., Crowell, M., & Odufuwa, E. (2015). Joint agency staff report on assembly bill 8: assessment of time and cost needed to attain 100 hydrogen refueling stations in California. Publication Number CEC-600-2015-016.

253. Meegoda, J. N., Li, B., Patel, K., & Wang, L. B. (2018). A review of the processes, parameters, and optimization of anaerobic digestion. International journal of environmental research and public health, 15(10), 2224.

254. Meier, D., Van De Beld, B., Bridgwater, A. V., Elliott, D. C., Oasmaa, A., & Preto, F. (2013). State-of-the-art of fast pyrolysis in IEA bioenergy member countries. Renewable and Sustainable Energy Reviews, 20, 619-641.

255. Melchior, T., Perkins, C., Lichty, P., Weimer, A. W., & Steinfeld, A. (2009). Solar-driven biochar gasification in a particle-flow reactor. Chemical Engineering and Processing: Process Intensification, 48(8), 1279-1287.

256. Metzger, J. O., & Hüttermann, A. (2009). Sustainable global energy supply based on lignocellulosic biomass from afforestation of degraded areas. Naturwissenschaften, 96(2), 279-288.

257. Mikkelsen, L. H., & Keiding, K. (2002). Physico-chemical characteristics of full scale sewage sludges with implications to dewatering. Water research, 36(10), 2451-2462.

258. Milieu Ltd., RPA, WRc. (2008). Environmental, economic and social impacts of the use of sewage sludge on land. Unpublished final Report. Part I: Overview Report. Study Contract DG ENV.G.4/ETU/2008/0076r. Retrieved from https://ec.europa.eu/environment/archives/waste/sludge/pdf/part_i_report.pdf

259. Mills, N., Pearce, P., Farrow, J., Thorpe, R. B., & Kirkby, N. F. (2014). Environmental & economic life cycle assessment of current & future sewage sludge to energy technologies. Waste management, 34(1), 185-195.

260. Mohan, D., Pittman Jr, C. U., & Steele, P. H. (2006). Pyrolysis of wood/biomass for bio-oil: a critical review. Energy & fuels, 20(3), 848-889.

261. Moon, J., Kim, T. K., VanSaders, B., Choi, C., Liu, Z., Jin, S., & Chen, R. (2015). Black oxide nanoparticles as durable solar absorbing material for high-temperature concentrating solar power system. Solar Energy Materials and Solar Cells, 134, 417-424.

262. Moore, H. L. and Collins, H. (2020). Decentralised renewable energy and prosperity for Lebanon. Energy Policy. Elsevier Ltd, 137(September 2019), p. 111102. doi: 10.1016/j.enpol.2019.111102.

263. Morales, S., Miranda, R., Bustos, D., Cazares, T., & Tran, H. (2014). Solar biomass pyrolysis for the production of bio-fuels and chemical commodities. Journal of Analytical and Applied Pyrolysis, 109, 65-78.

264. Morero, B., Montagna, A. F., Campanella, E. A., & Cafaro, D. C. (2020). Optimal process design for integrated municipal waste management with energy recovery in Argentina. Renewable Energy, 146, 2626-2636.

265. Morgano, M. T., Leibold, H., Richter, F., & Seifert, H. (2015). Screw pyrolysis with integrated sequential hot gas filtration. Journal of analytical and applied pyrolysis, 113, 216-224.

266. Morgano, M. T., Leibold, H., Richter, F., Stapf, D., & Seifert, H. (2018). Screw pyrolysis technology for sewage sludge treatment. Waste Management, 73, 487-495.

267. Morton, O. (6 September 2006). "Solar energy: A new day dawning?: Silicon Valley sunrise". Nature. 443 (7107): 19–22. https://doi.org/10.1038/443019a

268. Mulchandani, A., & Westerhoff, P. (2016). Recovery opportunities for metals and energy from sewage sludges. Bioresource technology, 215, 215-226.

269. Nachenius, R. W., Van De Wardt, T. A., Ronsse, F., & Prins, W. (2015). Residence time distributions of coarse biomass particles in a screw conveyor reactor. Fuel Processing Technology, 130, 87-95.

270. National Research Council. (1996). Use of reclaimed water and sludge in food crop production. National Academies Press. US EPA. Pp 47. Retrieved from https://www3.epa.gov/npdes/pubs/mstr-ch3.pdf

271. Neyens, E., & Baeyens, J. (2003). A review of thermal sludge pre-treatment processes to improve dewaterability. Journal of hazardous materials, 98(1-3), 51-67.

272. Ni, G., Li, G., Boriskina, S. V., Li, H., Yang, W., Zhang, T., & Chen, G. (2016). Steam generation under one sun enabled by a floating structure with thermal concentration. Nature Energy, 1(9), 16126.

273. Niessen, W. R. (2010). Combustion and incineration processes: applications in environmental engineering. CRC Press.

274. Niwagaba, C. B., Mbéguéré, M., & Strande, L. (2014). Faecal sludge quantification, characterisation and treatment objectives. In Faecal sludge management: systems approach for implementation and operation (pp. 19-44). London: IWA Publishing.

275. Nixon, J. D., Dey, P. K., & Davies, P. A. (2010). Which is the best solar thermal collection technology for electricity generation in north-west India? Evaluation of options using the analytical hierarchy process. Energy, 35(12), 5230-5240.

276. Nordin, A. (2015). Heavy metal removal from sewage sludge by pyrolysis treatment. Retrieved from http://www.diva-portal.org/smash/record.jsf?pid=diva2%3A902689&dswid=-5954

277. Nzihou, A., & Stanmore, B. (2013). The fate of heavy metals during combustion and gasification of contaminated biomass—a brief review. Journal of hazardous materials, 256, 56-66.

278. Ohm, T. I., Chae, J. S., Kim, J. E., Kim, H. K., & Moon, S. H. (2009). A study on the dewatering of industrial waste sludge by fry-drying technology. Journal of hazardous materials, 168(1), 445-450.

279. Ohm, T. I., Chae, J. S., Lim, K. S., & Moon, S. H. (2010). The evaporative drying of sludge by immersion in hot oil: Effects of oil type and temperature. Journal of hazardous materials, 178(1-3), 483-488.

280. Oladejo, J., Shi, K., Luo, X., Yang, G., & Wu, T. (2019). A review of sludge-to-energy recovery methods. Energies, 12(1), 60.

281. Olazar, M., Lopez, G., Amutio, M., Elordi, G., Aguado, R. & Bilbao J. (2009). Influence of FCC catalyst steaming on HDPE pyrolysis product distribution. Journal of Analytical and Applied Pyrolysis, 85, 359–365.

282. Oliveira, M., Ribeiro, A., Hylland, K., & Guilhermino, L. (2013). Single and combined effects of microplastics and pyrene on juveniles (0+ group) of the common goby Pomatoschistus microps (Teleostei, Gobiidae). Ecological Indicators, 34, 641-647.

283. Oommen, R., & Jayaraman, S. (2001). Development and performance analysis of compound parabolic solar concentrators with reduced gap losses–oversized reflector. Energy Conversion and Management, 42(11), 1379-1399.

284. Orosz, M., & Dickes, R. (2017). Solar thermal powered Organic Rankine Cycles. In Organic Rankine Cycle (ORC) Power Systems (pp. 569-612). Woodhead Publishing.

285. Owen, P. J., & Cleary, P. W. (2010). Screw conveyor performance: comparison of discrete element modelling with laboratory experiments. Progress in Computational Fluid Dynamics, An International Journal, 10(5-6), 327-333.

286. Oxford Economics, (2010). Oil price outlook to 2030: Executive summery.

287. Park, E. S., Kang, B. S., & Kim, J. S. (2008). Recovery of oils with high caloric value and low contaminant content by pyrolysis of digested and dried sewage sludge containing polymer flocculants. Energy & Fuels, 22(2), 1335-1340.

288. Park, H. J., Heo, H. S., Park, Y. K., Yim, J. H., Jeon, J. K., Park, J., ... & Kim, S. S. (2010). Clean bio-oil production from fast pyrolysis of sewage sludge: effects of reaction conditions and metal oxide catalysts. Bioresource technology, 101(1), S83-S85.

289. Pasek, A. D., Gultom, K. W., & Suwono, A. (2013). Feasibility of recovering energy from municipal solid waste to generate electricity. Journal of Engineering and Technological Sciences, 45(3), 241-256.

290. Patel, D. K., Brahmbhatt, P. K., & Panchal, H. (2018). A review on compound parabolic solar concentrator for sustainable development. International Journal of Ambient Energy, 39(5), 533-546.

291. Peccia, J., & Westerhoff, P. (2015). We should expect more out of our sewage sludge.

292. Pedroza, M. M., Sousa, J. F., Vieira, G. E. G., & Bezerra, M. B. D. (2014). Characterization of the products from the pyrolysis of sewage sludge in 1 kg/h rotating cylinder reactor. Journal of analytical and applied pyrolysis, 105, 108-115.

293. Peeters, B. (2010). Mechanical dewatering and thermal drying of sludge in a single apparatus. Drying Technology, 28(4), 454-459.

294. Peeters, B., Dewil, R., & Smets, I. (2014). Challenges of drying sticky wastewater sludge. Chem Eng, 121(9), 51-54.

295. Peeters, B., Dewil, R., & Smets, I. Y. (2012). Improved process control of an industrial sludge centrifuge-dryer installation through binary logistic regression modeling of the fouling issues. Journal of Process Control, 22(7), 1387-1396.

296. Peeters, B., Dewil, R., Vernimmen, L., & Smets, I. (2012). Avoiding activated sludge stickiness through addition of polyaluminiumchloride (PACl). In Proceedings of the 11th World Filtration Conference.

297. Peeters, B., Dewil, R., Vernimmen, L., Van den Bogaert, B., & Smets, I. Y. (2013). Addition of polyaluminiumchloride (PACl) to waste activated sludge to mitigate the negative effects of its sticky phase in dewatering-drying operations. Water research, 47(11), 3600-3609.

298. Peregrina, C. A., Lecomte, D., Arlabosse, P., & Rudolph, V. (2006). Life cycle assessment (LCA) applied to the design of an innovative drying process for sewage sludge. Process Safety and Environmental Protection, 84(4), 270-279.

299. Pheng, L. G., Affandi, R., Ab Ghani, M. R., Gan, C. K., Jano, Z., & Sutikno, T. (2014). A review of Parabolic Dish-Stirling Engine System based on concentrating solar power. Telkomnika, 12(4), 1142.

300. Philibert, C. (2011). Interactions of policies for renewable energy and climate.

301. Piatkowski, N., & Steinfeld, A. (2011). Solar gasification of carbonaceous waste feedstocks in a packed-bed reactor—Dynamic modeling and experimental validation. AIChE journal, 57(12), 3522-3533.

302. Pokorna, E., Postelmans, N., Jenicek, P., Schreurs, S., Carleer, R., & Yperman, J. (2009). Study of bio-oils and solids from flash pyrolysis of sewage sludges. Fuel, 88(8), 1344-1350.

303. Rackl, M., & Günthner, W. A. (2016). Experimental investigation on the influence of different grades of wood chips on screw feeding performance. Biomass and Bioenergy, 88, 106-115.

304. Rahman, M. A., & Aziz, M. A. (2018). Solar pyrolysis of scrap tire: optimization of operating parameters. Journal of Material Cycles and Waste Management, 20(2), 1207-1215.

305. Rahman, M. M., Mostafiz, S. B., Paatero, J. V., & Lahdelma, R. (2014). Extension of energy crops on surplus agricultural lands: A potentially viable option in developing countries while fossil fuel reserves are diminishing. Renewable and Sustainable Energy Reviews, 29, 108-119.

306. Ramadan, A. and Elistratov, V. (2019). Techno-Economic Evaluation of a Grid-Connected Solar PV Plant in Syria. Applied Solar Energy, 55(3), pp. 174–188. doi: 10.3103/S0003701X1903006X.

307. Rehman, S. (1998). Solar radiation over Saudi Arabia and comparisons with empirical models. Energy, 23(12), pp. 1077–1082. doi: 10.1016/S0360-5442(98)000.

308. Rhodes, C. (2009). Night-time solar energy. Great Britain. Retrieved at 16 June 2020 from http://ergobalance.blogspot.com/2009/

309. Ringer, M., Putsche, V., & Scahill, J. (2006). Large-scale pyrolysis oil production: a technology assessment and economic analysis (No. NREL/TP-510-37779). National Renewable Energy Lab.(NREL), Golden, CO (United States).

310. Rochman, C. M., Kurobe, T., Flores, I., & Teh, S. J. (2014). Early warning signs of endocrine disruption in adult fish from the ingestion of polyethylene with and without sorbed chemical pollutants from the marine environment. Science of the Total Environment, 493, 656-661.

311. Rodriguez, J., Canadas, I., & Zarza, E. (2014). PSA vertical axis solar furnace SF5. Energy Procedia, 49, 1511-1522.

312. Rogers, J. G., & Brammer, J. G. (2012). Estimation of the production cost of fast pyrolysis bio-oil. Biomass and Bioenergy, 36, 208-217.

313. Rollinson, A. N., & Oladejo, J. M. (2019). 'Patented blunderings', efficiency awareness, and self-sustainability claims in the pyrolysis energy from waste sector. Resources, Conservation and Recycling, 141, 233-242.

314. Romdhana, M. H., Hamasaiid, A., Ladevie, B., & Lecomte, D. (2009). Energy valorization of industrial biomass: Using a batch frying process for sewage sludge. Bioresource Technology, 100(15), 3740-3744.

315. Roubík, H., Mazancová, J., Le Dinh, P., Dinh Van, D., & Banout, J. (2018). Biogas quality across small-scale biogas plants: A case of central Vietnam. Energies, 11(7), 1794.

316. Roux, N., Jung, D., Pannejon, J., & Lemoine, C. (2010, June). Modelling of the solar drying process Solia. In Proceeding of 20th European symposium on computer aided process engineering.

317. Ruffino, B., Campo, G., Cerutti, A., Zanetti, M. C., Scibilia, G., Lorenzi, E., & Genon, G. (2016). Enhancement of Waste Activated Sludge (WAS) anaerobic digestion by means of pre-treatments and intermediate treatments. Proceedings of Cyprus, 23-25.

318. Ruiz, J. A., Juárez, M. C., Morales, M. P., Muñoz, P., & Mendívil, M. A. (2013). Biomass gasification for electricity generation: Review of current technology barriers. Renewable and Sustainable Energy Reviews, 18, 174-183.

319. Sakata, Y., Uddin, M. & Muto, A. (1999). Degradation of polyethylene and polypropylene into fuel oil by using solid acid and non-solid acid catalysts. Journal of Analytical and Applied Pyrolysis, 51, 135–155.

320. Salihoglu, N. K., Pinarli, V., & Salihoglu, G. (2007). Solar drying in sludge management in Turkey. Renewable Energy, 32(10), 1661-1675.

321. Sănduleac, M. (2019, March). Solar-Based Energy Resilience in Future Cities–A Preliminary Study in the Sub-Sunbelt Region. In 2019 11th International Symposium on Advanced Topics in Electrical Engineering (ATEE) (pp. 1-6). IEEE.

322. Sanin, F. D., Clarkson, W. W., & Vesilind, P. A. (2011). Sludge engineering: the treatment and disposal of wastewater sludges. DEStech Publications, Inc.

323. Saxena, A., Pandey, S. P., & Srivastav, G. (2011). A thermodynamic review on solar box type cookers. Renewable and Sustainable Energy Reviews, 15(6), 3301-3318.

324. Screw conveyor components and design: manual (2012). Conveyor Engineering and Manufacturing Co. [Accessed 25 August 2020]. Retrieved from 〈https://www.conveyoreng.com/conveyor-design-manual/?v=42983b05e2f2〉

325. Screw Conveyor design calculations - an Engineering Guide. (n.d.). Engineering resources for powder processing industry. Retrieved from https://powderprocess.net/Equipments%20html/Screw_Conveyor_Design.html

326. Segal, A., & Epstein, M. (1999). Comparative performances oftower-top'andtower-reflector'central solar receivers. Solar Energy, 65(4), 207-226.

327. Seginer, I., & Bux, M. (2005). Prediction of evaporation rate in a solar dryer for sewage sludge. Agricultural Engineering International: CIGR Journal.

328. Seginer, I., & Bux, M. (2006). Modeling solar drying rate of wastewater sludge. Drying Technology, 24(11), 1353-1363.

329. Seiple, T. E., Coleman, A. M., & Skaggs, R. L. (2017). Municipal wastewater sludge as a sustainable bioresource in the United States. Journal of environmental management, 197, 673-680.

330. Shaik Mohasin (2012, August 2012). Parabolic dish system. Retrieved from https://shaikmohasin.wordpress.com/2012/08/25/parabolic-dish-system/

331. Shakya, B. D. (2007). Pyrolysis of waste plastics to generate useful fuel containing hydrogen using a solar thermochemical process (Master's thesis, University of Sydney.).

332. Shakya, B. D. (2007). Pyrolysis of waste plastics to generate useful fuel containing hydrogen using a solar thermochemical process (Master's thesis, University of Sydney.).

333. Shao, J., Yan, R., Chen, H., Yang, H., & Lee, D. H. (2010). Catalytic effect of metal oxides on pyrolysis of sewage sludge. Fuel Processing Technology, 91(9), 1113-1118.

334. Sharuddin, S. D. A., Abnisa, F., Daud, W. M. A. W., & Aroua, M. K. (2016). A review on pyrolysis of plastic wastes. Energy conversion and management, 115, 308-326.

335. Shen, L., & Zhang, D. K. (2003). An experimental study of oil recovery from sewage sludge by low-temperature pyrolysis in a fluidised-bed☆. Fuel, 82(4), 465-472.

336. Singh, H. (2014). Design, fabrication and experimental study of grape cabinet dryer using forced convection. Doctoral dissertation, Symbiosis Institute of Technology. Symbiosis International University. Pune, India.

337. Sirijanusorn, S., Sriprateep, K., & Pattiya, A. (2013). Pyrolysis of cassava rhizome in a counter-rotating twin screw reactor unit. Bioresource technology, 139, 343-348.

338. Slim, R., Zoughaib, A., & Clodic, D. (2008). Modeling of a solar and heat pump sludge drying system. International journal of refrigeration, 31(7), 1156-1168.

339. Sloan, M. (2018, June 8). Gemsolar solar power plant with sunflower shape boosts efficiency.

340. Smestad, G., Ries, H., Winston, R., & Yablonovitch, E. (1990). The thermodynamic limits of light concentrators. Solar Energy Materials, 21(2-3), 99-111.

341. Smil, V. (2006). Transforming the twentieth century: technical innovations and their consequences (Vol. 2). Oxford University Press on Demand.

342. Smollen, M. (1986, April). Categories of moisture content and dewatering characteristics of biological sludges. In Proceedings of the Fourth World Filtration Congress (Vol. 14, pp. 35-41).

343. Solabolic technology (n.d.). Retrieved from http://www.solabolic.com/technology

344. Soria, J., Zeng, K., Asensio, D., Gauthier, D., Flamant, G., & Mazza, G. (2017). Comprehensive CFD modelling of solar fast pyrolysis of beech wood pellets. Fuel Processing Technology, 158, 226-237.

345. Spinosa, L. (Ed.). (2007). Wastewater Sludge: A Global Overview of the Current Status and Future Prospects. Iwa Publishing.

346. Spinosa, L. (Ed.). (2011). Wastewater Sludge. Iwa Publishing.

347. Steinfeld, A. (2005). Solar thermochemical production of hydrogen—a review. Solar energy, 78(5), 603-615.

348. Stelmachowski, M. (2010). Thermal conversion of waste polyolefins to the mixture of hydrocarbons in the reactor with molten metal bed. Energy Conversion and Management, 51, 2016–2024.

349. Strand, A., & Alsaker, J. (2009). U.S. Patent No. 7,562,465. Washington, DC: U.S. Patent and Trademark Office.

350. Strezov, V., & Evans, T. J. (Eds.). (2014). Biomass processing technologies. CRC Press (Taylor & Francis Group), Boca Raton London NY.

351. Suleiman, W., Gerba, C. P., Tamimi, A. H., Freitas, R. J., Al Sheraideh, A., & Hayek, B. (2010). Management practices of sludge and biosolid treatment and disposal in Jordan. J. Resid. Sci. Technol, 7(1), 63-67.

352. Syed-Hassan, S. S. A., Wang, Y., Hu, S., Su, S., & Xiang, J. (2017). Thermochemical processing of sewage sludge to energy and fuel: Fundamentals, challenges and considerations. Renewable and Sustainable Energy Reviews, 80, 888-913.

353. Tabatabaie-Raissi, A., & Antal Jr, M. J. (1986). Design and operation of a 30KWe/2KWth downward facing beam ARC image furnace. Solar energy, 36(5), 419-429.

354. Tawfeek, F. (2018). Sun rises on Egypt's solar energy market - Egypt Independent. Ww web. Available at: https://egyptindependent.com/sun-rises-on-egypts-solar-energy-market/?__cf_chl_jschl_tk__=bcf14cc1bd9fce798067505038f58a27bfd08a86-1586380847-0-AVxfVkkExkjEmqCD5ChZhnM8V7Dk03zhvEsGH7fo6800Wu0ToAlDA6ThHC92b0J75WoxGmNOyHy7AkotQFi6LPxizJHsoSVMuvXS4p2QBh4pqFE (Accessed: 9 April 2020).

355. Tchobanoglous, G., Theisen, H., & Vigil, S. (1993). Integrated Solid Waste Management: Engineering Principles and Management Issues. Water Science & Technology Library, 8(1), 63-90.

356. Tchobanoglous, G., Theisen, H., & Vigil, S. (1993). Integrated Solid Waste Management: Engineering Principles and Management Issues. Water Science & Technology Library, 8(1), 63-90.

357. Tesfay, A. H., Kahsay, M. B., & Nydal, O. J. (2014). Design and development of solar thermal Injera baking: steam based direct baking. Energy Procedia, 57, 2946-2955.

358. The Australian/New Zealand Standard, AS/NZS 3831:1998 – Waste Management – Glossary of Terms was published in September 1998. Retrieved from http://infostore.saiglobal.com/store2/Details.aspx?ProductID=375132

359. The Environmental Literacy Council (2015). What is Waste? Retrieved from https://enviroliteracy.org/environment-society/waste-management/what-is-waste/

360. Thipkhunthod, P., Meeyoo, V., Rangsunvigit, P., & Rirksomboon, T. (2007). Describing sewage sludge pyrolysis kinetics by a combination of biomass fractions decomposition. Journal of Analytical and Applied Pyrolysis, 79(1-2), 78-85.

361. Tian, M., Su, Y., Zheng, H., Pei, G., Li, G., & Riffat, S. (2018). A review on the recent research progress in the compound parabolic concentrator (CPC) for solar energy applications. Renewable and Sustainable Energy Reviews, 82, 1272-1296.

362. Tsai, W. T. (2012). An analysis of the use of biosludge as an energy source and its environmental benefits in Taiwan. Energies, 5(8), 3064-3073.

363. Tsoutsos, T., Gekas, V., & Marketaki, K. (2003). Technical and economical evaluation of solar thermal power generation. Renewable Energy, 28(6), 873-886.

364. Tuan, P. A., Mika, S., & Pirjo, I. (2012). Sewage sludge electro-dewatering treatment—A review. Drying Technology, 30(7), 691-706.

365. Tunçal, T., & Uslu, O. (2014). A review of dehydration of various industrial sludges. Drying Technology, 32(14), 1642-1654.

366. Tunçal, T., Jangam, S. V., & Güneş, E. (2011). Abatement of organic pollutant concentrations in residual treatment sludges: A review of selected treatment technologies including drying. Drying Technology, 29(14), 1601-1610.

367. U.S. Environmental Protection Agency (EPA), (2006). Municipal Solid Waste Generation, Recycling, and Disposal in the United States: Facts and Figures for 2006. USA.

368. U.S. EPA. Biosolids technology fact sheet. Use of composting for biosolids management. Accessed 15.06.2020. Retrieved from https://nepis.epa.gov/Exe/ZyPDF.cgi/P10053DF.PDF?Dockey=P10053DF. PDF September 2002, EPA/832-F-02-024

369. Umair, M., Akisawa, A., & Ueda, Y. (2014). Optimum settings for a compound parabolic concentrator with wings providing increased duration of effective temperature for solar-driven systems: a case study for Tokyo. Energies, 7(1), 28-42.

370. UNIVERSITY OF BABYLON (n.d.). Chemical engineering department. Drying. Retrieved from http://www.uobabylon.edu.iq/uobColeges/ad_downloads/4_13474_558.pdf

371. University of Southern Indiana. (n.d.). Recycling at USI: Solid Waste & Landfill Facts. Retrieved from https://www.usi.edu/recycle/solid-waste-landfill-facts/

372. Urbaniak, M., & Hillebrand, B. (2004). Sludge drying and granulation for their further use, Mat. In XVI Konferencji Naukowo-Technicznej nt. Aktualne problemy gospodarki wodno-ściekowej (pp. 27-28).

373. US Environmental Protection Agency EPA, (2018). Inventory of U.S. Greenhouse Gas Emissions and Sinks: 1990-2016. Washington, DC, USA.

374. Valo, A., Carrere, H., & Delgenes, J. P. (2004). Thermal, chemical and thermo-chemical pre-treatment of waste activated sludge for anaerobic digestion. Journal of Chemical Technology & Biotechnology: International Research in Process, Environmental & Clean Technology, 79(11), 1197-1203.

375. Van de Velden, M., Baeyens, J., Brems, A., Janssens, B., & Dewil, R. (2010). Fundamentals, kinetics and endothermicity of the biomass pyrolysis reaction. Renewable energy, 35(1), 232-242.

376. Vant-Hull, L. (2014). Issues with beam-down concepts. Energy Procedia, 49, 257-264.

377. Vaxelaire, J. (2001). Moisture sorption characteristics of waste activated sludge. Journal of Chemical Technology & Biotechnology: International Research in Process, Environmental & Clean Technology, 76(4), 377-382.

378. Vaxelaire, J., & Cézac, P. (2004). Moisture distribution in activated sludges: a review. Water research, 38(9), 2215-2230.

379. Vaxelaire, J., Bongiovanni, J. M., Mousques, P., & Puiggali, J. R. (2000). Thermal drying of residual sludge. Water Research, 34(17), 4318-4323.

380. Venderbosch, R. H., & Prins, W. (2010). Fast pyrolysis technology development. Biofuels, bioproducts and biorefining, 4(2), 178-208.

381. Vergara, S. E., & Tchobanoglous, G. (2012). Municipal Solid Waste and the Environment: A Global Perspective. Environment and Resources, 37(37), 277-309. https://doi.org/10.1146/annurev-environ-050511-122532

382. Vesilind, P. A. (1994). The role of water in sludge dewatering. Water Environment Research, 66(1), 4-11.

383. Vesilind, P. A., & Hsu, C. C. (1997). Limits of sludge dewaterability. Water science and technology, 36(11), 87-91.

384. Villamil, J. A. A., Hortúa, J. E., & Lopez, A. (2013). Design and construction of a solar collector parabolic dish for rural zones in Colombia. Tecciencia, 7(14), 14-22.

385. Wah, S. C., (2015). Moisture Control. Moisture control seminar, School of Bioscience, Taylor's University Lakeside. Retrieved from https://moisturecontrol.weebly.com/

386. Walsh, B. (Jan. 07, 2008). TIME USA, LLC. Trash Problems in Paradise. Retrieved from http://content.time.com/time/world/article/0,8599,1701095,00.html

387. Wang, N. Y., Shih, C. H., Chiueh, P. T., & Huang, Y. F. (2013). Environmental effects of sewage sludge carbonization and other treatment alternatives. Energies, 6(2), 871-883.

388. Wang, Q., Wang, J., & Tang, R. (2016). Design and optical performance of compound parabolic solar concentrators with evacuated tube as receivers. Energies, 9(10), 795.

389. Wang, T. (2019). Daily municipal solid waste generation per capita worldwide in 2018, by select country (in kilograms). Global Waste Generation - Statistics & Facts. Statista. Retrieved from https://www.statista.com/statistics/689809/per-capital-msw-generation-by-country-worldwide/

390. Wang, T. (2019). Percentage of global population and municipal solid waste generation share in 2018, by select country. Global Waste Generation - Statistics & Facts. Statista. Retrieved from https://www.statista.com/topics/4983/waste-generation-worldwide/

391. Wang, Z. (2019). Design of solar thermal power plants. Elsevier Inc. Retrieved from https://www.sciencedirect.com/book/9780128156131/design-of-solar-thermal-power-plants#book-info

392. Wang, Z. (2019). Thermal storage systems. In Z. Wang Editor (Eds.), Design of solar thermal power plants (1st ed., pp 387-415). Elsevier Inc. Retrieved from https://www.sciencedirect.com/book/9780128156131/design-of-solar-thermal-power-plants#book-info. Doi: https://doi.org/10.1016/C2017-0-03007-0

393. Weimer, A., Perkins, C., Mejic, D., Lichty, P. (2008). Rapid solar-thermal conversion of biomass to syngas. International patent application No. WO2008/027980

394. Weldekidan, H., Strezov, V., & Town, G. (2017). Performance evaluation of absorber reactors for solar fuel production. Chemical Engineering Transactions, 61, 1111-1116.

395. Weldekidan, H., Strezov, V., & Town, G. (2018). Review of solar energy for biofuel extraction. Renewable and Sustainable Energy Reviews, 88, 184-192.

396. Welford, W. & Winston, R. (1989). High Collection Nonimaging Optics. Academic Press, San Diego, 1989.

397. White, P. R., Franke, M., & Hindle, P. (1995). Integrated Solid Waste Management: A Lifecycle Inventory. Berlin: Springer.

398. White, P., Dranke, M., & Hindle, P. (2012). Integrated solid waste management: a lifecycle inventory. Berlin: Springer Science & Business Media.

399. Wiese-Fales, J. (2011). Nanoantenna reinvents solar energy. College of Engineering at the University of Missouri, U.S. Retrieved at 16 June 2020 from https://engineering.missouri.edu/2011/08/nanoantenna-reinvents-solar-energy/

400. Williams, P. T. (2013). Pyrolysis of waste tyres: a review. Waste management, 33(8), 1714-1728.

401. Wilson, D. C. (2007). Development drivers for waste management. Waste Management & Research, the Journal of the International Solid Wastes & Public Cleansing Association Iswa, 25(3), 198-207. https://doi.org/10.1177/0734242X07079149

402. Winkler, M. K., Bennenbroek, M. H., Horstink, F. H., Van Loosdrecht, M. C. M., & Van de Pol, G. J. (2013). The biodrying concept: An innovative technology creating energy from sewage sludge. Bioresource Technology, 147, 124-129.

403. Włodarczyk-Makuła, M. (2016). Persistence of two-, three-and four-ring of PAHs in sewage sludge deposited in different light conditions. Desalination and Water Treatment, 57(3), 1184-1199.

404. Wójcik, M., & Stachowicz, F. (2019). Influence of physical, chemical and dual sewage sludge conditioning methods on the dewatering efficiency. Powder technology, 344, 96-102.

405. Wu, C. C., Huang, C., & Lee, D. J. (1998). Bound water content and water binding strength on sludge flocs. Water research, 32(3), 900-904.

406. Wu, C. C., Huang, C., & Lee, D. J. (1998). Bound water content and water binding strength on sludge flocs. Water research, 32(3), 900-904.

407. Wu, L., Tu, J., Cai, Y., Wu, Z., & Li, Z. (2020). Biofuel production from pyrolysis of waste cooking oil fried sludge in a fixed bed. Journal of Material Cycles and Waste Management, 1-13.

408. Wu, Z., Zhang, J., Li, Z., Xie, J., & Mujumdar, A. S. (2012). Production of a solid fuel using sewage sludge and spent cooking oil by immersion frying. Journal of hazardous materials, 243, 357-363.

409. Xiang, X. (2017). U.S. Patent No. 9,671,171. Systems and methods of thermal transfer and/or storage. Washington, DC: U.S. Patent and Trademark Office.

410. Xiang, X., & Zhang, R. (2017). U.S. Patent No. 9,612,059. Washington, DC: U.S. Patent and Trademark Office.

411. Xie, Q., Peng, P., Liu, S., Min, M., Cheng, Y., Wan, Y., ... & Ruan, R. (2014). Fast microwave-assisted catalytic pyrolysis of sewage sludge for bio-oil production. Bioresource technology, 172, 162-168.

412. Xiong, S., Zhuo, J., Zhang, B., & Yao, Q. (2013). Effect of moisture content on the characterization of products from the pyrolysis of sewage sludge. Journal of analytical and applied pyrolysis, 104, 632-639.

413. Xiuguang, T. (谭修光), (2016). Sludge treatment method using solar pyrolysis carbonization technology. Patent Application WO2016127594A1, WIPO (PCT).

414. Xu, C., Chen, W., & Hong, J. (2014). Life-cycle environmental and economic assessment of sewage sludge treatment in China. Journal of Cleaner Production, 67, 79-87.

415. Xu, W. Y., & Wu, D. (2015). Comprehensive utilization of the pyrolysis products from sewage sludge. Environmental technology, 36(14), 1731-1744.

416. Yadav, D., & Banerjee, R. (2016). A review of solar thermochemical processes. Renewable and Sustainable Energy Reviews, 54, 497-532.

417. Yan, J. H., Deng, W. Y., Li, X. D., Wang, F., Chi, Y., Lu, S. Y., & Cen, K. F. (2009). Experimental and theoretical study of agitated contact drying of sewage sludge under partial vacuum conditions. Drying Technology, 27(6), 787-796.

418. Yang, G., Zhang, G., & Wang, H. (2015). Current state of sludge production, management, treatment and disposal in China. Water research, 78, 60-73.

419. Yang, H., Kudo, S., Kuo, H. P., Norinaga, K., Mori, A., Mašek, O., & Hayashi, J. I. (2013). Estimation of enthalpy of bio-oil vapor and heat required for pyrolysis of biomass. Energy & Fuels, 27(5), 2675-2686.

420. Yen, P. S., & Lee, D. J. (2001). Errors in bound water measurements using centrifugal settling method. Water research, 35(16), 4004-4009.

421. Yi, S., Jang, Y. C., & An, A. K. (2018). Potential for energy recovery and greenhouse gas reduction through waste-to-energy technologies. Journal of cleaner production, 176, 503-511.

422. Zadik, B., & Israel, F. (2011). Solar powered method and system for sludge treatment. U.S. Patent Application No. 13/254,277.

423. Zafar, S. (2018). Bioenergy consult. Promise of waste-to-energy. Retrieved from https://www.bioenergyconsult.com/author/salman/

424. Zeaiter, J., Ahmad, M. N., Rooney, D., Samneh, B., & Shammas, E. (2015). Design of an automated solar concentrator for the pyrolysis of scrap rubber. Energy conversion and management, 101, 118-125.

425. Zeaiter, J., Azizi, F., Lameh, M., Milani, D., Ismail, H. Y., & Abbas, A. (2018). Waste tire pyrolysis using thermal solar energy: An integrated approach. Renewable Energy, 123, 44-51.

426. Zeaiter, J., Azizi, F., Lameh, M., Milani, D., Ismail, H. Y., & Abbas, A. (2018). Waste tire pyrolysis using thermal solar energy: An integrated approach. Renewable Energy, 123, 44-51.

427. Zell, E. et al. (2015). Assessment of solar radiation resources in Saudi Arabia. Solar Energy. Elsevier Ltd, 119, pp. 422–438. doi: 10.1016/j.solener.2015.06.031.

428. Zeng, K., Flamant, G., Gauthier, D., & Guillot, E. (2015). Solar pyrolysis of wood in a lab-scale solar reactor: influence of temperature and sweep gas flow rate on products distribution. Energy Procedia, 69, 1849-1858.

429. Zeng, K., Gauthier, D., Li, R., & Flamant, G. (2015). Solar pyrolysis of beech wood: Effects of pyrolysis parameters on the product distribution and gas product composition. Energy, 93, 1648-1657.

430. Zeng, K., Gauthier, D., Lu, J., & Flamant, G. (2015). Parametric study and process optimization for solar pyrolysis of beech wood. Energy Conversion and Management, 106, 987-998.

431. Zeng, K., Gauthier, D., Soria, J., Mazza, G., & Flamant, G. (2017). Solar pyrolysis of carbonaceous feedstocks: A review. Solar Energy, 156, 73-92.

432. Zeng, K., Minh, D. P., Gauthier, D., Weiss-Hortala, E., Nzihou, A., & Flamant, G. (2015). The effect of temperature and heating rate on char properties obtained from solar pyrolysis of beech wood. Bioresource technology, 182, 114-119.

433. Zeng, K., Soria, J., Gauthier, D., Mazza, G., & Flamant, G. (2016). Modeling of beech wood pellet pyrolysis under concentrated solar radiation. Renewable energy, 99, 721-729.

434. Zhang, L., Xu, C. C., & Champagne, P. (2010). Overview of recent advances in thermo-chemical conversion of biomass. Energy Conversion and Management, 51(5), 969-982.

435. Zhao, L., Chen, D., & Xie, J. (2009, March). Sewage sludge solar drying practise and characteristics study. In 2009 Asia-Pacific Power and Energy Engineering Conference (pp. 1-5). IEEE.

436. Zheng, H. (2017). Solar energy desalination technology; Chapter 9: Solar Concentrating Directly to Drive Desalination Technologies. Amsterdam: Elsevier, pp. 671–707

437. Zhou, J., Liu, S., Zhou, N., Fan, L., Zhang, Y., Peng, P., ... & Chen, P. (2018). Development and application of a continuous fast microwave pyrolysis system for sewage sludge utilization. Bioresource technology, 256, 295-301.

438. Zhuang, L., Zhou, S., Wang, Y., Liu, Z., & Xu, R. (2011). Cost-effective production of Bacillus thuringiensis biopesticides by solid-state fermentation using wastewater sludge: Effects of heavy metals. Bioresource technology, 102(7), 4820-4826.